DEPARTAMENTO DE BIOQUÍMICA

FACULTAD DE MEDICINA

PRECLINICAL STUDIES FOR THE GENE THERAPY OF LEUKOCYTE ADHESION DEFICIENCY TYPE I

Memoria presentada por DIEGO LEÓN RICO para optar al grado de doctor por la Universidad Autónoma de Madrid, con mención internacional.

Directores de Tesis

Elena Almarza Novoa

Juan Antonio Bueren Roncero

CENTRO DE INVESTIGACIONES ENERGÉTICAS, MEDIO AMBIENTALES Y TECNOLÓGICAS (CIEMAT) – CENTRO DE INVESTIGACIONES BIOMÉDICAS EN RED DE ENFERMEDADES RARAS (CIBERER) – INSTITUTO DE INVESTIGACIÓN SANITARIA DE LA FUNDACIÓN JIMÉNEZ DÍAZ (IIS – FJD)

Elena Almarza Novoa, investigadora post doctoral de la División de terapias innovadoras del Sistema hematopoyético de Centro de Investigaciones Energéticas, Medioambientales y Tecnológicas, y **Juan Antonio Bueren Roncero**, jefe de la misma unidad, certifican que la memoria adjunta titulada *PRECLINICAL STUDIES FOR THE GENE THERAPY OF LEUKOCYTE ADHESION DEFICIENCY TYPE I* ha sido realizada por Diego León Rico bajo la dirección conjunto de los que suscriben, y cumple las condiciones exigidas para optar al título de Doctor con mención internacional por la Universidad Autónoma de Madrid.

Elena Almarza Novoa **Juan Antonio Bueren Roncero**

A mi padre

Agradecimientos

Muchas sois las personas que habéis hecho posible esta tesis doctoral por vuestro apoyo, ayuda y amistad.

Por eso, me gustaría agradecer…

En primer lugar a mis directores de tesis, **Juan y Elena**. A **Juan** por dejarme formar parte de un grupo de investigación tan bueno como el nuestro cuando tan solo era un recién licenciado en farmacia que buscaba un laboratorio donde realizar las prácticas de master. Durante estos años he seguido sintiendo el apoyo y la confianza que depositaste en mí, espero haber estado a la altura de esas expectativas. A **Elena**, por haberme guiado en mi formación como investigador y por haberme enseñado todo lo que sé, dejándome al mismo tiempo espacio para el error y para aprender por mí mismo. Gracias por haber sido jefa, compañera y amiga. Espero que lo sigas siendo durante mucho tiempo.

A todos **mis compañeros de Hemato**, tanto pequeños como grandes, tanto los que ya no estáis como los que seguís por aquí. Habéis sido muchos, pero todos habéis sido parte fundamental de mi vida ciematera.

A **Monserrat**, por ayudarme tanto durante estos años. Por soportar mis manías, mis nomenclaturas, mi orden caótico, mis "hojitas de instrucciones" y tantos otros defectos. Ha sido un placer ser tu compañero, espero que también lo haya sido para ti. A mis niñas del grupo LAD, **Clara, Raquel y Cris**. Ha sido genial trabajar con vosotras y enseñaros lo poco que he podido. Esta tesis es en parte gracias a vuestra ayuda y esfuerzo. Gracias por tantas risas compartidas y por esas inyecciones de ánimo que tanto se necesitan. Como diría Clara, espero no haber sido demasiado "repu".

A los pequehematos originales, **Sandra, Rocío, Laura P, Lara, Parra, Alberto, Álvaro, María peque, Elenita y Vic**. Por acoger y hacer sentir tan cómodo al joven y tímido Diego cuando llego por primera vez al CIEMAT. **Rocío**, la alegría del CIEMAT. ¡Qué fácil es quererte y que poco te dejas! Menos mal que con los años te hemos ido ablandando. Por quererme y cuidarme como si fuera tu hermano pequeño. **María**, mi mujer científica, por enseñarme la concentración del bromuro de etidio, la ampicilina… y tantas otras cosas. Eres igual de buena persona fuera del laboratorio como trabajadora y rigurosa dentro de él. **Sandra** y **Laura P,** menudo equipazo formabais. La de buenos momentos vividos juntos. Esto no ha sido lo mismo desde que os fuisteis. **Elenita**, mi primera compañera de atrás. Compartir el día a día contigo es vivir en una sorpresa constante. **Victoria**, nuestra galleguiña. Estarás acostumbrada a vivir en una tierra de nubes y lluvia, pero está claro que tú tienes luz propia. **Parra y Alberto,** mis iniciadores en el mundo de la maldad, se os echa de menos pareja. **Lara**, nunca olvidaré tus dichos y chascarrillos populares, eres toda una fuente de sabiduría popular. Nunca dejes de sonreír. **Álvaro,** lo que nos costó sacar la maldita banda. Fue un placer colaborar contigo y espero volver a hacerlo alguna vez. **Javi**, no dejes de emocionarte por las cosas y de ser un niño grande aunque te conviertas en un gran científico (que seguro que lo harás).

A mis niñas **Bego, María micro, Fati, MJ y Zita**. Ha sido un placer ser vuestro co-doctorando.

Juntos hemos aprendido, llorado, reído, trabajado, discutido y gracias a ello nos hemos convertido en los científicos que somos hoy en día. Sin vosotras no habría sido lo mismo. **María**, mi *mutual support*. Eres la responsabilidad y organización personificada, esa persona a la que un desastre como yo siempre necesita a su lado. Es un placer trabajar contigo. Por no hablar de lo buena persona que eres ¿Se puede pedir más? **Fati**, mi querida compañera de atrás. Soportar mis canticos durante tanto tiempo no ha tenido que ser fácil y tú lo has hecho estoicamente. La de confesiones que hemos compartido durante este tiempo. Sabes escuchar y se agradece. No dejes nunca de poner tanta pasión y energía en todo lo que haces. **Begoña**, mi compañera de beca y nombre. Ya no tendrás que preguntar en alto cuando llamen al teléfono ¿Bego o Diego? ¡Qué alivio! He conocido pocas personas tan cariñosas como tú. Deberían poner tu foto en el diccionario al lado de las palabras amor y cariño. Ya te dije una vez que eras el pegamento que mantenía este grupo unido. **MJ**, mi burgalesa, mi condesa de Tetuan. Por regañarme cuando me paso y por ser la diversión en estado puro. Eres única e irrepetible. No dejes que nunca te cambien. **Zita**, mi compañera de alegrías y frustraciones. Eres el claro ejemplo de que las primeras impresiones siempre son equivocadas. Sé que te irá muy bien en tu futuro profesional. Acuérdate de nosotros cuando seas una jefaza.

A **Rebeca y Omaira**, por aguantar tan bien todo el trabajo y todos los problemas que os damos. Sois tal cual la una para la otra. Tenéis gracia, salero y espontaneidad para dar y regalar.

A todos los recién llegados, **Sara, Laura J, Javier, Victoria, José, Sergio, Fran y Miguel**. Aunque me hagáis sentir un poco viejo, es una alegría teneros siempre alrededor. **José, Sergio, Fran y Miguel,** qué pena que no hayáis formado parte de esto desde el principio, porque sois maravillosos. Sabéis que solo puedo deciros una cosa: OHHHH.

A **Mari Luz, Raquel e Israel.** No se puede pedir compañeros de trabajo mas majos y mas "salaos" que vosotros. **Mari Luz**, he conocido poca gente tan trabajadora y con tantas ganas de ayudar como tú.

A las chicas de arriba, **Miriam y Laura**. Mira que da pereza subir a la planta de arriba, pero bien merece por veros a vosotras. **Laura**, siempre llevas una sonrisa en la cara. Gracias por descubrirme uno de los grandes secretos de tu tierra.

A los baticuevos, **Rosa, María, Susana, Oscar y Mercedes**, por acogerme siempre tan bien en vuestro despachito. Incluso a veces conseguíais hacerme sentir uno más de vosotros. **Rosa**, mi otra parte del *mutual support*, nos costó llevarnos bien pero se nota que al final nos hemos ganado el cariño y el respeto el uno del otro. Sigue cuidando tan bien de Elena. **María**, gracias por aportar ese punto de paz, sensibilidad y cordura que cualquier grupo necesita.

A **Paula, Maruja, Marina y Jaco**, por derrochar marcha, simpatía y buena ciencia a partes iguales. **Paula**, eres buena científica y mejor persona, amiga y compañera. Gracias por enseñarnos que el trabajo duro tiene sus recompensas. **Maru**, mi compañera de club. Toda la vida compartiendo nuestros veranos y nosotros sin saberlo, que pena no habernos conocido hace mucho más tiempo.

A **José Carlos y Guille**, por demostrar que se puede ser jefe y amigo al mismo tiempo. Vuestras dotes artísticas son inigualables. **Guille**, eres único, hablando contigo siempre se aprende algo nuevo y se llora de la risa a partes iguales.

A **Miguel,** por tantos pequeños problemas que me has solucionado. Contigo la burocracia no tiene misterios.

A **Aurora, Sole, Sergio y Mamen**. Sin vosotros no sería posible todo lo que hacemos más arriba. Gracias por hacernos la vida tan fácil.

A **Jesús, Edilia, Miguel Ángel** y toda la gente del animalario. Sin vosotros está tesis no tendría sentido. Por cuidar de nuestros ratones, los cuales deberían figurar prácticamente los primeros en la lista de agradecimientos.

A los **compañeros de las divisiones de biomedicina epitelial y oncología molecular**. Con vecinos así, da gusto venir a trabajar. Por compartir tan buenos consejos y por enseñarnos cosas tan interesantes como las que vosotros hacéis. En especial me gustaría dar las gracias a **Cloti, Mónica, Cris, Jose (La), Jose (Ariza), Águeda, Ana y Sara**. Nunca olvidaré los buenos ratos que hemos pasado y lo bien que me habéis tratado y acogido entre vosotros.

A mis compañeros del laboratorio de Londres, **María Eugenia, Pilar, Claudia, Miquel, Albert, Marlene y Karolin**. Por acogerme tan bien entre vosotros y hacerme sentir como en casa. Espero volver a veros a todos muy pronto.

Pero no todo es ciencia y laboratorio. Fuera de aquí también hay mucha gente que ha estado a mi lado antes y durante la realización de esta tesis. Espero que sigan estando ahi durante mucho tiempo.

A mis amigos del barrio**, Noelia, Isabel, Helena, Mari, Fátima, Patri, Sergio, Alex, Jorge y respectivos**. Poca gente puede presumir de tener tan buenos amigos como vosotros. A pesar de que nuestras vidas tomen rumbos tan diferentes, que tranquilo se vive sabiendo que vosotros estáis allí. No puedo dejar de darte las gracias en especial a ti, **Noelia**, por llevar toda la vida a mi lado. Espero que nunca te canses de mí y que nos queden todavía por vivir muchas más cosas.

A mis amigos de la facultad, **Marta, María, Juan, Javi, Leti y Pablo**. Que poco me cuesta reconocer que los 5 años de carrera han sido una de las mejores épocas de mi vida, y en gran parte es gracias a vosotros. Nunca pensé que podría llevarme tan bien y querer tanto a gente tan diferente a mí.

A **Aran, Isa, Almudena, Gazpa, Damián, Amor, Víctor y Rocío**. Por dejar que mi hermana me metiera en vuestras vidas. Hoy por hoy puedo decir que sois amigos míos con todas las letras. Si llego a

ser *Lisensiado* es en parte gracias a vosotros.

A **Ana, Nico, Pablo y Nacho**, por ser mi pequeña familia. Por cuidar tan bien de mí y de los míos en los malos y en los buenos momentos. Desde que tengo uso de razón, vosotros estáis en mis recuerdos.

A mi cuñado **Javi**, poco a poco te has hecho un hueco grande en nuestra pequeña familia, a pesar de la lata que das a veces. Gracias por ser mi compañero de gimnasio, de fiestas, de compras, de confesiones, de risas y de muchas tantas otras cosas. Hoy puedo decir con la boca grande que eres mi amigo.

A mi hermana **María**, ir detrás de ti no ha sido nada fácil, has dejado el listón muy alto. Gracias a lo cual he llegado hasta donde estoy hoy. Sé que nos queremos muchísimo aunque a veces nos saquemos de quicio, pero eso nos pasa por ser los dos tan cabezones y que los hermanos discuten es un hecho inherente a la condición de hermanos. Gracias por estar en los momentos buenos y en los momentos difíciles, por tus consejos, por indicarme el camino cuando estaba un poco perdido, por sacarme de casa cuando lo he necesitado… En definitiva, un GRACIAS con mayúsculas.

Y por último, a mis padres, **Carlos y Pilar**, por haberme criado de la forma en que lo hicisteis, por vuestro apoyo y cariño, y por haberme permitido estudiar y formarme. Siempre me habéis enseñado a ser responsable con los estudios y con el trabajo, pero también que todo eso no merece la pena sin amigos, momentos felices y diversión. **Papa**, aunque no estarás allí para ver como defiendo esta tesis, sé que de alguna manera estarás conmigo apoyándome. Gracias por ser como eras. **Mama**, tu sí que estarás allí, como siempre, a mi lado, apoyándome y preocupándote por mí. Por favor, no dejes de hacerlo nunca.

Seguro que se me queda alguien por agradecer, pero ya sabéis los que me conocéis que soy un poco despistado. En definitiva, Gracias a todos.

Resumen - Abstract

La Deficiencia de Adhesión Leucocitaria Tipo I (DAL-I) es una inmunodeficiencia primaria producida por mutaciones en el gen *ITGB2*, que codifica para la proteína CD18 o subunidad β_2. Esta proteína se asocia con diferentes subunidades CD11 para formar las integrinas β_2, las cuales se expresan en la membrana de los leucocitos y les permiten adherirse al endotelio como paso previo a la extravasación. Las mutaciones en el gen *ITGB2* producen una reducida, ausente o aberrante expresión de CD18, lo que se traduce en la ausencia de integrinas β_2 en la membrana leucocitaria. Los leucocitos de estos pacientes, principalmente los neutrófilos, son incapaces de abandonar el torrente sanguíneo y combatir las infecciones que se producen en los diferentes tejidos. Así, estos pacientes sufren infecciones bacterianas graves y recurrentes que pueden conducir a su muerte.

En la presente tesis doctoral nos propusimos inicialmente caracterizar una cepa de ratón que presenta una mutación hipomórfica en el gen *itgb2* ($CD18^{HYP}$) para su posterior uso como modelo animal de DAL-I. Estos ratones mostraban una expresión baja pero detectable de integrinas β_2 en células linfoides y mieloides y presentaban leucocitosis y defectos en la migración de neutrófilos en respuesta a agentes inflamatorios. Sorprendentemente, la médula ósea (MO) de estos ratones presentaba un mayor contenido de células madre hematopoyéticas (CMHs). Además, las células de MO de los ratones $CD18^{HYP}$ presentaban una mayor capacidad de repoblación competitiva que las de un ratón WT. A través de diferentes experimentos *in vivo* observamos que la ausencia de CD18 conduce a la expansión del compartimento de CMHs incluso en presencia de un ambiente hematopoyético WT, lo que demuestra por primera vez el papel de CD18 en la regulación del nicho hematopoyético.

Al tratarse de una enfermedad hematopoyética monogénica, DAL-I es una enfermedad idónea para ser tratada mediante terapia génica (TG) *ex vivo*. Por ello, generamos cuatro vectores lentivirales (VLs) autoinactivantes en los que la expresión del gen *ITGB2* está controlada por diferentes promotores, tanto ubicuos (PGK y UCOE) como mieloides (Chim y MIM). Estos VLs demostraron su eficacia para recuperar la expresión de integrinas β_2 y corregir el fenotipo en dos modelos *in vitro*: una línea linfoblastoide derivada de un paciente con DAL-I y CMHs sanas interferidas para la expresión de CD18 (mediante la utilización de un VL que expresa un RNAsh capaz de reconocer el RNAm de CD18).

Finalmente, pasamos a realizar experimentos de TG *ex vivo* en los ratones $CD18^{HYP}$. Los ratones tratados por TG presentaban células en sangre periférica y en MO que expresaban la proteína humana CD18 (hCD18). Además, estas células presentaban una mayor expresión de la proteína endógena CD11a (mCD11a) en comparación con ratones no tratados, lo que indicaba que la expresión ectópica de hCD18 rescataba la expresión de las integrinas β_2 de ratón. La expresión de hCD18 en todos los grupos tratados siempre fue mayor en neutrófilos que en linfocitos, aunque fueron aquellos ratones tratados con el vector LV:Chim.hCD18 en los que el ratio entre la expresión mieloide y la expresión linfoide fue mayor. Al retransplantar la MO de estos ratones, se observaron células $hCD18^{+}$ con expresión incrementada de mCD11a en los receptores secundarios, lo que indicaba que los VLs-hCD18 eran capaces de transducir CMHs con capacidad de repoblación a largo plazo. La recuperación de valores normales de leucocitos en la sangre y el restablecimiento de la capacidad de extravasación de los neutrófilos corroboraron la eficacia terapéutica de estos vectores.

Aunque se obtuvieron resultados muy similares con todos los VLs, el promotor ideal para la TG de DAL-I sería aquel que expresase hCD18 en todas las células hematopoyéticas y que dirija una alta expresión en el linaje mieloide, puesto que es el tipo celular más afectado por la deficiencia en esta proteína. Por eso, y en base a los resultados obtenidos, proponemos el uso del vector LV.Chim.hCD18 para un futuro ensayo de terapia génica en pacientes con DAL-I.

Leukocyte Adhesion Deficiency Type I (LAD-I) is a primary immunodeficiency caused by mutations in *ITGB2* gene, encoding for CD18 protein (also known as β_2 subunit). This protein binds to different CD11 subunits to form β_2 integrins, which are expressed in the leukocyte membrane and allow leukocytes to firmly adhere to the endothelium as a previous step to the extravasation. In LAD-I patients, *ITGB2* mutations lead to absent, low or aberrant CD18 expression, which results in absent or low β_2 integrin expression on the leukocyte membrane. CD18 deficient leukocytes, especially neutrophils, fail to extravasate from the bloodstream to infected tissues. LAD-I patients suffer from recurrent and severe infections leading normally to death.

In the present doctoral thesis, we initially aimed to characterize a mouse strain presenting an hypomorphic mutation in the *itgb2* gene ($CD18^{HYP}$), which would be later used as a LAD-I animal model. These mice displayed low but still present β_2 integrin expression in lymphoid and myeloid cells and showed leukocytosis and defects in neutrophil extravasation capacity in response to different inflammatory stimuli. Surprisingly, $CD18^{HYP}$ bone marrow (BM) showed enrichment in haematopoietic stem cells (HSCs). Moreover, BM cells from $CD18^{HYP}$ mice presented a higher competitive repopulation ability compared to WT cells. Through different *in vivo* experiments, we demonstrated that CD18 deficiency lead to the expansion of HSCs even in the presence of a WT haematopoietic environment, which pointed out the role of CD18 in the regulation of the haematopoietic niche for the first time.

As a monogenic haematopoietic disorder, LAD-I is a good candidate for *ex vivo* haematopoietic gene therapy (GT). For this, we generated four lentiviral vectors (LVs) in which *ITGB2* gene is expressed under ubiquitous (UCOE and PGK) or myeloid (Chim and MIM) promoters. These LVs succeeded in the CD18 expression and phenotype restoration in two different *in vitro* models: a lymphoblastic cell line derived from a LAD-I patient and in CD18-interferred healthy HSCs (generated by the use of a LV expressing a shRNA against the CD18 mRNA).

Finally, we carried our GT experiments in $CD18^{HYP}$ mice. GT-treated $CD18^{HYP}$ mice showed peripheral blood and BM cells expressing hCD18 protein, which in addition showed higher expression of mCD11a subunit in comparison with untreated mice. This indicated that ectopic hCD18 expression restores murine β_2 integrins. hCD18 expression was always higher in myeloid than in lymphoid cells in all treated groups, although LV.Chim.hCD18-treated animals showed the highest ratio between myeloid and lymphoid expression. When BM from these animals was re-transplanted into secondary recipients, $hCD18^{+}$ cells with increased mCD11a expression could be observed, indicating that all CD18-LVs were able to transduce true and long-term HSCs. The recovery of normal number of leukocytes and the reestablishment of inflammation-mediated neutrophil extravasation capacity supported the therapeutic effect of these LVs

Although similar results were obtained with all the hCD18-LVs, the ideal promoter for the GT of LAD-I would be the one driving a high expression of CD18 in the myeloid lineage but also expressing at a low level in other haematopoietic cells. For this reason, and on the basis of these results, we propose the use of LV.Chim.hCD18 for a future LAD-I GT clinical trial.

Index

List of abbreviations

ADA-SCID	Severe combined immunodeficiency due to adenosine deaminase deficiency
ALD	Adrenoleukodystrophy
A-MLV	Abelson murine leukaemia virus
AP	Air pouch
APC	Antigen-presenting cell
AV	Annexin V
BAL	Bronchoalveolar lavage
BM	Bone marrow
BMCs	Bone marrow cells
c	Canine
C3bi	Inactive complement component 3b
CalDAG-GEF1	Calcium and DAG-regulated Guanine exchange factor 1
CAR	CXCL12-abundant reticular
$CD18^{HYP}$	Hypomorphic CD18 mice
$CD18^{KO}$	Null CD18 mice
cDNA	Complementary DNA
CDS	Coding DNA sequence
CFU	Colony forming unit
CGD	Chronic granulomatous disease
CLAD	Canine leukocyte adhesion deficiency
CMC	Carboxymethylcellulose
CMH	Célula madre hematopoyética
CMP	Common myeloid progenitor
cPPT	Central polipurine tract
CR	Complement receptor
CRA	Competitive repopulation assay
Ct	Cycle threshold values
CXCL12	C-X-C motif ligand 12
DAG	Diacylglycerol
DAL-I	Deficiencia de adhesión leucocitaria tipo I
DiD	2-[5-(3,3-dimethyl-1-octadecyl-1,3-dihydro-2*H*-indol-2-ylidene)penta-1,3-dien-1-yl]-3,3-dimethyl-1-octadecyl-3*H*-indolium perchlorate
DOCK2	Dedicator of cytokinesis 2
ECM	Extracellular matrix
EF1α	Elongation factor 1 alpha
ESL-1	E-Selectin ligand 1
Fc	Fragment crystallizable
FcR	Fc Receptor
FIS	Foamyviral insertion site
Flt3L	FMS-like tyrosine kinase 3 ligand
FV	Foamyviral vector
GALV	Gibbon ape leukaemia virus
G-CSF	Granulocyte colony-stimulating factor
gDNA	Genomic DNA
GEF	Guanine-nucleotide-exchange factor
GMP	Granulocyte/monocytic progenitor
GOI	Gene of interest
GT	Gene therapy
h	Human
HEK	Human embryonic kidney
HIV-1	Human immunodeficiency virus type 1
HSC	Haematopoietic stem cell
HSCT	Haematopoietic stem cell transplantation
HUVEC	Human umbilical vein endothelial cells
iC3b	Inactive complement component 3b
ICAM	Intercellular adhesion molecule
IP3	Inositol triphosphate
JAM	Junctional adhesion molecule
LAC	Leukocyte adhesion cascade
LAD	Leukocyte adhesion deficiency
LCL	Lymphoblastoid cell line
LDA	Limiting dilution assay
LFA-1	Lymphocyte function-associated antigen 1
Lin^-	Lineage negative
LSK	$Lin^-Sca^+Ckit^+$

LT-HSC	Long-Term haematopoietic stem cell
LV	Lentiviral vector
m	Murine
Mac-1	Macrophage 1 antigen
MACS	Magnetic-activated cell sorting
MDS	Myelodysplastic syndrome
MEP	Megakaryotic/erythroid progenitor
MFI	Mean fluorescent intensity
MIDAS	Metal-ion-dependent adhesion site
miRNA	Micro RNA
MLD	Metachromatic leukodystrophy
MOI	Multiplicity of infection
MPP	Multipotent progenitor
MSCV	Murine stem cell virus
NK	Natural killer
O/N	Overnight
P/S	Penicillin/Streptomycin
PB	Peripheral blood
PBE	PBS with BSA and EDTA
PBL	Peripheral blood leukocyte
PBS	Primer binding site
PECAM1	Platelet endothelial cell adhesion molecule
PGK	Phosphoglycerate kinase
PID	Primary immunodeficiency
PLC	Phospoholipase C
PMA	Phorbol 12-myristate 13-acetate
PPT	Polypurine tract
PSGL-1	P-selectin glycoprotein ligand-1
Q-PCR	Quantitative PCR
Rap1	Ras-related protein 1
RIAM1	Rap1 GTP-interacting adaptor molecule
RIC	Reduced intensity conditioning
RIS	Retroviral insertion site
RISC	RNA Induced Silencing Complex
RN	Retronectin
RRE	Rev responsive element
SAE	Serious adverse effect
SCF	Stem cell factor
shSCR	Scrambled shRNA
sICAM-1	Soluble ICAM-1
SIN	Self-Inactivating
SRC	SCID Repopulating Cells
ST-HSC	Short-term haematopoietic stem cell
T-ALL	T-cell acute lymphoblastic leukaemia
TBI	Total body irradiation
TCR	T Cell receptor
TG	Terapia génica
TPO	Thrombopoietin
VCAM1	Vascular cell adhesion molecule 1
VCN	Vector copy number
VL	Vector lentiviral
VLA-4	Very late antigen-4
VSV-G	Glycoprotein of the vesicular stomatitis virus
WAS	Wiskott-Aldrich syndrome
wPRE	Post-transcriptional regulatory element of the Woodchuck hepatitis B virus
wPRE*	Mutated wPRE
X-SCID	X-linked SCID
γRV	γ-retroviral vector
ΔhCD4	Truncated human CD4

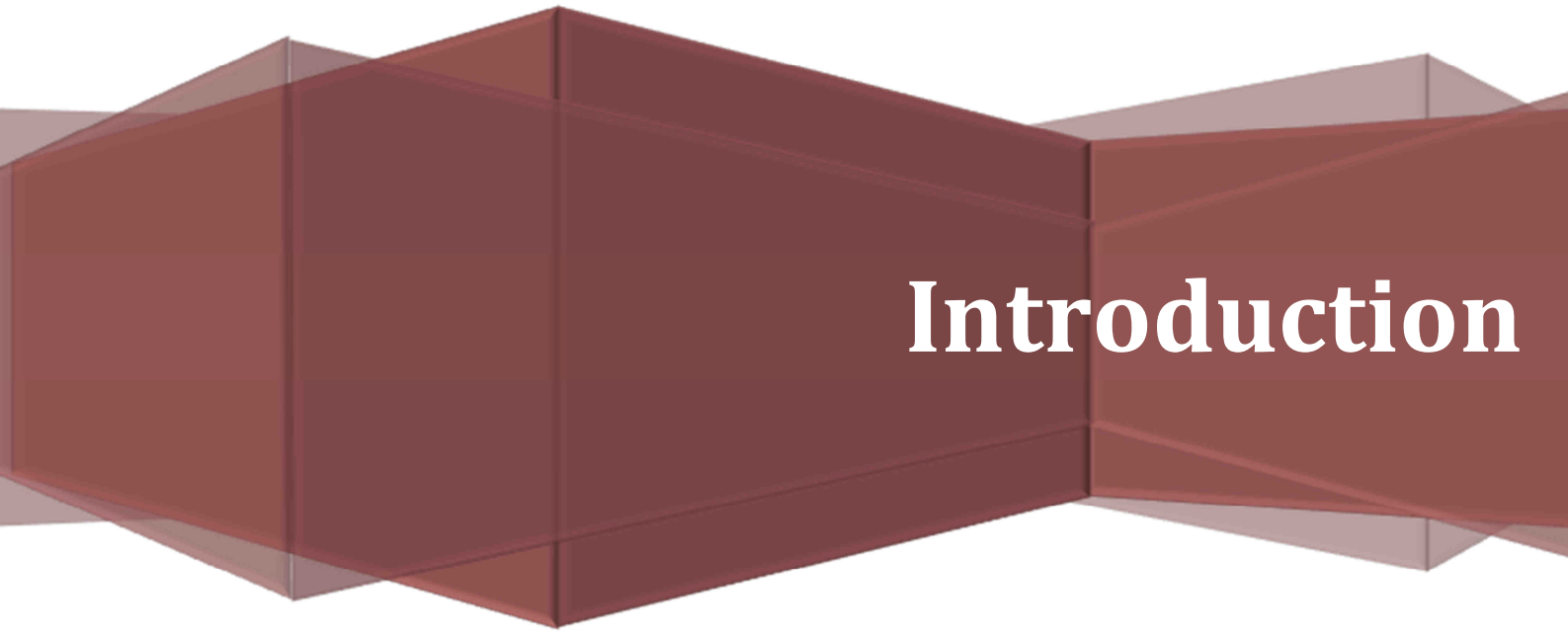

Introduction

1. Haematopoietic system

The haematopoietic system is responsible for the production, maturation and recycling of the cellular components of blood. The organs and tissues of the haematopoietic system include blood, bone marrow (BM), liver, spleen, thymus, lymph nodes and accessory lymphoid tissues.

Blood cells belong to two main lineages: lymphoid and myeloid. The lymphoid lineage consists of T, B, and natural killer (NK) cells, which perform adaptive and innate immune responses. The myeloid lineage includes very different cell types including granulocytes (neutrophils, eosinophils, mast cells, and basophils), monocytes, erythrocytes, and megakaryocytes/platelets; which play many different roles including innate immune response, oxygen transport and haemostasis.

Blood is one of the most highly regenerative tissues, with around one trillion mature cells being produced daily in adult human BM. Location of haematopoiesis changes throughout development, from the aorta-gonad-mesonephros[1] to foetal liver, spleen and finally to BM[2,3]. Haematopoiesis is mainly supported by the BM in healthy human adults, while spleen significantly contributes to the haematopoiesis in mice[4,5].

1.1. Organization of the haematopoiesis

Haematopoiesis follows a hierarchical organization as can be observed in Figure 1, where a small number of very primitive cells are able to generate a huge number of different mature cells.

The haematopoietic stem cells (HSCs) are the most primitive cells in the haematopoietic system and support all the haematopoiesis. As stem cells, they are characterized by their ability to generate different cell types (multipotency) and by their capability to self-renew.

The haematopoietic committed progenitors arise from the HSCs, but they have different properties: They have a higher proliferation activity than HSCs at the expense of having a reduced ability of self-renewal, and they are committed to produce a limited number of cell types.

Finally, cells with a recognizable morphology, either cells in maturation or mature and functional cells, complete the pyramid. These cells present a low or null capacity of proliferation and self-renewal, but carry out a variety of functions including immune defence, nutrient transport and blood clotting among others.

Haematopoiesis has to be tightly regulated since the requirements of the production of each cell type could change. This regulation is dependent on exogenous factors (endocrine and paracrine soluble mediators), cell-cell interactions with different components of the haematopoietic niche and neuroendocrine factors released by the nerve endings innervating the BM. On the other hand, there is an important regulation dependent on intrinsic factors of the HSCs like the greater or lesser expression of different transcription factors or epigenetic modifications[6].

1.2. Haematopoietic stem cells in mice

Mouse haematopoietic progenitors are defined as a heterogeneous population with short and long-term repopulation ability that do not express typical lineage markers expressed by blood cells so they are often defined as lineage negative (lin^-) cells. The Lin^- cell fraction contains a population of cells expressing Sca1 and c-kit markers known as LSK (Lin^-, $Sca1^+$ and $c\text{-}Kit^+$) cells corresponding to the true mouse HSCs. The LSK population represents a very low percentage of the BM cellularity, and only 100 LSK cells are sufficient to repopulate all the lineages of a mouse in the long term[4,7]. Additional markers can be used to define 3 different subpopulations of LSK cells[8]:

- Haematopoietic stem cells with the ability of self-renewal in the long-term (LT-HSC; LSK/Flk2$^-$/CD34$^-$/CD150$^+$)
- Haematopoietic stem cells with the ability of self-renewal in the short-term (ST-HSC; LSK/Flk2$^-$/CD34$^+$/CD150$^-$)
- Multipotent progenitors (MPP; LSK/IL7Rα^-/ Flk2$^+$), which no longer possess self-renewal ability yet keeping full-lineage differentiation potential.

1.3. Haematopoietic stem cells in humans

Xenotransplant models, where human cells are transplanted into immunodeficient mice, are typically used to define human HSCs. Human cells with the capacity to reconstitute a multilineage haematopoiesis in SCID mice are called SCID repopulating cells (SRCs)[9,10]. The CD34 marker was defined as a very important indicator of these SRCs[11,12]. Subsequent studies have identified other populations with higher SRC capacity, CD34$^+$CD38$^-$ and lin$^-$CD34$^+$CD38$^-$ cells[13], the latter being the more primitive among all of them. A more in-depth study identified two populations of cells with SRC capacity: cells with capacity to repopulate in the short term (short term SRCs) or in the long term (long term SRCs)[14].

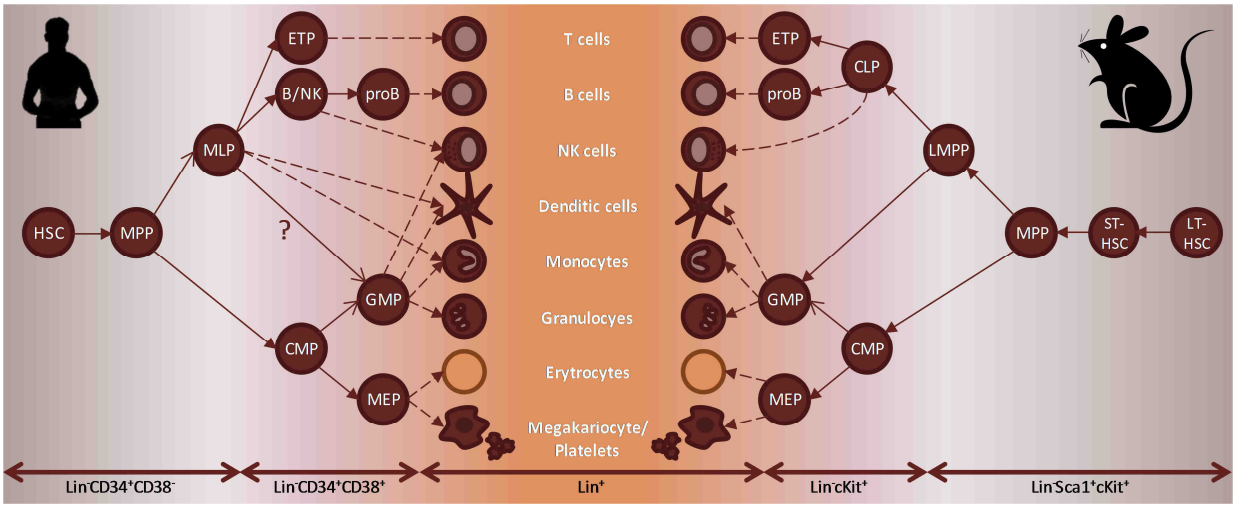

Figure 1. Current models of the haematopoietic system and lineage determination in the adult mouse and human. Modified from Doulatov et al[15].

1.4. Haematopoietic stem cells niche

The BM microenvironment appears to be uniquely adapted to support key properties of HSCs like multipotency, self-renewal and quiescence. The hypothesis of the HSC niche was first proposed by Schofield[16] and suggested that specialized niche cells in the BM are physically associated with HSCs and provide specific signals that help to maintain their function. Cell components of this HSC niche can be from haematopoietic and non-haematopoietic origin. A general model for the murine HSC niche (Figure 2) has been recently established supporting a perivascular location for most HSCs, with a preference for the endosteal region. Key components of the perivascular niche comprise endothelial cells, mesenchymal stromal cells and C-X-C motif Ligand 12 (CXCL12) expressing stromal cells, including CXCL12-abundant reticular (CAR) cells, leptin receptor$^+$ cells and nestin-GFP$^+$ cells[17]. All these cells provide signals, including CXCL12, Stem Cell Factor (SCF), and angiopoietin, that maintain the HSC function.

Monocytes/macrophages in the BM provide signals that support CXCL12 production from BM stromal cells and possibly act directly upon HSCs. Recently it has been described that circadian rhythms of neutrophil release from and migration back to the BM are able to modulate HSC niche. PB aged neutrophils (Ly6G$^+$/CD62$^-$/CXCR4^{Low}) migrate back to the BM where they are engulfed by BM-resident

macrophages. This process finally results in a reduction of the number of CAR cells and in the levels of CXCL12[18].

All these cellular components can also be regulated by physiological stimuli, such as sympathetic innervation, circadian rhythms and hormonal signals[19].

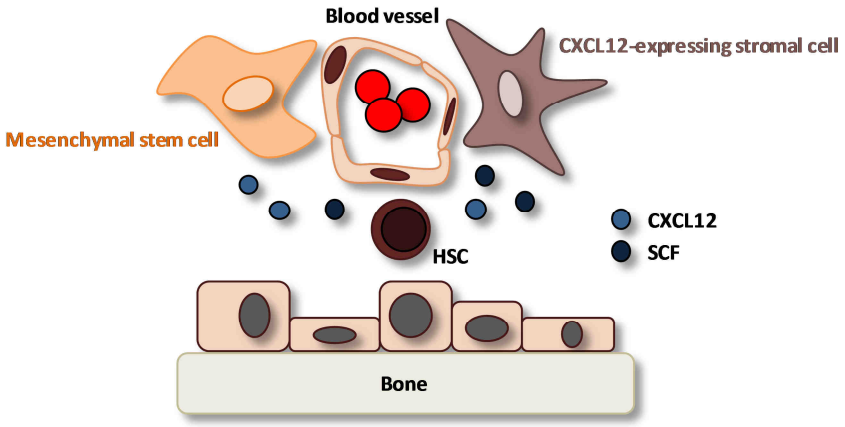

Figure 2. General Model for the mouse HSCs niche. Modified from Anthony et al[17].

2. Leukocyte adhesion cascade

Leukocytes or white blood cells are the cells of the immune system involved in defending the body against both infectious diseases and foreign materials. Leukocytes are classified into different groups according to morphological characteristics: granulocytes or polimorphonuclear leukocytes (including neutrophils, basophils and eosinophils) and agranulocytes or mononuclear leukocytes (including lymphocytes and monocytes). Leukocytes normally circulate in the blood but carry out most of their immune functions in tissues. Thus, leukocytes have to extravasate from circulation towards the site of tissue damage or infection in a multistep process known as leukocyte adhesion cascade (LAC) that is very similar for the different leukocyte subpopulations. In an inflammatory setting, recruitment of leukocytes occurs mainly in postcapillary venules beneath low haemodynamic shear forces. LAC implicates a large variety of cell-cell and cell-extracellular matrix (ECM) interactions. These interactions are mediated by a group of proteins known as adhesion molecules and their specific ligands. Integrins are some of these important adhesion molecules.

2.1. Integrins

Integrins are heterodimeric adhesion molecules that mediate cell-cell and cell-ECM interactions and also induce bidirectional signalling across the cell membrane. They are involved in important processes like immunity, wound healing and haemostasis and are able to regulate cell proliferation, activation, migration and homeostasis[20,21].

2.1.1. Structure

Twenty four different integrins can be found in humans and mice. They are formed by specific non-covalent associations of eighteen different α subunits and eight different β subunits (Figure 3). Both α and β subunits have a large extracellular region, a transmembrane domain and a short cytoplasmic tail. Nine of the eighteen α subunits contain an inserted or I domain with a Rossmann nucleotide-binding fold[22]. It is also known as αA domain because of its homology with the A domain of von Willebrand factor[23]. β subunits also contain an I-like domain (also known as βA domain) and their cytoplasmic tails share sequence homology (except for β_4 and β_8 subunits) including two very preserved NxxY/F motifs (where x could be any other amino-acid).

Integrins contain many different ion-binding sites because adhesion processes are dependent on bivalent cations. A metal-ion-dependent adhesion site (MIDAS) can be found in α subunits and it is the primary ligand-binding site in those integrins that contain an αA domain. Three different sites for ion-binding sites can be found in the βA domain of the β subunits. A pocket formed by these sites and the β-propeller of α subunits represents the major ligand-binding site in those integrins lacking the αA domain.

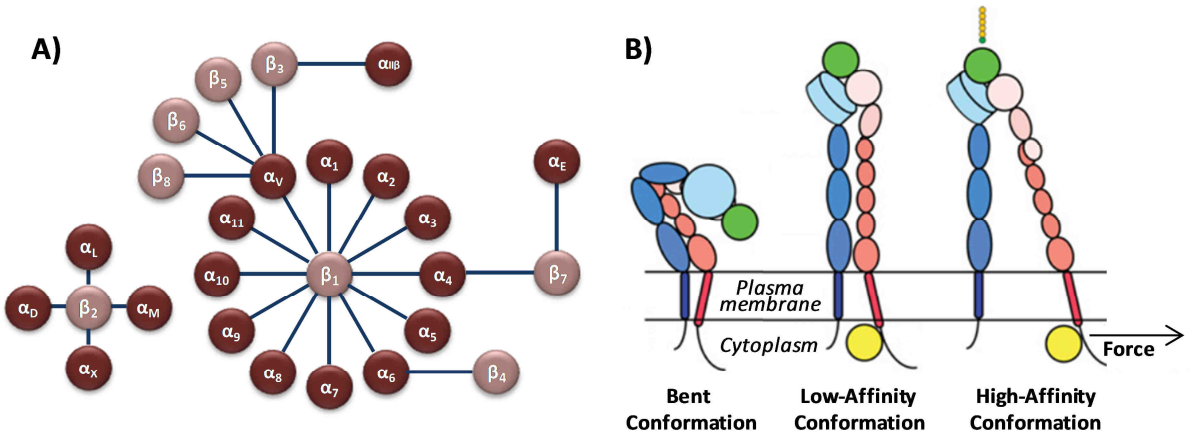

Figure 3. Integrins as a model of adhesion molecules. A) Combinatory scheme of human and mouse integrins. β subunits appear as dark blue circles and α subunits are represented as light blue circles. The lines represent the heterodimerization of an α and a β subunit to form an integrin. B) Conformational changes during integrin activation. Modified from Tan[24].

2.1.2. Signalling and conformational changes

Integrins transmit signals bidirectionally. They are able to respond to both intracellular and extracellular stimuli with conformational changes in their structure. Intracellular signals start the inside-out signalling leading to the activation of the integrins. When integrins are activated, they are able to recognize and bind their ligands. Ligand binding induce structural changes or clustering of integrins initiating different intracellular signalling cascades (outside-in signalling). This way cells are capable to sense the extracellular environment and react correspondingly[25].

A general model of the integrins activation is described in Figure 3 (Panel B). In their basal state, the extracellular region of the integrins adopts a bent conformation while cytoplasmic tails and transmembrane domains are strongly attached. The joining of a cytosolic activator results in the disruption of that attachment, allowing the extension of the extracellular regions. In this extended conformation, the headpiece is still closed and shows intermediate-affinity for the specific ligand. Tensile forces exerted by the cytoskeleton on the intracellular domain produce conformational changes along the entire length of the integrin thus integrins adopt the high-affinity ligand-binding conformation[24].

2.1.3. β_2 integrins

The β_2 integrins are those formed by the β_2 subunit and different I domain-containing α subunits. Its expression is restricted to the haematopoietic system. This integrin subfamily includes four members, with different patterns of expression and functions (Table 1)

All types of leukocytes express lymphocyte function-associated antigen 1 (LFA-1) on their surface. Six ligands have been described for integrin LFA-1, all belonging to the immunoglobulin superfamily. LFA-1 has been shown to bind its ligands through a conserved glutamate residue with different affinity for each one depending on the presence of different numbers of hydrophilic residues surrounding the acidic glutamate residue[24]. LFA-1 is mainly involved in the LAC, where its activation and

transition to the high affinity state allow its binding to intercellular adhesion molecule (ICAM) ligands and thus, the leukocyte firm adhesion to the endothelium. Transendothelial migration is also dependent on the interactions between LFA1 and endothelial ICAM-1 and junctional adhesion molecule 1 (JAM-1). LFA-1 is also involved in immune synapse formation between T cells and antigen-presenting cells (APCs). It is essential for maintaining a sustained contact between *naïve* T cells and APCs and for lowering the threshold of T cell activation by inducing a high level phosphorylation of ERK1/2 and IL-2 production in naïve T cells. Additional functions of LFA-1 include the mediation of cytolitic functions of cytotoxic T cells and NK cells.

Macrophage-1 antigen (Mac-1) binds a variety of ligands that do not share canonical binding sequences. This may be attributed to ligand-binding sites other than its αA domain[24]. It is mainly expressed in the myeloid lineage, where it mediates a range of functions like phagocytosis, degradation and remodelling of the ECM. Neutrophils use LFA-1 to attach to the vasculature and Mac-1 to crawl to an endothelial junction thus eventually leading to migration[26]. Mac-1-mediated outside-in signalling regulate neutrophil survival and apoptosis. Finally, Mac-1 has been implicated in immune tolerance in macrophages, dendritic cells and NK cells.

Integrin p150,95 shares many ligands with Mac-1. It is expressed in myeloid cells, dendritic cells, NK cells and populations of activated T and B cells. The differential expression of p150,95 serves as a marker to distinguish mature from immature dendritic cells. It also mediates phagocytosis of inactive complement component 3b (iC3b)-opsonized particles and it is involved in the adhesion of monocytes to endothelial cells.

Integrin $\alpha_D\beta_2$ is expressed at a basal level on the surface of most leukocytes and it is upregulated on phagocytic leukocytes present in regions of local inflammation. Although its specific role on leukocyte function remains unknown, $\alpha_D\beta_2$ has been implicated in eosinophil, neutrophil, and macrophage activation, lung inflammation, T cell proliferation and leukocyte infiltration into inflamed tissues[27,28].

Integrin	β subunit	α subunit	Ligands	Expression Pattern
LFA-1	β_2-CD18 (*ITGB2* gene)	αL-CD11a (*ITGAL* gene)	ICAM1-5, JAM-1, Type I collagen	T cell, B cell, monocyte/macrophages, NK cell, dendritic cell, neutrophil, eosinophil
Mac-1 (CR3)		αM-CD11b (*ITGAM* gene)	ICAM1, ICAM2, ICAM4, iC3b, fibrinogen, factor X, heparin, laminin, LPS, zymosan, oligodexosynucleotide, collagen, ellastase	Monocyte/macrophages, NK cell, neutrophil, eosinophil
p150.95 (CR4)		αX-CD11c (*ITGAX* gene)	C3bi, fibrinogen, collagen, CD23, heparin, LPS	Monocyte/macrophage, neutrophil, NK cell, dendritic cell
$\alpha_D\beta_2$		αD-CD11d (*ITGAD* gene)	ICAM3, VCAM1	Monocytes/macrophages, eosinophils, neutrophils

Table 1. The β2 subfamily of integrins: names, location and ligands. LFA-1 (Lymphocyte function-associated antigen 1), Mac-1 (Macrophage-1 antigen), CR (Complement receptor), ICAM (Intercellular adhesion molecule), JAM-1 (Junctional adhesion molecule 1), C3bi (Inactive complement component 3b), VCAM1 (Vascular cell adhesion molecule 1). Modified from Tan[29].

2.2. Phases of leukocyte adhesion cascade

The LAC (Figure 4) starts with the capture and rolling of free flowing leukocytes on the endothelium, which is mediated by the interaction between selectins and their glycosylated ligands. This initial contact slows down the velocity of the leukocytes and exposes them to signals coming from the inflamed endothelium, finally resulting in full integrins activation and firm adhesion to their ligands expressed by endothelial cells. This is followed by post -arrest modifications of leukocytes including reorganization of their cytoskeleton, cell spreading and intraluminal crawling. These modifications are

important for finding the optimal spot to pass through the endothelial lining either via the paracellular (between cells) or, more rarely, via the transcellular route (through cells).

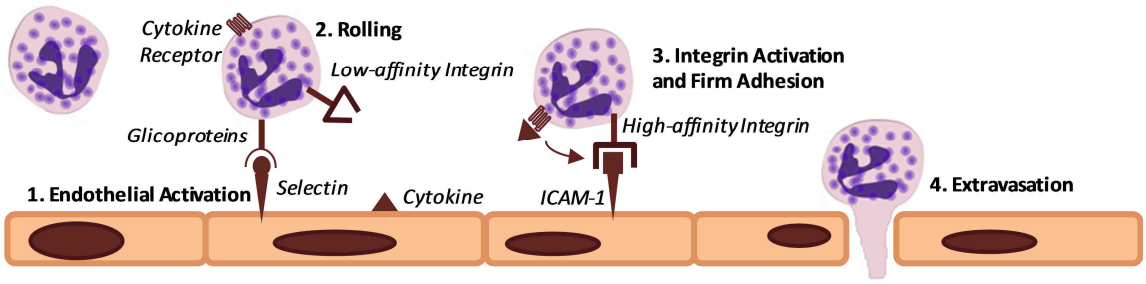

Figure 4. Phases of the leukocyte adhesion cascade (LAC).

2.2.1. Rolling

Leukocyte initial capture and rolling on the endothelium are mediated by the interaction between selectins and their glycosylated ligands. During this initial contact between endothelium and leukocytes, there is a continuous binding and release between selectins and their counter ligands[30,31]. Three members of the selectin family have been reported with different locations and functions. P-selectin is stored in Webel-Palade bodies of endothelial cells and is exposed in the membrane when these granules fuse to the cell membrane after cell activation by different stimuli. E-Selectin is constitutively expressed in skin microvessels. However, its expression can be rapidly induced by inflammatory cytokines such as TNFα and IL1b on endothelial cells. Basal levels of L-Selectin are expressed in most leukocytes. While E- and P-Selectin expressed by endothelial cells are considered as the most important rolling molecules, L-selectin is important for the lymphocyte homing to secondary lymphatic tissues[30].

Selectins are members of the C-type lectin family. As other members of this family, they are able to bind specific carbohydrate ligands. The minimal glycan determinant for selectin binding is Sialyl Lewis X, which can be found in different cell surface glycolipids and glycoproteins[32]. The best characterized ligand for selectins is P-selectin glycoprotein ligand-1 (PSGL-1), which is a mucin-type glycoprotein that can bind to all three selectins in an inflammatory environment. While P-Selectin interacts mainly with PSGL-1, E-Selectin has been shown to additionally use E-Selectin Ligand 1 (ESL-1) and CD44 as ligands. Selectin binding to PSGL-1 is critical for tethering and rolling of leukocytes on endothelial cells. In the case of E-Selectin, binding to PSGL-1 mediates initial leukocyte capturing while binding to ESL-1 and CD44 facilitates the characteristic E-selectin-mediated slow rolling of leukocytes[30,31]. L-selectin directs the migration of naive and central memory T cells to lymph nodes through recognition of glycoproteins expressed on the luminal surface of high endothelial venules[32].

Besides mediating leukocyte firm adhesion, α_4 integrins such as $\alpha_4\beta_1$ (Very late antigen-4, VLA4) and $\alpha_4\beta_7$ can mediate selectin-independent rolling. Although the role of LFA-1 and Mac-1 to mediate selectin-independent rolling is controversial, LFA-1 in its intermediate affinity conformation has been shown to be able to slow down the velocity of leukocytes rolling on selectins[30].

2.2.2. Integrin activation and firm adhesion

Integrins need to achieve a high-affinity ligand-binding state to mediate the leukocyte arrest and firm adhesion to the inflamed endothelium. During the rolling on the inflamed endothelium, chemokines, chemoattractants and selectin-initiated signaling pathways participates in fully integrin activation. The most relevant integrins for this process belong to the β_1 and β_2 integrin subfamilies, and, among them, the most studied are VLA-4 and LFA-1. These leukocyte integrins bind to immunoglobulin superfamily members such as vascular cell adhesion molecule 1 (VCAM-1) and ICAM-1, both expressed

by Inflammation-activated endothelial cells[31]

Integrin activation (Figure 5) is initiated when chemokines bind to their counterpart G-protein-coupled receptors leading to phospholipase C (PLC) activation and results in the cleavage of phosphatidylinositol 4,5-bisphosphate into inositol triphosphate (IP3) and diacylglycerol (DAG). IP3 is a soluble mediator able to initiate intracellular Ca^{2+} release. Both Ca^{2+} and DAG are able to activate guanine-nucleotide-exchange factors (GEFs) which activate the small GTPase Ras-related protein 1 (Rap1). Activated Rap1 forms a complex with Rap1 GTP-interacting adaptor molecule (RIAM1). RIAM1 acts as a scaffold to connect the membrane targeting sequences in Rap1 to talin, thereby recruiting talin to the plasma membrane[33]. Talin is a large cytoskeletal protein that binds to the membrane proximal NxxY/F moiety in the β tail and disrupts the interaction between the α and the β chains. Thus, talins initiate conformational changes leading to integrin activation. Kindlins are proteins able to bind the membrane distal NxxY/F motif of the β tails and have been proposed to modulate talin-mediated activation although the mechanism is still not completely understood[34].

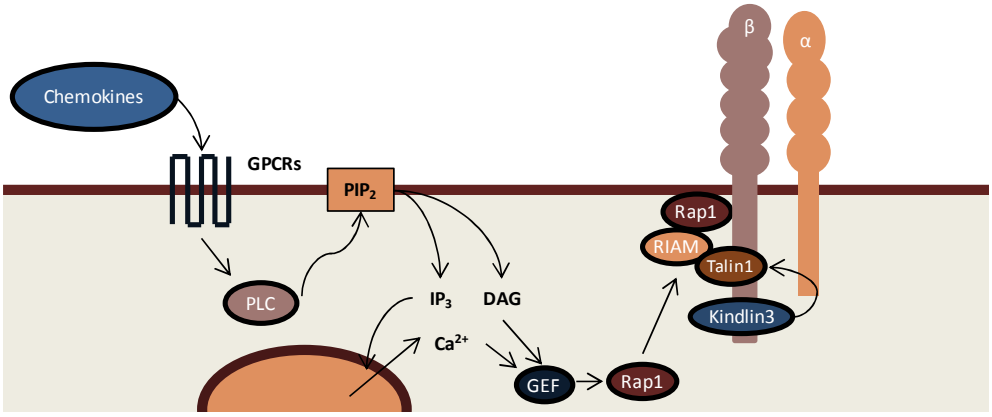

Figure 5. General mechanism for β_2 integrin activation.

2.2.3. Crawling and transendothelial migration

Adherent leukocytes crawl to nearby endothelial borders seeking for preferred sites of transmigration. Neutrophils and Monocytes intraluminal crawling is mediated by Mac-1 and ICAM-1 interactions[35]. Transendothelial migration, also known as diapedesis, is the point of no return in the LAC. Leukocytes cross the endothelium at the cell borders (paracellular route) or directly through endothelial cells (transcellular route). In addition to the heterophilic interactions mediated by β_1 and β_2 integrins and their ligands (ICAMs, VCAM-1 and JAMs), diapedesis requires homophilic adhesion of one leukocyte molecule interacting with the same molecule expressed by the endothelial cell. Among these molecules, platelet endothelial cell adhesion molecule (PECAM-1) and CD99 seem to be the most important[36].

3. Leukocyte adhesion deficiencies

Defects in the LAC lead to a number of primary immunodeficiencies (PID) known as leukocyte adhesion deficiencies (LAD). In LAD patients, leukocytes are unable to extravasate from blood to the infection sites. They are classified as defects in the myeloid function as neutrophils and monocytes are the most affected cells[37]. Three different types of LAD have been described according to which phase of the cascade is impaired. Table 2 summarizes the characteristics of each disease.

3.1. LAD-I

LAD-I is an autosomal recessive PID caused by the deficient cell surface expression of β_2 integrins. As a consequence neutrophils fail to firmly adhere to the inflamed endothelium. The

molecular basis underlying LAD-I are mutations in the *ITGB2* gene located at 21q22.3 (OMIM*600065) that encodes the β_2 common integrin subunit (CD18). More than 80 different mutations have been described in the *ITGB2* gene in LAD-I patients[38] including deletions, insertions, nonsense, splice site and missense mutations. Most of these mutations lead to null or reduced expression of β_2 integrins in the leukocyte surface, although in some cases they can lead to an aberrant and non-functional CD18 protein expressed at normal levels[39]. Although there is no hotspot for *ITGB2* mutations, most of the point mutations take place within the 5 and 9 introns, which encode for the βA domain[38]. βA domain seems to be implicated in the association and successful biosynthesis of integrins before been transported to the membrane[40].

		LAD-I	LAD-II	LAD-III
Aetiology	Gene	*ITGB2*	*SLC35C1*	*FERMT3*
	Protein	CD18	SLC35C1	KINDLIN-3
	Phase of LAC	Firm Adhesion	Rolling	Integrin Activation
Clinical Manifestations	Recurrent Severe Infections	+++	+	+++
	Skin Infection	++	+	++
	Delayed separation of the Umbilical cord	+++	-	+++
	Periodontitis	++	++	?
	Developmental abnormalities	-	+++	-/?
	Bleeding tendency	-	-	+++

Table 2. Principal Characteristics of the three Leukocyte adhesion deficiency syndromes. Modified from Eztioni[40].

Neutrophil adhesion defects are the functional abnormality responsible for the clinical picture in LAD-I patients, although β_2 integrins are deficient in all of their leukocytes[41]. This is likely because neutrophils are mainly dependent on the CD18 integrin expression for firm adhesion, while lymphocytes have redundant adhesion cascades[42]. CD18-deficient lymphocytes show decreased *in vitro* blastogenesis and proliferation. However, the clinical significance of these findings remains to be determined as LAD-I patients have no increased susceptibility to viral infections[43].

The severity of LAD-I is strictly related to the degree of CD18 deficiency[40]. Thus, two different phenotypes of LAD-I have been described according to the clinical manifestations and the levels of CD18 expression[44]:

- Severe Phenotype, when levels of CD18 expression are <2% of the normal levels.
- Moderate Phenotype, when levels of CD18 expression are 2-30% of the normal levels.

LAD-I patients suffer from recurrent and life-threatening infections in the skin, mucosa surface and digestive and respiratory tracts, that are usually indolent and necrotic and tend to lead to secondary bacteraemia. These infections appear in the childhood, when omphalitis and delayed umbilical cord separation are also very characteristic. Absence of pus formation is considered as a pathognomonic symptom[45,46]. *Staphylococcusaureus, Pseudomonas spp.* and gram-negative enterobacteria are the microorganisms leading to most of the infections, although mycoses caused by *Candida albicans* are also frequent[47,48]. Those patients surviving till the adulthood normally develop severe gingivitis and periodontitis[49]. Impaired healing of traumatic or surgical wounds is also very characteristic of LAD-I. These patients show moderate neutrophilia in the absence of apparent infections. As a consequence of acute infections, circulating granulocytes could reach levels of 10^5 / µL of blood[45,46]. Similar infections take place in patients with the moderate phenotype, although they are less frequent and severe[39].

3.1.1. Prevalence

LAD-I is considered as a rare disease due to the limited number of patients that have been

diagnosed all over the world. There are no available data of prevalence for LAD-I. The following table (Table 3) summarizes the number of LAD-I patients that have been reported in the literature in different geographic areas. As other PIDs, LAD-I seems to be more prevalent in Africa and Middle East because of the high rate of consanguinity, which reach more than 50% in some places[50,51].

Area	Organism	Patients	Observations
USA	Medscape	<400	75% with severe phenotype
Europe[52]	Orphanet	<350	
South-America[53]	Latin American Group for PID	7	All patients were diagnosed in Argentina
Iran[54]	Iranian PID Registry	37	
North-Africa[55]		33	Patients were diagnosed for LAD, but not for which type of LAD
India[56]		13	These patients were diagnosed in the same centre

Table 3. Reported cases of LAD-I in different geographic areas.

3.1.2. Diagnosis

According to the current diagnostic criteria of the European Society for Immunodeficiencies, LAD-I should be suspected in those children with soft-tissues recurrent infections and increased white blood cell count, even more if there is delayed umbilical cord separation. LAD-I diagnosis has to be confirmed by the analysis of CD18 and CD11 subunits expression by flow cytometry, although definitive criteria is the determination of CD18 mRNA levels or the identification of *ITGB2* mutations. Functional adhesion experiments are not necessary for the diagnosis and they are only performed for research[57]. Leukocytes express CD18 in their surface since week 20 of gestation allowing an early prenatal diagnosis in those families with a known history of LAD-I[40]. A procedure for preimplantation genetic diagnosis in human embryos generated by *in vitro* fertilization has been also developed [58].

3.1.3. Treatment

3.1.3.1. Symptomatic treatment

Those patients with the moderate form of LAD-I normally respond to conservative therapy based on the immediate use of antibiotics during acute infectious episodes and surgical debridement of wounds. Prophylactic antibacterial and/or antifungal may be used to reduce the risk of infections[40,59]. Although granulocyte transfusions may be useful to treat infections otherwise unresponsive to antibiotherapy[60], their use is limited because of difficulties in supply of daily donors and immune reactions to the allogeneic leukocytes[40].

3.1.3.2. Haematopoietic stem cell transplantation

Allogeneic haematopoietic stem cell transplantation (HSCT) is the only curative treatment for LAD-I and should be considered early in the course of the disease in patients with severe LAD-I phenotype[59]. Four large retrospective or prospective studies have been reported so far regarding HSCT for LAD-I patients (Table 4).

Time Period	Number of centres	Number of Patients	Overall Survival	Reference
1981-1993	2	14	71%	Thomas et al[61]
1993-2007	14	36	75%	Qasim et al[62]
1991-2008	1	11	91%	Al Dhekri et al[51]
2007-2009	1	10	80%	Hamidieh et al[63]

Table 4. HSCT in LAD-I patients.

From the published studies, a survival rate from 71 to 91 % can be achieved with HSCT in LAD-I patients. HLA-matched donors, both related or not, appear to be more suitable candidates for HSCT in LAD-I patients than haploidentical or mismatched related donors. The use of umbilical cord blood-derived HSC from mismatched unrelated donors has been lately introduced but appears as a very

promising alternative for those patients without a suitable donor. Full donor chimerism is not required, as mixed chimerism seems to be sufficient to maintain patients free of disease. This is in concordance with results from HSCT in Canine Leukocyte Adhesion (CLAD) affected dogs, where a reduced number of $CD18^+$ neutrophils is enough to correct the phenotype[64-66].

3.1.4. Somatic mosaicism

Five cases of somatic mosaicism have been detected in LAD-I patients[67-69]. All these patients presented a small subpopulation of $CD8^+$ T cells expressing normal levels of CD18. These cells presented revertant mutations leading to the WT sequence or to new functional CD18 variants. It remains unclear whether this revertant T cell population arises as a consequence of the survival of the patients into adulthood or, otherwise, it plays an active role in patient long-term survival. Furthermore, no reversions in progenitor or myeloid cells were observed suggesting that CD18 revertant mutations do not confer proliferative advantage outside the T-cell lineage. This phenomenon could be related to the role of LFA-1 as a costimulatory molecule during T-Cell Receptor (TCR)-mediated T cell activation[70]. Interestingly, it is very common the incidence of inflammatory bowel disease in this LAD-I mosaic patients[69].

3.1.5. LAD-I animal models

3.1.5.1. Canine leukocyte adhesion deficiency

CLAD is a lethal immunodeficiency typical of Irish (white and red) setter dogs. Symptoms appear from the early beginning, with omphalitis, following with severe and frequent bacterial infections accompanied by fever[41,71]. Afterwards, clinic progression is very homogenous with leukocytosis, severe gingivitis, lymphadenopathy, wound-healing delay and infectious episodes with pyrexia and cachexia. Skin lesions are also frequent in CLAD-affected dogs[41].

CLAD was first described in a dog with a clinical picture very similar to the one of LAD-I patients[72]. Flow cytometry analyses revealed an absent expression of CD18 and CD11b leukocyte integrins in the neutrophil surface[73]. Functional studies disclosed severe defects in adhesion-dependent functions of affected granulocytes. A mutation in the *ITGB2* gene was lately discovered as the cause of CLAD[74]. All the studied dogs were homozygous for a point mutation in the *ITGB2* gene (G107C) resulting in a substitution of a cysteine for a serine at position 36 (C36S) in the amino-terminal end of the CD18 protein. This cysteine is highly conserved among different species (human, dog, pig and mice) and its substitution for a serine likely leads to the disruption of a disulphide bridge and the alteration of the tertiary structure abrogating the correct dimerization of CD18 and CD11 subunits[41].

3.1.5.2. LAD-I mouse models

As mice with naturally occurring mutations in *Itgb2* have not been described, two transgenic models have been generated**.**

- **Hypomorphic CD18 mouse model** ($CD18^{HYP}$) was generated by homologous recombination of an integration-type gene targeting vector containing a neomycin resistance cassette[75]. The plasmid was linearized and electroporated into embryonic stem cells. Although the intention was to produce a null mutation, the presence of a cryptic promoter derived from the plasmid backbone finally resulted in an hypomorphic mutation, leading to a decreased but not absent expression of CD18, resembling the characteristics of the moderate LAD-I phenotype. Homozygous mutant mice presented mild leukocytosis, minimal to mild hyperplasia in spleen and BM, impaired inflammatory response assessed using a chemical peritonitis model (thioglycollate intraperitoneal injection) and delayed transplantation rejection of allografted neonatal hearts. These mice were originally generated in a mixed background

C57BL6/J and 129/Sv and then backcrossed for more than 10 generations to the C57BL/6J inbred strain.

- **Null CD18 mouse model** ($CD18^{KO}$) was generated by homologous recombination using the same gene targeting vector. However, the vector was used as a replacement-type vector in this case[76]. These animals display a phenotype very close to that observed in patients with the severe form of LAD-I: leukocytosis, spontaneous skin infections, impaired migration of neutrophils at infection sites and defective T cell function.

Previous studies have shown enrichment of LSK cells in the BM of $CD18^{KO}$ mice[77,78]. Similarly, when $CD18^{KO}$ foetal liver cells were used in competitive transplant assays against WT foetal liver cells, the proportion of $CD18^{KO}$ haematopoietic cells in recipient mice was always higher than expected[77,79]. Although these studies suggested a role of CD18 in HSC regulation, this need to be deeply studied.

3.1.5.3. Other models

Bovine Leukocyte Adhesion Deficiency (BLAD) is the bovine analogue of human LAD-I that affects Holstein-Friesian cattle worldwide[80]. It is an autosomal recessive congenital disease characterized by recurrent bacterial infections, persistent neutrophilia, delayed wound healing and retarded growth. BLAD is caused by a single point mutation A383G in the *ITGB2* gene, leading to the substitution of glycine for aspartic acid at 128 (D128G) in the CD18 protein. BLAD-affected calves have a severe deficiency in β_2 integrin expression on the leukocytes surface and aberrations in several adherence dependent functions of leukocytes[41].

4. *Ex vivo* haematopoietic stem cell gene therapy

Gene therapy (GT) and cell therapy are overlapping fields of biomedical research with the purpose of repairing the origin of genetic diseases or re-establishing the normal equilibrium in acquired diseases. GT is defined as the introduction of nucleic acids with the help of a vector into cells with the objective of modifying gene expression to prevent or reverse a specific disease. This new therapeutic approach can be carried out in three different ways: gene addition, gene correction/alteration and gene knockdown. On the other hand, cell therapy is based on the ability to isolate stem, progenitor or mature cells from a patient or a normal donor, expand them *ex vivo* and infuse them back into the patient to establish a short-lived or stable graft of the infused cells and their progeny.

In many diseases, gene and cell therapy have been used in combination to develop promising therapies. The best example of this combination is the GT through autologous transplantation of gene-modified HSCs. Thanks to the well-established knowledge and clinical application of HSCT, *ex vivo* gene transfer techniques have been applied to standard HSCT procedures and have reached rapid clinical translation. The key point of this combination of gene and cell therapy is that gene-modified autologous HSCs can be used for HSCT in the absence of a suitable donor for an allogeneic HSCT. Nowadays, autologous HSC GT represents an emerging therapeutic option for several monogenic diseases.

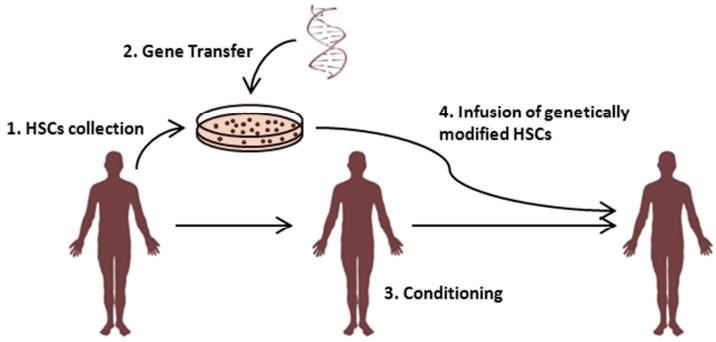

Figure 6. GT through autologous transplantation of gene-modified HSCs.

The biology of HSCs makes them amenable to be isolated *ex vivo,* genetically modified and transplanted by intravenous infusion. Prior to transplantation, patients could be conditioned or not. Once genetically modified HSCs have engrafted the recipient BM, they can produce new blood cells of all lineages for the whole life of the recipient, producing a long lasting effect (Figure 6). Autologous HSC GT has been successfully used in clinical trials since the Nineties (Table 5). Haematological disorders are the main indication, but not the unique, of this promising therapeutic approach, including PIDs such as SCID due to adenosine deaminase deficiency (ADA-SCID), X-linked SCID (X-SCID), chronic granulomatous disease (CGD) and Wiskott-Aldrich syndrome (WAS); erythroid diseases like β-thalassemia and HSC diseases like Fanconi anaemia. Storage disorders like metachromatic leukodystrophy (MLD) and adrenoleukodystrophy (ALD) can be also treated by autologous HSC GT because of the ability of haematopoietic cells to deliver the therapeutic enzyme to the nervous system.

	Target Cells	Treated Patients	Vector	SAE	Efficacy
***Haematological* disorders**					
ADA-SCID[81-83]	Lymphoid cells	40	γ-RV expressing *ADA*	None	Long-term cure comparable to HSCT
ADA-SCID[84]	Lymphoid cells		SIN LV expressing *ADA* from *EF1α* promoter	-	-
X- SCID[85,86]	Lymphoid cells	24	γ-RV expressing *IL2RG*	5 cases of T-ALL	Long-term cure comparable to HSCT
X- SCID[84,87]	Lymphoid cells	9	SIN γ-RV expressing *IL2RG* from *EF1α* promoter	-	Recovery of PB T cells that were functional and led to resolution of infections
CGD[88]	Myeloid cells	13	γ-RV expressing $gp91^{phox}$	3 cases of MDS / Transgene silencing	Transient or no clinical benefit. Long- term efficacy only in the 3 cases of clonal expansion
CGD (Personal Communication)	Myeloid cells	On Going	SIN LV expressing $gp91^{phox}$ from a myeloid promoter	-	-
WAS[89]	Multi-lineage	10	γ-RV expressing *WAS*	4 cases of T-ALL	Clear benefit at 2 year follow-up
WAS[90]	Multi-lineage	On Going	SIN LV expressing *WAS* from *WAS* promoter	-	Improvements in platelet counts, immune functions, and clinical scores
β-thalassemia[91]	Erythroid Cells	On Going	SIN LV; large LCR expressing *β-globin* and cHS4 insulator	Clonal Expansion	Transfusion independence
Fanconi anaemia[92,93]	Stem Cells		γ-RV expressing *FANCC* or *FANCA*	-	No clinical benefit
Fanconi anaemia[94-96]	Stem Cells	On Going	SIN LV expressing *FANC-A* from *PGK* promoter	-	-
Storage Disorders					
ALD[97]	Macrophages and microglia	On Going	SIN LV expressing *ABCD1* from *MND* promoter	-	Clear therapeutic benefit comparable to HSCT
MLD[98]	Macrophages and microglia	On Going	SIN LV expressing *ARSA* from *PGK* promoter	-	The disease did not manifest or progress beyond the predicted age of symptom onset

Table 5. *Ex vivo* HSC GT Clinical Trials. Serious adverse effect (SAE), T-cell acute lymphoblastic leukaemia (T-ALL), myelodysplastic syndrome (MDS), locus control region (LCR), phosphoglycerate kinase (*PGK*), aryl sulfatase A (ARSA), elongation factor 1α *(EF1α*), ATP-binding cassette sub-family D member 1 (*ABCD1*), interleukin 2 receptor, gamma chain (*IL2RG)*. Modified from Naldini[99] and Fischer et al[84].

4.1. Retrovirus

Viral vector-mediated gene transfer protocols have concentrated most of the efforts on developing clinical GT trials, taking advantage of the fact that viruses have naturally evolved to insert genetic information into target cells[100]. Concerning *ex vivo* HSC GT, retroviruses have been the most frequently used vectors. *Retroviridae* is a family of enveloped virus containing their genetic information in the form of RNA genome. The viral envelope is composed by the membrane of the host cell and glycoproteins encoded by the virus itself. Retroviruses are able to convert RNA into double-stranded DNA in a process known as retrotranscription. This DNA molecule is then integrated in the genome of the host cell allowing the replication of the virus. Retroviruses can be classified according to the complexity of their genome into two groups: simple and complex. Simple retroviruses contain only essential genetic information while complex ones also codify for additional regulatory proteins. A more detailed classification divides retroviruses into 7 genera (Table 6).

Genus	Subfamily	Representative species	Genome
Alpharetrovirus	*Orthoretrovirinae*	Avian sarcoma leukosis virus, Rous sarcoma virus	Simple
Betaretrovirus		Mouse mammary tumour virus	Simple
Deltaretrovirus		Bovine leukemia virus, human T-lymphotropic virus	Complex
Epsilonretrovirus		Walleye dermal sarcoma virus	Simple
Gammaretrovirus		Moloney murine leukemia virus (Mo-MLV), gibbon ape leukemia virus (GALV), Abelson murine leukemia virus, spleen focus-forming virus (SFFV)	Simple
Lentivirus		HumanImmunodeficiency virus 1 (HIV-1)	Complex
Spumavirus	*Spumaretrovirinae*	Human foamy virus	Complex

Table 6. Genera belonging to the *Retroviridae* family.

4.1.1. Retroviral genome and virion structure

Retroviral genome (Figure 7) consists of two single-stranded positive RNA molecules with an equivalent structure to an mRNA (contain a 5' cap and 3' polyA tail) that bind each other by hydrogen bonds to form a dimer. Retroviral genome has a variable size between 8 and 12 kb and contains at least three genes in an invariable order 5'-*gag-pol-env*-3'[101]:

- *Gag*, encoding capsid, matrix and nucleocapside proteins, which protect the viral genome.
- *Pol,* encoding the viral enzymes: RT, protease and integrase.
- *Env*, encoding the proteins of the viral envelope (surface and transmembrane proteins).

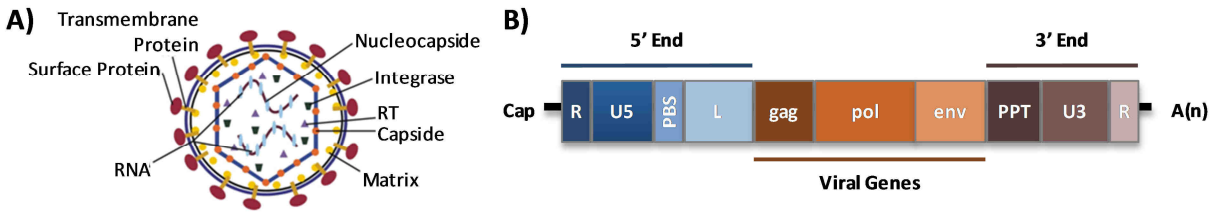

Figure 7. **A)** General structure of the retroviral virion. **B)** WT Retroviral RNA genome.

In addition to these major proteins, complex lentiviral genomes also codify for regulatory proteins such as *Tat,* which activates viral transcription, and *Rev*, involved in the control of splicing and nuclear export of viral transcripts[102]. Some of them also have accessory proteins such as *Vif, Vpr, Vpu and Nef*, whose combined action regulates viral gene expression, assembly and replication[103].

The retroviral RNA 5' end includes four regions, which are R, U5, primer binding site (PBS) and L.

- R is a short repeated sequence at each end of the genome used during the reverse transcription to ensure correct end-to-end transfer in the growing chain.
- U5 contains sequences important for polyadenylation and gives rise to the provirus 3' end

- PBS consists of 18 nucleotides complementary to 3' end of the specific tRNA primer, which and provides -OH group for initiation of reverse transcription.
- L is an untranslated region that contains the signal for packaging of the RNA genome (Ψ) and binding sites for transcription factors.

The 3' end includes 3 regions, which are PPT (polypurine tract), U3, and R.

- PPT is a short and purine-rich sequence used to initiate the plus-strand DNA synthesis during reverse transcription.
- U3 is a sequence between PPT and R and that give rise to the provirus 5' end contains promoter elements responsible for the transcription of the provirus. Att site is located in U3 and it is essential for the integration in the genome.

4.1.2. Retrovirus life cycle

A general scheme for the retrovirus life cycle can be found in Figure 8. The envelope proteins present in the viral membrane are able to bind receptor proteins in the membrane of the host cell (step 1). This step allows the viral membrane to fuse with the cell membrane (step 2) and proteins and RNA strands contained inside the virion can be released inside the cytoplasm (step 3). Within the cell, the retroviral RNA is reverse transcribed into double stranded DNA (step 4), which is transported to the nucleus (step 5) and integrated into the host cell genome with the help of the integrase (provirus, step 6). Proviral DNA is stable integrated so it can be replicated within the whole genome and transferred to the daughter cells. Proviral DNA is transcribed into RNA (step 7), which is spliced (step 8), transported to the cytoplasm (step 9) and used to synthesize the viral proteins (step 10). Full-length viral RNA and viral proteins are then assembled together (step 11) and a new viral particle escapes from the cell (step 12).

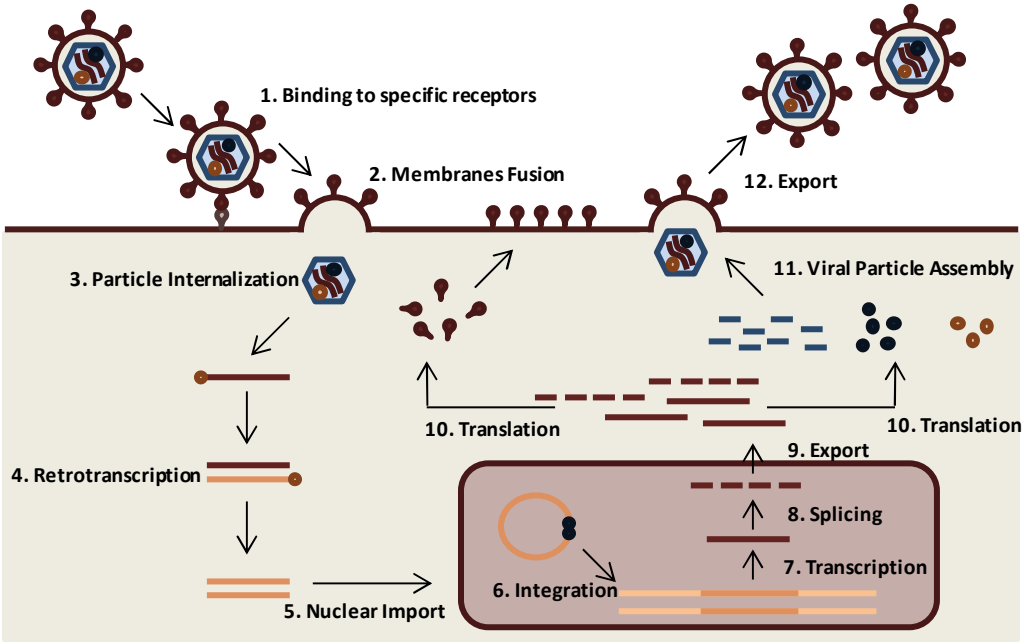

Figure 8. General Scheme of retrovirus life cycle.

As a consequence of the reverse transcription process, LTRs are generated on each end of the provirus. LTRs are sequences between 300 and 1800 nucleotides that are formed by U3-R-U5 regions and contain important transcriptional signals, including a cleavage/polyadenylation site in the R region and a promoter and enhancers in U3. Transcription is initiated at the U3-R boundary in the upstream LTR, and cleavage/polyadenylation takes place at the R-U5 boundary in the downstream LTR[101].

4.1.3. Lentiviral vectors

Lentiviral vectors (LVs) are lentiviruses that have been modified to be replication defective so once they are integrated, they cannot generate new replication-competent particles. That way, LVs are able to transduce the target cell and integrate an exogenous gene in its genome, but unable to propagate to other cells. These vectors are generated by the elimination of viral genes, which are replaced by a therapeutic transgene. Those viral genes that are essential are provided *in trans* during LV production.

Human immunodeficiency virus type 1 (HIV-1)-based LVs are currently commonly used in the HSC GT field. LVs have some characteristics that make them more suitable as vectors than classical γ-retroviral vectors (γRVs):

- Larger transgene capacity (up to 10 kb).
- Capability of transducing non-dividing cells.
- Safer integration profile.

Production of LVs is accomplished by the co-transfection in human embryonic kidney (HEK) 293T cells of a plasmid containing the modified lentiviral backbone, known as transfer plasmid, and other plasmids that supply *in trans* the elements that have been removed from the retroviral backbone and that are required for the production of the vectors (Figure 9)[104]. These plasmids are:

- Envelope plasmid: it contains the envelope protein. The properties of LVs can be modified supplying envelope proteins different from the WT one. This process is called pseudotyping. The most commonly used LV envelope is the G glycoprotein of the vesicular stomatitis virus (VSV-G) (Figure 9B), which allows the production of high-titer vectors[105]. Several studies have shown their ability to package LVs that are able to efficiently transduce different cellular types including HSCs from different species such as dog[106], mouse[107], non-human primates[108] and humans[109,110].
- Packaging plasmid: it contains the genes required for the viral cycle. Accessory viral genes (*vif*, *vpr*, *vpu* and *nef*) were removed as they are not required for the packaging of the vector[111] (second generation plasmids, Figure 9C). In third generation packaging plasmids, *tat* has been removed (as it was shown not to be required for the generation of functional vectors) and *gag-pol* and *rev* have been split into two plasmids[104].

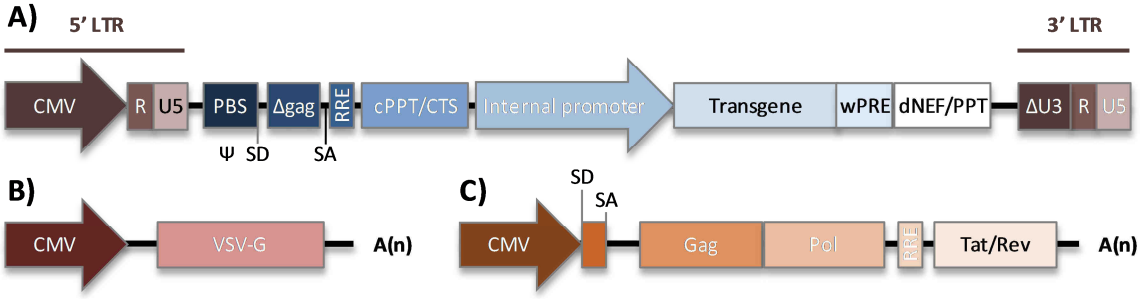

Figure 9. Split Packaging system for LV production. **A)** Transfer Plasmid **B)** Envelope Plasmid **C)** 2nd Generation Helper Plasmid.

- Transfer plasmid (Figure 9A): it encloses the therapeutical transgene and the lentiviral sequences that have to be supplied *in cis* to obtain a functional lentiviral particle (LTRs, PBS, Ψ signal, Δgag and att integration sites). Δgag is a non-coding residual element of *gag* gene giving rise to a secondary structure (SL4) that is required for the packaging[112]. The U3 region of the 5' LTR has been substituted for CMV or RSV promoters (among others) to enable an improved and TAT-independent RNA transcription[104]. None of these modifications are present in the transcribed RNA neither in the transduced cells.

Some additional modifications have been introduced to improve the safety of the lentiviral vectors. Among them, Self-inactivating (SIN) configuration is worthy of mention[113]. This modification implies a deletion of 400 bp within U3 region (including strong enhancer elements like CAAT and TATA boxes) making LTRs of the integrated provirus less likely to initiate any proto-oncogene activation (see section 1.4.2.).

SIN LVs require an internal promoter to drive the expression of the therapeutic transgene. The level of gene expression required for a specific application can be regulated by choosing a strong or a week promoter. Cellular and physiological promoters such as EF1α, PGK and VAV are weaker trans-activators as compared to viral promoters (such as CMV or SFFV)[114] so they are preferred when medium to low expression levels are required. Other promoters, such as inducible promoters, or lineage specific promoters (such as Cathepsin G/c-Fes Chimeric promoter[115]) can be incorporated in order to tightly regulate gene expression.

Some sequences have been incorporated into lentiviral backbones to increase both titers and gene expression:

- Post-transcriptional regulatory element of the woodchuck hepatitis B virus (wPRE): enhances the stability of viral RNA[116]. This sequence contains an open-reading frame (ORF) encoding a truncated peptide of the woodchuck hepatitis virus X protein, which has been related with hepatocarcinomas. For this reason, most of pre-clinical and clinical LVs include a version of the wPRE sequence where the ORF translation start codon was mutated (wPRE*)[117].
- The central polipurine tract (cPPT) facilitates the transport of the pre-integration complex to the nucleus[118,119].
- The central terminal sequence (CTS) is involved in the separation of reverse transcriptase[118].
- dNEF/PPT is essential for reverse transcription.
- The Rev responsive element (RRE) facilitates the transport of the viral RNA to the nucleus.

4.2. Safety of gene therapy

Genetic modification of HSCs using retroviral vectors has brought encouraging results in the correction of genetic diseases, but genotoxicity due to insertional oncogenesis is a risk that has to be taken in consideration. Several cases of haematological malignancies were described in the first γRV-based GT clinical trials. T-ALL cases described in SCID-X1 and WAS patients have been associated with LTR-mediated up-regulation of proto-oncogene, in most vases *LMO2*[120-122], while clonal dominance and MDSs described in γRV-treated CGD patients occurs by up-regulation of myeloproliferative genes like *MECOM, PRDM16 or SETBP1*[88]. Since then, research was focused on improving the safety of GT protocols through new vector designs and minimizing the *ex vivo* manipulation of HSCs.

Retroviral integration within or near a proto-oncogene could lead to its activation by different mechanisms. As mentioned before, the two LTRs contain strong enhancers and promoter elements in the U3 region, which can upregulate proto-oncogene transcription from its cellular promoter. Additionally, both LTRs could initiate the transcription originating a chimeric transcript encoding an N-terminally truncated form of the oncogene with constitutive activity and transforming potential. These LTR-dependent events are abrogated by the use of SIN RVs, where U3 regions are deleted from both LTRs during the transduction process and the vector expresses the therapeutic gene from an internal promoter. These internal promoters might also mediate upregulation of proto-oncogene transcription from its cellular promoter. However, the use of weak exogenous promoters results in lower proto-oncogene expression[99].

Retroviral vectors differ in their integration profile. γRVs show a strong preference for

integration close to transcription start sites and CpG islands while LVs prefer to integrate inside transcription units of actively transcribed genes that cluster in mega-base-wide chromosomal regions. On the other hand, vectors derived from foamy viruses and α-retroviruses show a largely random and uniform integration pattern[123].

Insertions of γRVs into gene regulatory elements make them more prone to induce insertional oncogenesis, while lentiviral integration pattern appears to be safer. However, lentiviral characteristic integration into transcribed genes can also deregulate gene expression on post transcriptional levels through the generation of chimeric transcripts. This phenomenon occurs when transcripts originated from upstream cellular promoters are spliced into provirus-derived RNAs through the use of constitutive and cryptic splice sites[124]. It has been recently described a clonal dominance in a LV-treated β-thalassemia patient as a consequence of a truncated HMGA2 transcript that escaped regulation by a miRNA directed at the 3' end of the full-length mRNA[91].

5. Alternative tools for genetic engineering: RNA interference

RNA interference is a mechanism of gene silencing produced by small non-coding RNAs, which include endogenous miRNA and exogenous siRNA or shRNA. This mechanism is deeply conserved during evolution and highly dependent on gene sequence. The process starts when a double-stranded small RNA is incorporated into the RNA induced silencing complex (RISC). The anti-sense strand guides RISC to the complementary or near-complementary region of the target mRNA leading to its cleavage (by the endonuclease Ago2) or to translation inhibition respectively[125].

miRNAs are non-coding RNAs encoded in the genome that help to regulate gene expression. They are expressed as a longer transcript, known as pri-miRNA which is processed in the nucleus to a stem-loop structure called a pre-miRNA by the microprocessor complex. Pre-miRNA is transported to the cytoplasm where it is cleaved by Dicer to produce a mature miRNA that can be incorporated into RISC [126]. A shRNA is a sequence of RNA emulating the pre-miRNA structure that can be used to stably silence target gene expression by its delivery through viral vectors[127]. This sequence is normally incorporated into a lentiviral backbone although, in some cases, a piggyback transposon has been used[128]. When the lentivirus is integrated into the genome, shRNA can be expressed by the internal promoter leading to the silencing of the desired gene (Figure 10).

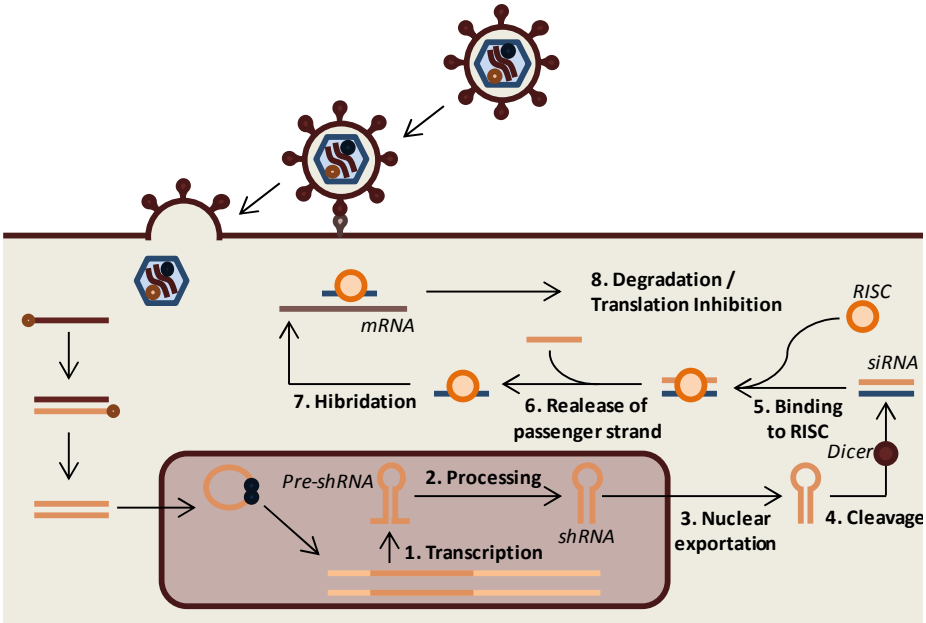

Figure 10. General mechanism for shRNA lentiviruses-mediated gene silencing.

Due to its strength and specificity, RNA interference-mediated gene silencing has been used in basic research to study the function of specific genes and in translational investigation to generate models of monogenic diseases such as Fanconi Anaemia[129] or CGD[130] in which it is possible to study new therapeutic approaches like GT.

6. Gene therapy for LAD-I

6.1. γ-retroviral vectors

GT for LAD-I was first attempted using γRVs expressing hCD18 from the LTR. These vectors were used to transduce a WT murine lymphoblastoid cell line (LCL)[131]. Transduced cells expressed the hCD18 protein in the cell surface as a chimeric heterodimer with the mCD11a protein and membrane expression of hCD18 was restricted to those cells expressing CD11 subunits. hCD18-γRVs were also used to transduce WT murine BM cells which were then transplanted into lethally irradiated recipients[132]. Expression of hCD18 could be detected in granulocytes 2 weeks after transplantation, but levels of expression decreased after 4 weeks.

γRVs expressing hCD18 from an internal promoter were also designed[133]. Sequences from the chicken *ACTB* gene and enhancer sequences derived from the immediate early gene of CMV were located internally into the viral transcription unit. This vector was used to transduce WT mouse BM cells that were infused back into lethally irradiated mice. 42% of surviving transplanted mice displayed expression of hCD18 in granulocytes at 6 weeks after transplantation and the number of hCD18-expressing granulocytes ranged from undetectable to 70% and was maintained for 6 months. hCD18 expression was always lower in lymphoid cells than in myeloid cells. hCD18 expression showed post-transcriptional regulation as it was upregulated after *in vitro* exposure of granulocytes to phorbol-12-myristate-13-acetate (PMA).

hCD18-γRVs pseudotyped with either A-MLV[132,134,135] or GALV[135] envelopes were used to transduce a LCL derived from a severe LAD-I patient with no detectable expression of either hCD18 or hCD11 subunits. hCD18-expressing LCLs recovered the ability to aggregate in the presence of PMA. This aggregation was CD18-dependent as it could be abrogated using an anti-CD18 blocking antibody.

The GALV-pseudotyped γRV mentioned above was used to transduce BM $CD34^+$ cells from a LAD-I patient. 31% of transduction was achieved in the presence of retronectin (RN). Corrected cells recovered mainly hCD11a expression while hCD11b and hCD11c expression were only detected upon expansion and differentiation. Corrected cells were assessed for functionality after sorting and myeloid differentiation. Corrected LAD-I neutrophils displayed increased binding to human umbilical vein endothelial cells (HUVEC) and underwent partially respiratory burst in response to opsonized zymosan, a stimulant that requires hCD11b/hCD18 expression. Based on these results, a phase-I GT clinical trial for human LAD-I was conducted in which 2 patients were enrolled[136,137]. Mobilized $CD34^+$ HSCs were collected from peripheral blood (PB), transduced with the γRV and infused back into the patients without any conditioning. A small percentage of corrected myeloid cells (up to 0.04%) were detected in PB at 2 and 4 weeks after transplantation but no corrected cells were detected by PCR 2 months after transplantation.

The failure observed in this clinical trial and in other similar phagocyte disorders[138] to achieve therapeutic levels of gene-corrected cells *in vivo*, despite high levels of transduction observed *in vitro*, suggested that conditioning was required in these cases to allow transduced $CD34^+$ cells to engraft.

A new γRV was designed, in which the canine CD18 (cCD18) was expressed from an internal murine stem cell virus (MSCV) LTR promoter/enhancer sequence[139]. This vector was evaluated for its

efficacy in the CLAD model. CLAD-affected dogs received a non-myeloablative conditioning with either 200 cGy total body irradiation (TBI) or busulfan prior to the administration of the gene-corrected $CD34^+$ cells (Figure 11). Both reduced-intensity conditioning (RIC) regimens resulted in low but detectable and long-term levels of $cCD18^+$ cells in PB with reversal or marked improvement of the CLAD clinical phenotype in 6 out of the 11 treated pups. Integration site analysis was performed on the 6 surviving dogs revealing the presence of 40 retroviral insertion sites (RIS) near oncogenes and 52 RIS near active genes out of a total of 321. Nevertheless, no evidence of vector-mediated transformation has been reported to date[140].

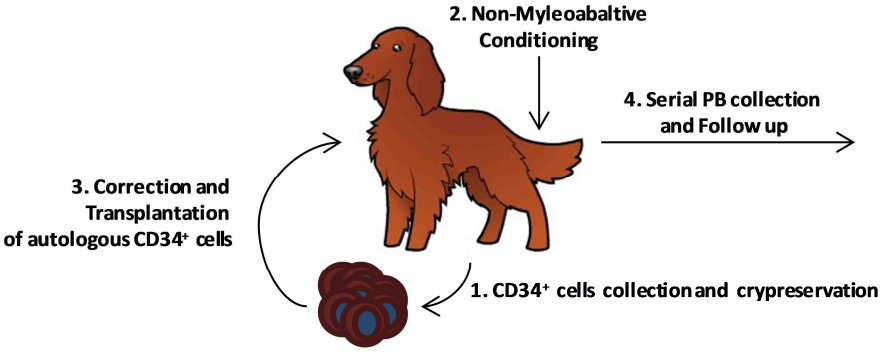

Figure 11. *Ex vivo* GT protocol in CLAD dogs.

6.2. Foamyviral vectors

New viral vectors have been developed to overcome the problems associated with γRV. A foamyviral vector (FV) expressing cCD18 from the MSCV LTR promoter/enhancer was used to conduct *ex vivo* GT experiments in 5 CLAD dogs after non-myeloablative conditioning[141]. Four dogs underwent complete reversal of the CLAD phenotype, which was sustained more than 4 years with no evidences of leukemia or MDS, as demonstrated by normal leukocytes counts, normal T-cell subsets and normal tri-lineage haematopoiesis in BM biopsies. Integration sites from early and late time-points were analysed in PB leukocytes[142]. cCD18-FVs integrated less close to oncogenes compared to cCD18-RVs and their integration pattern was very similar to computer-generated random sites. No foamyviral insertion sites (FIS) were found in oncogenes previously described as RIS in human GT clinical trials for CGD and X1-SCID like *PRDM16, SETBP1* and *LMO2* and only 6 FIS were found in the *MECOM* gene out of a total of 1528 unique FIS.

A FV incorporating a PGK promoter was also designed[143]. This vector was able to express cCD18 in canine neutrophils and $CD34^+$ cells after *in vitro* transduction. Nonetheless, CLAD dogs that received HSCs transduced with this vector did not experiment any clinical benefit and some of them died because of the disease.

6.3. Lentiviral vectors

SIN LVs for *ex vivo* LAD-I GT have been extensively studied in the CLAD model. Different internal promoters were used to drive the expression of the cCD18 cDNA (Table 7).

The use of a strong promoter–enhancer in a LV resulted in the successful correction of the typical CLAD phenotype in the two treated dogs, which became long-survivors in contrast to non-treated CLAD dogs, which normally die within the first 6 months of life. The outcome was not so conclusive when more physiological and weaker promoters were used. *In vitro* transduction of CLAD $CD34^+$ cells with the EF1α-LV resulted in similar cCD18 expression levels compared to that seen in $CD34^+$ cells from healthy dogs. Despite this fact, after transplantation of EF1α-LV-corrected $CD34^+$ cells, none

of the treated four CLAD dogs showed higher than 0.3% of $CD18^+$ PBLs and all died around 9 months after the procedure. EF1α promoter silencing was proposed as the reason of the failure of these experiments [144]. As shown in Table 7, only one dog survived after transplantation of PGK-LV-corrected $CD34^+$ cells. The surviving dog presented only 0.6% $CD18^+$ neutrophils in PB after 1 year, although a 19.2% of these positive neutrophils expressed cCD18 at normal levels. PGK and EF1α promoters in these particular settings (low multiplicity of infection (MOI), no $CD34^+$ cells pre-stimulation and reduced conditioning regimen) were not able to drive therapeutic levels of cCD18 expression.

Alternative physiological promoters were investigated. Different fragments of hCD18 and hCD11b promoters were cloned into LVs and checked for their ability to express cCD18 in CLAD $CD34^+$ cells[145]. Selected hCD18 and hCD11b LVs were assayed in *ex vivo* CLAD GT experiments resulting in 3 surviving dogs out of 4 treated dogs. Percentages of $cCD18^+$ PB neutrophils ranged from 0.7 to 1.5 % and expressed cCD18 from 12 to 24.3 % of normal levels. This study showed for the first time that lentiviral-mediated GT could be successful for LAD-I treatment.

Promoter	Reference	Free-disease Survival CLAD-dogs
MSCV LTR	Hunter et al[146]	2/2
EF1α	Nelson et al[147]	0/4
hPGK	Hunter et al[146]	1/4
hCD11b	Hunter et al[145]	1/2
hCD18	Hunter et al[145]	2/2

Table 7. LV-based *ex vivo* GT studies conducted in CLAD-affected dogs.

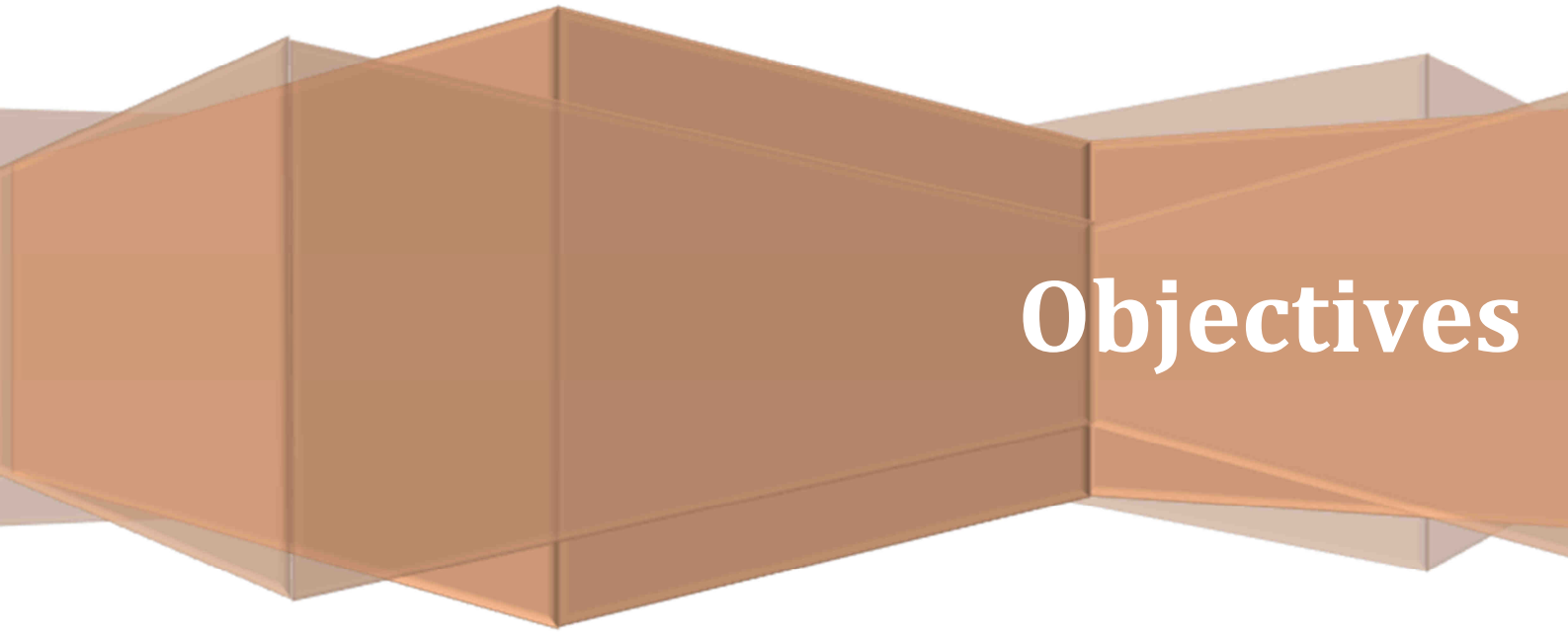

Objectives

LAD-I is an autosomal recessive disorder caused by mutations in the *ITGB2* gene resulting in null, low or aberrant expression of CD18. These defects affect the ability of the leukocytes to extravasate from the blood to the sites of infection. LAD-I symptomatology depends on the CD18 expression levels, resulting in a moderate or a severe phenotype, but in all cases it includes a high susceptibility to bacterial infections, neutrophilia and delayed wound healing. Patients with severe LAD-I normally die in the first years of life, while patient with the moderate phenotype can survive into the adulthood.

The standard treatment of these patients normally includes intensive antibiotherapy and even granulocyte transfusions, but the only current curative therapy is the allogeneic HSCT. However, the availability of HLA-compatible donors limits the number of patients that can benefit from this treatment. Additionally, HSCT complications can be very severe. As other monogenic PIDs, LAD-I is a good candidate to be treated by *ex vivo* HSC GT. The transplantation of autologous corrected HSCs could be available for all LAD-I patients and would limit the side effects associated with the allogeneic HSCT.

In order to develop new strategies of GT for LAD-I, we considered the following aims:

1. To study and characterize the HSC phenotype of the CD18 hypomorphic mouse model

2. To develop clinically applicable lentiviral vectors expressing hCD18 from ubiquitous and myeloid promoters.

3. To perform preclinical GT studies in different human and mouse *in vitro* and *in vivo* LAD-I models.

Materials and methods

1. Animal experimentation

All experimental procedures were carried out according to Spanish and European regulations (Spanish Royal Decree 53/2013 and Law 6/2013, which translate and comply with the European Directive 2010/63/UE about the use and protection of vertebrate mammals used for experimentation and other scientific purposes). Mice were maintained at the CIEMAT animal facility (registration number ES280790000183) under high standard conditions in line with FELASA recommendations:

- High-efficiency particulate air-filtered air with an exchange rate of 16–20 changes per hour.
- Regulated temperature of 20±2°C.
- Relative humidity of 55±10%.
- Light/dark cycle of 13/11 h with lights on at 07:00 h.
- 20 Gy-irradiated standard diet and ultraviolated-irradiated water ad libitum.
- Routinely pathogen screening.

1.1. Mouse strains

C57BL/6J (B6, stock number 000664), B6.SJL-*Ptprc*a/b*Pep*3b/BoyJ (P3B, stock number 002014) and B6.129S7-*Itgb2*^{tm1Bay}/J (CD18 hypomorphic mice, CD18^{HYP}, stock number 002128) colony founders were obtained from the Jackson Laboratory (Bar Harbor, USA).

B6 mice were used as WT controls in most of the experiments. P3B is a B6 congenic strain because it carries the differential B cell antigen designated CD45.1 (*Ptprc*^{a} allele), while the *b* allele (CD45.2) is present in the C57BL inbred strain.

Strain	Type	Background	CD45	ΔhCD4	Experiments
B6 **C57BL/6J**	Inbred		CD45.2	-	• Analysis of LAD-I classical phenotype: CD18^{WT} controls. • LSK cells determination, flow cytometry analysis and clonogenic assays: CD18^{WT} controls. • Limiting dilution assays: CD18^{WT} donor. • GT experiments: CD18^{WT} controls.
P3B[148] **B6.SJL-*Ptprc*^{a} *Pep3*^{b}/BoyJ**	Inbred	C57BL/6J	CD45.1	-	• Competitive repopulation experiments: recipients. • Limiting dilution assays: recipients and radioprotective donors. • Neutrophil donor in neutrophil transfer experiments.
CD18^{HYP} [75] **B6.129S7-Itgb2^{tm1Bay}/J**	Inbred Targeted Mutation	C57BL/6J	CD45.2	-	• Analysis of LAD-I classical phenotype. • LSK cells determination, flow citometry analysis and clonogenic assays. • Competitive repopulation experiments and limiting dilution assays • GT experiments: LAD-I model.
P3B-ΔhCD4[149] **vavHS21/45hCD4**	Inbred Targeted Mutation	C57BL/6J	CD45.1	+	• Competitive repopulation experiments: CD18^{WT} donor
PEdKO[150] **B6.129S2-*Sele*^{tm1Hyn} *Selp*^{tm1Hyn}/J**	Inbred Targeted Mutation	C57BL/6	CD45.2	-	• Study of aged neutrophils

Table 8. Mouse Strains: pan-leukocyte markers expression and experiments in which they have been used.

CD18^{HYP} mice contain the *Itgb2*^{tm1Bay} allele which is a hypomorphic mutation leading to the expression of low levels of mCD18. These animals were handled under sterile conditions and maintained in micro-isolators.

P3B-ΔhCD4 mice were previously generated in the laboratory[149]. Briefly, a vector consisting of a modified human CD4 gene (ΔhCD4, incapable of intracellular signalling and association with the MHC

class II) driven by the HS21/45 *vav* promoter (a kind gift from Jerry M. Adams, Walter and Eliza Hall Institute of Medical Research, Parkville, Australia) was linearized and microinjected into P3B eggs and then transferred into B6D2F1 pseudo pregnant females. These mice express the marker ΔhCD4 in all cells of the haematopoietic system.

PEdKO mice contain *Sele*^{tm1Hyn} and *Selp*^{tm1Hyn} alleles leading to absent E- and P-selectin expression respectively. These mice were kindly provided by Dr. Andrés Hidalgo (CNIC, Madrid, Spain).

1.2. Haematological sampling

Routine bleeding for PB collection of experimental mice was carried out by lateral tail vein sampling. A maximum volume of 200 µL was collected. PB was mixed with 20 µL of EDTA to prevent blood coagulation. Terminal blood collection was performed by cardiac puncture after CO_2 mice treatment. A maximum volume of 1 mL was collected. For haematological counts, 50 µl of EDTA-anticoagulated PB were analysed using an ABACUS Junior Vet Haematological Analyzer (Practice CVM, Tudela, Spain).

For BM collection, animals were sacrificed by cervical dislocation. Both tibiae and femora were surgically extracted and BM was harvested by flushing them under sterile conditions with DMEM + GlutaMAX (Gibco/Life Technologies/Thermo Fisher Scientific, Waltham, USA) and washed twice with PBE buffer (PBS + 0.5% BSA + 1mM EDTA, MACS/Miltenyi Biotec, Bergisch Gladbach, Germany). Cellularity was determined in the Neubauer chamber by diluting the sample in Türk solution (Merck KGaA, Darmstadt, Germany).

1.3. Transplantation experiments

1.3.1. Haematopoietic progenitors purification

Mouse haematopoietic progenitors, both Lin$^-$ and LSK cells, were purified from femora and tibiae BM samples by FACS. BM cells (BMCs) were stained for LSK or Lin$^-$ phenotype using a panel of monoclonal antibodies (Table S1) and FACS-sorted using a BD INFLUX (BD/Becton, Dickinson and Company, New Jersey, USA). FACS analysis of representative pre and post sorting BM samples from CD18^{HYP} mouse are represented in Figure 12.

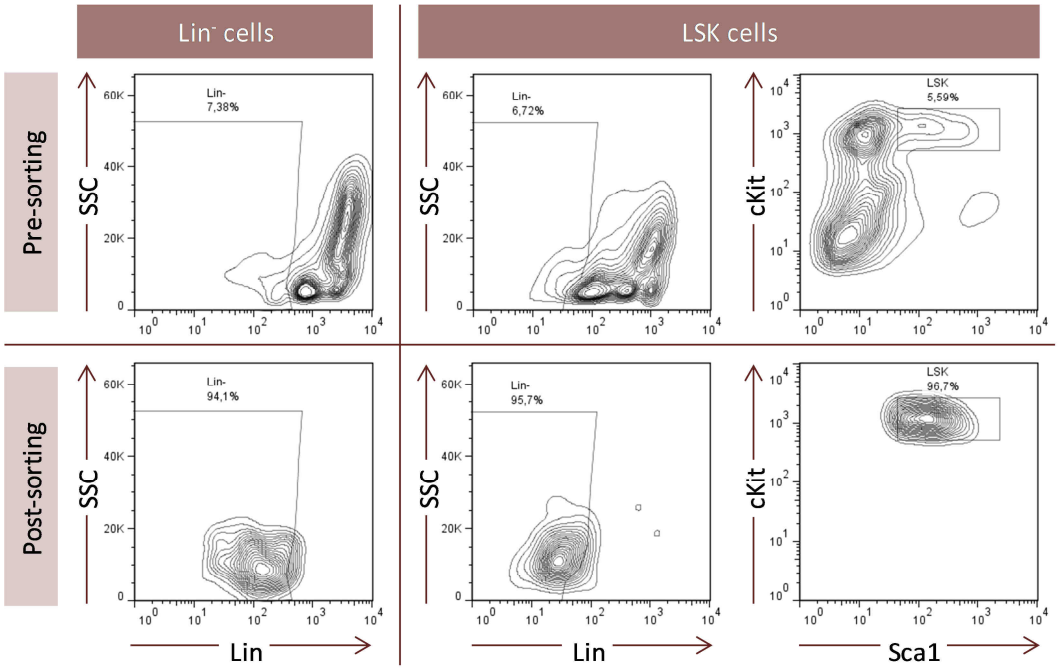

Figure 12. Representative flow cytometry analysis of a pre and post sorting BM sample.

1.3.2. Haematopoietic stem cell limiting dilution assay

BM single cell suspensions were obtained from $CD18^{HYP}$, $CD18^{WT}$ and P3B wild type mice (8 to 12 week old). Lethally irradiated (4.75 Gy + 4.75 Gy) recipient mice were competitively reconstituted by retro-orbital venous sinus injection with five different doses (5×10^5 cells, 1.5×10^5 cells, 5×10^4, 2.5×10^4 cells) of whole BMCs from test mice ($CD18^{HYP}$ or $CD18^{WT}$) and a radioprotective dose of 3×10^5 BMCs from P3B mice. Mice were bled at 3 months post transplantation (mpt) and analysed for the percentage of donor-reconstituted animals on each group. We considered as repopulated by donor cells those mice that had more than 1% donor-derived ($CD45.2^+$) cells in both lymphoid ($CD3^+$ and $B220^+$) and myeloid ($Gr\text{-}1^+$ and $CD11b^+$) subpopulations. Frequency of reconstituting haematopoietic stem cells from these limiting dilution experiments was calculated using ELDA software[151].

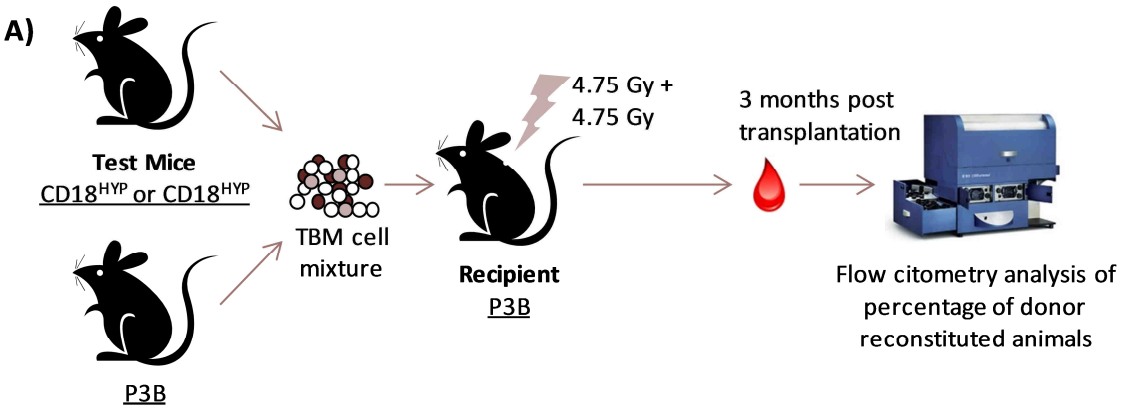

B)

Group	Readioprotective dose of P3B BM cells	BM cell dose from test mice
1	3×10^5	5×10^5
2		1.5×10^5
3		5×10^4
4		2.5×10^4
5		1.5×10^4

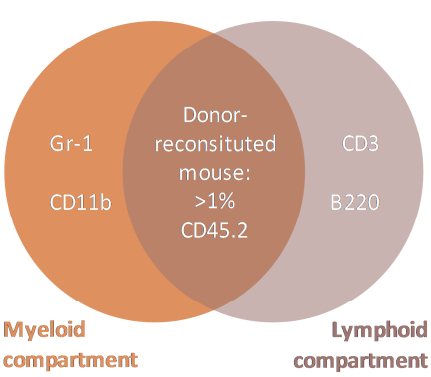

Figure 13. HSC limiting dilution assays. A) Experimental protocol. B) Groups of animals according to the dose of cells from each of the tested strains. C) Criteria used to determine if an animal had been reconstituted with donor cells.

1.3.3. Competitive repopulation assay

Competitive repopulation assays (CRAs) were conducted by mixing hematopoietic repopulating cells from male $CD18^{HYP}$ and P3B-ΔhCD4 mice ($CD18^{WT}$), that were subsequently intravenously transplanted into myeloablated P3B female mice that had received two doses of 4.75 Gy, spaced 24 hours apart, with x-ray equipment MG324 (300 kV, 12.8 mA, Philips, Hamburg, Germany). Proportion of both populations in the mixture was checked by flow cytometry prior to transplantation.

The percentage of cells derived from the transplanted competitor populations and from the endogenous BM was deduced from CD45.1, CD45.2 and ΔhCD4 FACS analyses carried out every 30 days. At 4 mpt, animals were culled and BMCs were harvested. BMCs and CFUs-derived cells were analysed for population content (CD45.1, CD45.2 and ΔhCD4). In addition, harvested BMCs were intravenously infused into myeloablated P3B secondary recipients, whose PB cells were periodically analysed for population content (CD45.1, CD45.2 and ΔhCD4). Two CRAs were performed with total

BMCs: one in which CD18^{HYP} and CD18^{WT} cells were mixed at the same proportion (1x10^6 cells of each stain) and other in which cells were mixed at 3:1 proportion CD18^{HYP} / CD18^{WT} (5x10^5 and 1,5x10^6 cells respectively). CRA was also conducted with MACS-sorted lin$^-$ cells. In this case 2x10^5 cells of both competitor populations were mixed and transplanted into the recipients (Figure 14).

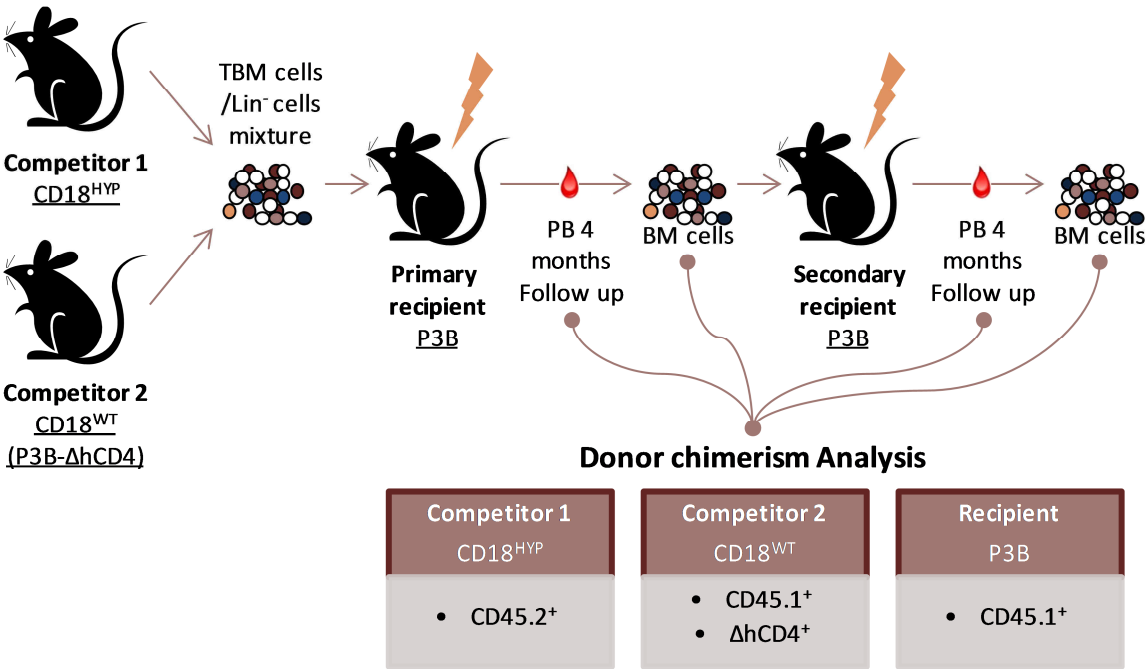

Figure 14. General protocol for CRAs. Population analysis was based on the determination by flow cytometry of pan-leukocyte markers CD45.1, CD45.2 and ΔhCD4.

1.3.4. Homing experiments

FACS-Sorted BM-derived LSK cells from 6 week old CD18^{HYP} and CD18^{WT} mice were washed with PBS (Sigma-Aldrich, St. Louis, USA) and resuspended at a density of 1 × 10^6 cells/mL. This suspension was incubated with 5 µl/ml of Vybrant® DiD cell-labelling solution (Molecular Probes/Life Technologies/Thermo Fisher Scientific, Waltham, USA) during 20 min at 37 ºC. After washing, LSK cells were resuspended and intravenously infused into myeloablated female B6 mice recipients. 6x10^4 LSK cells were administered to each mouse. At 14 h after transplantation recipients were culled and BMCs were harvested from the femora and tibiae and analysed for the presence of homed DiD$^+$ cells (Figure 15). A minimum of 5x10^5 viable cells were acquired.

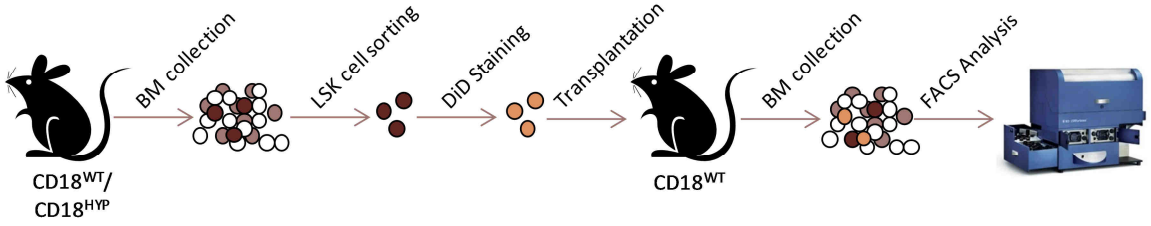

Figure 15. Protocol followed in LSK homing experiments.

Homing efficiency was calculated as published before[152]. Briefly, to determine the seeding efficiency to the BM we assumed that the two femora and tibiae contain approximately 20% of the total BM cellularity[153]. The seeding efficiency was calculated then on the basis of the total LSK cells retrieved related to the total LSK cells injected (all of them DID$^+$ as confirmed after the staining). The number of total homed LSK cells analysed (DID$^+$) was corrected for the total BMCs obtained from the 2 femora and tibiae.

$$Seeding\ efficiency = \frac{\%\ DiD^{+}\ cells * number\ of\ BM\ cells\ collected\ from\ both\ femora\ and\ tibiae}{20\% * number\ of\ injected\ LSK\ cells} * 100$$

1.3.5. Ex vivo gene therapy experiments

For *ex vivo* GT experiments, O/N transduced lin$^-$ cells were collected, washed and suspended in PBS at a density of 1.5 – 2.5x10^6 cell/mL. 200 µL of this cellular suspension (3 – 5x10^5 cells) were intravenously administered into lethally irradiated female CD18^{HYP} mice. These mice received a conditioning regimen consisting of two consecutive doses of irradiation (4.75 Gy + 4.75 Gy) the day before and the same day of the transplantation.

Transplanted mice were monthly followed-up for 4 months. Each month animals were bled. Collected PB was analysed by flow cytometry for the expression of hCD18 and the different murine CD11 subunits. 100 µL of PB were lysed and cells spun down. Genomic DNA (gDNA) was extracted from these pellets and used for vector copy number (VCN) determination (see section 5). 3 months after transplantation, animals were analysed by flow cytometry for hCD18 expression in different leukocytes subpopulations (T-Cells, B-cells and granulocytes) using specific markers (CD3, CD45R and Gr-1).

Transplanted mice were culled by cervical dislocation at 4 mpt. BMCs were harvested and analysed by flow cytometry. 3x10^6 of these BMCs were transplanted mouse to mouse into myeloablated secondary recipients. Two animals were transplanted with a pool of 3x10^6 BMCs from different animals.

Secondary recipients were similarly followed-up for 9 months. At the end of the experiments, mice were sacrificed by cervical dislocation. BM was subsequently harvested and analysed by flow cytometry.

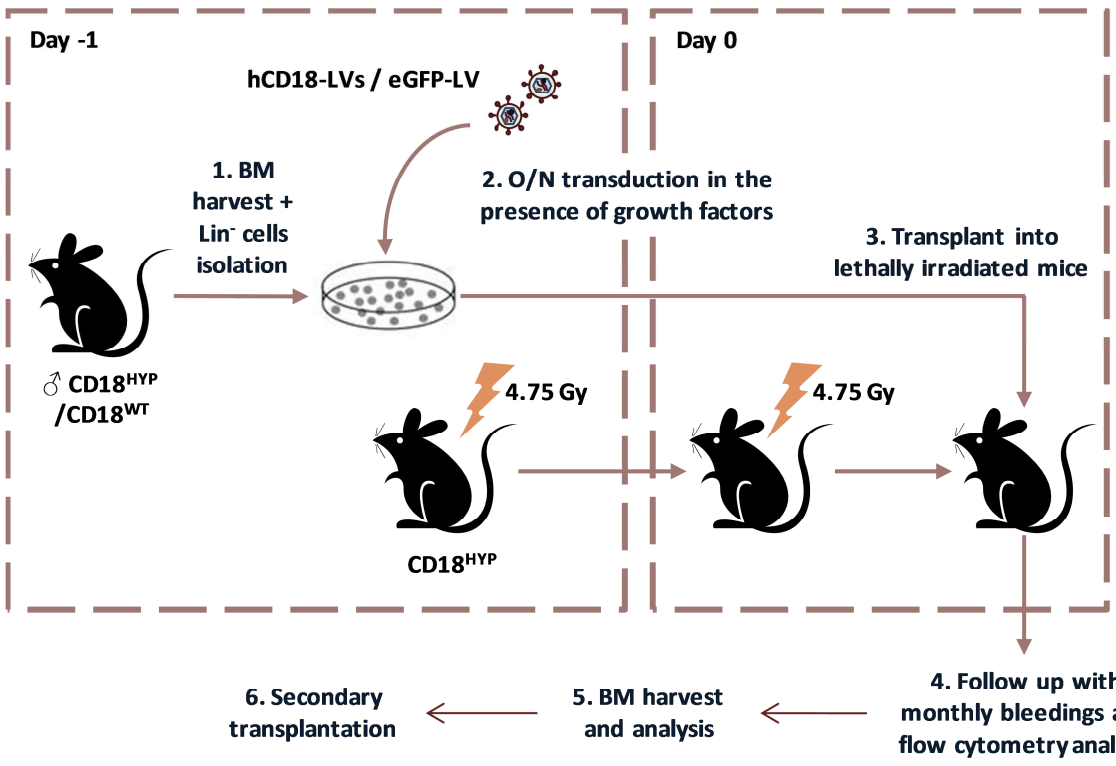

Figure 16. Ex vivo GT protocol in CD18^{HYP} mice.

1.4. Neutrophil transference

P3B mice were sacrificed and BMCs were collected by flushing both femora and tibiae with DMEM. Neutrophils were purified using Percoll 62% (GE Healthcare, Farfield, USA) (Figure 17) and erythrocytes lysed using a hypotonic buffer. Purities of 83-90% were achieved using this method. To induce senescence, neutrophils were cultured for 6 hours in RPMI 1640 (Roswell Park Memorial Institute) 1640 medium + GlutaMAX (Gibco/Life Technologies/Thermo Fisher Scientific, Waltham, USA) supplemented with 10% HyClone (GE Healthcare, Fairfield, USA) and 1% penicillin/streptomycin (P/S). 4-7x10^6 BM-derived *ex vivo*-senesced neutrophils were intravenously transferred into $CD18^{HYP}$ mice each 24 hours for 5 days. At day 6, mice were sacrificed and BMCs were collected and analysed for LSK cell content. PBS-treated $CD18^{HYP}$ mice and untreated $CD18^{HYP}$ and $CD18^{WT}$ mice were used as controls.

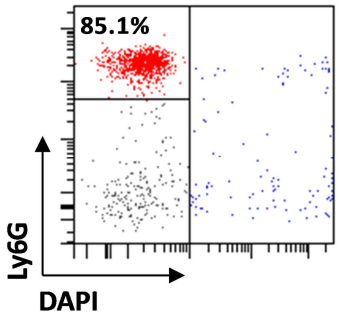

Figure 17. Representative example of the purity of Percoll (62%)-purified BM neutrophils from P3B mice.

1.5. Inflammation models

Two different models of local inflammation were performed to evaluate the capacity of neutrophils to extravasate from PB in two different anatomical locations: lung and subcutaneous air pouch.

1.5.1 Lipopolysaccharides-induced asthma model

Mice were administered intranasaly with 50 µL of 0.3 µg/µL LPS (from Escherichia coli 0111:B4, Sigma-Aldrich, St. Louis, USA) or PBS under isoflurane anaesthesia. 24 hours after LPS/PBS administration, bronchoalveolar lavages (BALs) were performed. BAL removes non-adherent cells and lung lining fluid from the mucosal surface so this technique allows sampling of innate, cellular and humoral responses within the lung. Mice were expired immediately prior to lavage by lethal injection of avertin (synthetized in the laboratory from 2,2,2-tribromoethanol and 2-methyl-2-butanol, both from Sigma-Aldrich, St. Louis, USA) and exsanguinated from both femoral arteries. Then, a small incision was made in the animal skin at the abdomen, skin around entire body was torn and skin upwards was peeled to expose thoracic cage and neck. Tissue from neck was dissected to expose trachea. A small incision in the trachea was performed taking care of not cutting the trachea all the way through and an 18G blunt fill needle (BD, 305180) was inserted through the incision. The needle and the trachea were stabilized with a bulldog serrefine. Utilizing 1 mL syringes, 3 lavages with 700 µL of PBS were performed and collected together. BAL samples were pulled down and resuspended into 200 µL of fresh PBS. Cell number was determined diluting these samples with trypan blue (Sigma-Aldrich, St. Louis, USA) and 50 µL of the suspension were used for FACS analysis (Ly6G/CD11c). Absolute numbers of neutrophils were determined as following:

Absolute numbers of migrating neutrophils were normalized to the values obtained in the $CD18^{HYP}$ animals.

1.5.2. Air-pouch inflammation model

The air pouch (AP) was generated by the dorsal subcutaneous injection of 5 ml of air on day 0 under isoflurane anaesthesia. On day 3 the pouches were reinflated with 3 ml of air and, on day 5, 40 ng of mouse recombinant TNF-α in PBS with 0.5% carboxymethylcellulose (CMC) as inert carrier were injected into the matured pouches. 4 hours after TNF-α administration, mice were sacrificed by CO_2 inhalation and PB collected by heart puncture and total leukocytes and neutrophils number counted using an ABACUS Junior Vet Haematological Analyser. The APs were then flushed with 8 ml of PBS and the collected cells centrifuged at 500g for 10min. The cells were resuspended in 0.5 ml of PBS and total leukocytes and neutrophils number in the AP were also counted using the haematological analyser. Emigration ratio for total leukocytes or neutrophils was calculated with the following equation:

$$Emigration\ Ratio = \frac{cells\ in\ the\ AP}{cells\ in\ PB} * 100$$

In the case of GT-treated animals, $hCD18^+$ or GFP^+ cells were determined in PB and in the AP and emigration ratio was calculated as following:

$$Emigration\ Ratio = \frac{hCD18^+\ or\ GFP^+\ cells\ in\ the\ AP}{hCD18^+\ or\ GFP^+\ cells\ in\ PB} * 100$$

2. Cell culture

2.1. Cell lines

The different cell lines used in the present work are summarized in Table 9.

Cell Line	Organism	Cell Type	Tissue	Disease	Growth	Origin	Purpose
293T	Human	Epithelial	Embryonic kidney	-	Adherence	ATCC - CRL-3216™	Production of LVs
HT1080		Epithelial	Connective tissue	Fibrosarcoma	Adherence	ATCC - CCL-121™	Titration of LVs
ZJ		B cell	Blood	LAD-I	Suspension	Kindly provided by Dr. Hickstein (NIH)	*In vitro* LAD-I experiments
MARK		B cell	Blood	-	Suspension	Kindly provided by Dr Regueiro (CIEMAT)	
GUS-1		B cell	Blood	-	Suspension	Kindly provided by Dr Regueiro (UCM)	

Table 9. Cell lines used for the in vitro experiments.

293T cell line, also known as HEK293T, is a cell line derived from human embryonic kidney cells and contains the SV40 (Simian vacuolating Virus 40) large T-antigen, which owes its transformation activity to the inhibition of the retinoblastoma and p53 tumour suppressor proteins. This allows for episomal replication of transfected plasmids containing the SV40 origin of replication. 293T cells are routinely used for LV production because of being easily grown and transfected[154].

HT1080 cell line was generated from tissue taken in a biopsy of a fibrosarcoma present in a 35 year old human male who died without having been treated with chemotherapy or radiotherapy[155]. HT1080 cells were widely used for LV titration.

ZJ cell line is a lymphoblastoid cell line (LCL) that was obtained by Epstein Barr virus infection of B cells from a LAD-I patient. This cell line expresses no detectable CD18 mRNA or protein levels[156]. ZJ cells have been widely used for *in vitro* transference of CD18 as a proof of concept for LAD-I GT[75,134]. MARK and GUS-1 LCLs were generated in Dr. Regueiro's laboratory from healthy samples and they were used as a $CD18^{WT}$ controls in these experiments.

2.1.1. Culture of adherent cells

HT1080 and 293T cells were cultured in complete medium based on DMEM + GlutaMAX supplemented with 10% Hyclone and 0.5% P/S. Cells were cultured in polystyrene cell culture flasks (Corning, New York, USA). Adherent cells were diluted using Trypsin-EDTA 1% (Sigma-Aldrich, St Louis, USA).

2.1.2. Culture of suspension cells

ZJ, GUS-1 and MARK cells were cultured in complete medium based on PRMI 1640 + GlutaMAX supplemented with 10% Hyclone and 0.5% P/S.

2.1.3. Transduction of lymphoblastoid cell lines

$2.5x10^5$ cells were normally transduced on RN (Takara Bio, Otsu, Japan)-coated 24-well non-treated tissue plates. Cells were O/N transduced with lentiviral supernatants at the desired MOI. The next day, cells were collected, washed and resuspended in fresh medium. The amount of viral supernatant was calculated as following:

$$Volume\ to\ add\ of\ viral\ supernatant\ (mL) = \frac{number\ of\ cells * MOI}{viral\ titre}$$

For the preparation of RN-coated plates, 500 µL of 19 µL/mL RN in PBS were added to each well (5 µg/cm^2). Plates were allowed to stand for 2 hours at room temperature or at 4°C overnight. After that, RN solution was removed and wells were washed once with PBS.

2.1.4. CD18-dependent functional assays in lymphoblastoid cells

2.1.4.1. PMA-induced aggregation

The aggregation assay was carried out as previously described[157]. Cells were washed two times and suspended in RPMI 1640 medium + GlutaMAX with 10% HyClone at a concentration of $2×10^6$ cells/ml and added to a flat-bottomed 96-well plate. Then, 50 µl of PBS or 1 µg/ml PMA solution (Sigma-Aldrich, St. Louis, USA) were added to each well and cells were incubated for one hour at 37ºC. An inverted microscope was used to view the aggregation. In blocking studies, a mouse monoclonal antibody against hCD18 (LEAF™ purified anti-human CD18, Clone TS1/18, BioLegend, San Diego, USA) was added at a final concentration of 7 µg/ml to the cell suspension 5 min before the addition of the PMA stimulus.

2.1.4.2. Soluble ICAM-1 binding assay

sICAM-1 binding assay was performed as formerly described[158]. sICAM-1 was prepared by incubating 20 µg/ml recombinant human ICAM-1/Fc (Chimera (R&D System, Minneapolis) with 100 µg/ml polyclonal PE-conjugated rabbit anti-human IgG Fc antibody (eBioscience, San Diego, USA) in 50 µl of RPMI 1640 medium + GlutaMAX containing 5% HyClone and HEPES 10 mM (Gibco/Life Technologies/Thermo Fisher Scientific, Waltham, USA) for 30 min at room temperature. $2x10^5$ cells were resuspended in the sICAM mixture with or without β_2-activating agents (10 mM $MgCl_2$ and 3 mM EGTA) for 30 min at 37 °C. Cells were washed with RPMI 1640 medium + GlutaMAX and analysed by flow cytometry.

2.2. Primary cells

2.2.1. Mouse lineage negative cells

2.2.1.1. Methyl-cellulose culture

$1.5x10^4$ BMCs or 10^3 BM-derived lin$^-$ cells were seeded in methylcellulose-based medium with

recombinant cytokines including mSCF, mIL-3 and mIL-6 (Methocult M3534, StemCell Technologies, Vancouver, Canada). The number of CFUs was scored on day 7 under an inverted microscope.

2.2.1.2. Lin$^-$ cell transduction and liquid culture

Mouse haematopoietic progenitors were transduced with hCD18-LVs and eGFP-LV at different MOIs (20 – 50) using an O/N protocol. Freshly isolated lin$^-$ cells were resuspended in StemSpan medium (StemCell Technologies, Vancouver, Canada) containing 100 ng/mL hIL-11 and 100 ng/mL mSCF (Eurobiosciences, Friesoythe, Germany) and the required amount of lentiviral supernatant was added (calculated using the formula described in section 2.1.3 of Material and Methods). Next day cells were washed and either resuspended in fresh medium for their expansion in liquid culture or resuspended in PBS to be used in GT *ex vivo* experiments (see section 1.3.5). Lin$^-$ cells were allowed to grow in liquid culture for 7 days for flow cytometry analysis and VCN determination.

2.2.2. Human CD34$^+$ cells

2.2.2.1. Purification of cord blood CD34$^+$ cells

Cord blood samples from healthy donors were obtained from the Madrid Community Transfusion Centre. Mononuclear cells were purified by Ficoll-Paque PLUS (GE Healthcare, Fairfield, USA) density gradient centrifugation. Then, CD34$^+$ cells were selected using CD34 MicroBead Kit. Magnetic-labelled cells were positive selected firstly with a LS column and then with a MS column in QuadroMACS™ and OctoMACS™ separators respectively (All from MACS, Miltenyi Biotec, Bergisch Gladbach, Germany). Purified CD34$^+$ were then evaluated for their purity by flow cytometry. Purities from 80-95% were routinely obtained.

2.2.2.2. Transduction of human CD34+ cells and neutrophil differentiation

Freshly isolated CD34$^+$ cells were cultured for 2 days in StemSpam medium supplemented with human cytokines including SCF (300 ng/ml), thrombopoietin (TPO, 100 ng/ml) and FMS-like tyrosine kinase 3 ligand (Flt3l, 100 ng/ml), and 1% P/S. Cells were collected at day 2 and O/N transduced with shRNA-LVs at a MOI of 100 vp/cell on non-treated retronectin-coated 24-multiwell plates. The following day, cells were washed and resuspended in fresh medium.

In the case of lentiviral correction, interfered-CD34$^+$ cells were allowed to grow for 3 additional days and then GFP$^+$ cells were FACS-sorted and resuspended in fresh medium. The next day, cells were collected and transduced with hCD18-LVs at a MOI of 100 vp/cell. The day after transduction cells were washed and resuspended in neutrophil differentiation medium (IMDM supplemented with 20% Hyclone, 1% P/S and human cytokines including IL-3 (20 ng/ml), SCF (20 ng/ml) and G-CSF (100 ng/ml) and allowed to proliferate for 12 days. These 12-day differentiated neutrophils were used in different functional assays described below (Figure 18).

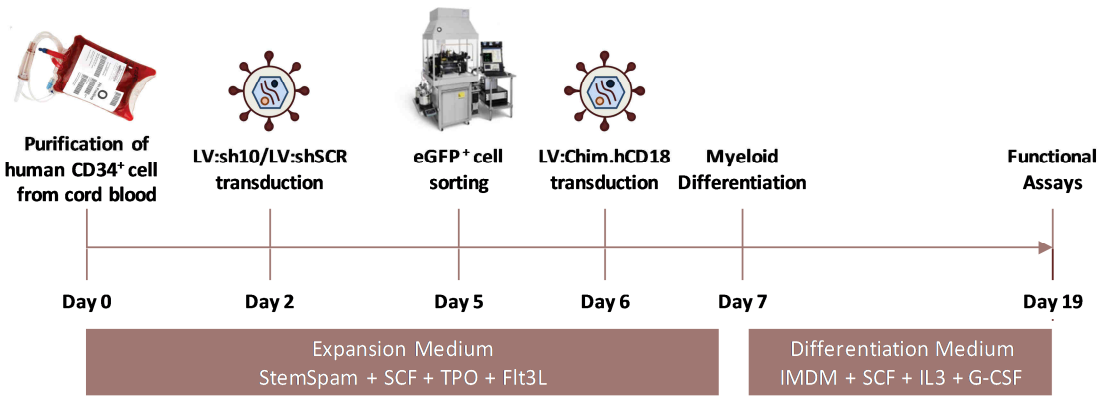

Figure 18. Transduction and differentiation of cord blood CD34$^+$ cells from healthy human donors.

2.2.2.3. Soluble ICAM-1 binding assay

This assay was performed similarly as described for LCLs in 2.1.4.2. section, but with one exception; cells were incubated with 1 µL of Fc receptor (FcR) blocking reagent (MACS, Miltenyi Biotec, Bergisch Gladbach, Germany) for 20' at 4 ºC and then washed prior to the incubation with the ICAM-1-Fc reagent. This step was performed in order to avoid the recognition of the ICAM-1-Fc reagent by the FcR typically expressed by myeloid cells.

2.2.2.4. Flow chamber assay

Flow chamber assays were performed as previously described[159]. $1x10^5$ twelve-day differentiated neutrophils were mixed with $1x10^5$ control untransduced neutrophils and resuspended in 500 µL of RPMI 1640 medium + GlutaMAX with 10% Hyclone. Plastic slides were coated with fibrinogen (2.5 mg/ml) for one hour at 37 ºC. Flow chambers (Department of Medical Engineering, Imperial College School of Medicine, London, United Kingdom) were assembled with 0.2-mm spacers, pre-coated slides, and an exit tubing (Medex/Smiths Medical, London, United Kingdom). Four 50 ml syringes were filled with PBS and connected to the chamber using tubing (Medex/Smiths Medical, London, United Kingdom), a three-way tap (BD/Becton, Dickinson and Company, New Jersey, USA), and Y-connectors (Alaris/CareFusion, San Diego, USA). The tubing and chambers were primed to eliminate bubbles and mounted on a microscope stage inside of an environmental chamber (37 ºC). Syringes were assembled on a BS-9000-6 multi-syringe programmable syringe pump with flow-rate control (Braintree Scientific, Braintree, United Kingdom). Cells were injected through the three-way tap and passed into the chamber with about 1 ml PBS from the syringes. After 10 min adherence, PBS was pumped into the chamber at low flow (1 dyn/cm^2/min) for 1 min to remove non-adherent cells. Afterwards, flow rates were augmented in 10–20 dyn/cm^2 increments in 1-min intervals to a maximum sheer stress of 80 dyn/cm^2. Images of bright field and eGFP fluorescence were acquired after each flow rate increment using Zeiss Axiovert 135 microscope with a 10X phase contrast lens (Zeiss, Oberkochen, Germany), a digital camera (Hamamatsu Photonics, Hamamatsu, Japan) and Volocity 4.2 software (PerkinElmer, Waltham, USA).

The shear stress for each flow rate was calculated from the following formula:

$$\text{Shear stress} = \frac{6 * \text{flow rate} * \text{viscosity}}{\text{channel width} * (\text{channel height})^2}$$

Where: shear stress is expressed in dyn/cm^2, flow rate is expressed in ml/sec, viscosity of PBS is 0.0076 Poise, channel height = chamber width = 0.7 cm and channel height = spacer height = 0.02 cm.

The number of cells detaching at each increment of shear stress was calculated and expressed as a percentage of the total number of adherent cells in the same field immediately after the low flow wash. eGFP$^+$ cells correspond to the LV:shSCR and LV:sh10-transduced cells and eGFP$^-$ cells correspond to the untransduced cells.

2.2.2.5. Chemiluminescence assay of neutrophil respiratory burst

12-day *in vitro* differentiated neutrophils were compared in a chemiluminescence assay of respiratory burst activity in response to complement-opsonized zymosan. Activation of the respiratory burst in response to C3bi-opsonized zymosan has been shown to be a CD11/CD18-mediated function activity[160,161]. Luminol-enhanced chemiluminescence was used as a sensitive measure of the respiratory burst of human phagocytes as previously described[162]. $1x10^5$ cells were preincubated for 15 min in a 160 µL of RPMI 1640 medium + GlutaMAX with 15 µg/mL human serum albumin at room temperature in an Isoplate-96 Microplate White Frame Clear Well (PerkinElmer, Waltham, USA). At the beginning of the assay, 10 µmol/L luminol (Sigma-Aldrich, St. Louis, USA) and 1 mg/mL opsonized zymosan were

added to the reaction mixture. Luminol-enhanced chemiluminescence was read for 10-second intervals at the designated time points with a Genios Pro reader (Tecan, Männedorf, Switzerland). The assay was performed at room temperature and chemiluminescence was reported as relative light units (RLU)/10^6 cells/10 s.

Zymosan (Sigma-Aldrich, St. Louis, USA) was opsonized with human serum as previously described[163]. Briefly, Zymosan was resuspended in PBS at 20 mg/mL, heated and shaken at 100 ºC for 20 minutes, sonicated for 60 s and washed in PBS by centrifugation (300g, 2 min). Finally Zymosan was resuspended in fresh PBS at 20 mg/mL and incubated with an equal volume of pooled human serum. The mixture was incubated at 37 ºC for 1 hour (keeping Zymosan in suspension). Opsonized Zymosan was washed twice in PBS by centrifugation (300g, 2 min), resuspended in PBS at 10 mg/mL and stored at –80°C.

3. Flow cytometry analyses

Flow cytometry analyses were performed in the LSRFortessa cell analyser (BD/Becton, Dickinson and Company, New Jersey, USA). Off-line analysis was performed with the FLowJo Software v7.6.5. (Tree star, Ashland, USA).

A minimum of 10^4–10^5 viable cells were normally acquired. Samples were always resuspended in flow cytometry buffer (PBS containing 0.5% BSA and 0.05% sodium azide) containing 1 µg/ml DAPI as a viability marker. In the case of PB and BM samples, erythrocytes were lysed in ammonium chloride lysis solution (0.155 mM NH_4Cl, 0.01 mM $KHCO_3$, 10^{-4} mM EDTA) before antibody staining. Table S1 summarize all the labelled antibodies used in the different experiments. Fluorochrome-conjugated streptavidins were used as a second step reagent to detect biotinylated primary antibodies.

Mean fluorescent intensity (MFI) was used to determine the surface expression of antigens detected by fluorescent-labelled antibodies. In those cases where relative surface expression was used, this was calculated by normalizing the MFI value from the sample to that of a control as following:

$$Relative\ surface\ expression = sample\ MFI * 100/control\ MFI$$

3.1. Haematopoietic progenitor population study

For haematopoietic progenitor population studies, harvested BMCs from 6 week old $CD18^{HYP}$ and $CD18^{WT}$ mice were stained with the cocktail of monoclonal antibodies listed on Table S1. Cell-surface markers for the harvested haematopoietic populations are summarized as indicated in Table 10.

	Positive	Negative
Long-term haematopoietic stem cells (LT-HSC)	ckit, Sca1, CD150	CD3, B220, Gr1, Mac1, Ter119, Flk2, CD34
Short-term haematopoietic stem cells (ST-HSC)	ckit, Sca1, CD34	CD3, B220, Gr1, Mac1, Ter119, Flk2, CD150
Multipotent progenitor (MPP)	ckit, Sca1, Flk2	CD3, B220, Gr1, Mac1, Ter119
Megakaryotic/erythroid progenitor (MEP)	Ckit,	CD3, B220, Gr1, Mac1, Ter119, Sca1, CD34, FcγR
Granulocyte/monocytic progenitor (GMP)	ckit, CD34, FcγR	CD3, B220, Gr1, Mac1, Ter119, Sca1,
Common myeloid progenitor (CMP)	Ckit, CD34	CD3, B220, Gr1, Mac1, Ter119, Sca1, FcγR

Table 10. Subpopulation of BM haematopoietic progenitors identified on the basis of FACS-detection of surface markers.

3.2. LSK cell cycle analysis

For the LSK cell cycle status and apoptosis analysis, $5x10^5$ BM-derived MACS-sorted lineage negative cells from 6 week old $CD18^{HYP}$ and $CD18^{WT}$ mice were resuspended in Hoesch binding buffer (Hank's balanced salt solution containing 20 mM HEPES, 5.5 mM Glucose and 10% HyClone) and stained for DNA and RNA using Hoechst 33342 (Sigma-Aldrich, St. Louis, USA) and Pyronin Y (Sigma-Aldrich, St.

Louis, USA). These cells were then labelled for LSK phenotype analyses using a cocktail of monoclonal antibodies listed on Table S1. Cells were analysed by flow cytometry in the Influx cell sorter (BD/Becton, Dickinson and Company, New Jersey, USA).

3.3. Annexin V apoptosis study

Apoptosis was studied in $Gr1^+$ BMCs using FITC apoptosis detection Kit I (BD Pharmingen/Becton, Dickinson and Company, New Jersey, USA). $2x10^5$ fresh isolated BMCs were first stained with a Gr1-PE antibody. Then cells were resuspended in 200 µL of binding buffer at 10^6 cells/mL. 100 µL were stained with 5 µL of FITC-annexin V (AV). Cells were gently vortexed and incubated for 15 min at RT in the dark. Finally, 400 µL of binding buffer containing DAPI were added to the cells. The samples were immediately analysed by flow cytometry. Cells in early apoptosis were identified as the AV^+ $DAPI^-$ population. In contrast, cells in late apoptosis or already dead were identified as AV^+ $DAPI^+$ population.

4. Lentiviral vectors

4.1. Plasmids

Bacterial plasmids containing the different lentiviral constructs used were generated using typical procedures of molecular biology. All the enzymes used during the cloning such as restriction enzymes, ligases, polymerases, kinases and phosphatases were obtained from New England Biolabs (Ipswich, USA). After each ligation, the resulting products were transformed in TOP10 bacteria (Invitrogen/Life Technologies/Thermo Fisher Scientific, Waltham, USA). Plasmid DNA was purified from selected colonies and analysed by restriction analysis.

4.1.1. CD18-LV cloning

Four different promoters were selected to drive the expression of the human CD18 cDNA (hCD18). Two of them are ubiquitous promoters, PGK and UCOE, and the other two are myeloid promoters, chimeric promoter (Chim) and MIM.

Chim promoter is a fusion of the *FES* and the *CTSG* minimal 5'-flanking regions (where the TATA box of the *CTSG* promoter is mutated in order to limit transcriptional initiation to the *FES* minimal promoter only). *CTSG* gene encodes a protein known as cathepsin G, which is a serine protease expressed during neutrophil maturation. *FES* gene codifies for a protein known as tyrosine-protein kinase Fes/Fps, which is implicated in the normal development of macrophages and neutrophils. Chim promoter drives a specific myeloid expression both in human cell lines and in mice, where the highest levels of expression are seen in $Gr\text{-}1^+$ and $CD41^+$ cells. A SIN LV expressing $gp91^{Phox}$ protein under the control of the Chim promoter has been successfully used for haematopoietic *ex vivo* GT in a mouse model of X-CGD[115] and has been proposed for a future clinical trial.

MIM promoter is a fusion of the promoter and the enhancer sequences of the chicken *LECT2* gene, containing several C/EBP-beta binding sites[164]. This gene encodes for a protein known as myeloid protein 1 (MIM-1), implicated in granulocytic differentiation. In a xenotransplantation model, where human $CD34^+$ cells were transduced with a lentiviral vector expressing GFP under the control of the MIM promoter, the highest levels of expression were observed in $CD15^+CD33^-$ and $CD15^+CD14^-$ neutrophils (Personal communication).

Ubiquitin chromatin opening elements (UCOEs) consist of methylation-free CpG islands surrounding dual divergently transcribed promoters of housekeeping genes[165]. These genetic elements have some characteristics that make them suitable for GT such as resistance to transcriptional silencing

and consistent and stable transgene expression in tissue culture systems[166]. The UCOE from the human *HNRPA2B1-CBX3* locus (A2UCOE) have been successfully used within the context of a SIN LV to drive the expression of IL2GR for *ex vivo* GT experiments in a mouse model of X1-SCID[167]. The A2UCOE promoter displays little or no methylation both *in vivo* and *in vitro* and can provide protection from methylation to other promoters when linked upstream[168-170].

The plasmids containing Chim, MIM and A2UCOE promoters, pCCL.Chim.GFP.Wpre*[115], pCCL.mim.gp91.Wpre* (data not published) and pHR'.A2UCOE.GFP[167] plasmid were kindly provided by Dr. Adrian Thrasher and Dr. Giorgia Santilli (Institute of Child Health – University College of London, London, United Kingdom). The plasmid containing the hCD18 (HsCD00044736) was obtained from Harvard PlasmID (Harvard Medical School, Boston, USA).

An ampicylin-resistant plasmid containing the pCCL SIN lentiviral backbone with an internal PGK promoter and the Wpre* sequence (pCCL.PGK.eGFP.Wpre*), kindly provided by Dr. Luigi Naldini (San Raffaele-Telethon Institute for Gene Therapy, Milan, Italy), was used to clone the four hCD18-LVs.

4.1.1.1. pCCL.PGK.CD18.Wpre* plasmid

A fragment containing the lentiviral backbone and the PGK promoter (7181 bp) was obtained by digestion of pCCL.PGK.eGFP.Wpre* plasmid (7929 bp) with *Bam*HI. The generated overhang ends were blunted using a T4 DNA polymerase. This fragment was treated with Antarctic phosphatase to prevent self-ligation. HsCD00044736 plasmid (4854 bp) was digested with *Psi*I to generate a blunt fragment containing the hCD18 (2370 bp). Both fragments were ligated with the T4 DNA Ligase and transformed in TOP10 bacteria to obtain the pCCL.PGK.CD18.Wpre* plasmid (Figure S1).

4.1.1.2. pCCL.Chim.CD18.Wpre* plasmid

Lentiviral backbone lacking the cPPT sequence (6500 bp) was obtained by digestion of pCCL.PGK.eGFP.Wpre* plasmid (7929 bp) with *Hpa*I and *Bam*HI restriction enzymes. On the other hand, a fragment containing Chim promoter together with the cPPT sequence (1021 bp) was obtained from the pCCL.Chim.GFP.Wpre* plasmid (8109 bp) by digestion with the same restriction enzymes. Both fragments were ligated with the T4 DNA Ligase and transformed in TOP10 bacteria to obtain the intermediate plasmid pCCL.Chim.Wpre*. This plasmid was digested with *Pst*I, and treated with Antarctic phosphatase to remove the 5´ phosphate and thus avoid self-ligation. HsCD00044736 plasmid (4854 bp) was digested with *Psi*I to generate a blunt fragment containing the hCD18 (2370 bp). Both fragments were ligated with the T4 ligase and transformed in TOP10 bacteria to obtain the pCCL.Chim.CD18.Wpre* plasmid (Figure S2).

4.1.1.3. pCCL.MIM.CD18.Wpre* plasmid

Lentiviral backbone lacking cPPT sequence (6500 bp) was obtained by digestion of pCCL.PGK.eGFP.Wpre* plasmid (7929 bp) with *Hpa*I and *Bam*HI restriction enzymes. On the other hand, a fragment containing MIM promoter together with the cPPT sequence (1283 bp) was obtained from the pCCL.mim.gp91.Wpre* plasmid (9486 bp) by digestion with the same restriction enzymes. Both fragments were ligated with the T4 DNA Ligase and transformed in TOP10 bacteria to obtain the intermediate plasmid pCCL.MIM.Wpre*. This plasmid was digested with *Sma*I to generate two blunt ends between the promoter and the Wpre* sequence. This fragment containing the lentiviral backbone and the promoter was then treated with Antarctic phosphatase. HsCD00044736 plasmid (4854 bp) was digested with *Psi*I to generate a blunt fragment containing the hCD18 (2370 bp). Both fragments were ligated with the T4 ligase and transformed in TOP10 bacteria to obtain the pCCL.MIM.CD18.Wpre* plasmid (Figure S3).

4.1.1.4. pCCL.A2UCOE.CD18.Wpre* plasmid

Lentiviral backbone (6648 bp) was obtained by sequential digestion of pCCL.PGK.eGFP.Wpre* plasmid (7929 bp) with *Eco*RV and *Xma*I restriction enzymes. On the other hand, a fragment containing A2UCOE promoter (2653 bp) was obtained from the pHR'.A2UCOE.GFP plasmid (11156 bp) following three steps: Digestion with *Eco*RI, generation of blunt ends with T4 DNA polymerase and digestion with *Age*I. *Xma*I and *Age*I are restriction enzymes that generate compatible cohesive ends. Both lentiviral backbone and promoter fragments were ligated with the T4 DNA Ligase and transformed in TOP10 bacteria to obtain the intermediate plasmid pCCL.A2UCOE.Wpre*. This plasmid was digested with *Eco*RV to generate two blunt ends and then treated with Antarctic phosphatase. HsCD00044736 plasmid (4854 bp) was digested with *Psi*I to generate a blunt fragment containing the hCD18 (2370 bp). Both fragments were ligated with the T4 ligase and transformed in TOP10 bacteria to obtain the pCCL.A2UCOE.CD18.Wpre* plasmid (Figure S4).

4.1.2. shRNA-LV cloning

Seven different shRNAs were designed against different regions of the human CD18 mRNA, including the coding DNA sequence (CDS) and the 3' UTR (Figure 19). A scrambled shRNA (shSCR) was previously generated in the laboratory that did not recognize any sequence in the human transcriptome. This sequence was obtained from the plasmid pSilencer 3.1-H1 puro (Ambion/Life Technologies/Thermo Fisher Scientific, Waltham, USA).

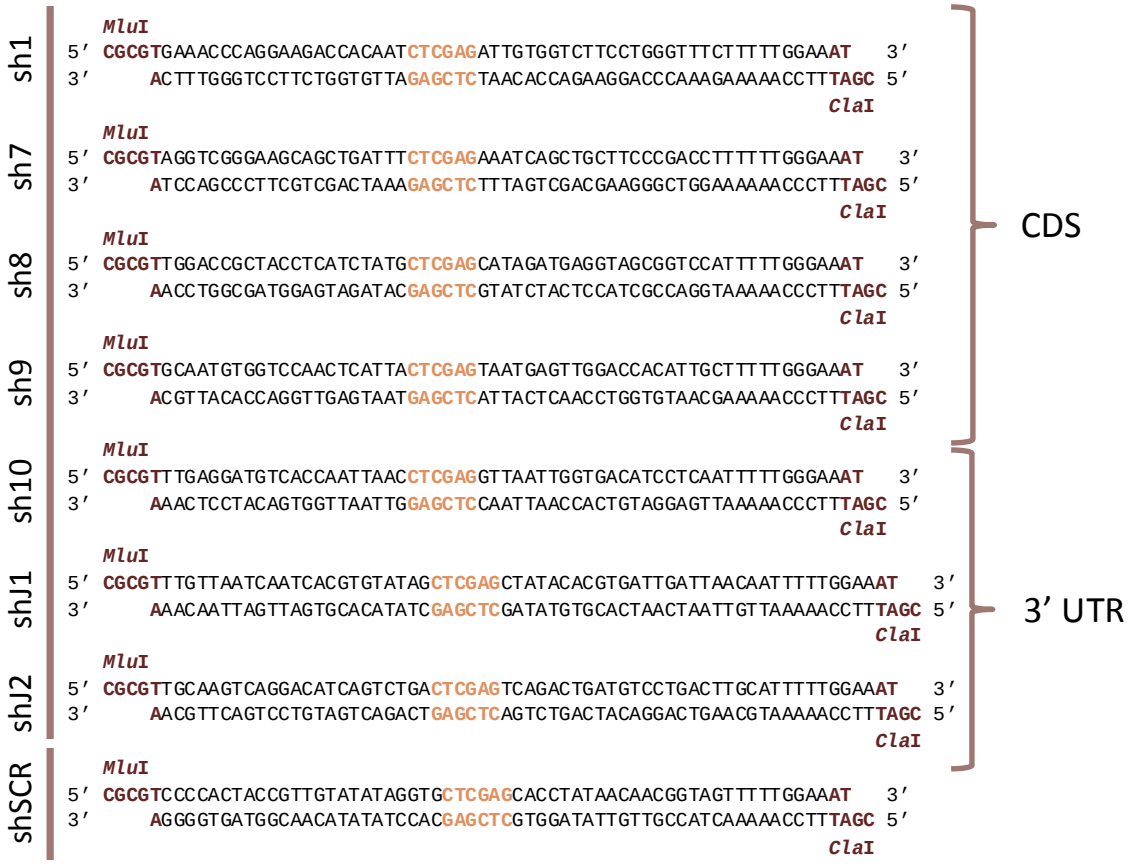

Figure 19. shRNA designed to recognised human CD18 mRNA. Nucleotides corresponding to the restriction sites used for cloning into the LVTHM backbone (*Mlu*I and *Cla*I) are marked in brown and nucleotides corresponding to the central loop are marked in orange. The shSCR was designed not to recognize any sequence of the human transcriptome so it could be used as a negative control.

All the designed shRNAs were cloned into the LVTHM plasmid[171,172]. This plasmid contains a lentiviral backbone where the shRNA expression cassette is incorporated into the 3' LTR. In this

cassette, the expression of the shRNA is driven by an H1 promoter and the presence of a TetO operator allows the regulation of the shRNA expression if desired. It also includes an EF1α promoter driving the expression of the eGFP reporter protein that allows an easy detection of the transduced cells (Figure 20).

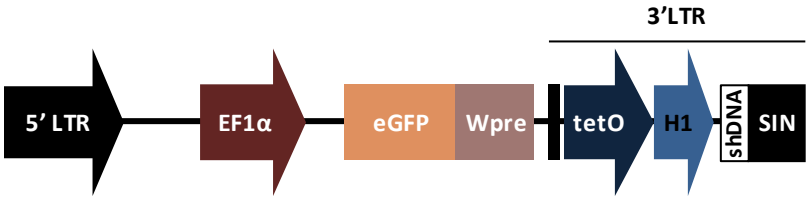

Figure 20. LVTHM Lentiviral Backbone containing an shRNA expression cassete in the 3' LTR

First of all, double-stranded DNA sequences (as described in Figure 19) were generated by using complementary oligonucleotides that were flanked by *Mlu*I and *Cla*I restriction sites. For that, oligos were mixed in annealing buffer (100 mM KCH_3COO; 30 mM HEPES pH7.4; 2 mM $Mg(CH_3COO)_2$) and hybridized at 95ºC for 4 min and then at 70ºC for 10 min. T4 polynucleotide kinase was subsequently used to transfer a P_i from the γ position of ATP to the 5´-hydroxyl terminus of the double-stranded DNA. Reaction was carried out at 37 ºC for 30 min and then the enzyme was inactivated at 70ºC for 10 min.

LVTHM plasmid was digested with *Mlu*I and *Cla*I and then dephosphorylated using Antarctic Phosphatase. Digested LVTHM and double-stranded inserts were ligated by the use of T4 DNA ligase (Figure S5).

4.2. Production of lentiviral vectors

All SIN LVs were generated by a second generation packaging system in which 293T cells were transiently transfected with the transfer, helper (pCMVdR8.74) and envelope (pMD2.VSVg) plasmids, obtaining VSV-G-pseudotyped lentiviral particles (Figure 21). The pMD2.VSVg and pCMVdR8.74 plasmids used were obtained from PlasmidFactory (Bielefeld, Germany). Transfections were performed on 293T cells at 70-80 % confluence in 150 mm diameter plates following the $CaCl_2$ DNA precipitation method previously described[104,173]. Briefly, culture medium was replaced for Iscove's Modified Dulbecco's Medium + GlutaMAX (IMDM, Gibco/Life Technologies/Thermo Fisher Scientific, Waltham, USA) supplemented with 10% Hyclone and 0.5% P/S one hour before transfection.

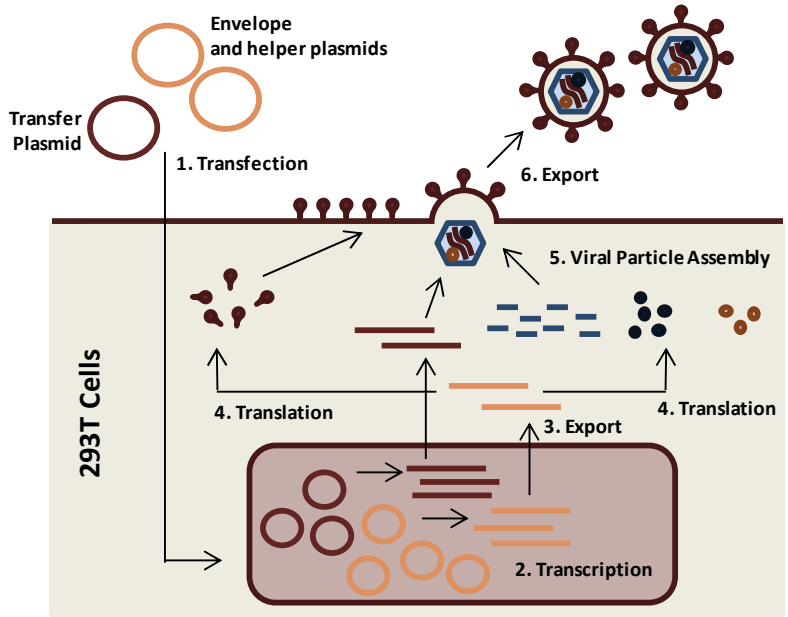

Figure 21. Second generation packaging strategy for lentiviral vector production.

The amounts described below correspond to one plate of 293T cells. Mixtures of the three plasmids were prepared freshly containing 40 µg of the corresponding transfer plasmid, 16.25 µg of the second generation pCMVdRd8.74 helper plasmid and 7 µg of the pMD2-VSV-G envelope plasmid. These mixtures were prepared in a final volume of 1125 µl of 0.1x Tris-EDTA buffer/dH_2O (2:1) per plate and then 125 µl of 2.5 M $CaCl_2$ were added. After 5 min incubation at RT, 1250 µl of 2x HBS buffer (100 mM HEPES, 281 mM NaCl, 1.5 mM Na_2HPO_4, pH 7.15) were added dropwise while vortexing at full speed, allowing the formation of Ca^{2+}/DNA^- precipitates. Immediately the total volume was added to the plates of 293T cells, which will subsequently phagocyte the precipitates. After 14 h, culture medium was replaced by fresh medium. Lentiviral supernatants were collected 24 and 48 h post-transfection, filtered through 0.1 µm pore-size filter (Milipore/Merck KGaA, Darmstadt, Germany) and concentrated by ultracentrifugation (25000 rpm, 2 h, 4 ºC). Viral pellets were then resuspended in StemSpam medium, quickly spun to eliminate insoluble junk, aliquoted and stored at -80 ºC.

4.3. Titration of lentiviral vectors

Viral titers were determined by infection of HT1080 cells with serial dilutions of the supernatants. $5x10^4$ cells/well were seeded in 24-well tissue culture plates the day before. The same day of the titration, cell number in each well was determined. Serial dilutions of the lentiviral supernatants were prepared in DMEM-based complete medium from 1:100 to 1:100000 and then used to infect the HT1080 cells. After 3 days, cells were collected.

4.3.1. Titration of GFP-containing lentiviral vectors

Those vectors containing a GFP-expressing cassette were titered in the base of their ability to express this reporter protein in HT1080 cells. Thus, collected cells were analysed by flow cytoemtry for the percentage of GFP^+ cells. Taking into account that the percentage of GFP^+ cells can only take values from 0 to 100, so with a high amount of lentiviral particles the system reaches saturation, only those dilutions giving rise to values with a linear distribution were used for the calculation. An average of two-three values was used as the final titer. The formula used for titer calculation is the following:

$$Viral\ titer\ (vp/mL) = \frac{cell\ number\ at\ the\ day\ of\ the\ infection * \%\ GFP^+\ cells * dilution\ factor}{100}$$

4.3.2. Titration of GFP-non containing lentiviral vectors

Those vectors not containing a GFP-expressing cassette were titered by Q-PCR. DNA was obtained from the infected HT1080 cells and then analysed for the VCN (see section 5). The titer was calculated for each dilution and then an average of them was used as the final titer. The formula used for titer calculation is the following:

$$Viral\ titer\ (vp/mL) = Cell\ number\ at\ the\ day\ of\ the\ infection * VCN * Dilution\ Factor$$

5. Quantitative PCR

Quantitative PCR (Q-PCR) was used in order to determine VCN in transduced murine and human cells (using gDNA as template) or to measure mRNA levels of hCD18 and hCD11a (using cDNA as template).

gDNA was extracted from a minimum of $5x10^5$ cells using NucleoSpin® Tissue (Macherey-Nagel, Duren, Germany). Total RNA was isolated using Trizol reagent (Ambion/Life Technologies/Thermo Fisher Scientific, Waltham, USA). 1 µg of total RNA was reverse transcribed into cDNA by the use of the RetroScript RT kit (Ambion/Life Technologies/Thermo Fisher Scientific, Waltham, USA).

gDNA/cDNA was further amplified by Q-PCR using specific primers (Table 11). Q-PCR

amplification was performed in a 7500 fast real-time PCR system (Applied Biosystems/Life Technologies/Thermo Fisher Scientific, Waltham, USA) using fast SYBR green PCR master mix or TaqMan. In the last case, the use of fluorescent probes was required (Table 12). After 95 ºC (20 s) incubation, amplification was performed as 40 consecutive cycles of 95 ºC (3 s) and 60 ºC (30 s). Primers were acquired from Grupo Taper (Alcobendas, Spain) and fluorescent probes were acquired from Sigma-Aldrich (St Louis, USA).

	Primer	Sequence (5' to 3')	Tm (ºC)
TaqMAN	PsiF	CAGGACTCGGCTTGCTGAAG	63
	PsiR	TCCCCCGCTTAATACTGACG	59
	AlbF	GCTGTCATCTCTTGTGGGCTG	64
	AlbR	ACTCATGGGAGCTGCTGGTTC	63
	TtnF	AAAACGAGCAGTGACGTGAGC	61
	TtnR	TTCAGTCATGCTGCTAGCGC	60
SyBR Green	hCD18F	CAGCAATGTGGTCCAACT	58
	hCD18R	GAGGGCGTTGTGATCCAG	58
	hCD11aF	GGGAATGAACCATTGACA	58
	hCD11aR	GCCAGCAACGAAGTCTTT	58
	GAPDHF	GGCATGGACTGTGGTCATGA	60
	GAPDHR	TGCACCACCAACTGCTTAGC	60

Table 11. List of Primers used for the different Q-PCR amplifications performed.

Probe	Sequence (5' to 3')	Tm (ºC)
PsiP	[6FAM]-CGCACGGCAAGAGGCGAGG-[BHQ1]	75.7
AlbP	[TxRd]-CCTGTCATGCCCACACAAATCTCTCC-[BHQ2]	73.9
TtnP	[TxRd]-TGCACGGAAGCGTCTCGTCTCAGTC-[BHQ2]	75.7

Table 12. List of fluorescent probes used in the TaqMan-based Q-PCR amplifications performed.

5.1. Vector copy number determination

The VCN is the parameter that indicates the number of integrated proviral copies per transduced cell. Proviral genome and host cell genome were amplified and quantified by TaqMAN-based multiplex Q-PCR. *Psi* packaging sequence was used to quantify viral genome while albumin gene (*Alb*) or titin (*Ttn*) gene were used to quantify human or murine genome respectively.

Quantification of viral and cell genomes was performed by interpolating the cycle threshold values (Ct) from the gDNA samples into a standard curve with ten-fold dilutions of plasmids containing known copies of both relevant sequences: *Psi/Alb* (contained in the pRRL.PGK.eGFP/Alb plasmid) and *Psi/Ttn* (pRRL.PGK.eGFP/Ttn). Both plasmids were kindly provided by Dr. Sabine Charrier (Genethon, Evry, France). Cell number corresponding to the calculated number of *Alb* or *Ttn* copies was determined assuming that each cell contains two copies of them. VCN was finally calculated as:

$$VCN\ (proviral\ copies/cell) = \frac{number\ of\ proviral\ copies}{\left(\frac{number\ of\ Alb\ or\ Ttn\ copies}{2}\right)}$$

5.2. Relative expression of hCD18 and hCD11a

Gene expression was calculated in based on ΔΔCt calculation, which yields a normalized and relative gene expression value. This is accomplished by normalization of the gene of interest to an endogenous reference gene whose expression is considered to be invariable among samples. Afterwards, this value is normalized to the gene expression detected in a separate control sample.

hCD18 and hCD11a expression in transduced lymphoblastoid cells and $CD34^+$ cells was normalized to GAPDH reference gene expression levels within the same sample to determine ΔCt. This

step serves to correct for non-treatment-related variation among wells such as potential differences in cell number.

$$\Delta\mathrm{Ct} = Ct\ GOI - Ct\ GAPDH$$

This value was exponentially transformed and normalized to the expression of hCD18 and hCD11a respectively in untransduced cells.

$$\text{Relative expression } (\Delta\Delta\mathrm{Ct}) = \frac{2^{(\Delta\mathrm{Ct}^{transduced\ cells})}}{2^{(\Delta\mathrm{Ct}^{untransduced\ cells})}}$$

6. Statistical analysis

The statistical analysis was performed using GraphPad Prism version 5.00 for Windows (GraphPad Software, San Diego, USA, www.graphpad.com). For the analyses we performed a non-parametric Mann-Whitney test or Kruskal-Wallis test. The significances are expressed as P<0.0001(****), P<0.001(***), P<0.01(**) or P<0.05(*).

Results

1. Haematopoietic characterization of CD18^{HYP} mice

1.1. Study of the LAD-1 phenotype

1.1.1. Haematological counts

LAD-I human patients and different LAD-I animal models have a characteristic increment of circulating leukocytes in PB. We studied absolute numbers of total leukocytes, lymphocytes and granulocytes in PB samples from CD18^{WT} and CD18^{HYP} mice. As shown in Figure 22, all the parameters were statistically increased in CD18^{HYP} PB samples in comparison with CD18^{WT} PB samples

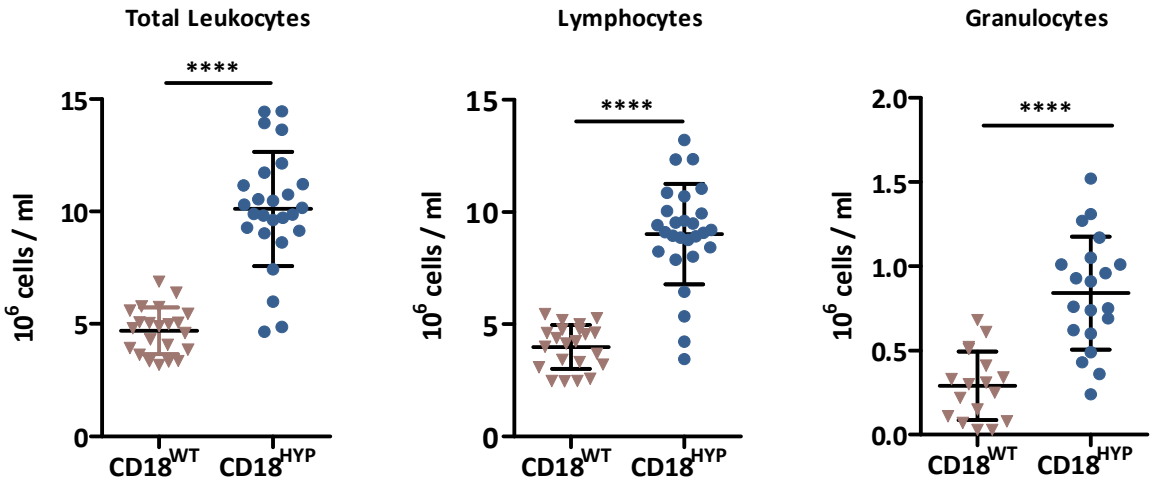

Figure 22. Haematological counts for total leukocytes, lymphocytes and granulocytes in CD18^{WT} and CD18^{HYP} mice PB samples. The significance of differences between groups are expressed as P<0.0001 (****).

1.1.2. β_2-integrins expression in peripheral blood leukocytes and total bone marrow cells

Peripheral blood leukocytes (PBLs) from CD18^{WT} and CD18^{HYP} mice were analysed by flow cytometry for the expression of the β_2 common subunit (CD18) and the three different α subunits that are associated with it (CD11a, CD11b and CD11c).

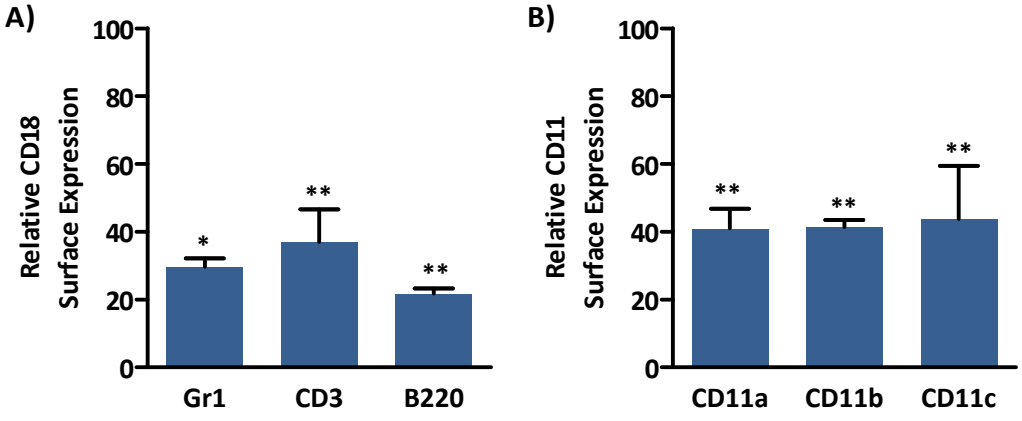

Figure 23. Expression of β_2-integrins subunits in CD18^{HYP} mice PBLs relative to the expression found in CD18^{WT} mice PBLs. A) Relative CD18 surface expression in granulocytes (Gr-1), T cells (CD3) and B cells (B220) from CD18^{HYP} mice. B) Relative CD11a, CD11b and CD11c surface expression in PBLs from CD18^{HYP} mice. The significance of differences between CD18^{HYP} and CD18^{WT} expression is expressed as P<0.05 (*) and P<0.01 (**).

CD18 expression was analysed in three different subpopulations of PBLs (T cells, B cells and granulocytes), that were identified on the basis of their characteristic expression of surface markers CD3, B220 and Gr-1 respectively (Figure 23). An 80% reduction in CD18 surface expression levels was

found in B cells from CD18^{HYP} mice in comparison with CD18^{WT} mice while 70% and 63% reductions in CD18 expression levels were found in granulocytes and T cells respectively compared with CD18^{WT} mice (Figure 25A). In line with these results, expression levels obtained for the three analysed α subunits (CD11a, CD11b and CD11c) were approximately 40% of the expression levels found in CD18^{WT} PBLs (Figure 25B). Not only expression levels but also proportion of β_2-integrins expressing cells was reduced in CD18^{HYP} mice in comparison with CD18^{WT} mice, apart from Mac-1$^+$ cells (CD18$^+$/CD11b$^+$) that were slightly increased (Figure 24).

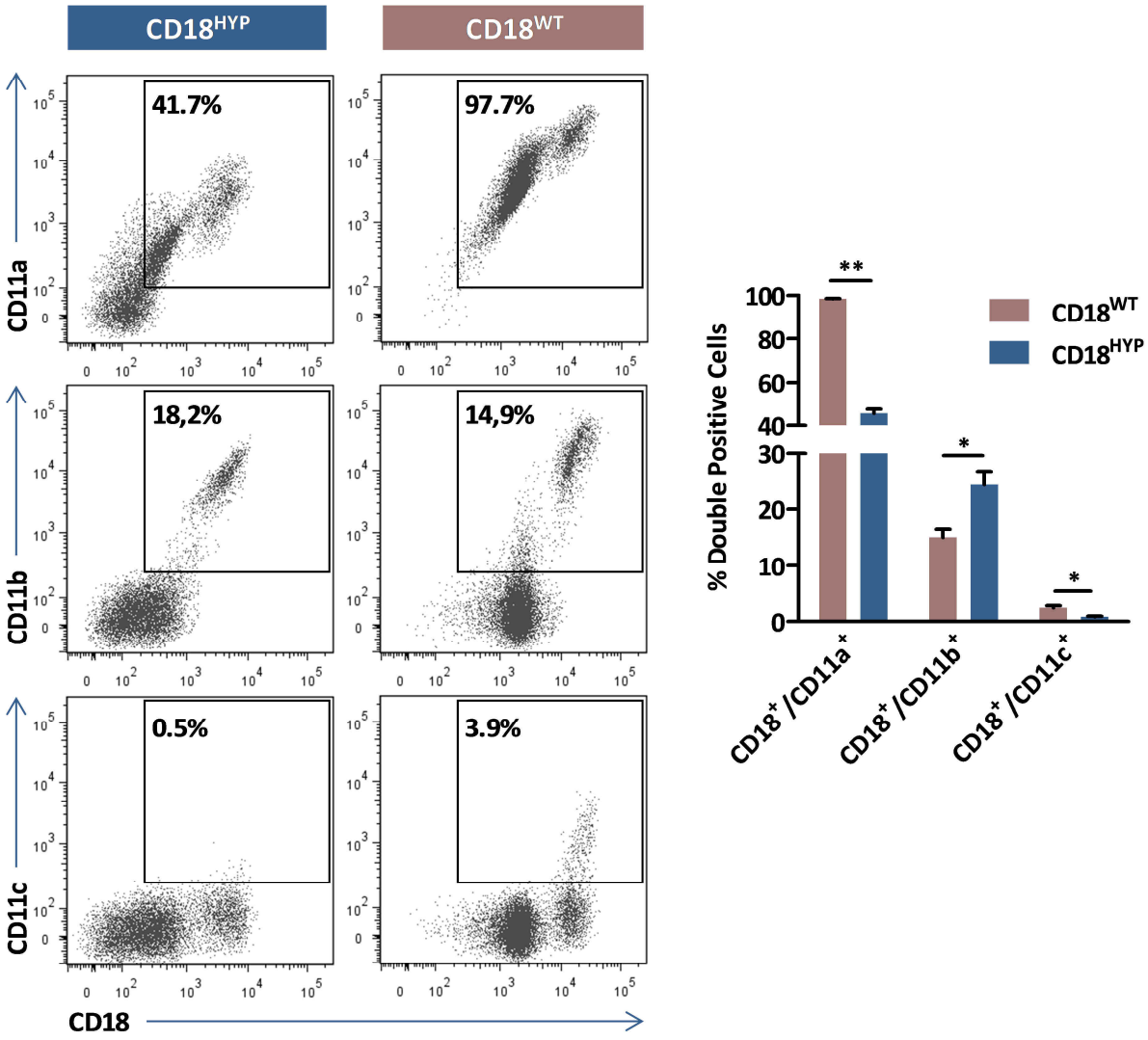

Figure 24. Flow cytometry analysis of the expression of β_2-integrins in PBLs. A) Dot Plots from representative CD18^{WT} and CD18^{HYP} mice PB samples. B) Percentage of β_2-integrins$^+$ cells in the studied mice groups. The significance of differences between groups is expressed as P<0.05 (*) and P<0.01 (**).

The same analysis was performed in bone marrow cells (BMCs) from CD18^{WT} and CD18^{HYP} mice (Figure 25). A similar reduction of that observed in PBLs was noticed in BMCs for the four β_2-integrins subunits from CD18^{HYP} mice in comparison to CD18^{WT} mice.

1.1.3. LFA-1 and VLA-4 expression in mouse haematopoietic progenitors

After confirming a deep reduction of β_2-integrins expression in mature PBLs and in total BMCs, mouse haematopoietic progenitors (LSK cells) from CD18^{WT} and CD18^{HYP} mice were interrogated for the expression of LFA-1 (CD18/CD11a) and the expression of the β_1-integrin VLA-4 (CD24/CD49d) (Figure 26A). Almost all LSK cells from CD18^{WT} and CD18^{HYP} mice expressed both VLA-4 subunits. In the case of LFA-1 integrin, only a tiny population of LSK cells from CD18^{HYP} mice expressed CD18 and CD11a

subunits while 80% of LSK cells from the $CD18^{WT}$ mice expressed both subunits.

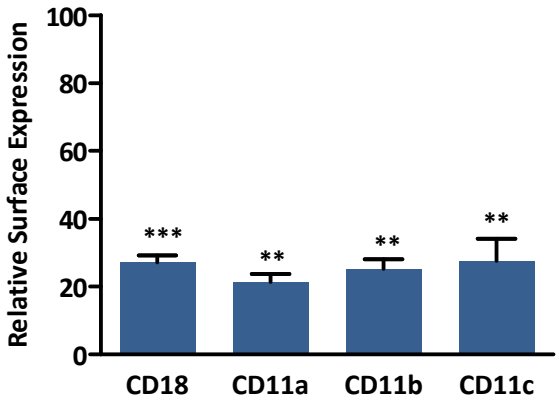

Figure 25. Relative surface expression of β_2-integrin subunits (CD18, CD11a, CD11b and CD11c) in BMCs from $CD18^{HYP}$ mice normalized to that of BMCs from $CD18^{WT}$ mice. The significance of differences between $CD18^{HYP}$ and $CD18^{WT}$ expression is expressed as P<0.01 (**) and P<0.001 (***).

The small LFA-1-expressing population of LSK cells in $CD18^{HYP}$ mice displayed a marked reduction in expression levels of CD18 and CD11a in comparison with $CD18^{WT}$ mice while no differences in CD29 and CD49a expression levels were observed between groups (Figure 26B).

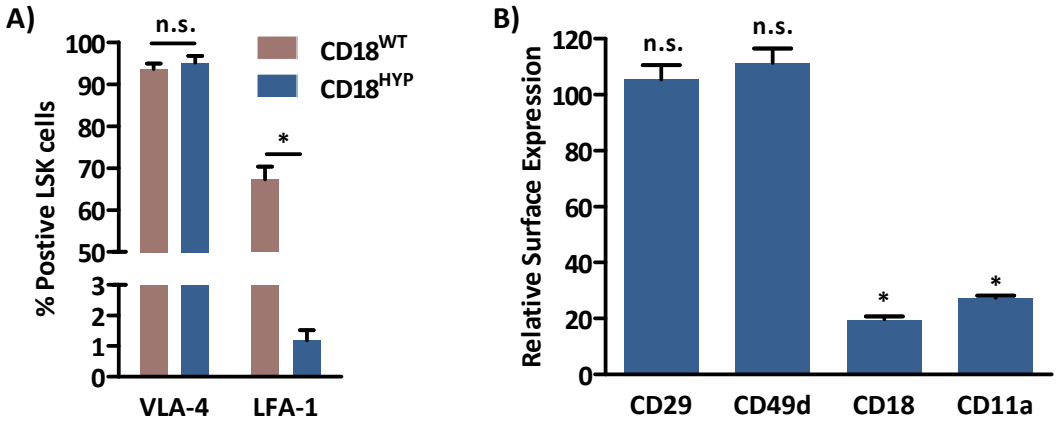

Figure 26. Flow cytometry analysis of LFA-1 and VLA-4 expression in LSK cells from $CD18^{WT}$ and $CD18^{HYP}$ mice. A) VLA-4^+ and LFA-1^+ LSK cells found within BM of $CD18^{WT}$ and $CD18^{HYP}$ mice. B) Relative surface expression of VLA-4 subunits (CD29 and CD49d) and LFA-1 subunits (CD18 and CD11a) in LSK cells from $CD18^{HYP}$ mice normalized to that of LSK cells from $CD18^{WT}$ mice. The significance of differences between groups is expressed as P<0.05 (*).

1.1.4. Study of neutrophil migration capacity in a LPS-induced asthma model

As a consequence of *ITGB2* mutations, leukocytes (mainly neutrophils) from LAD-I patients are unable to extravasate from PB to the infection sites. In order to confirm if the partial reduction of β_2-integrins expression in $CD18^{HYP}$ mice give rise to an impaired neutrophil migration capacity, $CD18^{WT}$ and $CD18^{HYP}$ mice were subjected to a LPS-induced asthma model. In this assay, mice were intranasally treated with LPS or PBS (as an untreated control). 24 hours later BAL was performed to collect the content of the epithelial lining fluid and determine the cellular composition of the pulmonary airways. In this context, the BAL fluid is mainly composed by alveolar macrophages ($Ly6G^{LOW}/CD11c^+$) and neutrophils ($Ly6G^{HIGH}/CD11c^-$) (Figure 27A). Cell count was determined and the percentage of neutrophils was analysed by flow cytometry in order to calculate the absolute number of neutrophils that had migrated to the lungs in response to the LPS stimulus (Figure 27B). A 55% reduction in the neutrophil migration capacity was observed in $CD18^{HYP}$ mice in comparison with $CD18^{WT}$ mice, indicating that the observed partial reduction of β_2-integrins expression is sufficient to generate a LAD-I phenotype in $CD18^{HYP}$ mice.

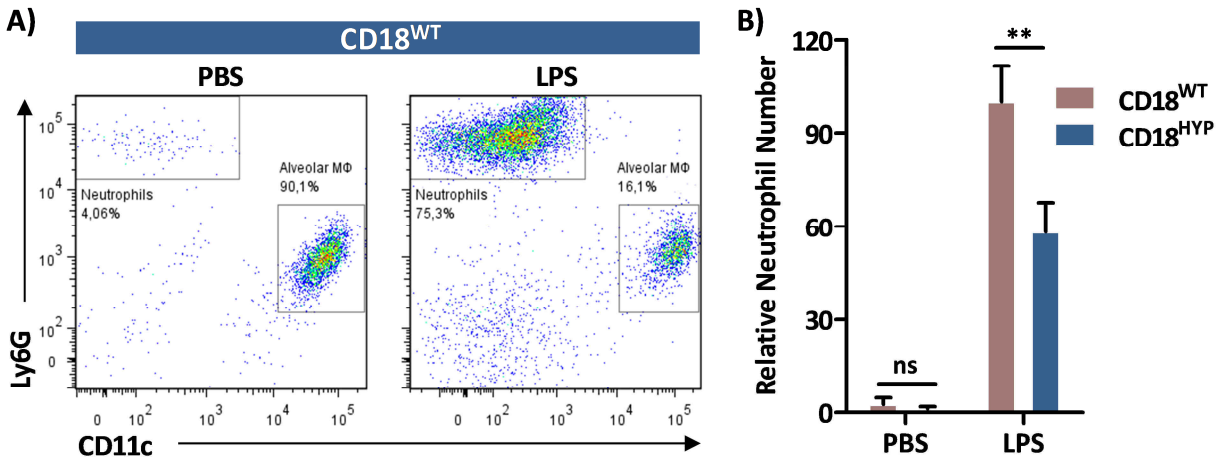

Figure 27. LPS-induced asthma model. A) Representative flow cytometry analysis of the hematopoietic population that can be found in a BAL from $CD18^{WT}$ mice treated intranasaly with PBS and LPS respectively. B) Relative numbers of neutrophils collected by BAL. Total collected cells were counted with the haemocytometer and the proportion of neutrophils was determined by flow cytometry to determine absolute number of neutrophils. Relative number of neutrophils in $CD18^{HYP}$ vs. $CD18^{WT}$ is shown. The significance of differences between groups is expressed as P<0.01 (**).

1.1.5. Study of neutrophil migration in the air pouch model

Ding et al[174] described defects in neutrophil migration to a subcutaneous air pouch (AP) in response to TNF-α in $CD11a^{-/-}$ and $CD18^{KO}$ in comparison to WT animals. We performed a similar comparison with $CD18^{HYP}$ and $CD18^{WT}$ mice. Four hours after TNF-α injection, the content of the AP was collected and analysed. $CD18^{WT}$ animals were able to mount a proper inflammatory response after TNF-α stimulus as observed by the increment of the leukocyte emigration ratio (Figure 28). On the contrary, no significant difference in the emigration ratio was observed between TNF-α and vehicle group in $CD18^{HYP}$ mice. These results indicated that $CD18^{HYP}$ leukocytes are not able to migrate to a subcutaneous air pouch in response to TNFα stimulus. This migration defect was more pronounced when the emigration ratio was studied in the neutrophil population. Interestingly, the neutrophil emigration ratio was also decreased in basal conditions in $CD18^{HYP}$ mice in comparison with $CD18^{WT}$ mice.

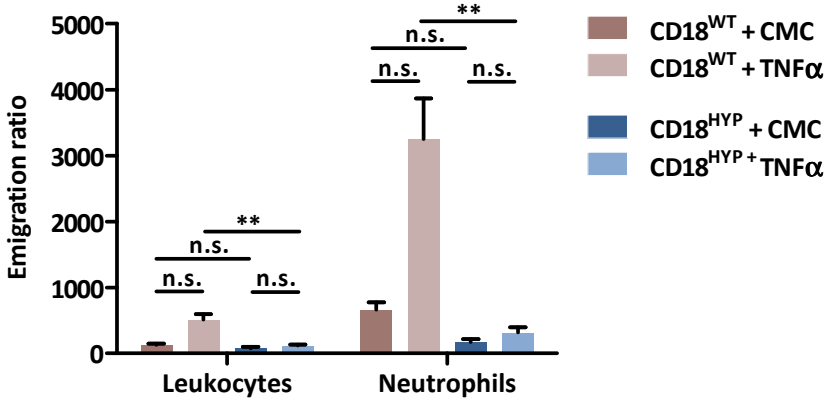

Figure 28. TNFα-induced inflammation model in a subcutaneous AP. The emigration ratios for total leukocytes and neutrophils are shown. The significance of differences between groups is expressed as P<0.01 (**).

1.2. Study of the role of β_2-integrins in the regulation of haematopoietic stem cells

1.2.1. In vitro analyses of the haematopoietic stem cell content in $CD18^{HYP}$

Adhesion molecules can play roles other than their canonical functions during the LAC. Mice

with mutations in different selectin genes have been recently described to present a higher content of haematopoietic progenitors[18]. To study the impact of *Itgb2* mutations in the BM HSC content, BM samples from $CD18^{WT}$ and $CD18^{HYP}$ mice were interrogated by flow cytometry for the percentage of LSK cells (Figure 29). A 2.1-fold increase in the percentage of LSK cells was in $CD18^{HYP}$ mice in comparison with $CD18^{WT}$ mice, while no changes in cellularity were observed between these mice. A similar enrichment in BM LSK cells was observed in another adhesion molecule-deficient mouse model, PEdKO, which is a knock-out model for P- and E-Selectins. Although the role of adhesion molecules such as integrins or selectins in mature leukocytes have been extensively studied and described, little is known regarding its possible function in HSCs.

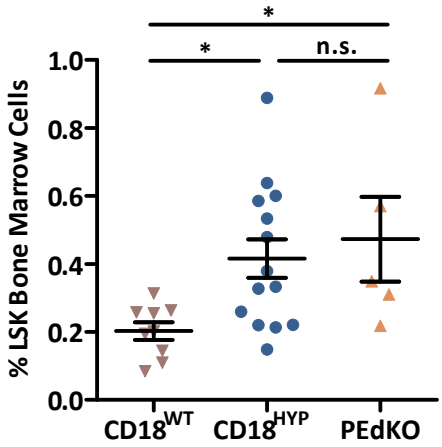

Figure 29. Proportion of HSCs with LSK phenotype in BM samples from $CD18^{WT}$ and $CD18^{HYP}$ mice. The significance of differences between groups is expressed as P<0.05 (*).

A more detailed study of the HSCs content was performed by flow cytometry using a complex panel of surface markers that allowed us to distinguish three subpopulations inside the LSK population: LT-HSCs, ST-HSCs and MPPs (Figure 30). A significant increment in the proportion of LT-HSCs and ST-HSCs and a non-significant increment in the MPP were observed in BM samples from $CD18^{HYP}$ mice in comparison with $CD18^{WT}$ mice.

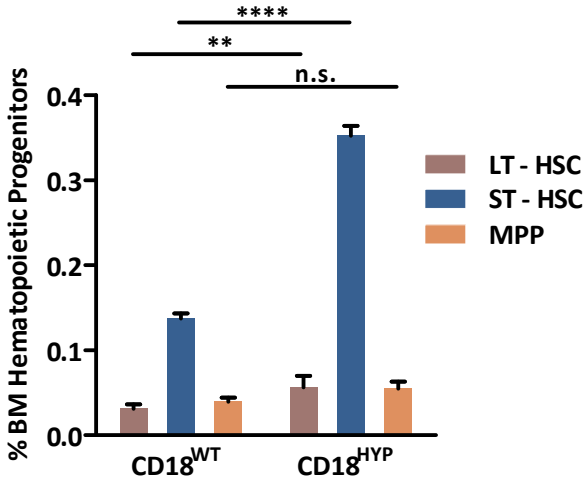

Figure 30. Flow cytometry characterization of different subpopulations of LSK cells from $CD18^{HYP}$ and $CD18^{WT}$ mice: long-term haematopoietic stem cells (LT-HSC), short-term haematopoietic stem cells (ST-HSC) and multipotent progenitors (MPP). Specific markers are shown in Materials and Methods Section. The significance of differences between groups are expressed as P<0.01 (**) and P<0.0001 (****).

Clonogenic studies in methylcellulose were performed with BMCs and MACS-sorted Lin^- cells from $CD18^{WT}$ and $CD18^{HYP}$ mice. In both cases, $CD18^{HYP}$ samples gave rise to a higher number of CFUs in

comparison with $CD18^{WT}$ samples (Figure 31).

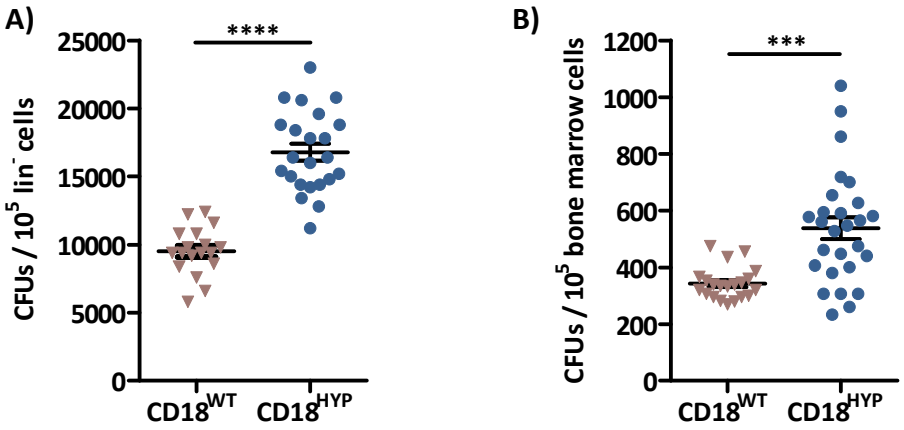

Figure 31. Analysis of the haematopoietic progenitor content in 6 week-old $CD18^{WT}$ and $CD18^{HYP}$ mice. The number of CFUs present in purified lin^- (Panel A) and total BMCs (Panel B) from $CD18^{WT}$ and $CD18^{HYP}$ mice is shown. The significance of differences between groups is expressed as P<0.0001(****) and P<0.001(***).

1.2.2. In vivo quantification of haematopoietic stem cells by limiting dilution assay

The LDA, which is considered the gold standard method to assess the HSC content, is based on the fact that it is possible to estimate the number of HSCs by injection of distinguishable cell mixtures of a control and the population of study into irradiated recipients. In these mixtures, the proportion of the population of the study is progressively reduced. After transplantation, the percentage of differentiated cells produced by the population of the study is used to estimate the number of HSCs.

	$CD18^{WT}$		$CD18^{HYP}$	
Transplanted Cell number	*Tested*	*Positive*	*Tested*	*Positive*
500,000	4	4	4	4
150,000	4	4	7	7
50,000	5	5	5	5
25,000	7	3	5	3
15,000	4	2	7	4
HSC Frequency	1/26,054		1/18,769	
P value	0.483			

Table 13. LDA with $CD18^{HYP}$ and $CD18^{WT}$ BMCs. The table summarizes the number of tested and positive animals for each of the transplantation groups, the estimated frequency of HSCs and the statistical analysis.

Five doses of BMCs from $CD18^{HYP}$ and $CD18^{WT}$ were transplanted (together with a radioprotective dose of BMCs) into lethally irradiated P3B mice. At 3 mpt, levels of CD45.2 (corresponding to the population of study) were determined within myeloid and lymphoid populations (see Materials and Methods section 1.3.2.). Based on these results, positive engrafted animals (>1% of both myeloid and lymphoid donor cells) were identified (Table 13). ELDA analysis performed on these results allowed us to estimate the frequency of HSCs within the initial dose of transplanted BMCs. There was a trend for HSCs to be more frequent within CD18-defficient BMCs (1/18,769) than in CD18-proficient BMCs (1/26,054), although these results were not statistically significant.

1.2.3. Characterization of $CD18^{HYP}$ LSK cells: Cell cycle, apoptosis and homing capacity

LSK cells were evaluated for their cell cycle and apoptosis status by co-staining with Hoechst 33342 and Pyronin Y. Hoechst 33342 is an exclusive DNA dye while Pyronin Y reacts with both DNA and RNA, but in the presence of Hoechst 33342, Pyronin Y reaction with DNA is blocked, so Pyronin Y stains only RNA. This staining allowed us to distinguish among cells in G_0, G_1, and $S+G_2+M$ cell cycle phases. A

significant increase in the proportion of LSK cells in G_0 phase was found in $CD18^{HYP}$ mice BM samples (Figure 32A), while no significant differences were found in the proportion of LSK cells in the rest of the cell cycle phases. This result indicated that CD18 deficiency leads to an enrichment in quiescent HSCs.

The role of CD18 in the regulation of apoptosis in neutrophils has been extensively studied. The engagement of β_2-integrin Mac-1 on neutrophils can either inhibit or enhance apoptosis depending on the activation state of the integrin and the presence of proapoptotic stimuli. $Gr1^+$ BMCs were stained with a fluorescent AV conjugate, with a high affinity for phosphatidylserine, which is translocated from the inner to the outer leaflet of the plasma membrane in apoptotic cells. $Gr1^+$ BMCs from $CD18^{HYP}$ mice have reduced levels of apoptosis compared to WT cells, as previously described for mature circulating neutrophils (Figure 32B). Apoptotic cells are characterized by a reduced DNA content due to that fragmented DNA leak out of the cells. Thus, apoptotic LSK cells were identified as the $subG_0$ population. We did not detect any difference in the proportion of $SubG_0$ cells in BM LSKs, suggesting that CD18 does not play a role in the regulation of apoptosis in HSCs (Figure 32A).

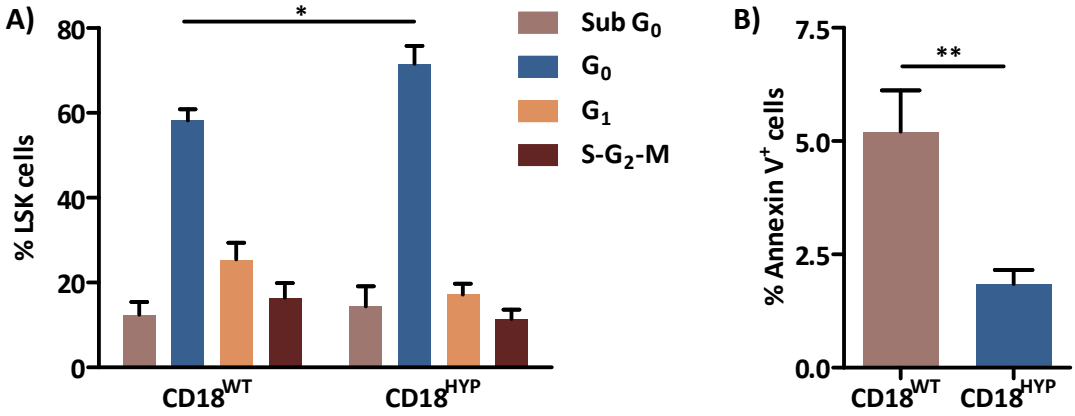

Figure 32. Apoptosis and cell cycle status in BMCs from $CD18^{WT}$ and $CD18^{HYP}$ mice. A) Cell cycle study of LSK cells by co-staining with Hoechst 33342 and Pyronin Y. B) Apoptosis study of $Gr\text{-}1^+$ BMCs by AV staining. The significance of differences between groups are expressed as $P<0.05$ (*) and $P<0.01$ (**).

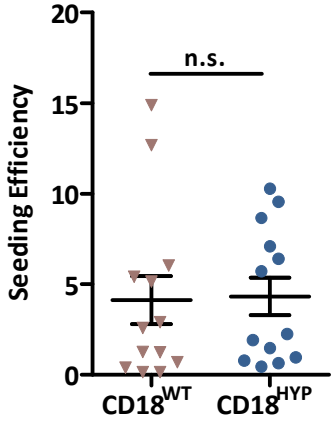

Figure 33. Seeding efficiency of FACS-sorted and DiD-stained BM LSK cells from $CD18^{HYP}$ or $CD18^{WT}$ mice intravenously transplanted into lethally irradiated WT recipients.

Although current data indicate that β_2-integrins do not play a direct role in HSC homing, it has been described that if the function of β_1-integrins is compromised, defects in β_2-integrin expression lead to a synergistic impairment in HSC homing[78,175]. To determine whether the seeding efficiency was affected in $CD18^{HYP}$ HSCs, BM samples were obtained from $CD18^{HYP}$ or $CD18^{WT}$ mice and LSK cells were FACS-sorted. These cells were stained with DiD and subsequently intravenously administered into lethally irradiated WT recipients. These animals were culled after 16 h and their BMCs were collected to

detect homed DiD^{+} LSK cells. We found that defective CD18 expression in HSCs has no effect on their homing capacity in irradiated CD18^{WT} recipients (Figure 33).

1.2.4. Regulation of the haematopoietic stem cell compartment by aged neutrophils clearance

Clearance of PB aged neutrophils to the BM has recently been described to play an important role in mouse HSC regulation[18]. P- and E-selectin deficiency affects neutrophil migration back to the BM leading to enrichment in HSCs as observed in PEdKO mice. Aged neutrophils are defined in PB by high expression levels of CXCR4 and low levels of CD62L (Ly6G^{+} CXCR4^{high} CD62L^{low}).

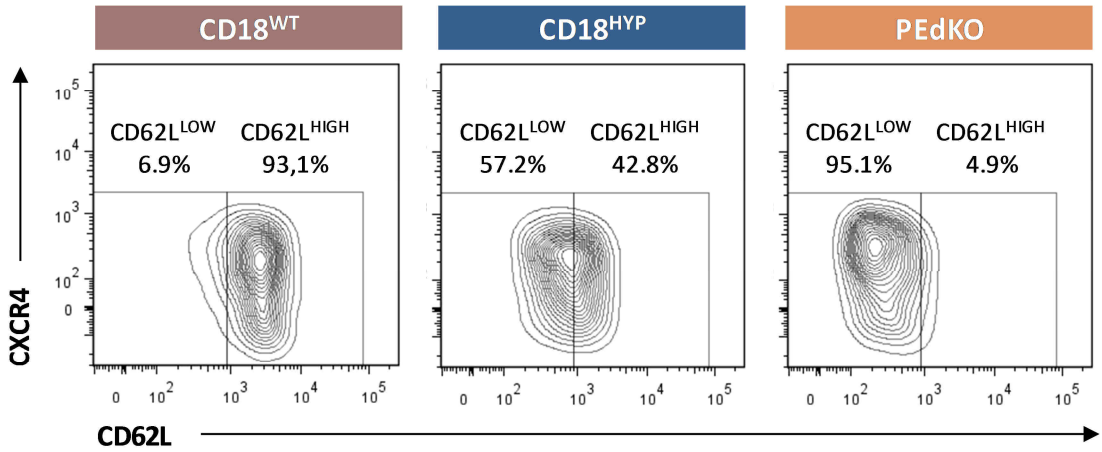

Figure 34. FACS analysis of aged neutrophils (Ly6G^{+} CXCR4^{high} CD62L^{low}) in representative PB samples from PEdKO, CD18^{HYP} and CD18^{WT} mice.

PB samples from PEdKO, CD18^{HYP} and CD18^{WT} mice were analysed for the presence of aged neutrophils (Figure 34). While a small proportion of aged neutrophils could be detected in CD18^{WT} mice (7%), PEdKO mice presented a huge accumulation of these cells (95%). In the case of CD18^{HYP} mice, we could observe an intermediate situation between PEdKO and CD18^{WT} (57%), likely due to the reduced but detectable presence of β_2-integrins expression. This result suggested that clearance of CD18-defective neutrophils to the BM was partially impaired in comparison with CD18^{WT} mice.

To clarify if the partial accumulation of aged neutrophils in the PB of CD18^{HYP} is responsible for the observed HSC enrichment in the BM, we carried out an experiment where *ex vivo* senesced WT neutrophils were daily transferred during 5 days into CD18^{HYP} mice. If the observed HSCs enrichment in CD18^{HYP} BM occurs as a consequence of the lack of the signalling pathway initiated by the clearance of aged neutrophils to the BM, the transfer of WT neutrophils, which are able to properly migrate back to the BM, should restore a normal proportion of LSK cells. At day 6, BMCs were collected and the percentage of LSK cells was determined. As shown in Figure 35A, no significant differences were detected in the proportion of LSK cells among non-treated, PBS-treated or neutrophil-transferred CD18^{HYP} mice.

Donor neutrophils were purified from the BM of P3B mice (CD45.1) with a purity of 85.5±2.7 of Ly6G^{+} cells (Figure 17). To discard the possibility that donor neutrophils samples could have some contaminating LSK cells that could have homed in the recipient BM, thus masking a possible reduction in the proportion of LSK cells after WT neutrophil transference, we analysed the presence of donor cells in the recipient BM. Although it was possible to detect donor cells within recipient BM by the analyses of CD45.1^{+} cells, no CD45.1^{+} donor LSK cells were detected (Figure 35B). All together, these results indicate that the HSC enrichment observed in CD18^{HYP} mice BM is not caused by defects in neutrophil extravasation and that, in this particular mouse strain, other factors should play a role in the observed

HSC phenotype.

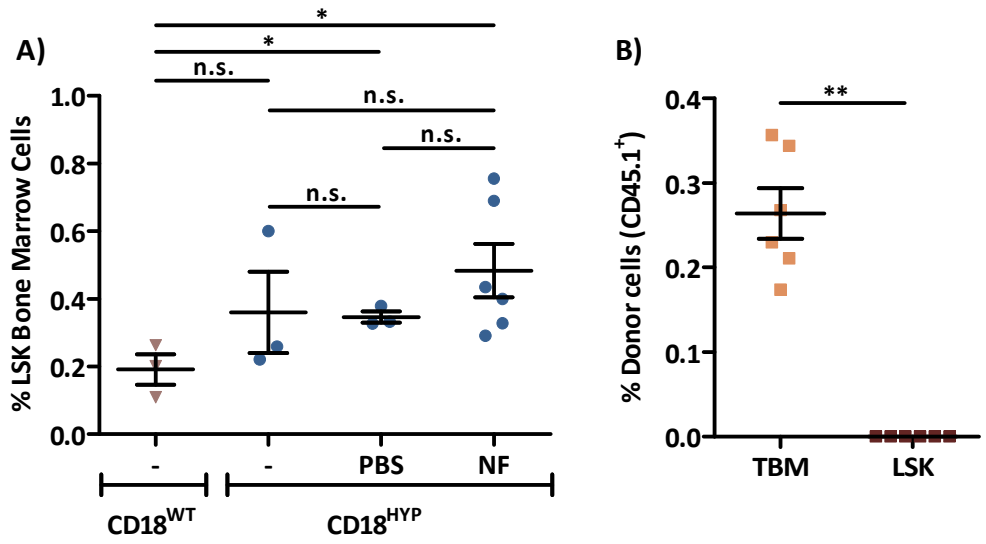

Figure 35. A) Determination of LSK cell proportion in non-treated (-) $CD18^{WT}$ mice and non-treated (-), PBS-treated (PBS) and neutrophils-transferred (NF) $CD18^{HYP}$ mice. B) Analysis of donor cells in the BM of neutrophil-transferred $CD18^{HYP}$ mice. The significance of differences between groups are expressed as P<0.05 (*) and p<0.01 (**).

1.2.5. Competitive repopulation assays

As clearance of aged neutrophils seemed not to be the mechanism responsible for the HSC enrichment observed in the BM of the $CD18^{HYP}$ mice, we decided to study whether this HSC enrichment could be due to other factors. CD18 deficient expression in HSCs could affect their interaction with other BMCs in the niche or could mediate an autonomous effect on HSCs self-renewal. In order to study the different possible mechanisms involved in the observed phenotype we conducted *in vivo* CRAs. In this kind of experiments, two different competitor populations of haematopoietic repopulating cells (total BMCs, lin^- cells, purified HSCs…) are mixed and transplanted together in conditioned recipients, thus making possible to study which is the contribution of each competitor population to the recipient haematopoiesis. To this aim, we mixed together different populations of haematopoietic cells from $CD18^{HYP}$ and $CD18^{WT}$ mice to evaluate the repopulation properties of CD18-defficient HSCs. In our case P3B-ΔhCD4 mice, which were previously generated in the laboratory[149], were used as a $CD18^{WT}$ BM competitor population and P3B mice as WT recipients. These mice express a truncated hCD4 protein (ΔhCD4) as a panleukocytic marker. In combination with the classical CD45.1 and CD45.2 markers, ΔhCD4 detection allowed us to distinguish both competitor populations and the possible remaining endogenous haematopoiesis (see Materials and methods for the identification of the different populations on the basis of these surface markers).

We performed two different CRAs where total BMCs or purified lin^- cells from $CD18^{HYP}$ and $CD18^{WT}$ mice were mixed at the same proportion and transplanted into lethally irradiated WT recipients (Table 14). Donor chimerism levels were evaluated both in PB and BM.

	Cell type	Proportion $CD18^{WT}/CD18^{HYP}$	Administered cell dose
Experiment 1	Total BMCs	50:50	$3x10^6$
Experiment 2	Lin^- cells	50:50	$3x10^5$
Experiment 3	Total BMCs	70:30	$3x10^6$

Table 14. Competitive repopulation assays performed with haematopoietic repopulating cells from $CD18^{WT}$ and $CD18^{HYP}$ mice.

In the first experiment, a mixture of total BMCs from $CD18^{HYP}$ and $CD18^{WT}$ at the same proportion was used to transplant lethally irradiated WT recipients. Four months after transplantation, primary recipients were culled and their BMCs were collected and transplanted into secondary

recipients. The study of donor chimerism levels in PB revealed a higher contribution of CD18^{HYP} cells to the haematopoietic reconstitution of recipient mice (Figure 36A). CD18-deficient derived haematopoiesis increased over time in PB and increased from primary to secondary recipients. Donor chimerism was also evaluated in total BMCs and in BM-derived CFUs, showing that CD18-deficient cells represented more than 80% of the cellularity in these populations (Figure 36B).

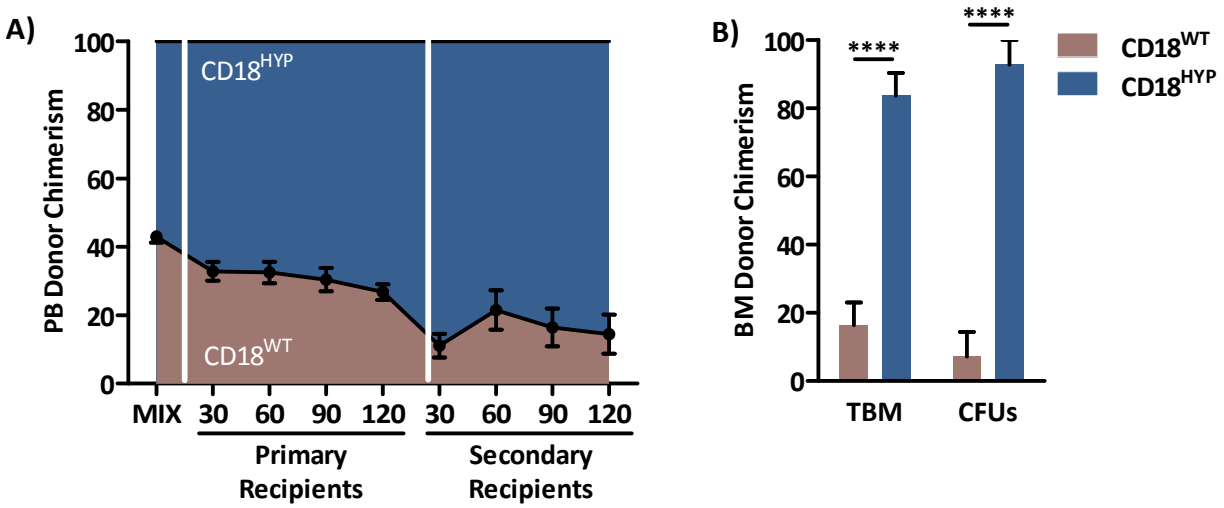

Figure 36. Donor chimerism levels in lethally irradiated WT (P3B) animals transplanted with a mixture of BMCs from CD18^{HYP} and CD18^{WT} (P3B-ΔhCD4) mice at the same proportion. A) PB donor chimerism levels in primary and secondary recipients. B) Donor chimerism levels in total BMCs and BM-derived CFUs in primary recipients 4 months after transplantation. The significance of differences between groups is expressed as P<0.0001 (****).

In a second experiment, BM-derived purified lin$^-$ cells from CD18^{HYP} and CD18^{WT} mice were mixed at the same proportion and then transplanted into lethally irradiated WT recipients. The use of lin$^-$ cells, which represent a BM population enriched in haematopoietic progenitors, resulted in a much higher contribution of CD18-deficient cells to the haematopoietic reconstitution of recipient mice, both in PB (Figure 37A) and BM (Figure 37B)

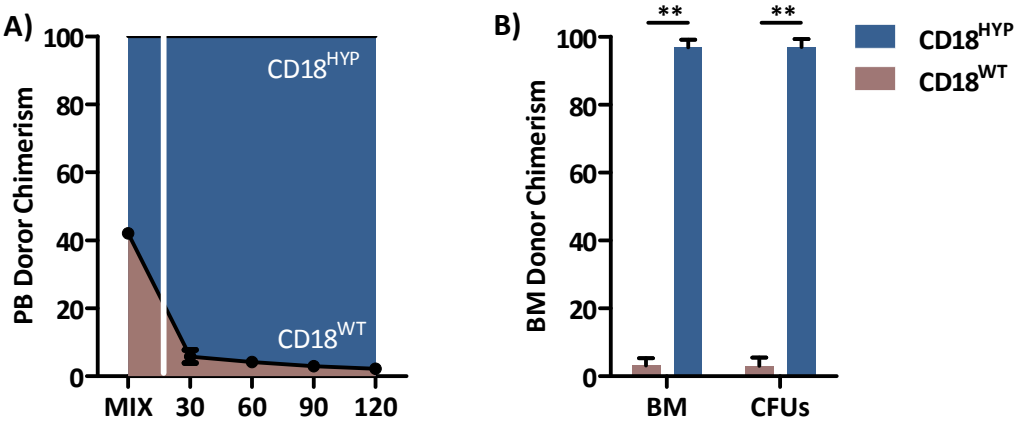

Figure 37. Donor chimerism levels in lethally irradiated WT animals (P3B) transplanted with a mixture of BM-derived lin$^-$ cells from CD18^{HYP} and CD18^{WT} (P3B-ΔhCD4) mice at the same proportion. A) PB donor chimerism levels during 4-month's follow up. B) Donor chimerism levels in total BMCs and BM-derived CFUs 4 months after transplantation. The significance of differences between groups is expressed as P<0.01 (**).

Finally, we conducted a third CRA in which non-purified BMCs from CD18^{HYP} and CD18^{WT} mice were mixed at a 30:70 proportion and transplanted into lethally irradiated WT recipients (Table 14). Taking into account the different LSK cell content of each BM population, similar numbers of LSK cells would have been infused at this ratio. In spite of the low proportion of total CD18^{HYP} BMCs transplanted in these animals, a progressive increase of CD18^{HYP}-derived haematopoiesis could be observed in PB

analyses from primary recipients. In secondary recipients, a 50% of CD18^{HYP} PB chimerism was observed up to 120 days post-transplantation, consistent with the initial proportion of CD18^{HYP} transplanted LSK cells. (Figure 38A). Analyses of BM chimerism revealed similar contribution of both populations to BM cellularity. This was also observed when donor chimerism was analysed within LSK population and BM-derived CFUs (Figure 38B, upper panel). Remarkably, when BM-chimerism from secondary recipients was analysed, a tendency for the CD18-defficient haematopoiesis to be predominant was observed, reaching statistical significance within the LSK cell population. (Figure 38B, lower panel).

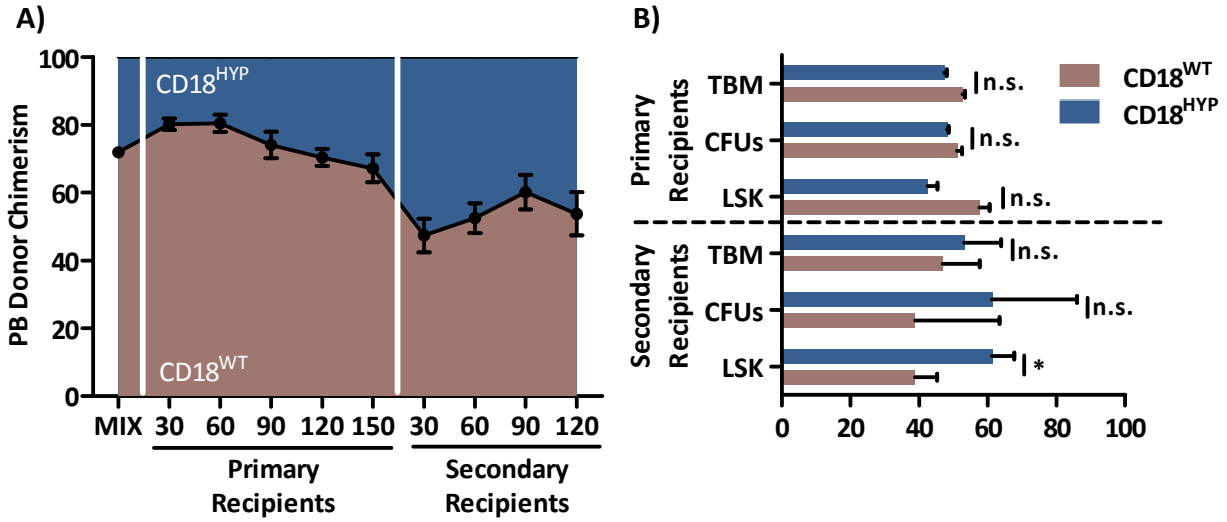

Figure 38. Donor chimerism levels in lethally irradiated WT animals (P3B) transplanted with a mixture of total BMCs from CD18^{HYP} and CD18^{WT} mice (P3B-ΔhCD4) at 30:70 proportion. A) PB donor chimerism levels in primary and secondary recipients. B) Donor chimerism levels in total BMCs, LSK population and BM-derived CFUs in primary and secondary recipients at 5 and 4 months after transplantation respectively. The significance of differences between groups is expressed as P<0.05 (*).

2. LAD-I gene therapy in human models

2.1. Phenotypic correction of LAD-I lymphoblastoid cells

The ZJ cell line is a LAD-I patient derived LCL with no detectable expression of β_2-integrins. As a proof of concept for the *in vitro* GT of LAD-I, ZJ cells were transduced with a LV where the human CD18 cDNA is expressed under the control of the Chimera promoter (LV:Chim.hCD18) at increasing MOI values (from 1 to 100 vp/cell).

hCD18 and hCD11a surface expression levels were first analysed by flow cytometry (Figure 39). Transduction of ZJ cells with LV:Chim.hCD18 at all the tested MOIs resulted in the recovery of both hCD18 and hCD11a membrane expression. The use of a MOI of 10 vp/cell was sufficient to recover the expression of both hCD18 and hCD11a in most of the cells (Figure 39A). Surface expression levels of both subunits were rapidly saturated from MOI 10 onward (Figure 39B). hCD18 and hCD11a surface expression levels showed a high degree of linear dependence with a Pearson's correlation coefficient of 0.9888 (p-value 0.0002) (Figure 39C). On the other hand, there was no correlation between hCD18 surface expression levels and the used MOI (data not shown).

On the contrary, hCD18 mRNA levels in transduced ZJ cells increased proportionally to the MOI used (Figure 39D). This increment in hCD18 mRNA levels did not translate into any modification on hCD11a mRNA levels, which remained stable despite of the transduction conditions (Figure 39D).

VCN determination, which was performed by Q-PCR using primers against LTR and hAlb, confirmed that increasing doses of LVs resulted in increasing levels of integrated proviral copies (Figure 39E).

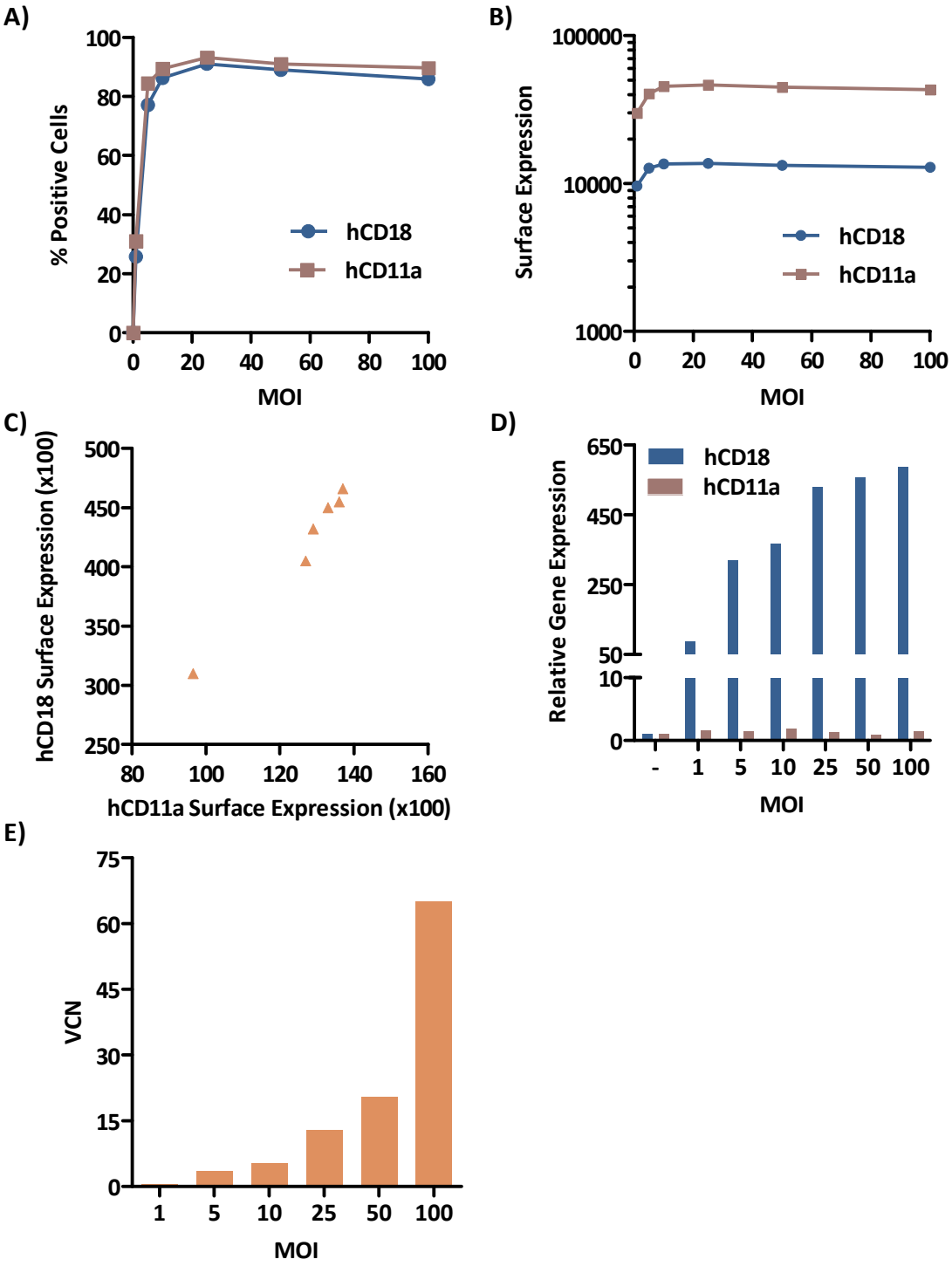

Figure 39. Transduction of ZJ cells with increasing MOIs of LV:Chim.hCD18: Flow citometry and Q-PCR Analysis. A) Percentage of hCD18/hCD11a expressing cells. B) hCD18 and hCD11a surface expression levels C) Correlation between hCD18 and hCD11a surface expression levels. D) mRNA CD18 and CD11a expression levels relative to untransduced ZJ cells. E) VCN determination.

Based on the previous results we decided to perform the next experiments with a MOI of 10. As control for these experiments we used two WT LCLs, MARK and GUS-1, derived from two different healthy donors. Thus, ZJ cells were transduced with the four hCD18-LVs that we have designed. In two of them, CD18 is expressed under the control of ubiquitous promoters (LV:PGK.hCD18 and LV:UCOE.hCD18) and in the other two, hCD18 expression is driven by myeloid promoters (LV:Chim.hCD18 and LV:MIM.hCD18). These transduction conditions resulted in ZJ cells recovering WT

levels of hCD18 and hCD11a membrane expression with all LVs tested (Figure 40A). Transduced ZJ cells showed between 4 and 5.5 proviral copies per cell (Figure 40B). hCD18 surface expression levels were determined by flow cytometry and expressed as MFI per integrated proviral copy (MFI/VCN). The UCOE promoter drove the highest expression levels while the other 3 promoters provided very similar expression levels. The hCD18 expression levels drove by these promoters were very similar to the basal level of hCD18 expression in the GUS-1 WT cell line and a little bit higher than that of MARK WT cell line, indicating that the 4 designed hCD18-LVs are able to drive physiological levels of the transgene when one proviral copy is integrated (Figure 40C).

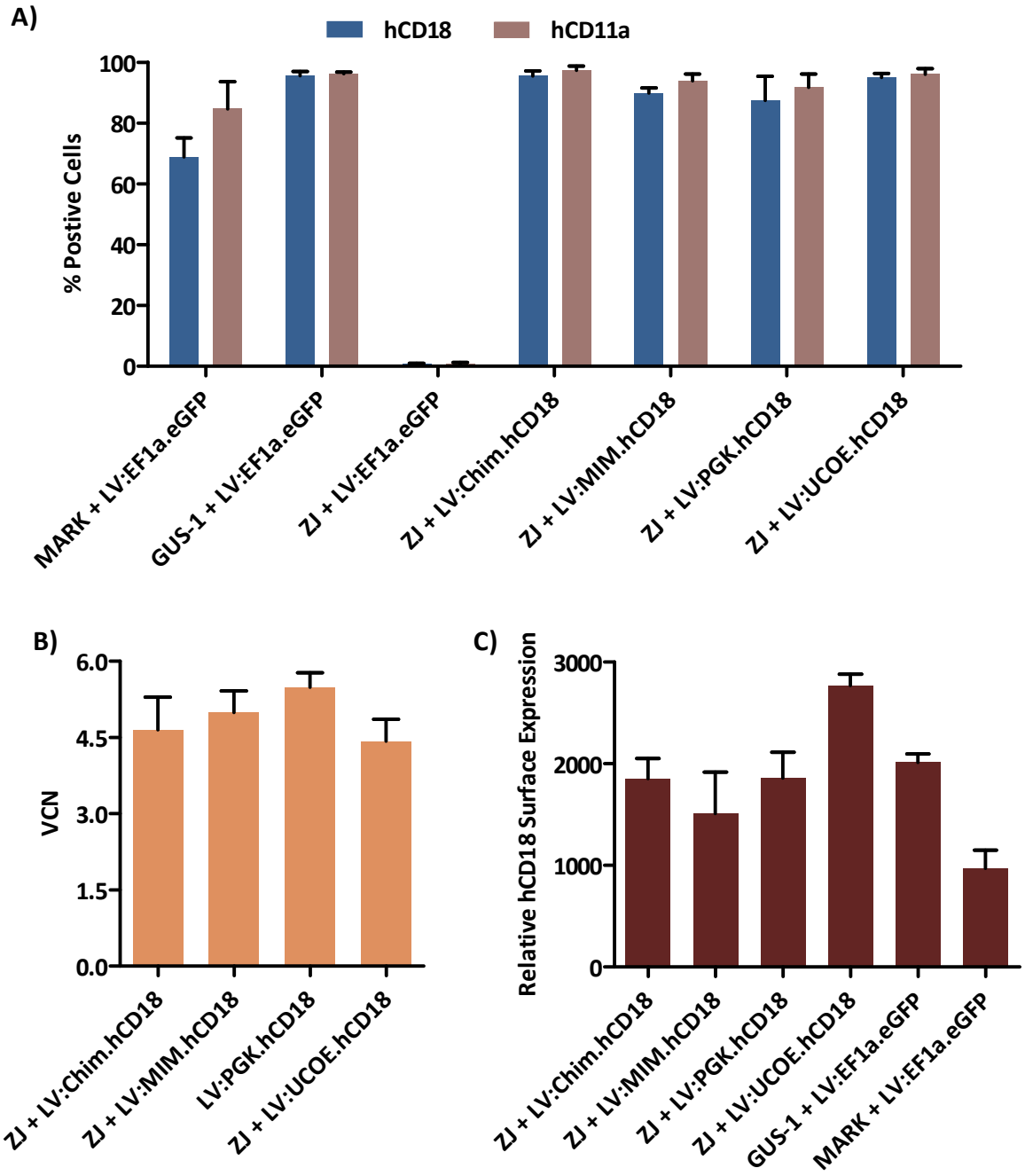

Figure 40. Transduction of ZJ, GUS-1 and MARK cells with hCD18-LVs and control eGFP-LV. A) Percentage of $hCD18^+$ and $hCD11a^+$ cells 5 days after transduction. B) VCN determination in gDNA from CD18-LVs-transduced ZJ cells 10 days after transduction. C) Relative hCD18 surface expression. In the case of hCD18-LVs-transduced cells, surface expression is corrected with the VCN.

In order to study if restoration of hCD18 membrane expression in ZJ cells can lead to the

phenotypic correction of these cells, we conducted two functional assays: A PMA-induced aggregation assay and a sICAM-1 binding assay. As controls for these experiments we used two WT LCLs (MARK and GUS-1) and ZJ LAD-I cells transduced at an MOI of 10 vp/cell with a LV expressing eGFP (LV:EF1α.eGFP).

The aggregation assay is based on the ability of LCLs to aggregate when they are stimulated with PMA, which is a potent and sustained activator of PKC. As it could be observed in Figure 41, eGFP-transduced MARK and GUS-1 cells were able to aggregate after PMA stimulus while eGFP-transduced ZJ cells presented no aggregation, either in the presence or in the absence of PMA. ZJ cells that had been transduced with each of the hCD18-LVs recovered the ability to aggregate after PMA stimulus, indicating that the ectopic provided hCD18 is functionally active. The aggregation observed in MARK and GUS-1 control cells and in corrected ZJ cells was abrogated in the presence of an anti-hCD18 blocking antibody, indicating that the observed aggregation was actually dependent on hCD18 expression.

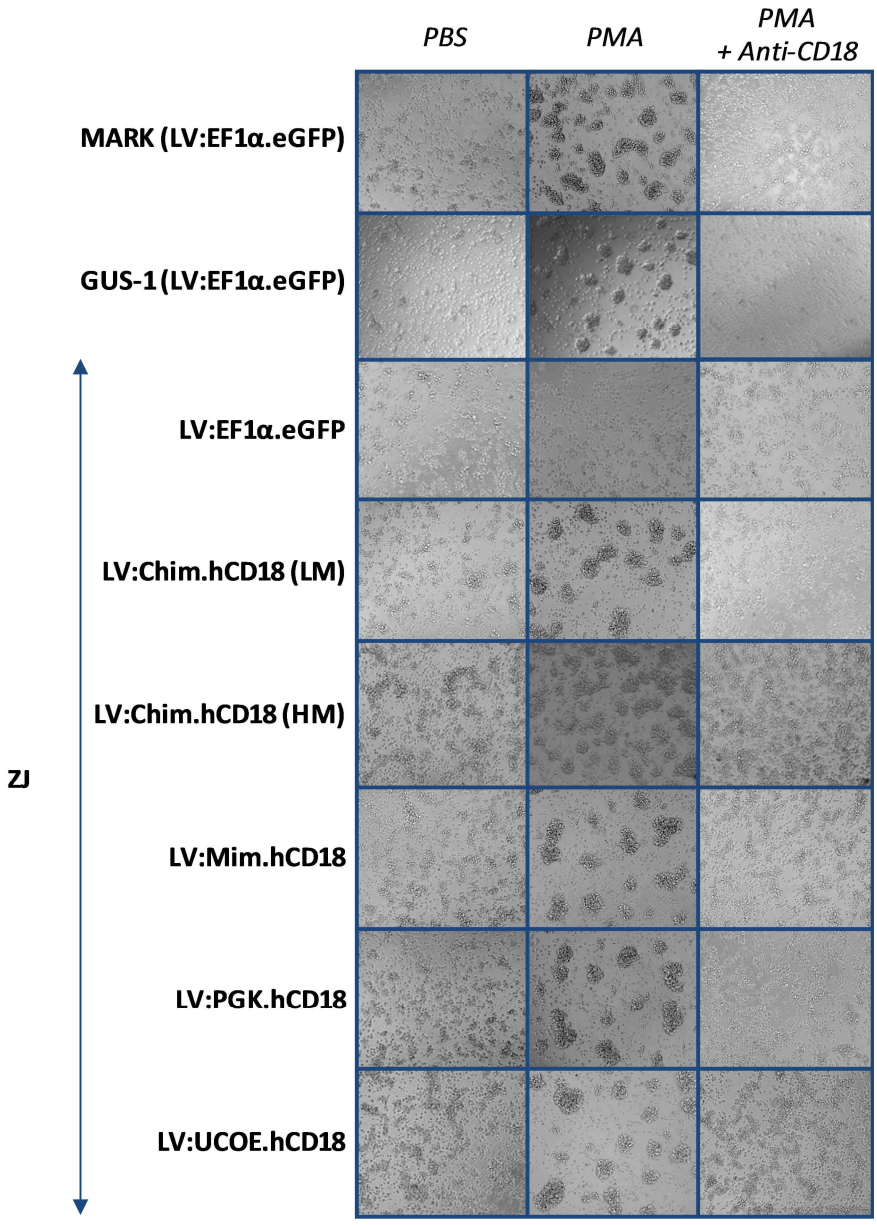

Figure 41. PMA-induced aggregation assay. Cells were incubated either with PBS (first column) or PMA (second column) and let to aggregate for 1 h. Anti-CD18 blocking antibody (third column) was also added to demonstrate that the observed aggregation was dependent on hCD18. Two types of ZJ cells transduced with LV:Chim.hCD18 were used: LM, transduced at low MOI (10 vp/cell) and HM, transduced at high MOI (100 vp/cell).

In the second functional assay we measured the ability of corrected cells to bind to a soluble form of the typical β_2-integrins ligand ICAM-1. sICAM-1 has been found in different body fluids including serum, cerebrospinal liquid, urine and synovial fluid. It is normally released by endothelial cells by proteolytic cleavage of pre-existing ICAM-1 proteins or directly synthetized from specific mRNA after an inflammation stimulus[176]. In this assay, integrin activation of LFA-1 molecules was induced (directly from outside the cells) by altering the extracellular divalent cation conditions, in particular by the addition of millimolar levels of Mg^{2+} when Ca^{2+} is removed with a chelating agent such as EGTA. The two different WT LCLs showed a similar basal sICAM-1 binding capacity. However, after stimulation with Mg^{2+}/EGTA, GUS-1 cells bound to ICAM-1 at a higher level than MARK cells. ZJ cells did not present any sICAM-1 ability either in the absence or in the presence of activating agents. On the contrary, hCD18-LV-transduced ZJ cells bound to sICAM-1 at a similar degree than GUS-1 cells (Figure 42).

Both functional assays were also carried out with ZJ cells that had been transduced with LV:Chim.hCD18 vector at a high MOI (100 vp/cell, HM). Similar outcomes were obtained in both tests with those cells in comparison with ZJ cells transduced at a lower MOI (10 vp/cell, LM) (Figures 43 and 44).

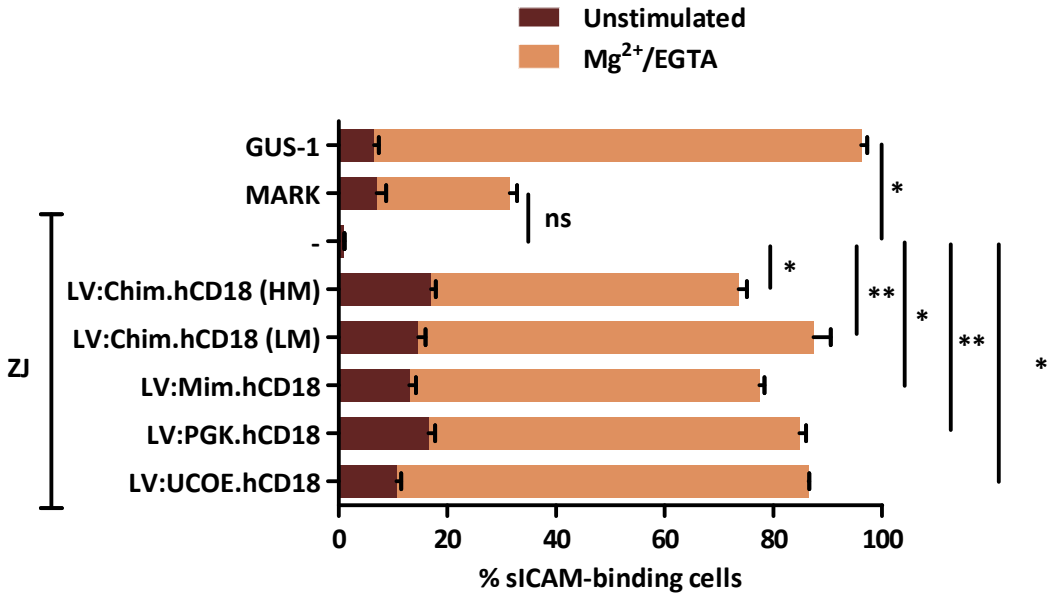

Figure 42. Soluble ICAM-1 binding assay. Fc-ICAM-1 chimeric protein was incubated with a PE-conjugated Anti-Fc antibody so ICAM-1 binding cells could be identified by flow cytometry. Cells were let to bind ICAM-1 in the presence or in the absence of Mg^{2+} and EGTA. Two types of ZJ cells transduced with LV:Chim.hCD18 were used: ones transduced at low MOI (10, LM) and others transduced at high MOI (100, HM). The significance of differences between groups is expressed as $P<0.05$ (*) and $P<0.01$ (**).

2.2. CD18-interferred human CD34⁺ cells as a new model for LAD-I gene therapy

2.2.1. Screening of different shRNA-LVs against hCD18 mRNA

Six different shRNA sequences were cloned in a LV backbone to target different regions of the hCD18 mRNA. These shRNA-LVs also contained an eGFP-expression cassette, which enabled us to identify the interfered cells. As a proof of concept, 50 µL of the shRNA-LV supernatants were used to transduce both MARK and cord blood $CD34^+$ cells from a healthy donor in order to evaluate the level of hCD18 downregulation driven by each shRNA-LV after 5 days in culture. Transductions were performed on RN and, in the case of $CD34^+$ cells, after 2 days of cytokine prestimulation. LV:sh10 was the most efficient for downregulating hCD18 expression in both cell types (Figure 43A and 43B), taking into

account that similar levels of transduction (% eGFP$^+$ cells) were observed in the different conditions (Figure 43C). LV:sh10 was therefore selected to perform the rest of the experiments.

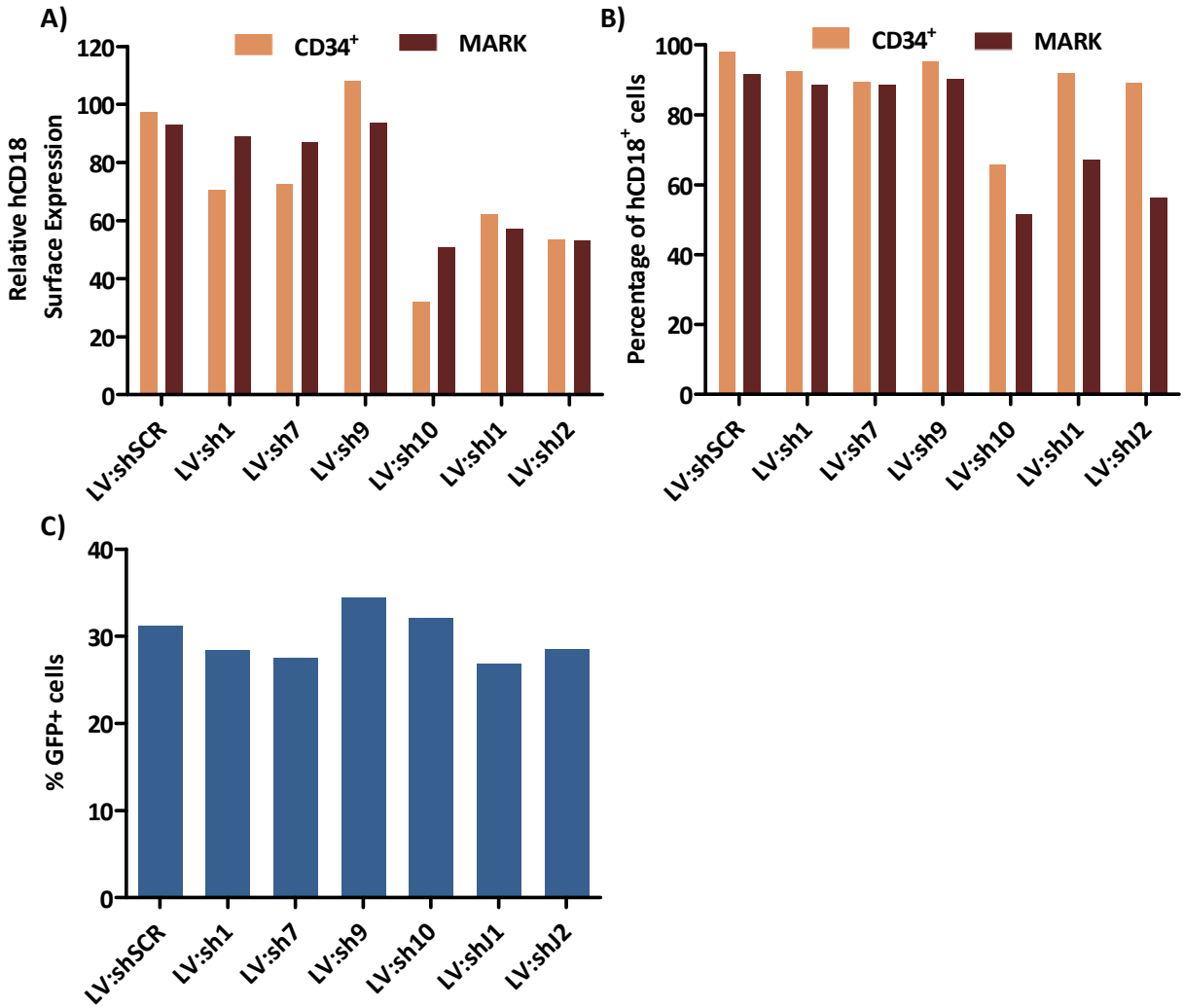

Figure 43. Transduction of MARK cells and cord blood CD34$^+$ cells from a healthy donor with anti-hCD18 shRNA LVs. Relative hCD18 surface expression normalized to expression levels found in untransduced cells (A) and percentage of hCD18 expressing cells (B) after shRNA-LV transduction. C) Percentage of GFP$^+$ CD34$^+$ cells after shRNA-LV transduction.

2.2.2. Generation of LAD-I like haematopoietic stem cells

Cord blood CD34$^+$ cells from different healthy donors were purified, prestimulated and transduced with LV:sh10 and LV:shSCR at a MOI of 100 vp/cell. After 6 days in culture, hCD18 and hCD11a expression was evaluated by flow cytometry (to detect cell surface expression levels) and by Q-PCR (to determine total mRNA expression levels) (Figure 44). Consistent with data in Figure 43, levels of hCD18 determined by flow citometry were dramatically and significantly reduced in LV:sh10-transduced cells in comparison with LV:shSCR-transduced cells (Figure 44A and 44B). This effect resulted in a concomitant reduction of hCD11a surface expression levels (Figure 44B) in concordance with the requirement of this subunit to be co-expressed with hCD18. In order to evaluate if there was a direct relationship between higher levels of eGFP reporter gene and hCD18/hCD11a downregulation, hCD18 and hCD11a expression were evaluated in a population of high eGFP expression. Expression of both β_2-integrin subunits was reduced in this population in comparison with the total eGFP-expressing population, being this difference significant in the case of hCD18 expression (Figure 44B). When the expression of β_2-integrin subunits was analysed by Q-PCR, also a marked reduction in the hCD18 expression was observed. However, CD11a expression levels remained unchanged after LV:sh10

transduction (Figure 44C), consistent with the specificity of the sh10 against hCD18 mRNA.

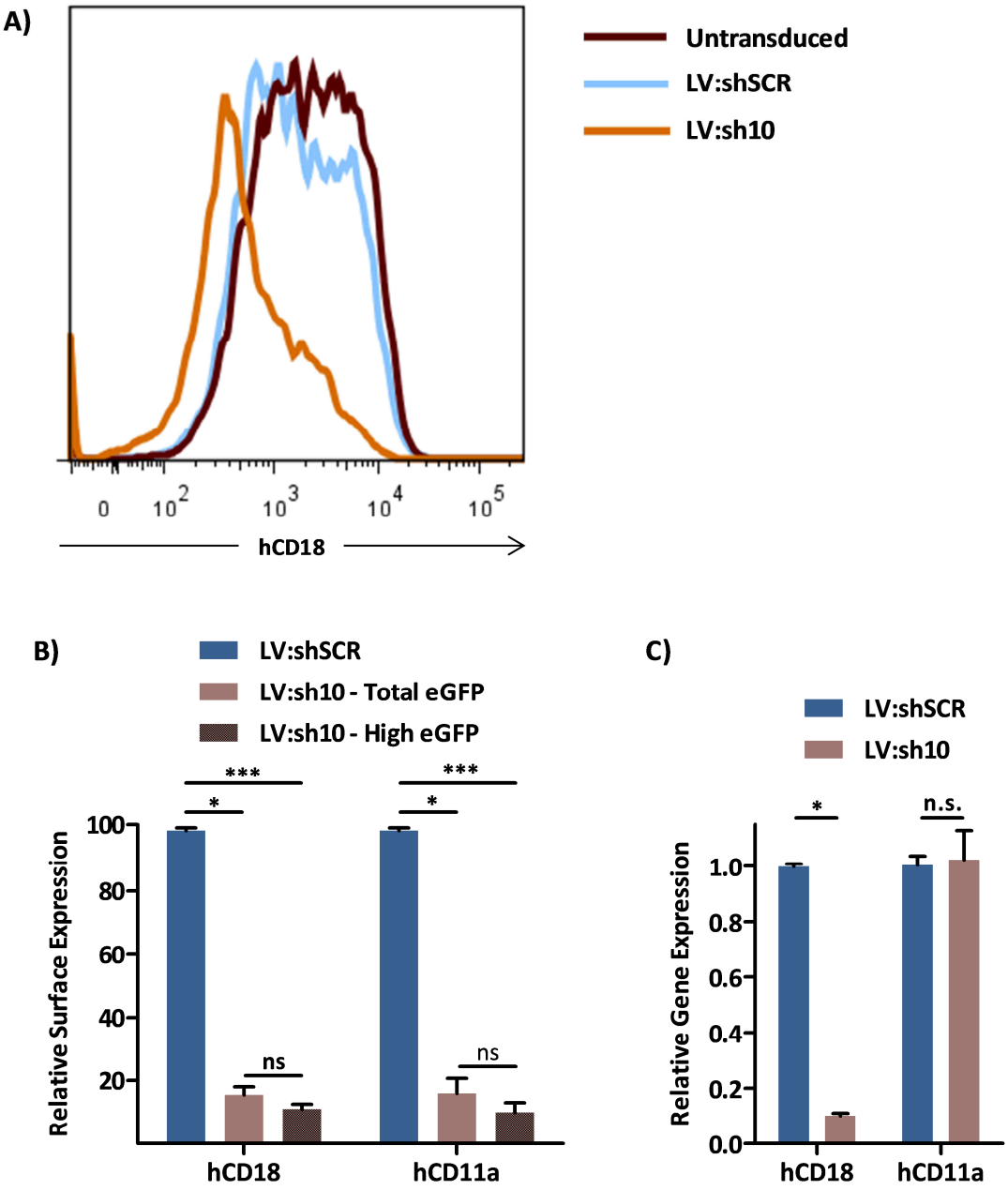

Figure 44. Expression of β_2-integrin subunits in LV:shSCR and LV:sh10-transduced healthy cord blood CD34$^+$ after 5 days of culture. A) Representative histogram of CD18 surface expression. B) hCD18 and hCD11a surface expression levels. MFI values were normalized to MFI values of untransduced cells. C) hCD18 and hCD11a relative gene expression assessed by Q-PCR data using a $\Delta\Delta C_t$ method with GAPDH as an endogenous reference gene and normalized to untransduced cells. The significance of differences between groups is expressed as P<0.05(*) and P<0.001 (***).

2.2.3. Neutrophil differentiation and functional evaluation

In order to generate CD18-interferred neutrophils *in vitro*, healthy cord blood CD34$^+$ cells were transduced with LV:shSCR and LV:sh10 and expanded for 2 days. Then, transduced eGFP$^+$ cells were sorted out and cultured for 1 day in expansion medium. On the next day an aliquot of LV:sh10-transduced cells was transduced with the therapeutic LV:Chim.hCD18 at a MOI of 100 vp/cell. Transduced and untransduced cells were then cultured for 12 additional days in differentiation media containing G-CSF, IL3 and SCF. Thus, four types of neutrophils were generated: untransduced, control (LV:shSCR), LAD-I like (LV:sh10) and corrected LAD-I like (LV:sh10 + LV:Chim.hCD18) (Figure 45).

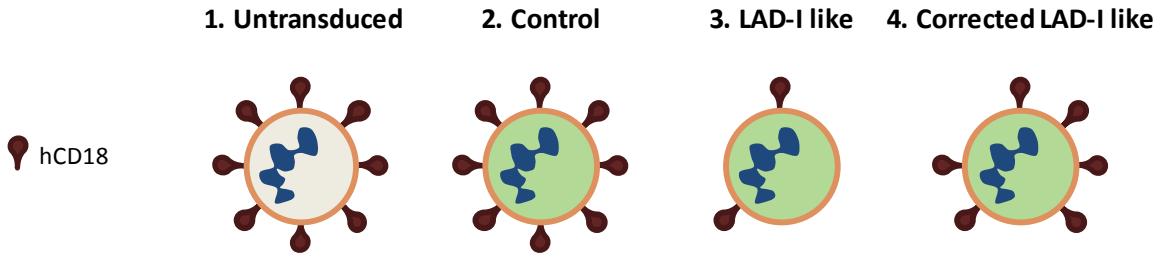

LV:sh10	-	-	+	+
LV:shSCR	-	+	-	-
eGFP Expression	-	+	+	+
LV:Chim.hCD18	-	-	-	+

Figure 45. Different types of *in vitro* differentiated neutrophils generated from cord blood healthy human $CD34^+$ cells and their characteristics.

The expression of β^2-integrin subunits (hCD18, hCD11a and hCD11b) was evaluated at day 12 of differentiation (Figure 46). As expected, no significant differences were observed in hCD18 expression between untransduced (Type 1) and control (Type 2) neutrophils. Consistent with previous observations in undifferentiated $CD34^+$ cells, LAD-I like (Type 3) neutrophils showed a drastic and significant reduction of hCD18 expression. Additionally, the expression of its counterpart subunits, hCD11a and hCD11b, was also significantly reduced. Transduction with the LV:Chim.hCD18 (Type 4) resulted in 43% recovery of untransduced neutrophil hCD18 levels. As expected, similar increments for hCD11a and hCD11b β_2-integrins subunits expression were observed in corrected LAD-I like neutrophils (Figure 46).

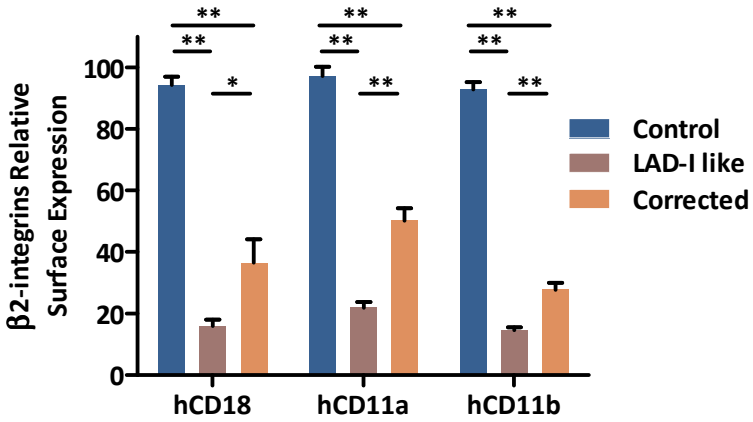

Figure 46. β_2-integrins expression in control, LAD-I like and corrected neutrophils obtained by *in vitro* differentiation of cord blood $CD34^+$ cells. Differentiation was carried out in the presence of SCF, IL3 and GCSF for up to 12 days. Expression levels were determined by flow cytometry as MFI and then normalized to the MFI of untransduced cells. The significance of differences between groups are expressed as $P<0.05$(*) and $P<0.01$ (**).

VCN was also determined in 12-day differentiated neutrophils (Figure 47). Between 1.5 and 1.3 copies per cell of the LV:sh10 and LV:shSCR were detected. VCN from LAD-I like neutrophils (Type 3) was subtracted from VCN detected on corrected LAD-I like neutrophils (Type 4) in order to determine the VCN for LV:Chim.hCD18. Thus, around 2 copies of the therapeutic LV:Chim.hCD18 were deduced to be integrated in corrected LAD-I like neutrophils (Type 4).

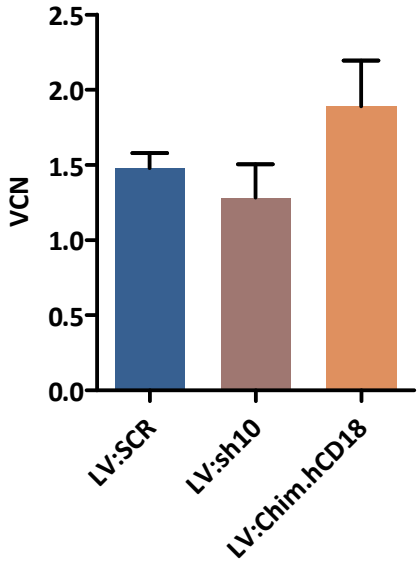

Figure 47. VCN determination in 12-day differentiated control (Type 2), LAD-I like (Type 3) and corrected LAD-I like (Type 4) neutrophils. VCN from LAD-I like neutrophils was subtracted from VCN detected on corrected LAD-I like neutrophils in order to determine the VCN for LV:Chim.hCD18.

Three different functional assays were carried out to evaluate if the moderate hCD18 recovery obtained after LV:Chim.hCD18 had an impact on the functionality of the corrected LAD-I like neutrophils. In the first set of experiments, we evaluated the ability of neutrophils to bind to sICAM-1. As shown in Figure 48, untransduced and control neutrophils showed very similar levels of sICAM-1 binding, both before and after stimulation. On the contrary, LAD-I like neutrophils presented a marked reduction in their capacity to bind sICAM-1, which was partially restored after LV.Chim.hCD18 transduction.

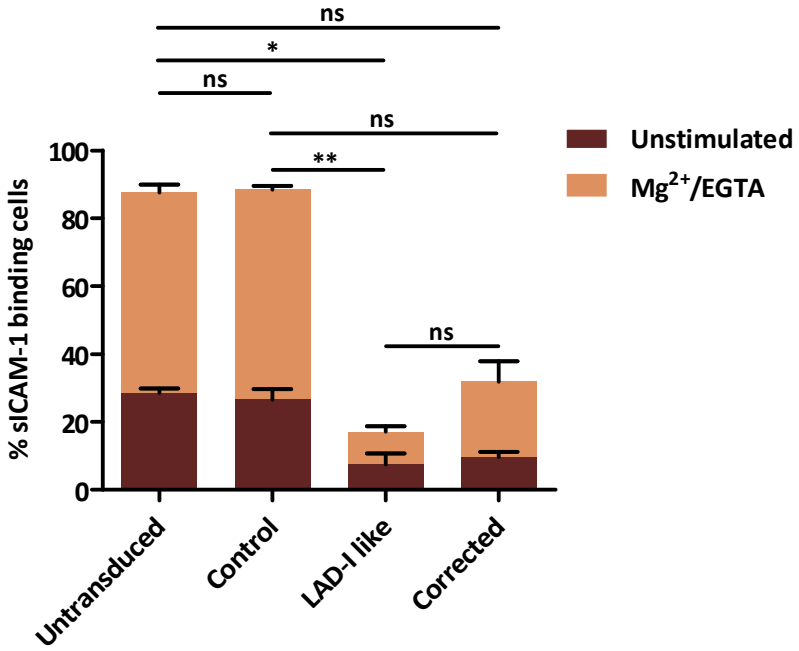

Figure 48. sICAM-1 binding assay on *In vitro* differentiated neutrophils. Cells were incubated with a chimeric sICAM-1-Fc protein that can be detected easily by flow cytometry. Percentage of sICAM-1 was determined before and after stimulation with Mg^{2+}/EGTA.

In the second set of experiments, we evaluated the adhesion capacity in a dynamic setting (Figure 49). For this purpose we performed a flow chamber assay in which differentiated cells were allowed to attach to fibrinogen, a Mac-1 ligand. Afterwards, flow rates were increased at 10–20

dyn/cm^2 increments in 1-min intervals to a maximum sheer stress of 80 dyn/cm^2. The percentage of adherent cells was evaluated after each increment of fluid shear stress. As expected, no differences were found between untransduced and control cells. However, LV:sh10 transduction resulted in a decreased ability to resist shear stress when cells were bound to fibrinogen. LV:Chim.hCD18 transduction of hCD18-interferred cells resulted in a higher resistance to shear stress indicating that LV-mediated hCD18 actopic expression was able to improve the adhesion properties of LAD-I like neutrophils, thus partially restoring the WT phenotype.

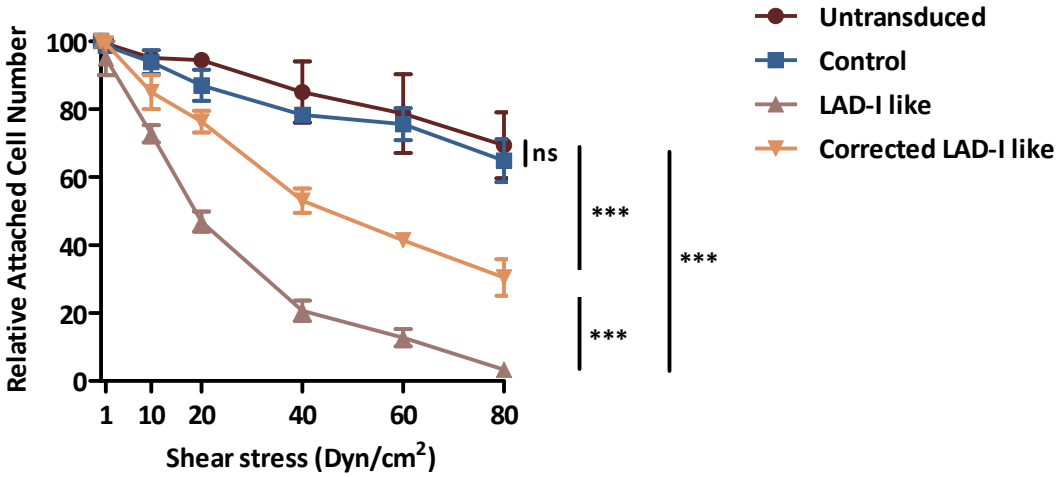

Figure 49. Flow chamber experiments with control, LAD-I like neutrophils and corrected LAD-I like neutrophils. Cells were allowed to attach to fibrinogen and then non-adherent cells were removed at low flow. Subsequently, flow rates were increased in 10–20 dyn/cm^2 increments in 1-min intervals to a maximum sheer stress of 80 dyn/cm^2. The number of attached cells after each increment of shear stress was calculated and expressed as a percentage of the total number of adherent cells in the same field after the low flow wash. The significance of differences between groups is expressed as P<0.001(***).

Finally, we evaluated the ability of *in vitro* differentiated neutrophils to undergo a respiratory burst response (Figure 50). The respiratory burst in neutrophils plays an important role in host defence against pathogens and has been shown to be a CD11b/CD18-mediated function when C3bi-opsonized Zymosan is used as the stimulus. It is based on a rapid release of reactive oxygen species that can be detected by different techniques including the use of luminol, a chemical compound that exhibits chemiluminescence, in the presence of oxidizing agents.

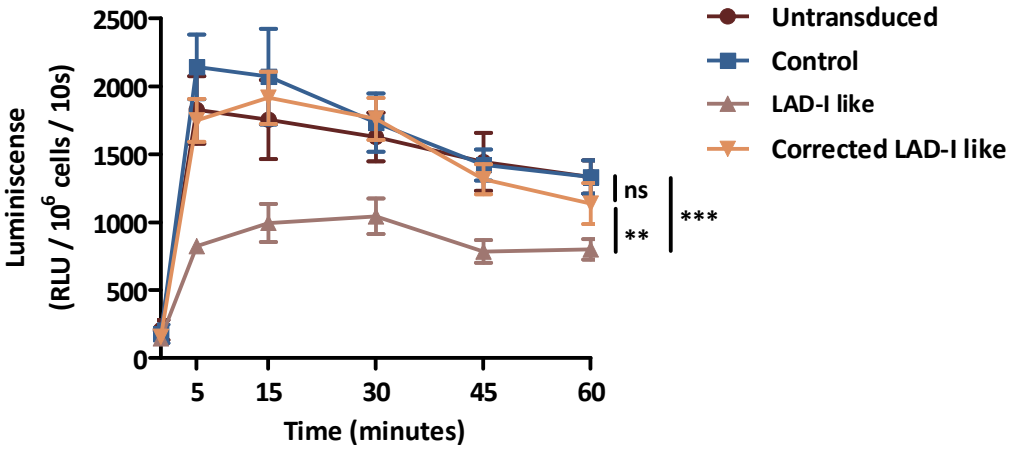

Figure 50. Respiratory Burst on *in vitro* CD34$^+$ cells-derived neutrophils. Respiratory burst response was induced by C3bi-opsonized Zymosan (specifically recognized in a CD11/CD18-dependent manner) and detected by luminol-enhanced chemoluminescence. Luminescence detected for each sample was extrapolated for 10^6 cells with the following equation: 10^6 cell luminescence = sample luminescence * 10^6 cells / cell number. The significance of differences between groups are expressed as P<0.01 (**) and P<0.001(***).

As shown in Figure 50 control untransduced and LV:shSCR-transduced neutrophils were able to mount a rapid respiratory burst in the presence of opsonized zymosan that was maintained at least during an hour. Respiratory burst of LAD-I like neutrophils was clearly diminished in comparison to control neutrophils. Major differences were observed for the first two time points also showing statistical significance. Surprisingly, despite of the low recovery of hCD11b surface expression after LV:Chim.hCD18 transduction (Figure 46), corrected LAD-I like neutrophils mounted a respiratory burst very similar to that of the control cells. These results show that very low levels of correction are sufficient to restore phagocytic ability of CD18-defficient cells.

3. *Ex vivo* gene therapy in CD18^{HYP} mice

3.1. *In vitro* transduction of mouse haematopoietic progenitors

BM lin$^-$ cells, which is a population enriched in mouse haematopoietic progenitors, are often used as target cells in *ex vivo* GT experiments conducted in mice.

Lin$^-$ cells were purified from CD18^{HYP} BMCs by FACS. Purities from 82.3 to 97.3 % were usually obtained (Figure 12). Once purified, lin$^-$ cells were transduced with the different hCD18-LVs in the presence of haematopoietic growth factors (hIL-11 and mSCF) capable to preserve the long-term repopulating ability of the HSCs[177]. On next day cells were washed and maintained both in expansion medium and in myeloid differentiation medium (containing G-CSF and IL-3). Cells were differentiated towards the myeloid lineage since neutrophils are the mainly affected cells as a consequence of CD18 deficiency.

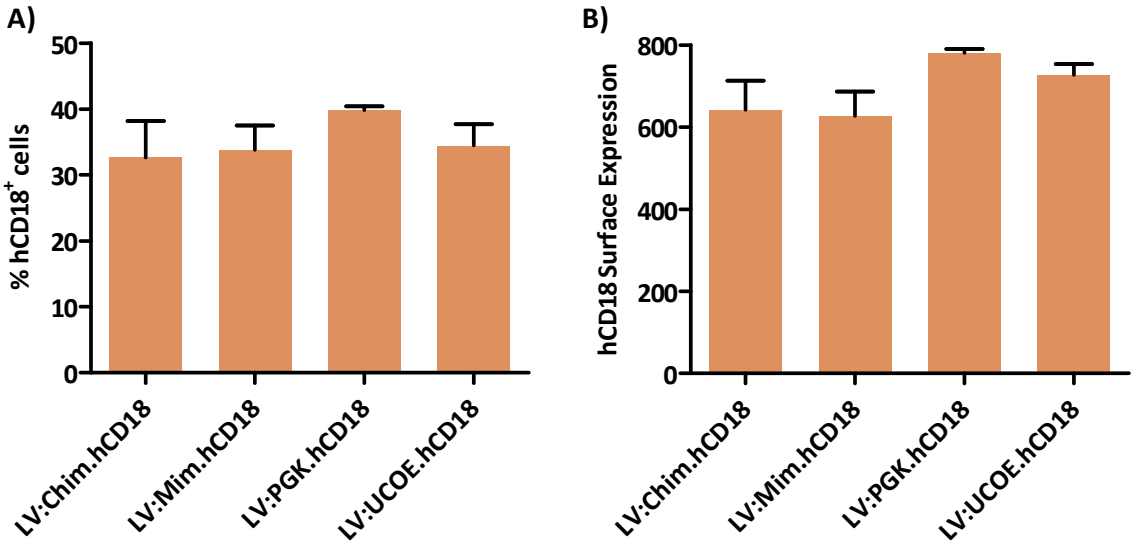

Figure 51. hCD18 expression in LV-transduced myeloid-differentiated CD18^{HYP} lin$^-$ cells. A) Percentage of hCD18$^+$ cells. B) Levels of hCD18 expression expressed as MFI.

hCD18 and mCD11a surface expression levels were evaluated after 7 days of myeloid differentiation (Figures 51 and 52). hCD18$^+$ cells were detected in a range between 30 and 40%, with no statistically significant differences among the different hCD18-LVs. In addition, hCD18 was expressed at very similar levels among the different hCD18-LVs (Figure 51). After 7 days of myeloid differentiation, untransduced and eGFP-transduced CD18^{HYP} cells expressed about 50% of mCD11a levels observed in untransduced CD18^{WT} cells. In the case of the hCD18-transduced cells, lentiviral-mediated enforced hCD18 expression resulted in mCD11a levels between 70 and 80% of WT levels, indicating that exogenous hCD18 is able to bind to mCD11a subunits and form new β_2 chimeric integrins composed by murine and human subunits (Figure 52).

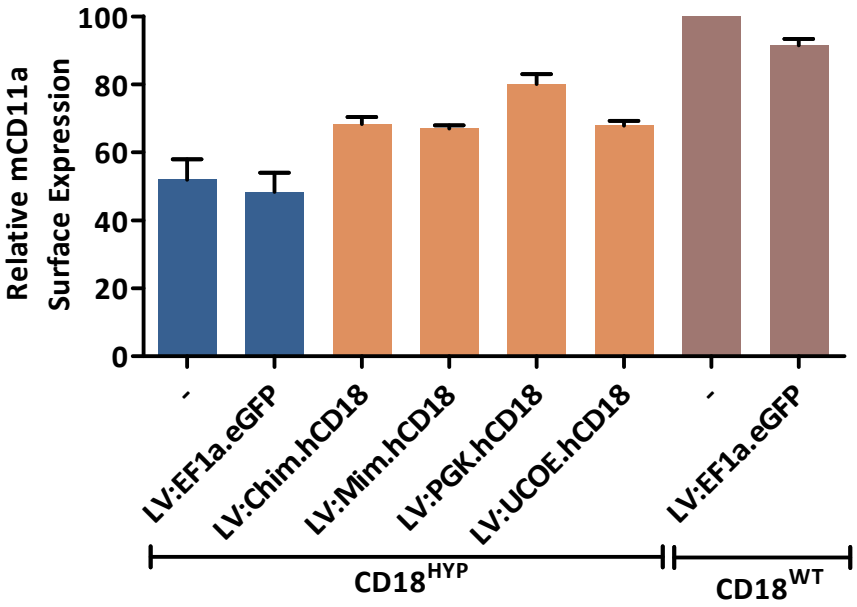

Figure 52. Surface expression of mCD11a in transduced, untransduced and myeloid-differentiated $CD18^{HYP}$ and $CD18^{WT}$ lin^- cells. mCD11a surface expression levels were determined by flow cytometry and then normalized to those found in untransduced $CD18^{WT}$ cells.

hCD18 expression was also evaluated after PMA stimulation and compared to non-PMA treated cells. PMA stimulus resulted in a slight increment in the percentage of $hCD18^+$ cells as can be observed in Figure 53. These results indicate that ectopic hCD18 is able to be up-regulated in a physiological way under an activating stimulus.

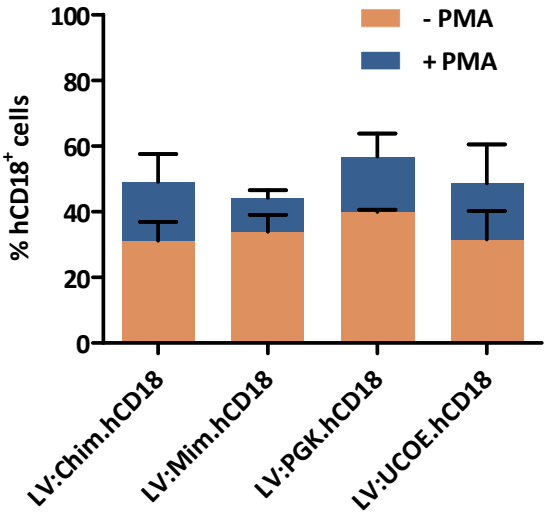

Figure 53. Post-transductional hCD18 regulation in response to PMA in neutrophils generated *in vitro* form transduced $CD18^{HYP}$ lin^- cells. $hCD18^+$ cells were determined by flow cytometry before and after PMA stimulation.

Haematological toxicity of lentiviral transduction was evaluated by 7-day culture in methylcellulose (Figure 54). No differences in CFUs were observed among untransduced, eGFP-transduced and hCD18-transduced $CD18^{HYP}$ lin^- cells suggesting that neither lentiviral transduction nor hCD18 exogenous expression affects clonogenic capacity of $CD18^{HYP}$ murine haematopoietic progenitors.

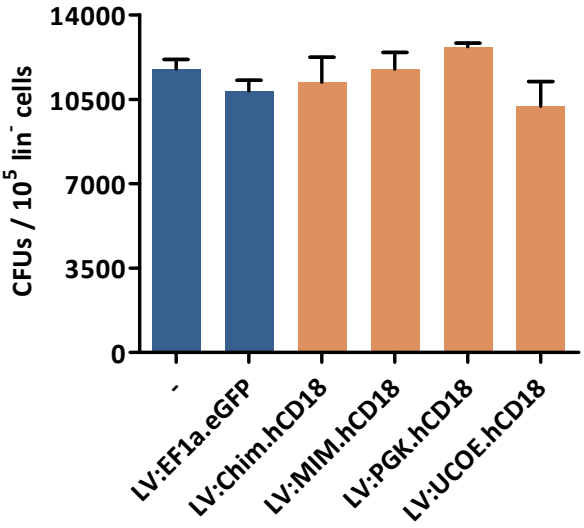

Figure 54. Clonogenic assays in methylcellulose with transduced and untransduced CD18^{HYP} lin$^-$ cells.

3.2. *Ex vivo* gene therapy in CD18^{HYP} mice

Lin$^-$ cells from CD18^{HYP} mice were isolated and transduced with the four hCD18-LVs as described in section 3.2 of Results. One day after transduction cells were washed and resuspended in PBS and transplanted into lethally irradiated CD18^{HYP} mice. As control groups, CD18^{HYP} mice were transplanted with LV:SFFV.eGFP-transduced CD18^{HYP} and CD18^{WT} lin$^-$ cells. Six independent GT experiments were carried out (Table 15). In experiments 1 and 2, secondary transplants were also performed. As similar outcomes were observed in the different experiments, results were treated together.

Experiment	MOI	Donor Cells	Vector	Number of Recipients
1*	20	CD18^{HYP}	LV:Chim.hCD18	3
			LV:UCOE.hCD18	4
2*	20	CD18^{HYP}	LV:Chim.hCD18	3
			LV:MIM.hCD18	3
			LV:PGK.hCD18	5
			LV:SFFV.eGFP	5
		CD18^{WT}	LV:SFFV.eGFP	3
3	20	CD18^{HYP}	LV:Chim.hCD18	5
			LV:MIM.hCD18	2
			LV:PGK.hCD18	6
			LV:UCOE.hCD18	4
			LV:SFFV.eGFP	4
		CD18^{WT}	LV:SFFV.eGFP	4
4	50	CD18^{HYP}	LV:Chim.hCD18	3
			LV:PGK.hCD18	4
			LV:UCOE.hCD18	4
			LV:SFFV.eGFP	3
		CD18^{WT}	LV:SFFV.eGFP	2
5	50	CD18^{HYP}	LV:Chim.hCD18	7
			LV:PGK.hCD18	5
			LV:SFFV.eGFP	4
		CD18^{WT}	LV:SFFV.eGFP	6
6	50	CD18^{HYP}	LV:Chim.hCD18	8
			LV:PGK.hCD18	2
			LV:SFFV.eGFP	4
		CD18^{WT}	LV:SFFV.eGFP	3

Table 15. *Ex vivo* GT experiments carried out in CD18^{HYP} lethally irradiated animals. Total numbers of treated animals were: LV:Chim.hCD18 n=29; LV:UCOE.hCD18 n= 12; LV:MIM.hCD18 n= 5; LV:PGK.hCD18 n= 22. *In experiments 1 and 2, secondary transplants were also performed (See Table 15).

3.2.1. β_2 integrins' expression in gene therapy-treated CD18^{HYP} primary recipients

From the first month, hCD18$^+$ PBLs could be detected in all recipients that had been transplanted with LV:hCD18-transduced cells. Interestingly, hCD18 was co-expressed with the three CD11 murine subunits (Figure 55).

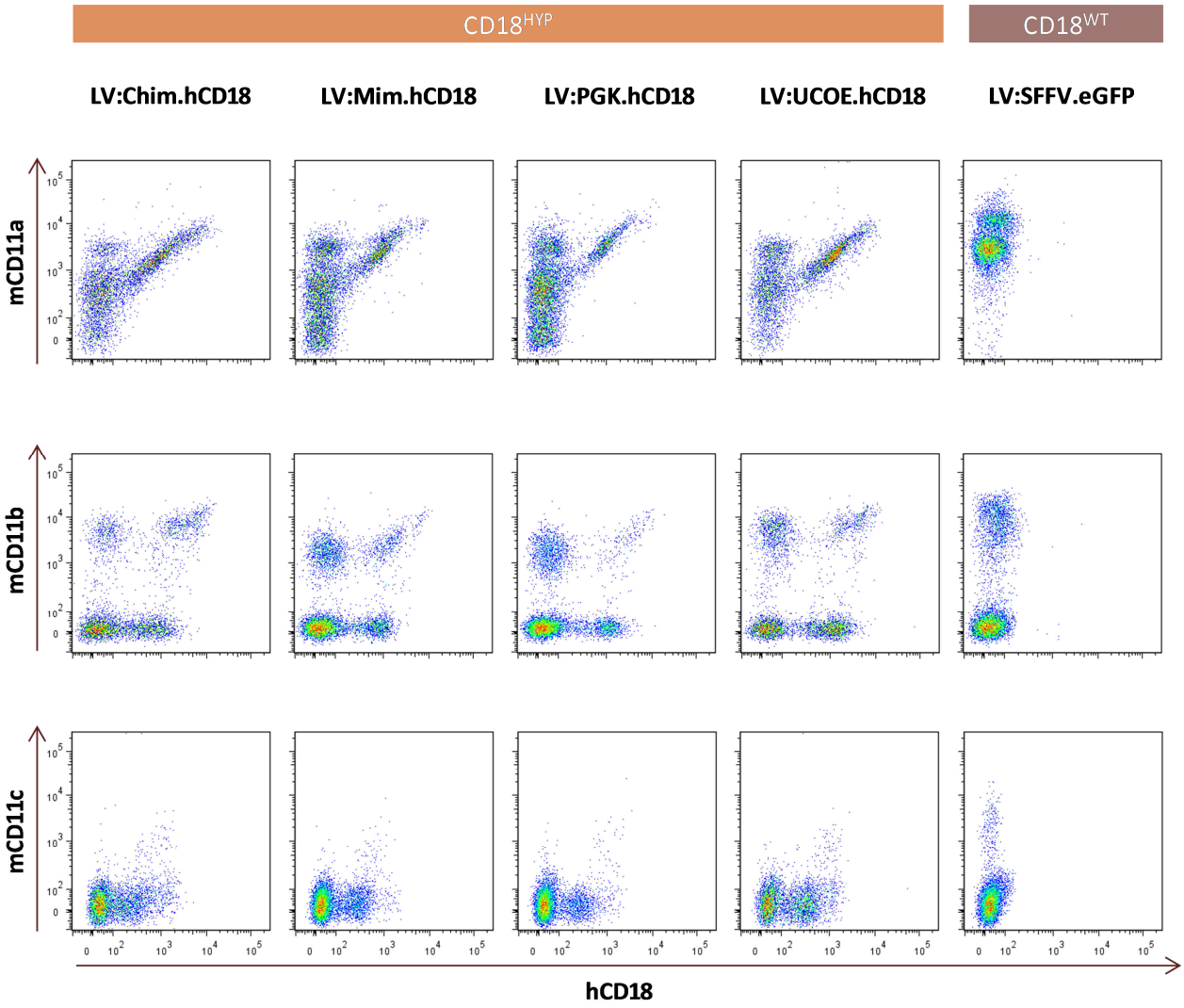

Figure 55. β_2 integrins' expression of representative GT-treated CD18^{HYP} primary recipients.

Similar proportion of hCD18$^+$/mCD11a$^+$ cells was observed in PB of transplanted mice at 1 and 3 mpt (Figure 56A). In hCD18$^+$ cells, levels of mCD11a were higher than the ones of CD18^{HYP} untransduced cells (Figure 57) indicating that hCD18 is able to heterodimerize with mCD11a increasing the expression of murine β_2 integrins. hCD18$^+$ cells recovered approximately a 50% of the CD18^{WT} mCD11a expression levels in all treated groups.

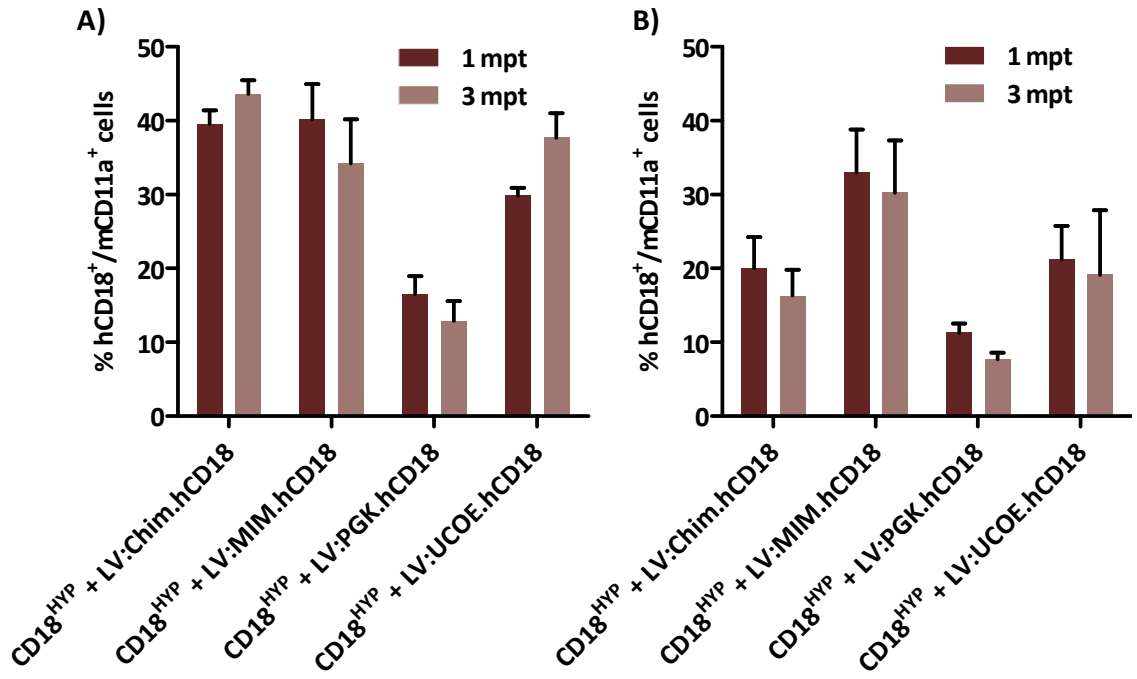

Figure 56. Percentage of hCD18^{+}/mCD11a^{+} PBLs at 1 and 3 mpt in *ex vivo* primary (A) and secondary (B) GT-treated CD18^{HYP} mice. Presented results correspond to 6 independent experiments.

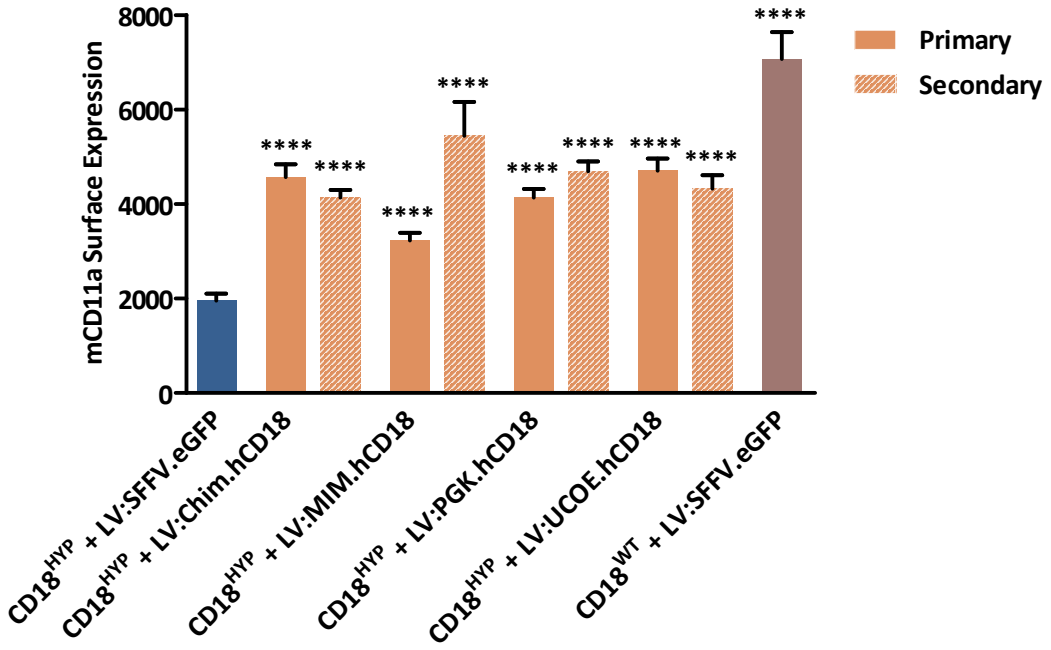

Figure 57. Mean of mCD11a surface expression levels (MFI) in PBLs at the different time points after transplant of transduced cells in primary (orange) and secondary (scratched orange) CD18^{HYP} recipient mice and eGFP control animals (dark blue and brown). Presented results correspond to 6 independent experiments (primary recipients) and secondary recipients from experiments 1 and 2. The significance of differences between groups is expressed as P<0.0001(****) and is always referred to the CD18^{HYP} + LV:SFFV.eGFP group.

Three months after transplantation, hCD18 expression was evaluated in different subpopulations of PBLs (T cells, B cells and neutrophils). These subpopulations were identified on the basis of the expression of specific markers (CD3^{+} for T cells, B220^{+} for B cells and Gr1^{HIGH} for neutrophils). It was possible to detect hCD18^{+} neutrophils, B and T cells in all the transplanted groups (Figure 58A). Surface hCD18^{+} expression levels (MFI) in myeloid cells were always higher than the ones observed in lymphoid cells, regardless of the nature of the promoter (ubiquitous or myeloid promoters) that was driving hCD18 expression (Figure 58B). However, the ratio between hCD18 expression levels in

myeloid and lymphoid cells in LV:Chim.hCD18 and LV:MIM.hCD18-transduced cells was higher than in the other groups, being statistically significant and the most similar to the $CD18^{WT}$ mice in the case of LV:Chim.hCD18 (Figure 58C).

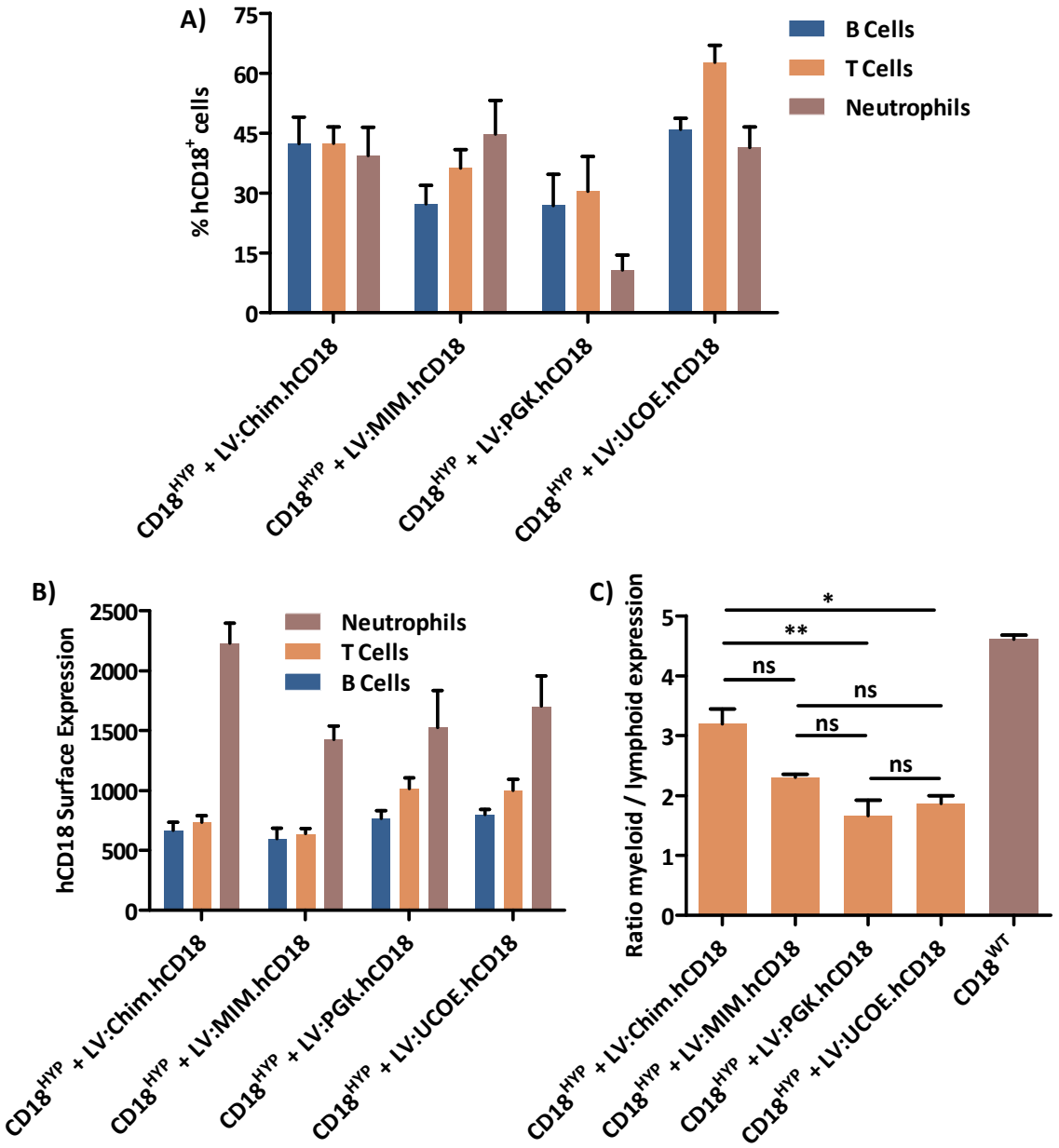

Figure 58. Lineage hCD18 surface expression after transplant of transduced cells in $CD18^{HYP}$ recipient mice. Presented results correspond to independent experiments 1 and 2. A) Percentage of neutrophils, B cells and T cells expressing hCD18. B) Surface hCD18 expression levels (MFI) in different haematopoeitic lineages. C) Ratio of myeloid and lymphoid hCD18 expression. This ratio was calculated as following: hCD18 MFI in Gr^{HIGH} cells / (hCD18 MFI in $CD3^+$ cells + hCD18 MFI in in $B220^+$ cells). The significance of differences between groups is expressed as P<0.05(*) and P<0.01 (**).

Four months after transplantation, primary recipients were culled and BMCs were also analysed for hCD18 and mCD11a expression (Figure 59). Percentages of $hCD18^+/mCD11a^+$ cells ranged from 11 % (in the case of LV:PGK.hCD18-treated mice) to 38 % (in the case of LV:MIM.hCD18-treated mice) in a very similar way to that noted in PB (Figure 59A). Furthermore, similar levels of mCD11a upregulation were observed in BMCs (Figure 59B). $hCD18^+$ BMCs expressed from 51 to 62 % of the mCD11a expression levels observed in LV.SFFV.eGFP-treated $CD18^{WT}$.

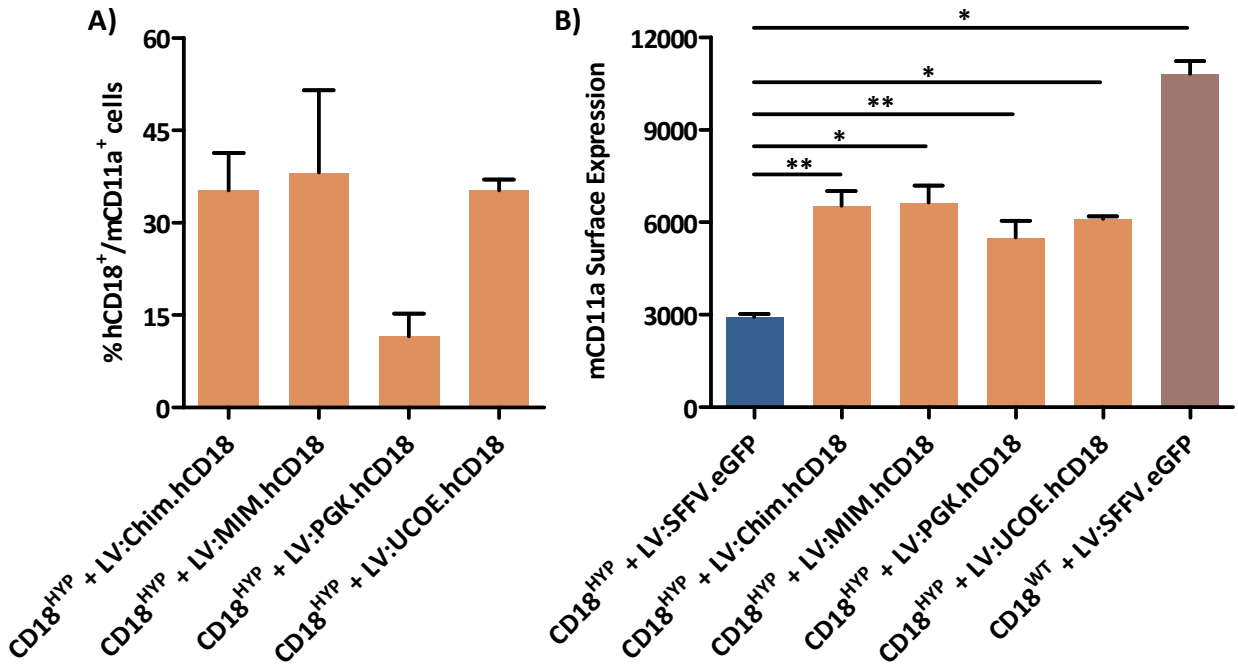

Figure 59. CD11a expression in BMCs of GT-treated CD18^{HYP} mice. Presented results correspond to experiments 1 and 2. A) Percentage of hCD18^{+}/mCD11a^{+} cells in the total BMC population at 4 months post transplantation B) mCD11a surface expression levels observed in the transplanted mice. The significance of differences between groups is expressed as P<0.01 (**) and P<0.05 (*).

3.2.2. Long term β$_2$ integrins' expression in gene therapy-treated CD18^{HYP} mice

In order to evaluate if hCD18-LVs were able to transduce true LT-HSCs, when primary recipients from experiments 1 and 2 were culled at 4 mpt, total BMCs from these recipients were harvested and transplanted into lethally irradiated CD18^{HYP} secondary recipients (Table 16).

Experiment	Donor Cells	Vector	Number of recipients	
			Pool	Mouse to mouse
1	CD18^{HYP}	LV:Chim.hCD18	1	3
		LV:UCOE.hCD18	1	4
2	CD18^{HYP}	LV:Chim.hCD18		3
		LV:MIM.hCD18		3
		LV:PGK.hCD18		3

Table 16. Secondary recipients from GT-treated primary CD18^{HYP} recipients.

Similar proportion of hCD18^{+}/mCD11a^{+} cells was observed in PB of secondary recipients at 1 and 3 mpt. In any case, these levels were reduced in comparison with primary recipients with the exception of LV:MIM.hCD18 group, which maintained very similar levels to that of the primary recipients. This reduction in the percentage of hCD18^{+} mCD11a^{+} cells is likely more related to the loss of engraftment ability of transduced cells after secondary transplantation rather than to epigenetic silencing of the promoters. Despite of the diminished proportion of hCD18^{+} cells, this population showed similar mCD11a upregulation to that of the primary recipients (Figure 57B), confirming the hypothesis that no epigenetic silencing was taking place.

9 months after transplantation, secondary recipients were sacrificed and BM was collected and analysed for hCD18 expression. As can be observed in Figure 60, both in TBM cells and in the LSK population, low but still detectable levels of hCD18^{+} cells were observed, with the exception of LV:MIM.hCD18 group, which maintained a high proportion of hCD18^{+} cells despite of the long-time of analysis.

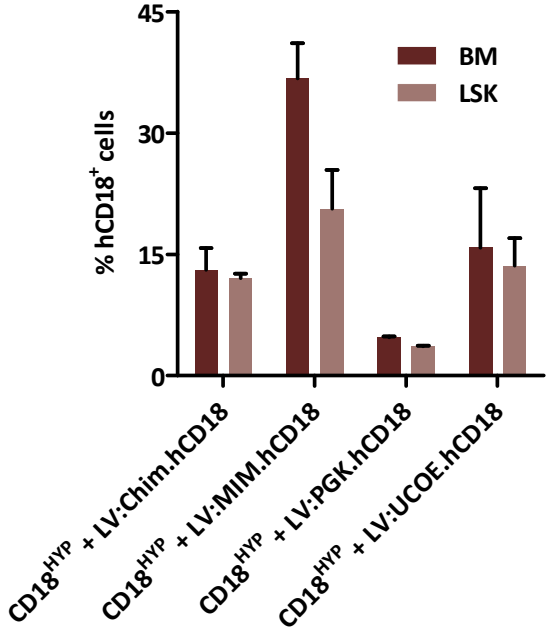

Figure 60. Long-term analysis of BM in secondary $CD18^{HYP}$ recipients. Analysis of $hCD18^{+}$ cells at 9 mpt in total BMCs and in the LSK subpopulation.

All these results indicate that hCD18-LVs were able to transduce true and primitive LT-HSCs, which can generate $hCD18^{+}$ haematopoiesis in secondary recipients, and thus it is possible to detect $hCD18^{+}$ BM cells even at 9 months after secondary transplantation.

3.2.3. Assessment of the lentiviral vector-associated risk

Secondary transplantation is a powerful tool to detect possible leukaemogenic events induced by insertional oncogenesis. However, none of the secondary recipients from hCD18-LV-treated mice showed symptoms of leukaemia, and all of them presented normal levels of WBCs (Figure 62) and normal multilineage distribution (Figure 61).

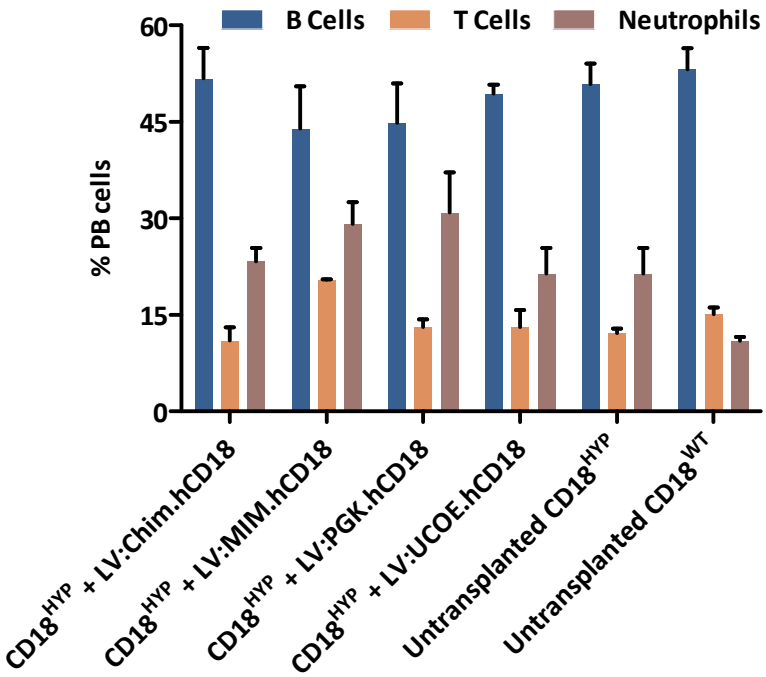

Figure 61. Multilineage distribution in PB at 4 months post-transplantation of secondary recipients and age-matched untransplanted $CD18^{WT}$ and $CD18^{HYP}$ mice.

Although LVs have been shown to be safer in terms of insertional oncogenesis than classical γRVs[114,178], this phenomenon is still a potential risk when using integrative viral vectors, particularly if multicopy insertion takes place. Therefore, in GT protocols, the number of vector copies per cell (VCN) is generally limited because of safety purposes. VCN was determined by Q-PCR in gDNA extracted from PBLs from both primary and secondary recipients. Between 1 and 0.5 proviral copies per cell were detected in PBLs from primary recipients and between 0.3 and 0.6 in secondary recipients. (Table 17).

	LV:Chim.hCD18	LV:MIM.hCD18	LV:PGK.hCD18	LV:UCOE.hCD18
Primary recipients	0.897±0.430	0.703±0.130	0.738±0.162	0.438±0.005
Secondary recipients	0.457±0.145	0.613±0.090	0.358±0.112	0.350±0.087

Table 17. VCN determination in gDNA extracted from PBLs from primary and secondary recipients at 3 mpt.

3.2.4. Correction of LAD-1 phenotype in gene therapy-treated CD18^{HYP} mice

As mentioned in section 1.1.1., CD18^{HYP} mice displayed leukocytosis as a typical symptom of CD18 deficiency. Levels of leukocytes were evaluated in *ex vivo* GT-treated primary and secondary CD18^{HYP} mice recipients (Figure 62). Primary recipients maintained the characteristic leukocytosis along the analysis time. This behaviour was very similar to that observed in the control eGFP CD18^{HYP} group. However, normalization in white blood cell counts could be observed in secondary recipients despite of having a considerable lower proportion of hCD18^{+} cells in PB.

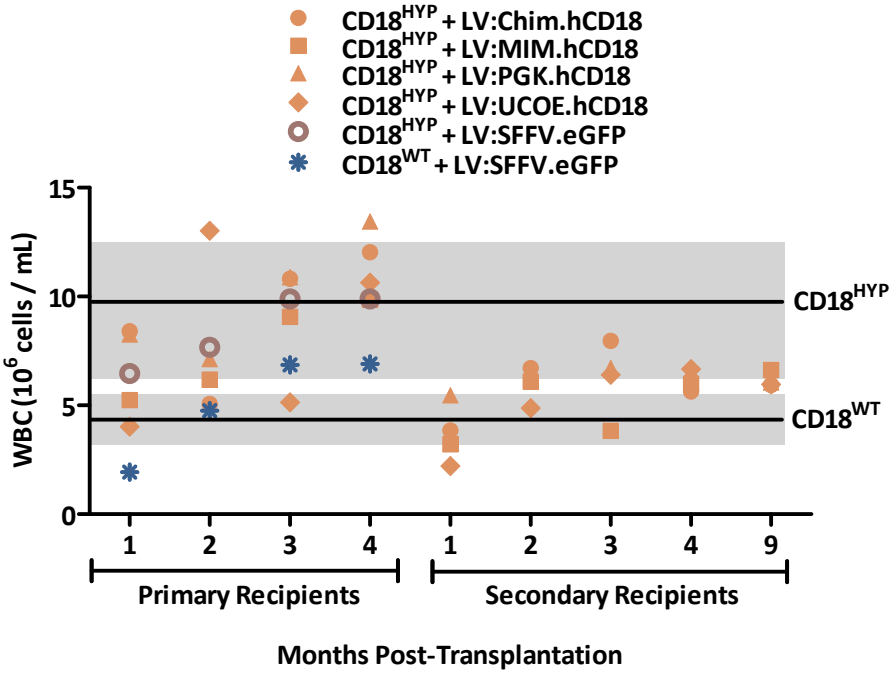

Figure 62. White blood cell counts in *ex vivo* GT-treated primary and secondary CD18^{HYP} mice recipients. Control mice were transplanted with eGFP transduced CD18^{WT} and CD18^{HYP} mice.

CD18 deficiency leads mainly to defects in neutrophil extravasation from PB to inflamed tissues. As shown before in section 1.1.5., neutrophils from CD18^{HYP} mice showed reduced capacity of extravasation in an air-pouch-based inflammation model. Therefore, we performed the same experiment with *ex vivo* GT-treated primary CD18^{HYP} mice and control animals. As can be observed in Figure 63, hCD18^{+} CD18^{HYP} neutrophils migrated to the air-pouch significantly better than eGFP^{+} CD18^{HYP} control neutrophils and in a similar way to eGFP^{+} and untransduced CD18^{WT} indicating that ectopic hCD18 expression was able to correct neutrophil migration defects in CD18^{HYP} mice.

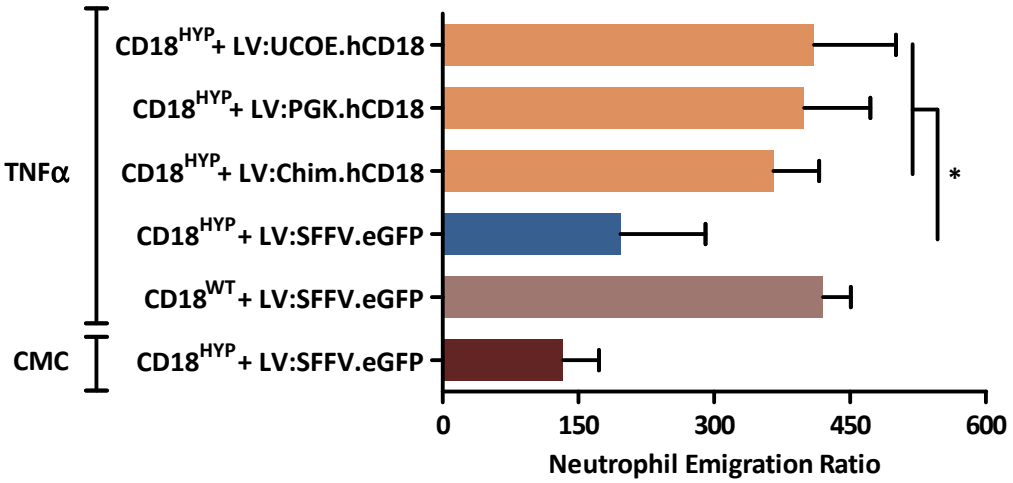

Figure 63. Air pouch-based inflammation model in *ex vivo* GT-treated primary $CD18^{HYP}$ recipients and control mice treated either with TNFα (proinflammatory stimulus) or CMC (vehicle). Neutrophils emigration ratio is calculated as described in material and methods from the total cell number found within the pouch and the percentage of $Gr1^+$ cells determined by flow cytometry. The significance of differences between groups is expressed P<0.05 (*).

Furthermore, in the group of LV:Chim.hCD18-treated $CD18^{HYP}$ mice we could performed a second functional assay to evaluate neutrophil migration capacity based on the intranasal administration of LPS. Although differences were not significant, we could observe a clear trend for GT-treated neutrophils to migrate similarly or even higher than those from $CD18^{WT}$ animals (Figure 64). These two functional experiments demonstrated that $hCD18^+$ $CD18^{HYP}$ neutrophils recovered the capability to extravasate from PB to inflamed tissues.

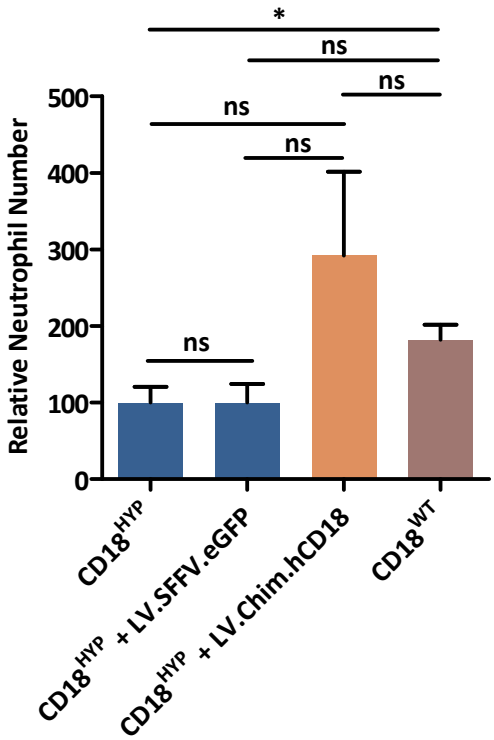

Figure 64. Neutrophil migration to a lung inflammation model based on LPS intranasal administration. The relative neutrophil number is calculated as described in material and methods from the absolute cell number found in the BAL and the percentage of $Ly6G^+$ $CD11c^-$ cells determined by flow cytometry. The significance of differences between groups is expressed P<0.05 (*).

Discussion

In the present thesis we have characterised a mouse model of LAD-1 immunodeficiency ($CD18^{HYP}$ mice), which allowed us to uncover new roles of β_2 integrins in HSC regulation. Moreover, we have developed new LVs for the GT of LAD-I, testing them in three different models: human LCLs, human CD18-interferred CD34-derived neutrophils and $CD18^{HYP}$ mice. In any case, hCD18-LVs have appeared as a powerful tool for LAD-I GT.

1. Characterization of the $CD18^{HYP}$ mouse model: New role of β_2 integrins in HSC regulation

$CD18^{HYP}$ mice (B6.129S7-*Itgb2*^{tm1Bay}/J) were generated by homologous recombination of a targeting vector containing the neomycin resistance gene[75]. The presence of a cryptic promoter in the plasmid backbone resulted in a hypomorphic mutation, leading to a decreased but not absent expression of CD18, resembling the characteristics of the moderate LAD-I phenotype. These mice were originally generated and described in a mixed background C57BL6/J and 129/Sv. They have been backcrossed for more than 10 generations to the C57BL/6J inbred strain but no description has been performed after backcrossing. Our first aim was then to characterize the $CD18^{HYP}$ haematopoietic phenotype in the C57BL6/J background.

LAD-I human patients and different LAD-I animal models have a characteristic increment of circulating leukocytes in PB[41]. $CD18^{HYP}$ mice recapitulate this symptom, with high numbers of lymphocytes and granulocytes in PB in comparison to $CD18^{WT}$ mice (Figure 22). This neutrophilia has been extensively studied and several hypotheses have been proposed to explain this phenotype. The first one is that the defective antimicrobial function of CD18-deficient neutrophils leads to the occurrence of infections and thus to a continuous BM stimulation and granulocyte production[79]. The second one is an increased production of hematopoietic cytokines, including IL-17, by unidentified cells in tissues due to the incapacity of CD18-deficient neutrophils to extravasate from PB. IL17 contributes to increase G-CSF levels thus enhancing granulopoiesis[179]. A third hypothesis propose that CD18-defficiency leads to an apoptosis delay in neutrophils, leading to an alteration in their homeostasis and their accumulation in PB[180]. Related to this last mechanism, Casanova-Acebes et al[18] demonstrated the importance of the granulocyte homeostasis maintenance in the regulation of haematopoiesis and showed that defects on adhesion molecules expression can alter the hematopoietic stem cell niche. All of these studies demonstrated that β_2 integrins' expression may be implicated in complex HSC regulation, that need to be further explored.

First, total PBLs and BMCs were interrogated for β_2 integrins' expression and, as expected, they showed a marked decrease in CD18 and CD11 subunits membrane expression (Figures 23 and 25). CD18 expression was equally reduced in T cells, B cells and neutrophils. The reduction of β_2 integrins' expression found in $CD18^{HYP}$ mice was very similar to that observed in LAD-I patients with a moderate phenotype. Not only the expression levels but also proportion of β_2 integrin expressing cells was reduced in $CD18^{HYP}$ mice in comparison with $CD18^{WT}$ mice, apart from Mac-1^+ (CD18-CD11b) cells that were slightly increased (Figure 24). Mac-1 is mainly expressed by neutrophils so this increment in Mac-1^+ cells could be related to the expansion of neutrophil population. Similar analysis was performed in mouse HSCs (defined as LSK cells) from $CD18^{HYP}$ mice. They barely expressed LFA-1 β_2 integrin (CD18

and CD11a) while no differences were found in VLA-4 β_1-integrin, suggesting that β_2 integrin deficiency is not compensated by an overexpression of other hematopoietic integrins (Figure 26).

β_2 integrins play an important role during leukocyte extravasation[24]. As a consequence of CD18 deficiency, this process is particularly impaired in neutrophils[41]. This extravasation defect was corroborated in $CD18^{HYP}$ mice in two different inflammation models: an LPS-induced pulmonary damage model[181] and a TNFα-induced air-pouch model. In both cases, where two different stimuli and two different body locations (respiratory tract and subcutaneous space) were employed, migration to the inflamed tissue of $CD18^{HYP}$ neutrophils was highly reduced in comparison to $CD18^{WT}$ ones (Figures 27 and 28). These results correlated with the impaired migration of $CD18^{HYP}$ neutrophils to the peritoneal cavity described by Wilson et al[75] when a chemical peritonitis was induced by intraperitoneal injection of thioglycollate medium. In addition, Ridger et at[182] had already described that intravenous administration of anti-CD18 antibodies inhibited neutrophil migration after LPS instillation. Impaired leukocyte influx in a subcutaneous air pouch in response to TNFα was already described by Ding et al for both $CD18^{KO}$ and $CD11a^{-/-}$ mice while in $CD11b^{-/-}$ mice was markedly increased [174]. According to these results, migration is response to TNFα can be definied as a LFA-1-dependent process.

Adhesion molecules, specially integrins, do not only mediate cell-cell and cell-ECM adhesion, but can also play roles other than their canonical functions and affect the multitude transduction cascades that control cell survival, proliferation, differentiation and organ development[21]. In addition, some authors have described implications of adhesion molecules in the regulation of HSCs[18,183]. Thus, we further investigated a possible implication of β_2 integrins in HSC regulation.

When the LSK cell content was investigated in $CD18^{HYP}$ mice, a significant increment was found in comparison to $CD18^{WT}$ mice (Figure 29) and was consistent with that observed in a transgenic mouse model deficient in other adhesion molecules: E- and P-selectins (PEdKO mice)[18]. A more detailed FACS analysis revealed a significant increment of ST and LT-HSCs within $CD18^{HYP}$ BM in comparison to $CD18^{WT}$ mice (Figure 30). This enrichment was confirmed as an increased clonogenic capacity in methylcellulose cultures (Figure 31). These results pointed out an important role of different adhesion molecules in the regulation of the HSC content in BM.

The gold standard test to estimate the number of HSC is the LDA[184], in which graded decreasing donor BM cell numbers of a particular genotype are mixed with a radio-protective and constant dose of BMCs from a distinguishable donor. The engraftment of test donor cells is evaluated then at 3 months post-transplantation, both in the lymphoid and in the myeloid lineages. The number of engrafted animals on each transplantation group could be used to estimate the frequency of HSCs using different mathematical models. When using the ELDA software to analyse our results of LDAs[151,185] assays with $CD18^{WT}$ and $CD18^{HYP}$ mice, we observed a trend showing increased number of HSCs within $CD18^{HYP}$ BM in comparison with $CD18^{WT}$ BM, although this difference was not statistically significant (Table 13).

As previously mentioned, CD18 deficiency might be related with altered apoptosis in deficient cells. Gomez et al[77] described reduced apoptotic levels in $Gr\text{-}1^+$ cells in the BM of mice transplanted with different proportions of CD18-deficient and WT cells. We obtained similar results in $Gr1^+$ PB cells

of $CD18^{HYP}$ mice (Figure 32B). There are many other papers in which the role of CD18 in the regulation of apoptosis in mature circulating neutrophils has been studied. Engagement of β_2 integrin on these cells can either inhibit or enhance apoptosis depending on the activation state of the integrin and the presence of pro-apoptotic stimuli such as TNFα or FAS[186,187]. In our studies, a significant increment in the proportion of LSK cells in G_0 phase within $CD18^{HYP}$ BM in comparison with $CD18^{WT}$ was found (Figure 32A). When apoptosis in LSK cells was analysed, no differences were found between $CD18^{WT}$ and $CD18^{HYP}$ mice. Thus, our results suggested that CD18 is not playing a relevant role in the regulation of apoptosis on early hematopoietic progenitors.

Previous reports showed that deficiencies in β_2 integrins by themselves do not affect the ability of BM cells to home to the hematopoietic niche once intravenously administered[175,188]. However, inhibition of VLA-4 in CD18 deficient HSCs resulted in a dramatic reduction in BM homing in comparison to the inhibition of VLA-4 in WT mice. This suggests that CD18 can contribute to BM homing when the function of VLA-4 is compromised[175,189]. Our studies on the homing ability of $CD18^{WT}$ and $CD18^{HYP}$ LSK cells revealed that LSK cells migrate equally to the BM regardless of the level of CD18 expression (Figure 33). β_1 integrins have shown to be essential for the retention of HSCs within the hematopoietic niche[78,189]. Thus, disrupting VCAM-1/VLA-4 axis (with antibodies or small molecules) provides modest mobilization in mice, macaques and humans[190,191]. Mobilization induced by the combination of CXCR4 and VLA-4 blockage has been described to have an additive effect and could provide an alternative to G-CSF treatment[190]. A possible role of β_2 integrins in HSC mobilization remains to be defined and $CD18^{HYP}$ mice could provide a useful model in this respect.

Casanova-Acebes et al [18] described a new role of an specific population of aged neutrophils in HSCs regulation. These PB aged neutrophils are able to migrate back to the BM as a clearance mechanism. in BM, these cells are phagocytized by BM-resident macrophages, thus initiating a signalling cascade that leads to a reduction in the number of CAR cells and in the levels of CXCL12 that eventually produces the mobilization of HSCs from the BM to PB. However, the physiological significance of this link between hematopoietic and immune system remains to be defined. In PEdKO mice, deficient for the adhesion molecules P- and E-selectins, aged neutrophils are not able to migrate back to the BM, leading to their accumulation in PB and to the enrichment in primitive HSCs within BM. A more moderate accumulation of aged neutrophils was observed in $CD18^{HYP}$ mice (Figure 34). To clarify if this partial accumulation of aged neutrophils could explain the observed enrichment in HSCs in $CD18^{HYP}$ mice, we daily injected I.V. *ex vivo*-senesced WT neutrophils into $CD18^{HYP}$ mice. This procedure did not result in a recovery of normal levels of LSK cells in the BM of recipient mice (Figure 35). Thus, a possible defect in CD18-defficient neutrophil BM clearance may not be sufficient to produce the enrichment in BM HSCs observed in $CD18^{HYP}$ mice.

In order to investigate if the higher content of HSCs could lead to a higher hematopoietic repopulation capacity of $CD18^{HYP}$ cells, we performed a CRA where equal proportion of $CD18^{HYP}$ and $CD18^{WT}$ total BMCs were mixed together and transplanted into irradiated WT recipients. For the CRAs we took advantage of the P3B-ΔhCD4 mice previously generated in the laboratory[149], which are characterized by the expression of a truncated form of the human CD4 protein (hCD4) in all the hematopoietic system. The use of three isogenic mouse strains (P3B-ΔhCD4 and $CD18^{HYP}$ as donors and P3B as recipients), each one expressing a different specific panleukocytic marker ($hCD4^{+}CD45.1^{+}$,

CD45.2^{+}, CD45.1^{+} respectively) allowed us to obtain a detailed and accurate follow up of the HSC repopulating kinetics. After the transplantation of this mixture it was possible to observe that CD18^{HYP} cells contribute greater than CD18^{WT} cells to the hematopoietic reconstitution of recipients, both in PB and BM, confirming a higher repopulation capacity of CD18^{HYP} BM cells. This repopulation capacity must be only due to higher capacity of the CD18^{HYP} HSCs to repopulate as the receptor microenvironment of the BM is WT. The BM of primary recipients was infused into lethally irradiated WT secondary recipients, where the contribution of CD18^{HYP} cells to the hematopoietic reconstitution was even higher than that observed in primary recipients (Figure 36). This increment in the hematopoietic reconstitution capacity of the CD18^{HYP} cells could be attributed to cells in the BM, other than the primitive HSCs, that could be contributing to the engraftment or helping the deficient cells to engraft. When we enriched the BM in HSCs and haematopoietic progenitors by lineage depletion (so less accessory cells were infused) and performed the CRA as defined, an even higher repopulating capacity of CD18^{HYP} cells was observed (Figure 37).

To demonstrate that the increased engraftment was due to the CD18^{HYP} true HSCs we would need to infuse the exact same number of this true HSC population in a CRA. To this aim, a third CRA was carried out mixing BMCs from CD18^{HYP} and CD18^{WT} in a 70:30 proportion. Taking into account the percentage of LSK cells on each type of competitor population, the actual proportion of LSK cells in this mixture would be the same. At 1 mpt, CD18^{HYP} cells contributed less than WT cells to the haematopoietic reconstitution, something that would be expected as less cells were infused. Nevertheless, the CD18^{HYP} engraftment increased along time and when BM was analysed at 5 mpt, similar donor chimerism was observed from both competitor populations although the initial proportion of CD18^{HYP} was more than two times lower. BMCs from these animals were transplanted into secondary recipients and donor chimerism was analysed. While similar engraftment levels of CD18^{HYP} and CD18^{WT} cells were observed in PB, a higher engraftment of CD18^{HYP} cells was observed in the BM, being possible to detect statistically significant differences in the proportion of LSK cells (Figure 38) at the end of the experiment. Gomez et al[77] described very similar observations for CD18^{KO} mice. These mice showed increased proportion of LSK cells within the BM. CRAs were conducted mixing different proportions of CD18^{KO} and WT fetal liver cells and in every case the contribution of CD18^{KO} to the recipient hematopoietic reconstitution was higher than the proportion in the initial mixture.

On the basis of these results, we hypothesized that CD18 deficiency leads itself to a cell-autonomous expansion of HSCs. CD18-defficiency may deprive HSCs from specific signalling leading to deregulation of the normal HSC pool. The fact that the deficiency of CD18 in HSC might be the mechanism underlying the enrichment in HSCs was confirmed by the observations in secondary recipients. CD18^{HYP} HSCs transplanted in a WT environment are able to expand and contribute in a higher extent to the secondary recipient's hematopoietic reconstitution. If the enrichment of CD18^{HYP} HSCs was due to CD18-defficiency in other cells different from HSCs themselves, the presence of WT cells either by the *ex vivo* neutrophil transfer or by the cotransplantation with CD18^{WT} HSCs would have reduced LSK cell content to normal levels and similar repopulation ability would have been observed in secondary recipients.

CD18 deficiency may private BM cells from many signals coming from the extracellular matrix and the hematopoietic niche. On the one hand, β_2 integrins can play a role as intracellular signal

transducers[24]. Ligand-induced clustering of the β_2 integrins induces SFK activation, leading to the activation of important signalling molecules as PKC, ERK1/2 and Akt, which can regulate gene transcription. β_2 integrin-induced SFK activation also regulates actin reorganization via Syk/Vav1/3 pathway and many other molecules have been found to be directly associated with the β_2 integrin intracellular region. On the other hand, the relationship between stem cells and their niches has been largely characterized. Stem cell niches regulate such important aspects as self-renewal, proliferation and survival[189,192]. Therefore, the lack of communication between CD18-defficent HSCs and the hematopoietic niche is sufficient to explain the deregulation in the HSC pool observed in the $CD18^{HYP}$ mice. HSC deregulation due to deficiencies in other adhesion molecules such as E-selectin[183] or α_{II} integrin[193] have been previously reported, but our results constitute the first link between CD18 and HSCs.

One of the bottlenecks for the *ex vivo* GT of some hematopoietic disorders is the availability of enough numbers of autologous HSCs. Patients with some genetic diseases, such as Fanconi anaemia, are characterised by a progressive loss of HSCs[194] and current efforts have been focused on the early diagnosis of the disease aiming the collection of the HSCs before the patients develop the BM failure[195]. In the case of LAD, no relationship between β_2 integrins and HSCs has been described in humans. For this reason, and on the basis of the results observed in $CD18^{HYP}$ mice, the study of HSC content in the BM of LAD-I patients would be highly relevant, as such a potential HSC enrichment in LAD-I patients would be very useful for the GT of these patients.

In some PIDs such as X1-SCID or WAS, that have been successfully treated by *ex vivo* haematopoietic GT, corrected cells present a proliferative advantage over uncorrected ones. Thus, although a limited number of corrected cells engraft, these can overcome the non-corrected cells and residual defective haematopoiesis[196,197]. The availability of a great number of autologous HSCs would be of special interest for the GT of LAD-I because a proliferative advantage of the corrected cells is not expected, except for corrected T cells (as described in HSCT and GT experiments in CLAD dogs[64,141]).

2. Gene Therapy for LAD-I

LAD-I is a severe immunodeficiency disorder leading to the death of most of the patients within the first two years of their life, in the case of those patients with the severe phenotype. Despite the fact that allogeneic HSCT has resulted in survival rates from 71 to 91 %[51,61-63], the access to HLA-matched donors is still a major limitation for this therapy.

Haematopoietic *ex vivo* GT is a promising therapeutic approach for many genetic haematological and non-haematological disorders and a powerful alternative to the allogeneic HSCT. Indeed, in some diseases such as ADA-SCID, haematopoietic GT is currently considered an alternative to unrelated HSCT. Much research has been done in preclinical models in terms of efficacy and safety that has enabled GT to make a great leap forward and nowadays GT clinical trials have become a reality. Patients from different diseases such as X1-SCID, ADA-SCID, ALD, or WAS have actually benefited from this new approach[84,99,197]. The appearance of some cases of acute lymphoid leukaemia due to LTR-mediated insertional oncogenesis has changed the vector of choice from γ-RVs to LVs. The most

common form of insertional oncogenesis occurs when the vector is integrated close to a proto-oncogene and the viral LTR is able to transactivate its expression. Some additional modifications have been made in the LV backbone to minimize its transactivation capacity. Among them, it is worth to point out the elimination of specific enhancer sequences in the LTR regions leading to the so-called SIN LVs. This modification requires the introduction of internal promoters with less transactivation capacity in the SIN LVs to drive the expression of the therapeutic transgene[99]. Moreover, LVs themselves have a safer integration profile than classical γ-RV. LVs do not integrate in regulatory regions but have a preference for integration into the body of genes, which lowers considerably the risk of genotoxicity as shown by different *in vitro* and *in vivo* studies[114,198]. Although there are other retroviral vectors derived from foamy viruses and α-retroviruses and even non-viral vectors such as transposons with a considered more random and safer integration profile[123] that are being investigated for GT[199-201], SIN LVs are nowadays the vector of choice for *ex vivo* hematopoietic GT. A great efficacy with a very good safety profile has been recently published for SIN LVs for the treatment of WAS[90] and MLD[98] and new LV-based GT clinical trials are currently on going for PIDs such as X-CGD, ADA-SCID and X1-SCID. Furthermore, LVs can be produced in large scale under GMP conditions, something that will be required for any hematopoietic GT clinical trial[202].

In the last few years, new approaches of GT have emerged based on gene editing, as an alternative to vector-mediated gene addition strategies. Gene editing is based on the modification of the cell genome taking advantage of the process of homologous recombination to correct a pathogenic mutation or to introduce a correct copy of the affected gene in a safe harbour. Many efforts have been made to improve the efficacy of gene editing but the use of engineered genetic scissors has allowed the huge boom that gene editing has experience over the last decade[203,204]. There is currently one clinical trial based on these technology which aims the disruption of the CCR5 gene in T cells as a new therapeutic approach for AIDS[205] and the modification of human HSCs is still at a preclinical level[206].

For all these reasons, we have attempted to develop new GT approaches for LAD-I based on SIN LVs where hCD18 cDNA was expressed under the control of 4 different internal promoters. Two of them are ubiquitous promoters, the PGK and the UCOE promoter. As CD18 is expressed in all the leukocytes and in some populations of HCS and hematopoietic progenitors, the use of ubiquitous promoters will allow us to drive transgene expression in all the cells lacking CD18 expression as a consequence of *ITGB2* mutations. Many data has been already published regarding the PGK promoter in preclinical GT studies[95,207,208]. In addition, a PGK LV has been recently used in the GT clinical trial for MLD[98] and another is going to be used in a future clinical trial for Fanconi Anaemia[95]. SIN PGK γRV displayed a similar immortalization capacity than a full-length PGK γRV[209] probably due to the presence of an enhancer sequence[210]. In addition, some authors described aberrant transcript arising from the antisense strand of the PGK-neomycin constructs intended for KO mice generation[211,212]. However, no transformation capacity was observed for the PGK promoter in the context of LVs by the *in vitro* immortalization assay[114] and no clonal dominance has been observed in the MLD GT clinical trial, confirming the attractive safety profile of this promoter. The other ubiquitous promoter used to drive the expression of hCD18 was A2UCOE, which has several interesting features for GT. This promoter has been shown to be more resistant to epigenetic silencing than other frequently used promoters, such as SFFV, CMV or EF1α[168]; and to lack classic enhancer activity[167], which in the context of GT vectors may be useful to reduce the risk of enhancer-mediated insertional oncogenesis. It has also been shown to provide relatively efficient therapeutic correction of different preclinical disease mouse models such as

X1-SCID[167] and Recombination activating gene 2 (RAG2)-SCID[213], with no significant adverse effects. Furthermore, this promoter was also capable to confer resistance to epigenetic silencing to an adjacent promoter[168,214]. However, it has the potential to cause insertional mutagenesis through aberrant splicing, so a refined version has been designed recently[215].

The other two promoters used in this study are promoters preferentially active in myeloid cells. Although CD18 is expressed in all leukocytes, LAD-I is considered as a phagocytic disorder rather than a lymphocytic disorder. The use of myeloid promoters would thus induce a higher CD18 expression in the cell type that is most markedly affected in this disease. In the case of Chim promoter, it has been already used in the context of a SIN LV for the GT of a mouse model of X-CGD with very promising results[115], based on which a new clinical trial will be carried out for the GT of X-CGD patients. Actually, two X-CGD patients have been already treated with this LV on a compassionate-use: The first one died early after the transplant because of complications not related to the gene therapy. In the second patient, neutrophil function recovery could be observed *in vitro,* although the patient died early after the transplant also due to a GT-unrelated complication (Personal communication, ESGCT 2014, The Hague).

In these four hCD18-LVs, a WT sequence of the hCD18 cDNA has been included. Aditionally, we analysed hCD18 cDNA for coding optimization. Using OptimumGene codon optimization tool we obtained a codon adaptation index (CAI) of 0.84 for the WT sequence, which is very close to the optimal CAI (1). Although many authors have proposed the utilization of codon-optimised transgenes for GT[207,216], other authors support the need of a deep safety analysis of codon optimised-constructs intended for clinical application[217].

We aimed to test these four hCD18-LVs in *in vitro* human LAD-I models. For this objective, we first took advantage of the ZJ cell line, which is a human lymphoblastoid cell line obtained by immortalization of B cells obtained from a LAD-I patient[156]. This cell line showed no detectable levels of β_2 integrins in the cell membrane and has been previously used for CD18 transference studies [132,134,135]. Transduction of ZJ cells with increasing doses of LV:Chim.hCD18 resulted in the recovery of hCD18 and hCD11a membrane expression (Figure 39). Interestingly, surface expression levels of both subunits were rapidly saturated from the MOI of 10 vp/cell onward. To investigate the effect of the transduction on the mRNA levels of both subunits, QPCR gene expression analysis were performed and thus it was possible to observe a progressive increment in the expression of hCD18 mRNA while no alteration of hCD11a mRNA levels was observed. All these results indicated that ectopic expression of hCD18 had no apparent impact on the endogenous regulation of CD11a expression. As CD18 has to be expressed in the membrane together with CD11 subunits, CD18 membrane expression got saturated by endogenous levels of CD11 proteins.

Transduction of ZJ cells with each of the four hCD18-LVs (at a MOI of 10 vp/cell) resulted in full recovery not only of CD18 but also of CD11a subunit expression at a very similar VCN in all the cases (between 4 and 5.5; Figures 40A and 40B). When transduced ZJ cells were interrogated for CD18 expression levels, no significant differences could be observed between these levels and the ones found in the GUS-1 cell line (a human WT LCL; Figure 40C). However, levels of CD18 membrane expression were significantly higher than those obtained for the MARK cell line, a WT LCL from a different donor.

This could be due to differences on CD18 expression between different individuals as it has been described that there are many factors that can alter the levels of expression of β_2 integrins such as life habits[218], environmental factors[219], traumatic processes[220] and even diseases[221,222]. With each of the hCD18-LVs, transduced ZJ cells were able to aggregate in the presence of PMA and to bind to sICAM-1 after Mg^{2+}/EGTA activation (Figure 41 and 42). These results indicated that hCD18-LVs are able to restore β_2 integrin expression and to correct LAD-I phenotype in a cell line derived from a patient. Similar recovery of PMA-dependent aggregation was shown for γ-RV-transduced ZJ cells by Wilson et al[132,134] although the proportion of $CD18^+$ cells was much lower in all the cases and FACS-sorted $CD18^+$ cells were used for the functional assays. Moreover, this aggregation assay is not easily quantifiable so the utilization of the sICAM-1 binding assay provided a more objective and easy-to-measure information regarding the functionality of the β_2 integrins.

An ideal *in vitro* model for LAD-I GT would be the use of patient's HSCs that could be transduced and then *in vitro* differentiated into neutrophils or even transplanted into immunodeficient mice. However, it is important to keep in mind that LAD-I is a very rare condition (around 350 patients have been diagnosed in Europe and, to our knowledge, there are no alive LAD-I patients in Spain up to date). In addition, BM aspirations are not routinely performed on these patients as this procedure is not required for the diagnosis or the follow-up of these patients. For these reasons, we aimed to generate LAD-I like human HSCs taking advantage of the RNA interference technology. This strategy has been previously used to generate human models to study the efficacy of GT for other diseases[129,130].

To this end, we used a previously reported LV construct[171,172] to clone our shRNAs. After studying the efficacy of different constructs, a LV expressing a shRNA against the 3' UTR region of the hCD18 mRNA (LV:sh10) was selected for the experiments because of its high efficiency. Transduction of healthy cord blood human $CD34^+$ cells with this LV resulted in a 90% reduction of hCD18 expression levels determined by QPCR and by FACS, with a concomitant reduction in the hCD11a surface expression levels (Figure 44). β_2 integrins are obligated heterodimers thus, although LV:sh10 transduction did not alter hCD11a transcription, hCD11a cannot be expressed at the membrane without hCD18. The expression levels found on these LAD-I like HSCs (10 % of that found on control cells) allowed us to mimic HSCs obtained from LAD-I patients with the moderate phenotype.

These LAD-I like HSCs were subsequently used to test the efficacy of the LV:Chim.hCD18 to correct the LAD-I like HSCS. Neutrophils were generated *in vitro* from these HSCs. LAD-I like neutrophils showed surface expression levels of CD18, CD11a and CD11b that were drastically reduced in comparison with control neutrophils (Figure 45). Moreover, LAD-I neutrophils showed defects in their functionality as seen in three different CD18-dependent assays: they were unable to properly bind to β_2 integrins' ligands like ICAM-1 and fibrinogen and they could not mount a proper respiratory burst upon opsonised zymosan activation (Figures 48, 49 and 50).On the other hand, neutrophils derived from LAD-I like HSCs that had been transduced with the therapeutical LV, showed partial recovery on CD18, CD11a and CD11b surface expression levels. As a consequence of this expression restoration, they showed improved capacity to bind to ICAM-1 and fibrinogen in comparison with uncorrected neutrophils and, moreover, full restoration of the ability to mount a respiratory burst in response to opsonized-zymosan (Figures 48, 49 and 50). These results pointed out that CD18-dependent adhesion and physical functions are more sensitive to CD18 expression levels while CD18-dependent signalling

functions (e.g. sensing the environment to mount a respiratory burst) only required a partial CD18 expression to be run properly. In other GT clinical trials for diseases in which the affected protein is involved in signalling pathways (such as X1-SCID), very low transgene expression has been shown to be enough to correct the phenotype of the disease[196].

The fact that the therapeutic LV:chim.hCD18 was not able to restore more than 50% of the CD18 expression levels found in control cells could be explained by different reasons. Sh10 was designed to target the 3' UTR of hCD18 mRNA, which is the mRNA sequence that immediately follows the translation termination codon and contains regulatory regions involved in post-transcriptional gene expression. This strategy has the advantage that LV-mediated expression of hCD18 would not be recognised by the shRNA as the ectopic CD18 mRNA does not contain that region. However, regulatory motifs in UTRs are often conserved in genes belonging to the same family[223]. Actually, using the results received through BLAST analyses we can predict that the sh10 would potentially be able to recognise at least 6 human mRNAs. We hypothesize that downregulation of some of these genes could be affecting the ability of hCD18 to be re-expressed in the membrane, limiting somehow the utility of this model. Although more recent and accurate tools like CRISPR-Cas9 genome editing could be used as an alternative to shRNAs to generate a LAD-I disease-model in primary mouse[224] and human HSCs[225], our results provide a human model to test our vectors *in vitro*.

In vitro models are always very powerful tools for testing the efficacy of new therapeutic approaches and reduce the number of experimental animals. However, *in vitro* experiments cannot reproduce the complexity of a haematopoietic *ex vivo* GT protocol, so *in vivo* experiments are always required to finally assess its efficacy and safety. To test our hCD18-LVs we took advantage of the $CD18^{HYP}$ mouse model. Although $CD18^{KO}$ mice could appear as a good experimental model due to the absence of CD18 expression the fact that these animals are poor breeders make them problematic for these kind of experiments. The $CD18^{HYP}$ mice behave as normal breeders and previous works[75] and our own experiments demonstrated that $CD18^{HYP}$ mice had a sufficient phenotype to study the efficacy of the GT.

BM-derived lin^- cells, that is a population enriched in haematopoietic progenitors and HSCs, was selected as the target population for the gene transfer. These cells, once transduced and transplanted into irradiated animals, are able to repopulate the animals generating hematopoietic cells of all the lineages carrying the provirus integrated in their genomes. Although more primitive populations can be used as target cells, like lin^-cKit^+ cells[226] or even LSK cells[227], lin^- cells are common target cells for haematopoietic *ex vivo* GT in mice[95,149,196,207].

First, we wanted to analyse the *in vitro* transduction process. With this aim, freshly isolated lin^- cells were transduced with the different hCD18-LVs and then differentiated towards the myeloid lineage for seven additional days. hCD18 was detected in every case, in a range between 30 and 40% (Figure 51). hCD18-LV transduction resulted in increased mCD11a surface expression levels which indicated that new β_2 integrins were formed and transported to the membrane, consisting of hCD18 and mCD11a subunits (Figure 52). These results indicated that hCD18 can be expressed in mouse haematopoietic cells, in concordance with previous works[131,132], leading to the recovery of mCD11a expression in the cell membrane.

Leukocytes have been reported to develop an important posttranscriptional regulation of β_2 integrins both *in vitro* and *in vivo*, in response to a variety of stimuli such as cytokines, phorbol esters, and complement[228]. Neutrophils derived from transduced lin^- cells did show upregulation of hCD18 expression upon PMA stimulation (Figure 53), which pointed out that the ectopic hCD18 expression can be regulated in a physiological way in mouse hematopoietic cells.

Finally, the toxicity of the transduction process was evaluated in a methylcellulose-based colony forming cell assays (Figure 54). No differences in the number of CFUs were observed among untransduced, GFP- or hCD18-transduced cells indicating that neither the LV-transduction or the ectopic hCD18 expression mediate a significant hematopoietic toxicity. Other therapeutic transgenes used in GT studies have been proposed to result in toxicity for transduced HSCs. This is the case of $gp91^{phox}$ (for the GT of X1-CGD), whose constitutive expression may lead to the inappropriate production of ROS, limiting their functionality or engraftment potential. However, there is no currently enough evidence supporting this hypothesis and expression of $gp91^{phox}$ and induction of intracellular ROS in HSCs has to be studied in more detail[88].

Once we had checked that hCD18-LVs were able to efficiently transduce $CD18^{HYP}$ lin^- cells, we moved to the *ex vivo* GT experiments. Freshly-isolated lin^- cells were transduced at low MOI and transplanted into lethally irradiated $CD18^{HYP}$ mice. After transplantation of transduced cells, $hCD18^+$ cells could be detected in the PB of all the GT-treated animals. hCD18 was co-expressed with the three murine CD11 subunits (mCD11a, mCD11b, mCD11c; Figure 55). A similar proportion of $hCD18^+$ $mCD11a^+$ cells was observed in all the GT-treated mice at 1 and 3 mpt, in a range between 14 and 44%; (Figure 56A). Interestingly, these animals expressed higher levels of mCD11a in comparison with mice transplanted with LV:SFFV.eGFP-transduced $CD18^{HYP}$ cells (Figure 57). This increment was very similar in all the groups and led to the recovery of 50% of the levels found in control mice transplanted with $CD18^{WT}$ cells. The increased expression of mCD11a resulted from the formation of new chimeric β_2-integrins composed by the association of hCD18 and mCD11a as observed *in vitro*. At the end of the experiment similar levels of $hCD18^+/mCD11a^+$ cells and a comparable upregulation of mCD11a expression was found in the BM of *ex vivo* GT-treated $CD18^{HYP}$ mice (Figure 59).

hCD18 was expressed in T cells, B cells and neutrophils (Figure 58A), despite of the promoter used to drive the expression of the therapeutic transgene. As mentioned before, Chim and MIM have been proposed as myeloid-specific promoters. However, when the Chim promoter was first described by Santilli et al[115], it was observed that this promoter was actived both in lymphoid and non-hematopoietic cell lines, although at a lower level as compared to that observed in myeloid cells. A similar behaviour was observed for the MIM promoter, both *in vitro* and *in vivo* (Personal Communication). In our experiments, when PB cells were interrogated for hCD18 expression levels, it was possible to observe that neutrophils always showed higher hCD18 levels than B and T cells, as happens with the physiological mCD18 expression in these cells. This was observed in all GT-treated mice, no matter the nature of the promoter used to regulate the expression of hCD18. However, the ratio between the myeloid and lymphoid hCD18 expression was higher in cells that have been transduced with the LV:Chim.hCD18 group, which thus closely mimicked the physiological CD18 expression pattern (Figure 58C).

CD18 is expressed in most leukocytes and play other roles outside the LAC. LFA-1 is essential in the immune synapse formation since it enables a maintained contact between T cells and APCs and initiates a signalling pathway leading to the decrease of the T cell activation threshold. In addition, LFA-1 has been implicated in the cytolitic function of $CD8^+$ T cells and NK cells[24]. Lymphocytes from LAD-I patients show impaired *in vitro* proliferation and blastogenesis. Nevertheless the role that CD18 deficiency in lymphocytes plays in the pathogenesis of LAD-I is still unknown[43]. LAD-I symptomatology has been associated with defects on neutrophil function[41]. CD18-defficient neutrophils fail to extravasate from the blood flow while lymphocytes can take advantage of other adhesion molecules[42]. For that reason, we believe that a promoter driven expression of hCD18 in all haematopoietic lineages, though with high levels of expression in neutrophils would be ideal for the GT of LAD-I.

Our results confirm for the first time that hCD18 can be expressed *in vivo* in $CD18^{HYP}$ hematopoietic cells after LV-mediated GT. Previous studies showed that hCD18 can be expressed after γRV-mediated *ex vivo* hematopoietic GT in C3H/HeJ mice (a general purpose mouse strain with WT mCD18 expression)[133]. A similar pattern of hCD18 expression was observed in this previous work, where neutrophils expressed higher hCD18 levels than lymphocytes.

Safety is a major concern in the GT field. In the first GT clinical trials, several cases of T-ALL and MDS took place as a consequence of LTR-mediated insertional oncogenesis[120,121,229,230]. New SIN-LVs have a safer integration profile and have shown to be safer than classical γ-RVs. However, insertional oncogenesis is still possible, and safety has to be always evaluated for the new vectors. For that reason, secondary transplants are commonly performed in GT experiments as a powerful tool to detect possible leukemogenic events and, in addition, to study the long-term expression of the therapeutic transgene.

In secondary recipients, $hCD18^+/mCD11a^+$ cells were observed in a range from 8 to 32% (Figure 56B). In all the cases, this percentage was lower in comparison with primary recipients from the same group, except in the case of the MIM group. However, similar upregulation of mCD11a in $hCD18^+$ cells of these animals was observed to that found in primary recipients (Figure 57). The reduction in cells expressing therapeutic or reporter transgenes in secondary recipients has been described in previous experiments[115,231] in mice and it is more related to the exhaustion of hematopoietic reconstitution capacity of transduced cells after the secondary transplant than to a process of epigenetic silencing of the promoters. Actually, replication stress has been associated to the functional exhaustion of mouse HSCs[232]. The four different promoters that have been used in this work to drive the expression of hCD18 are physiological and eukaryotic promoters that are less prone to be silenced[167,233] in comparison with other viral promoters such as CMV or SFFV. This fact was confirmed in the VCN determination (Table 17), where it was possible to observe a reduction in the VCN of PBLs from primary recipients (0.9 – 0.4) in comparison with secondary recipients (0.6 – 0.3). No evidences of leukemia were noted in GT-treated mice since normal WBC counts (Figure 62) and normal multilineage distribution (Figure 61) were routinely observed even in secondary recipients.

Different important aspects can be concluded from these results: First, hCD18-LVs are able to transduce true LT-HSCs as transgene expression was observed in secondary recipients even at 9 mpt. Second, manipulation of mouse hematopoietic stem cells with hCD18-LVs seemed to be a safe GT

approach, with no appearance of multicopy insertions or signs of malignant transformation. Despite of this preliminary safety analysis, other kind of studies remained to be performed, including the study of the integration pattern and the clonal distribution, the biodistribution of hCD18-LV-transduced cells or the absence of replicative competent lentiviral particles in the *ex vivo* GT-treated animals.

In GT experiments, it is crucial not only to demonstrate that LVs are able to induce the expression of the therapeutic transgene, but also that this expression has a major impact on the phenotype of the disease. To evaluate the efficacy of the hCD18-LV-mediated GT in the correction of the LAD-I phenotype in $CD18^{HYP}$ mice, we analysed neutrophil migration capacity in the two inflammation scenarios used to characterise this mouse model; the TNFα-induced air pouch inflammation model and the LPS-induced pulmonary inflammation model(Figures 63 and 64). In both of them, *ex vivo* GT-treated animals showed similar neutrophil migration than WT controls indicating the recovery of the migration capacity of the donor neutrophils. It is important to highlight that our data show for the first time that GT restores *in vivo* functional defects associated to CD18 deficiency.

In summary, we have demonstrated in different *in vitro* human and *in vivo* mouse models the safety and the efficacy of the use of hCD18-LVs to correct different alterations in the leukocyte function associated to CD18 deficiency. These results, together with the on-going integration pattern analyses allow us to propose that a GT trial based on the use of LVs for the GT of human LAD-I patients would be reasonable. To our knowledge, there is only another group working in the GT of LAD-I in the Center for Cancer Research (Bethesda, USA). They had developed several LV and FVs containing different internal promoters to drive the expression of cCD18 and they have tested them in the CLAD model. While cCD18-FV expressing cCD18 from MSCV or PGK promoter succeeded in the correction of CLAD, more modest results were obtained with LVs expressing the therapeutic transgene from physiological promoters such as PGK or EF1a, or even when using fragments of the promoter regions of the human genes encoding for CD18 or CD11b. In these experiments, $CD34^{+}$ cells were transduced at a very low MOI and animals received a RIC regimen[145-147], which could explain the failure observed on these experiments.

Although it has been shown that RIC is sufficient to allow the engraftment of corrected cells leading to the reversion of the phenotype in GT experiments conducted in CLAD-affected dogs[64,66], we believe that the use of full-myeloablative conditioning will be required for the efficient LAD-I GT due to the absence of selective advantage of corrected cells. This is the case of other myeloid immunodeficiencies such as X-CGD[88].

CLAD GT experiments pointed out that high CD18 expression levels are required to correct the disease phenotype. One way to achieve high levels of transgene expression is based on the use of a very strong promoter like the MSCV promoter/enhancer. Although no clonal dominance or malignant transformation has been observed in the long-term follow up of the MSCV-FV-treated CLAD dogs, the use of such a strong promoter would not be desirable according to the standards currently applied in human GT and it is not easily accepted by the regulatory agencies. Therefore, we believe that the use of moderate MOI of LVs (20 – 50 vp/cell) in which the expression of hCD18 is driven by a more physiological promoter would be desirable to achieve required transgene expression levels to correct the phenotype of the disease. Recent data from the MLD GT clinical trial, in which a PGK-LV was used to

achieve a supraphysiological expression of the therapeutic transgene, has shown that there is no increment in the genotoxic risk when LVs are used at a high MOI[98].

The use of large animal models for the preclinical evaluation of new GT vectors has been proposed by many authors[234,235]. It has been described that approximately 75% of mouse HSCs are outside G_0 and that mouse HSCs divide every 2.5 weeks. In contrast, studies in non-humane primates indicate that HSCs from these animals are more quiescent and divide approximately every 36 weeks, more similar to human HSCs, which are estimated to divide every 45 weeks. As a next step in the preclinical development of our hCD18-LVs, the use of CLAD-affected dogs or humanised mice transplanted with LAD-I patient cells could de considered, although for many GT studies, mice are considered as good predictor of the efficacy and safety in humans and preclinical research in mouse model is currently enough for the approval by the regulatory agencies.

FVs have several important advantages for GT. Foamyviruses are endemic in non-human primates and other mammals, but have not been observed in humans except in cases of benign zoonosis. FVs have a large packing capacity, broad host and cell-type tropism and an attractive safe integration profile relative to γRVs and LVs as it is considered almost random[236]. Moreover, transduction efficiencies of FV vectors in HSCs are comparable to those of LVs[237]. Despite all these characteristics that made FVs very good GT vectors, there is no clinical experience with FVs and the low titer of FV currently limits their utilization in large-scale GT[238]. On the other hand, LVs are already used in the clinics, can be easily produced at a large scale under GMP conditions and have an enough safety profile, so the development of new hematopoietic GT strategies based on LVs will become more rapidly a reality for patients with severe diseases like LAD-I.

The preclinical results obtained in this study allow us to propose the LV:Chim.hCD18 as a good candidate for LAD-I *ex vivo* hematopoietic GT. It is clear that a promoter driving a high expression of the therapeutic transgene in the myeloid lineage, but with some activity in the lymphoid lineage and in hematopoietic progenitors and stem cells, is a very good choice for LAD-I. In addition, the LV:Chim.hCD18 is the LV that had led to the best and more consistent results in different *in vivo* experiments. Pending from the integration profile study, we are currently drafting the application for orphan drug designation for which we fulfill all the criteria currently required to achieve this designation. We have many research and clinical European collaborators in the fields of GT and PIDs that would be interested in participate in a future LAD-I GT clinical trial. Although HSCT is nowadays the only curative therapy for LAD-I, GT may become a good alternative for those patients with the severe phenotype which, because of their low life expectancy, do not have enough time to find a compatible donor.

Conclusions

1. $CD18^{HYP}$ mice recapitulate the characteristics and symptoms of the moderate form of LAD-I disease in humans.

2. $CD18^{HYP}$ mice show an increased content of quiescent HSCs in BM, in comparison with $CD18^{WT}$ mice.

3. $CD18^{HYP}$ mice show an increased proportion of aged neutrophils in PB. However, this phenomenon does not account for the increment of BM HSCs in this animal model.

4. Competitive repopulation experiments of $CD18^{HYP}$ and $CD18^{WT}$ BM cells demonstrate that CD18 deficiency leads to a self-autonomous expansion of mouse HSCs.

5. We have generated new LVs expressing the hCD18 cDNA under the regulation of the PGK, UCOE, Chim and MIM promoters.

6. All the hCD18-LVs generated in this study promote the ectopic expression of hCD18 and also the endogenous expression of hCD11a in the membrane of LAD-I lymphoblastoid cells and mediate the phenotypic correction of these cells.

7. LAD-I like neutrophils have been generated by the transduction of human $CD34^{+}$ cells with a LV expressing a specific anti-hCD18 shRNA, showing defects in a variety of CD18-dependent functions.

8. LAD-I like HSCs recover almost a 50% of WT hCD18 expression after transduction with the LV:Chim.hCD18. Neutrophils generated from these corrected LAD-I like HSCs show improved ability to bind β_2-integrin ligands and restored ability to undergo a respiratory burst.

9. Haematopoietic cells from *ex vivo* GT-treated mice expressed with a concomitant increment of endogenous mCD11a expression in the membrane of these cells. In addition, these animals recover normal numbers of leukocytes in PB and neutrophil extravasation in response to inflammatory stimuli.

10. Taken together, our work constitutes the first preclinical GT study conducted in a LAD-I mouse model with new therapeutic LVs designed for clinical application. Based on the results obtained in our study, the LV:Chim.hCD18 will be proposed for a future GT clinical trial of LAD-I patients.

1. Los ratones CD18 ^{HYP} recapitulan las características y síntomas del fenotipo moderado de la enfermedad denominada deficiencia de adhesión leucocitaria tipo I (DAL-I) en humanos.

2. Los ratones CD18^{HYP} muestran un incremento en el contenido de células madre hematopoyéticas (CMHs) quiescentes en la médula ósea en comparación con ratones CD18^{WT}.

3. Los ratones CD18^{HYP} muestran una mayor proporción de neutrófilos envejecidos en sangre periférica. Sin embargo, este fenómeno no justifica el incremento de CMHs en la médula ósea de este modelo animal.

4. Los experimentos de repoblación competitiva con células de médula ósea procedentes de ratones CD18^{HYP} y CD18^{WT} demuestran que la deficiencia en CD18 produce una expansión autónoma de las CMHs de ratón.

5. Se han desarrollado cuatro vectores lentivirales (VLs) que expresan la proteína CD18 humana bajo el control de los promotores PGK, UCOE, Chim y MIM.

6. Los cuatro VLs-hCD18 generados en este estudio promueven la expresión ectópica de hCD18 así como la expresión endógena de hCD11a en la membrana de células linfoblastoides DAL-I, lo que resulta en la corrección del fenotipo característico de estas células.

7. Se han generado neutrófilos "semejantes a DAL-I" mediante la transducción de células CD34^{+} humanas con un VL que expresa un ARNsh específico anti-hCD18, los cuales muestran defectos en diferentes funciones celulares dependientes de hCD18.

8. Las CMHs "semejantes a DAL-I" recuperan el 50% de la expresión WT de hCD18 cuando son transducidas con el VL:Chim.hCD18. Los neutrófilos generados a partir de estas CMHs "semejantes a DAL-I" corregidas muestran una mejoría en la capacidad de unirse a ligandos de integrinas β_2 y una recuperación de la capacidad para producir un estallido respiratorio normal.

9. Las células hematopoyéticas de ratones CD18^{HYP} tratados por terapia génica (TG) muestran expresión de hCD18 en la membrana con una concomitante recuperación de la expresión endógena en membrana de mCD11a. Además recuperan valores normales de leucocitos en sangre periférica y la capacidad de extravasación de los neutrófilos en respuesta a diferentes estímulos inflamatorios.

10. En conjunto, nuestro trabajo constituye el primer estudio preclínico de TG en un modelo de ratón de DAL-I con nuevos VLs terapéuticos diseñados para su aplicación clínica. Teniendo en cuenta los resultados obtenidos en este estudio, el VL:Chim.hCD18 será propuesto para un futuro ensayo clínico de TG para pacientes con DAL-I.

Bibliography

1. Medvinsky A, Dzierzak E. Definitive hematopoiesis is autonomously initiated by the AGM region. Cell. 1996;86:897-906.

2. Dieterlen-Lievre F, Godin IE, Garcia-Porrero JA, Marcos MA. Initiation of hemopoiesis in the mouse embryo. Ann N Y Acad Sci. 1994;718:140-146.

3. Tavassoli M. Embryonic and fetal hemopoiesis: an overview. Blood Cells. 1991;17:269-281; discussion 282-266.

4. Morrison SJ, Uchida N, Weissman IL. The biology of hematopoietic stem cells. Annu Rev Cell Dev Biol. 1995;11:35-71.

5. Till JE, Mc CE. A direct measurement of the radiation sensitivity of normal mouse bone marrow cells. Radiat Res. 1961;14:213-222.

6. Barquinero J. Células madre hematopoyéticas. Monografía XXVII: Células Madre y Terapia regenerativa: Real Academia Nacional de Farmacia; 2009:59-81.

7. Wilson A, Trumpp A. Bone-marrow haematopoietic-stem-cell niches. Nat Rev Immunol. 2006;6:93-106.

8. Seita J, Weissman IL. Hematopoietic stem cell: self-renewal versus differentiation. Wiley Interdiscip Rev Syst Biol Med. 2010;2:640-653.

9. Kamel-Reid S, Dick JE. Engraftment of immune-deficient mice with human hematopoietic stem cells. Science. 1988;242:1706-1709.

10. McCune JM, Namikawa R, Kaneshima H, Shultz LD, Lieberman M, Weissman IL. The SCID-hu mouse: murine model for the analysis of human hematolymphoid differentiation and function. Science. 1988;241:1632-1639.

11. Civin CI, Trischmann T, Kadan NS, et al. Highly purified CD34-positive cells reconstitute hematopoiesis. J Clin Oncol. 1996;14:2224-2233.

12. Larochelle A, Vormoor J, Hanenberg H, et al. Identification of primitive human hematopoietic cells capable of repopulating NOD/SCID mouse bone marrow: implications for gene therapy. Nat Med. 1996;2:1329-1337.

13. Bhatia M, Bonnet D, Murdoch B, Gan OI, Dick JE. A newly discovered class of human hematopoietic cells with SCID-repopulating activity. Nat Med. 1998;4:1038-1045.

14. Guenechea G, Gan OI, Dorrell C, Dick JE. Distinct classes of human stem cells that differ in proliferative and self-renewal potential. Nat Immunol. 2001;2:75-82.

15. Doulatov S, Notta F, Laurenti E, Dick JE. Hematopoiesis: a human perspective. Cell Stem Cell. 2012;10:120-136.

16. Schofield R. The stem cell system. Biomed Pharmacother. 1983;37:375-380.

17. Anthony BA, Link DC. Regulation of hematopoietic stem cells by bone marrow stromal cells. Trends Immunol. 2014;35:32-37.

18. Casanova-Acebes M, Pitaval C, Weiss LA, et al. Rhythmic modulation of the hematopoietic niche through neutrophil clearance. Cell. 2013;153:1025-1035.

19. Calvi LM, Link DC. Cellular complexity of the bone marrow hematopoietic stem cell niche. Calcif Tissue Int. 2013;94:112-124.

20. Hynes RO. Integrins: bidirectional, allosteric signaling machines. Cell. 2002;110:673-687.

21. Zhang Y, Wang H. Integrin signalling and function in immune cells. Immunology. 2012;135:268-275.

22. Lee JO, Rieu P, Arnaout MA, Liddington R. Crystal structure of the A domain from the alpha subunit of integrin CR3 (CD11b/CD18). Cell. 1995;80:631-638.

23. Tuckwell D. Evolution of von Willebrand factor A (VWA) domains. Biochem Soc Trans. 1999;27:835-840.

24. Tan SM. The leucocyte beta2 (CD18) integrins: the structure, functional regulation and signalling properties. Biosci Rep. 2012;32:241-269.

25. Shen B, Delaney MK, Du X. Inside-out, outside-in, and inside-outside-in: G protein signaling in integrin-mediated cell adhesion, spreading, and retraction. Curr Opin Cell Biol. 2012;24:600-606.

26. Phillipson M, Heit B, Colarusso P, Liu L, Ballantyne CM, Kubes P. Intraluminal crawling of neutrophils to emigration sites: a molecularly distinct process from adhesion in the recruitment cascade. J Exp Med. 2006;203:2569-2575.

27. McKillop WM, Barrett JW, Pasternak SH, Chan BM, Dekaban GA. The extracellular domain of CD11d regulates its cell surface expression. J Leukoc Biol. 2009;86:851-862.

28. Yakubenko VP, Belevych N, Mishchuk D, Schurin A, Lam SC, Ugarova TP. The role of integrin alpha D beta2 (CD11d/CD18) in monocyte/macrophage migration. Exp Cell Res. 2008;314:2569-2578.

29. Smith CW. 3. Adhesion molecules and receptors. J Allergy Clin Immunol. 2008;121:S375-379; quiz S414.

30. Schmidt S, Moser M, Sperandio M. The molecular basis of leukocyte recruitment and its deficiencies. Mol Immunol. 2013;55:49-58.

31. Ley K, Laudanna C, Cybulsky MI, Nourshargh S. Getting to the site of inflammation: the leukocyte adhesion cascade updated. Nat Rev Immunol. 2007;7:678-689.

32. Zarbock A, Ley K, McEver RP, Hidalgo A. Leukocyte ligands for endothelial selectins: specialized glycoconjugates that mediate rolling and signaling under flow. Blood. 2011;118:6743-6751.

33. Lee HS, Lim CJ, Puzon-McLaughlin W, Shattil SJ, Ginsberg MH. RIAM activates integrins by linking talin to ras GTPase membrane-targeting sequences. J Biol Chem. 2009;284:5119-5127.

34. Calderwood DA, Campbell ID, Critchley DR. Talins and kindlins: partners in integrin-mediated adhesion. Nat Rev Mol Cell Biol. 2013;14:503-517.

35. Muller WA. Getting leukocytes to the site of inflammation. Vet Pathol. 2013;50:7-22.

36. Muller WA. Mechanisms of leukocyte transendothelial migration. Annu Rev Pathol. 2011;6:323-344.

37. Al-Herz W, Bousfiha A, Casanova JL, et al. Primary immunodeficiency diseases: an update on the classification from the international union of immunological societies expert committee for primary immunodeficiency. Front Immunol. 2011;2:54.

38. van de Vijver E, Maddalena A, Sanal O, et al. Hematologically important mutations: leukocyte adhesion deficiency (first update). Blood Cells Mol Dis. 2012;48:53-61.

39. Etzioni A. Genetic etiologies of leukocyte adhesion defects. Curr Opin Immunol. 2009;21:481-486.

40. Etzioni A. Defects in the leukocyte adhesion cascade. Clin Rev Allergy Immunol. 2010;38:54-60.

41. Gu YC, Bauer TR, Jr., Ackermann MR, et al. The genetic immunodeficiency disease, leukocyte adhesion deficiency, in humans, dogs, cattle, and mice. Comp Med. 2004;54:363-372.

42. Oppenheimer-Marks N, Davis LS, Lipsky PE. Human T lymphocyte adhesion to endothelial cells and transendothelial migration. Alteration of receptor use relates to the activation status of both the T cell and the endothelial cell. J Immunol. 1990;145:140-148.

43. Bauer TR, Jr., Gu YC, Creevy KE, et al. Leukocyte adhesion deficiency in children and Irish setter dogs. Pediatr Res. 2004;55:363-367.

44. Harris ES, Weyrich AS, Zimmerman GA. Lessons from rare maladies: leukocyte adhesion deficiency syndromes. Curr Opin Hematol. 2013;20:16-25.

45. Anderson DC, Springer TA. Leukocyte adhesion deficiency: an inherited defect in the Mac-1, LFA-1, and p150,95 glycoproteins. Annu Rev Med. 1987;38:175-194.

46. Etzioni A, Doerschuk CM, Harlan JM. Of man and mouse: leukocyte and endothelial adhesion

molecule deficiencies. Blood. 1999;94:3281-3288.

47. Movahedi M, Entezari N, Pourpak Z, et al. Clinical and laboratory findings in Iranian patients with leukocyte adhesion deficiency (study of 15 cases). J Clin Immunol. 2007;27:302-307.

48. Simon A, Pillai S, Raghupathy P, Chandy M. Leucocyte adhesion deficiency-1. Indian Pediatr. 2002;39:963-966.

49. Waldrop TC, Anderson DC, Hallmon WW, Schmalstieg FC, Jacobs RL. Periodontal manifestations of the heritable Mac-1, LFA-1, deficiency syndrome. Clinical, histopathologic and molecular characteristics. J Periodontol. 1987;58:400-416.

50. Al-Muhsen S, Alsum Z. Primary immunodeficiency diseases in the Middle East. Ann N Y Acad Sci. 2013;1250:56-61.

51. Al-Dhekri H, Al-Mousa H, Ayas M, et al. Allogeneic hematopoietic stem cell transplantation in leukocyte adhesion deficiency type 1: a single center experience. Biol Blood Marrow Transplant. 2011;17:1245-1249.

52. Prevalence of rare diseases: Bibliographic data; 2013.

53. Leiva LE, Zelazco M, Oleastro M, et al. Primary immunodeficiency diseases in Latin America: the second report of the LAGID registry. J Clin Immunol. 2007;27:101-108.

54. Rezaei N, Aghamohammadi A, Moin M, et al. Frequency and clinical manifestations of patients with primary immunodeficiency disorders in Iran: update from the Iranian Primary Immunodeficiency Registry. J Clin Immunol. 2006;26:519-532.

55. Barbouche MR, Galal N, Ben-Mustapha I, et al. Primary immunodeficiencies in highly consanguineous North African populations. Ann N Y Acad Sci. 2011;1238:42-52.

56. Madkaikar M, Mishra A, Desai M, Gupta M, Mhatre S, Ghosh K. Comprehensive report of primary immunodeficiency disorders from a tertiary care center in India. J Clin Immunol. 2013;33:507-512.

57. Hanna S, Etzioni A. Leukocyte adhesion deficiencies. Ann N Y Acad Sci. 2012;1250:50-55.

58. Lorusso F, Kong D, Jalil AK, Sylvestre C, Tan SL, Ao A. Preimplantation genetic diagnosis of leukocyte adhesion deficiency type I. Fertil Steril. 2006;85:494 e415-498.

59. Bonilla FA, Bernstein IL, Khan DA, et al. Practice parameter for the diagnosis and management of primary immunodeficiency. Ann Allergy Asthma Immunol. 2005;94:S1-63.

60. Mellouli F, Ksouri H, Barbouche R, et al. Successful treatment of Fusarium solani ecthyma gangrenosum in a patient affected by leukocyte adhesion deficiency type 1 with granulocytes transfusions. BMC Dermatol. 2010;10:10.

61. Thomas C, Le Deist F, Cavazzana-Calvo M, et al. Results of allogeneic bone marrow transplantation in patients with leukocyte adhesion deficiency. Blood. 1995;86:1629-1635.

62. Qasim W, Cavazzana-Calvo M, Davies EG, et al. Allogeneic hematopoietic stem-cell transplantation for leukocyte adhesion deficiency. Pediatrics. 2009;123:836-840.

63. Hamidieh AA, Pourpak Z, Hosseinzadeh M, et al. Reduced-intensity conditioning hematopoietic SCT for pediatric patients with LAD-1: clinical efficacy and importance of chimerism. Bone Marrow Transplant. 2012;47:646-650.

64. Bauer TR, Jr., Gu YC, Tuschong LM, et al. Nonmyeloablative hematopoietic stem cell transplantation corrects the disease phenotype in the canine model of leukocyte adhesion deficiency. Exp Hematol. 2005;33:706-712.

65. Gu YC, Bauer TR, Sokolic RA, et al. Conversion of the severe to the moderate disease phenotype with donor leukocyte microchimerism in canine leukocyte adhesion deficiency. Bone Marrow Transplant. 2006;37:607-614.

66. Sokolic RA, Bauer TR, Gu YC, et al. Nonmyeloablative conditioning with busulfan before matched littermate bone marrow transplantation results in reversal of the disease phenotype in canine

leukocyte adhesion deficiency. Biol Blood Marrow Transplant. 2005;11:755-763.

67. Tone Y, Wada T, Shibata F, et al. Somatic revertant mosaicism in a patient with leukocyte adhesion deficiency type 1. Blood. 2007;109:1182-1184.

68. Uzel G, Tng E, Rosenzweig SD, et al. Reversion mutations in patients with leukocyte adhesion deficiency type-1 (LAD-1). Blood. 2008;111:209-218.

69. Marsili M, Lougaris V, Lucantoni M, et al. Successful Anti-TNF-alpha Treatment in a Girl with LAD-1 Disease and Autoimmune Manifestations. J Clin Immunol. 2014;34:788-791.

70. Damle NK, Klussman K, Aruffo A. Intercellular adhesion molecule-2, a second counter-receptor for CD11a/CD18 (leukocyte function-associated antigen-1), provides a costimulatory signal for T-cell receptor-initiated activation of human T cells. J Immunol. 1992;148:665-671.

71. Debenham SL, Millington A, Kijast J, Andersson L, Binns M. Canine leucocyte adhesion deficiency in Irish red and white setters. J Small Anim Pract. 2002;43:74-75.

72. Renshaw HW, Chatburn C, Bryan GM, Bartsch RC, Davis WC. Canine granulocytopathy syndrome: neutrophil dysfunction in a dog with recurrent infections. J Am Vet Med Assoc. 1975;166:443-447.

73. Giger U, Boxer LA, Simpson PJ, Lucchesi BR, Todd RF, 3rd. Deficiency of leukocyte surface glycoproteins Mo1, LFA-1, and Leu M5 in a dog with recurrent bacterial infections: an animal model. Blood. 1987;69:1622-1630.

74. Kijas JM, Bauer TR, Jr., Gafvert S, et al. A missense mutation in the beta-2 integrin gene (ITGB2) causes canine leukocyte adhesion deficiency. Genomics. 1999;61:101-107.

75. Wilson RW, Ballantyne CM, Smith CW, et al. Gene targeting yields a CD18-mutant mouse for study of inflammation. J Immunol. 1993;151:1571-1578.

76. Scharffetter-Kochanek K, Lu H, Norman K, et al. Spontaneous skin ulceration and defective T cell function in CD18 null mice. J Exp Med. 1998;188:119-131.

77. Gomez JC, Doerschuk CM. The role of CD18 in the production and release of neutrophils from the bone marrow. Lab Invest. 2010;90:599-610.

78. Papayannopoulou T, Priestley GV, Nakamoto B, Zafiropoulos V, Scott LM, Harlan JM. Synergistic mobilization of hemopoietic progenitor cells using concurrent beta1 and beta2 integrin blockade or beta2-deficient mice. Blood. 2001;97:1282-1288.

79. Horwitz BH, Mizgerd JP, Scott ML, Doerschuk CM. Mechanisms of granulocytosis in the absence of CD18. Blood. 2001;97:1578-1583.

80. Nagahata H. Bovine leukocyte adhesion deficiency (BLAD): a review. J Vet Med Sci. 2004;66:1475-1482.

81. Aiuti A, Cattaneo F, Galimberti S, et al. Gene therapy for immunodeficiency due to adenosine deaminase deficiency. N Engl J Med. 2009;360:447-458.

82. Gaspar HB, Cooray S, Gilmour KC, et al. Hematopoietic stem cell gene therapy for adenosine deaminase-deficient severe combined immunodeficiency leads to long-term immunological recovery and metabolic correction. Sci Transl Med. 2011;3:97ra80.

83. Candotti F, Shaw KL, Muul L, et al. Gene therapy for adenosine deaminase-deficient severe combined immune deficiency: clinical comparison of retroviral vectors and treatment plans. Blood. 2012;120:3635-3646.

84. Mukherjee S, Thrasher AJ. Gene therapy for PIDs: progress, pitfalls and prospects. Gene. 2013;525:174-181.

85. Hacein-Bey-Abina S, Hauer J, Lim A, et al. Efficacy of gene therapy for X-linked severe combined immunodeficiency. N Engl J Med. 2010;363:355-364.

86. Fischer A, Hacein-Bey-Abina S, Cavazzana-Calvo M. 20 years of gene therapy for SCID. Nat Immunol. 2010;11:457-460.

87. Hacein-Bey-Abina S, Pai SY, Gaspar HB, et al. A modified gamma-retrovirus vector for X-linked severe combined immunodeficiency. N Engl J Med. 2014;371:1407-1417.

88. Grez M, Reichenbach J, Schwable J, Seger R, Dinauer MC, Thrasher AJ. Gene therapy of chronic granulomatous disease: the engraftment dilemma. Mol Ther. 2011;19:28-35.

89. Boztug K, Schmidt M, Schwarzer A, et al. Stem-cell gene therapy for the Wiskott-Aldrich syndrome. N Engl J Med. 2010;363:1918-1927.

90. Aiuti A, Biasco L, Scaramuzza S, et al. Lentiviral hematopoietic stem cell gene therapy in patients with Wiskott-Aldrich syndrome. Science. 2013;341:1233151.

91. Cavazzana-Calvo M, Payen E, Negre O, et al. Transfusion independence and HMGA2 activation after gene therapy of human beta-thalassaemia. Nature. 2010;467:318-322.

92. Kelly PF, Radtke S, Kalle C, et al. Stem cell collection and gene transfer in fanconi anemia. Mol Ther. 2007;15:211-219.

93. Liu JM, Kim S, Read EJ, et al. Engraftment of hematopoietic progenitor cells transduced with the Fanconi anemia group C gene (FANCC). Hum Gene Ther. 1999;10:2337-2346.

94. Jacome A, Navarro S, Rio P, et al. Lentiviral-mediated genetic correction of hematopoietic and mesenchymal progenitor cells from Fanconi anemia patients. Mol Ther. 2009;17:1083-1092.

95. Gonzalez-Murillo A, Lozano ML, Alvarez L, et al. Development of lentiviral vectors with optimized transcriptional activity for the gene therapy of patients with Fanconi anemia. Hum Gene Ther. 2010;21:623-630.

96. Tolar J, Becker PS, Clapp DW, et al. Gene therapy for Fanconi anemia: one step closer to the clinic. Hum Gene Ther. 2012;23:141-144.

97. Cartier N, Hacein-Bey-Abina S, Bartholomae CC, et al. Hematopoietic stem cell gene therapy with a lentiviral vector in X-linked adrenoleukodystrophy. Science. 2009;326:818-823.

98. Biffi A, Montini E, Lorioli L, et al. Lentiviral hematopoietic stem cell gene therapy benefits metachromatic leukodystrophy. Science. 2013;341:1233158.

99. Naldini L. Ex vivo gene transfer and correction for cell-based therapies. Nat Rev Genet. 2011;12:301-315.

100. Nienhuis AW. Development of gene therapy for blood disorders: an update. Blood. 2013;122:1556-1564.

101. Fan H, Johnson C. Insertional oncogenesis by non-acute retroviruses: implications for gene therapy. Viruses. 1998;3:398-422.

102. Sakuma T, Barry MA, Ikeda Y. Lentiviral vectors: basic to translational. Biochem J. 2012;443:603-618.

103. Coil DA, Miller AD. Phosphatidylserine is not the cell surface receptor for vesicular stomatitis virus. J Virol. 2004;78:10920-10926.

104. Dull T, Zufferey R, Kelly M, et al. A third-generation lentivirus vector with a conditional packaging system. J Virol. 1998;72:8463-8471.

105. Burns JC, Friedmann T, Driever W, Burrascano M, Yee JK. Vesicular stomatitis virus G glycoprotein pseudotyped retroviral vectors: concentration to very high titer and efficient gene transfer into mammalian and nonmammalian cells. Proc Natl Acad Sci U S A. 1993;90:8033-8037.

106. Horn PA, Keyser KA, Peterson LJ, et al. Efficient lentiviral gene transfer to canine repopulating cells using an overnight transduction protocol. Blood. 2004;103:3710-3716.

107. Hanawa H, Persons DA, Nienhuis AW. High-level erythroid lineage-directed gene expression using globin gene regulatory elements after lentiviral vector-mediated gene transfer into primitive human and murine hematopoietic cells. Hum Gene Ther. 2002;13:2007-2016.

108. Horn PA, Topp MS, Morris JC, Riddell SR, Kiem HP. Highly efficient gene transfer into baboon marrow repopulating cells using GALV-pseudotype oncoretroviral vectors produced by human packaging cells. Blood. 2002;100:3960-3967.

109. Guenechea G, Gan OI, Inamitsu T, et al. Transduction of human CD34+ CD38- bone marrow and cord blood-derived SCID-repopulating cells with third-generation lentiviral vectors. Mol Ther. 2000;1:566-573.

110. Hanawa H, Kelly PF, Nathwani AC, et al. Comparison of various envelope proteins for their ability to pseudotype lentiviral vectors and transduce primitive hematopoietic cells from human blood. Mol Ther. 2002;5:242-251.

111. Zufferey R, Nagy D, Mandel RJ, Naldini L, Trono D. Multiply attenuated lentiviral vector achieves efficient gene delivery in vivo. Nat Biotechnol. 1997;15:871-875.

112. Miller AD. Development and Applications of Retroviral Vectors. 1997.

113. Zufferey R, Dull T, Mandel RJ, et al. Self-inactivating lentivirus vector for safe and efficient in vivo gene delivery. J Virol. 1998;72:9873-9880.

114. Modlich U, Navarro S, Zychlinski D, et al. Insertional transformation of hematopoietic cells by self-inactivating lentiviral and gammaretroviral vectors. Mol Ther. 2009;17:1919-1928.

115. Santilli G, Almarza E, Brendel C, et al. Biochemical correction of X-CGD by a novel chimeric promoter regulating high levels of transgene expression in myeloid cells. Mol Ther. 2011;19:122-132.

116. Zufferey R, Donello JE, Trono D, Hope TJ. Woodchuck hepatitis virus posttranscriptional regulatory element enhances expression of transgenes delivered by retroviral vectors. J Virol. 1999;73:2886-2892.

117. Zanta-Boussif MA, Charrier S, Brice-Ouzet A, et al. Validation of a mutated PRE sequence allowing high and sustained transgene expression while abrogating WHV-X protein synthesis: application to the gene therapy of WAS. Gene Ther. 2009;16:605-619.

118. Follenzi A, Ailles LE, Bakovic S, Geuna M, Naldini L. Gene transfer by lentiviral vectors is limited by nuclear translocation and rescued by HIV-1 pol sequences. Nat Genet. 2000;25:217-222.

119. Zennou V, Petit C, Guetard D, Nerhbass U, Montagnier L, Charneau P. HIV-1 genome nuclear import is mediated by a central DNA flap. Cell. 2000;101:173-185.

120. Hacein-Bey-Abina S, Von Kalle C, Schmidt M, et al. LMO2-associated clonal T cell proliferation in two patients after gene therapy for SCID-X1. Science. 2003;302:415-419.

121. Howe SJ, Mansour MR, Schwarzwaelder K, et al. Insertional mutagenesis combined with acquired somatic mutations causes leukemogenesis following gene therapy of SCID-X1 patients. J Clin Invest. 2008;118:3143-3150.

122. Avedillo Diez I, Zychlinski D, Coci EG, et al. Development of novel efficient SIN vectors with improved safety features for Wiskott-Aldrich syndrome stem cell based gene therapy. Mol Pharm. 2011;8:1525-1537.

123. Gabriel R, Schmidt M, von Kalle C. Integration of retroviral vectors. Curr Opin Immunol. 2012;24:592-597.

124. Moiani A, Paleari Y, Sartori D, et al. Lentiviral vector integration in the human genome induces alternative splicing and generates aberrant transcripts. J Clin Invest. 2012;122:1653-1666.

125. Wang Z, Rao DD, Senzer N, Nemunaitis J. RNA interference and cancer therapy. Pharm Res. 2011;28:2983-2995.

126. Gregory RI, Chendrimada TP, Shiekhattar R. MicroRNA biogenesis: isolation and characterization of the microprocessor complex. Methods Mol Biol. 2006;342:33-47.

127. Moore CB, Guthrie EH, Huang MT, Taxman DJ. Short hairpin RNA (shRNA): design, delivery, and assessment of gene knockdown. Methods Mol Biol. 2010;629:141-158.

128. Zhou F, Liang S, Chen AH, et al. A transgenic Marc-145 cell line of piggyBac transposon-derived

targeting shRNA interference against porcine reproductive and respiratory syndrome virus. Vet Res Commun. 2012;36:99-105.

129. Banos R, Valeri A, Alvarez L, et al. Efficacy of a gene therapy approach using a humanized model of Fanconi anemia. Human Gene Therapy. 2012;23:A111-A111.

130. Brendel C, Kaufmann KB, Krattenmacher A, Pahujani S, Grez M. Generation of X-CGD cells for vector evaluation from healthy donor CD34+ HSCs by shRNA-mediated knock down of gp91phox. Molecular Therapy - Methods & Clinical Development. 2014;1.

131. Krauss JC, Bond LM, Todd RF, 3rd, Wilson JM. Expression of retroviral transduced human CD18 in murine cells: an in vitro model of gene therapy for leukocyte adhesion deficiency. Hum Gene Ther. 1991;2:221-228.

132. Wilson RW, Yorifuji T, Lorenzo I, et al. Expression of human CD18 in murine granulocytes and improved efficiency for infection of deficient human lymphoblasts. Hum Gene Ther. 1993;4:25-34.

133. Krauss JC, Mayo-Bond LA, Rogers CE, Weber KL, Todd RF, 3rd, Wilson JM. An in vivo animal model of gene therapy for leukocyte adhesion deficiency. J Clin Invest. 1991;88:1412-1417.

134. Wilson JM, Ping AJ, Krauss JC, et al. Correction of CD18-deficient lymphocytes by retrovirus-mediated gene transfer. Science. 1990;248:1413-1416.

135. Bauer TR, Jr., Miller AD, Hickstein DD. Improved transfer of the leukocyte integrin CD18 subunit into hematopoietic cell lines by using retroviral vectors having a gibbon ape leukemia virus envelope. Blood. 1995;86:2379-2387.

136. Bauer TR, Jr., Adler RL, Hickstein DD. Potential large animal models for gene therapy of human genetic diseases of immune and blood cell systems. Ilar J. 2009;50:168-186.

137. Bauer TR, Jr., Hickstein DD. Gene therapy for leukocyte adhesion deficiency. Curr Opin Mol Ther. 2000;2:383-388.

138. Barese CN, Goebel WS, Dinauer MC. Gene therapy for chronic granulomatous disease. Expert Opin Biol Ther. 2004;4:1423-1434.

139. Bauer TR, Jr., Hai M, Tuschong LM, et al. Correction of the disease phenotype in canine leukocyte adhesion deficiency using ex vivo hematopoietic stem cell gene therapy. Blood. 2006;108:3313-3320.

140. Hai M, Adler RL, Bauer TR, Jr., et al. Potential genotoxicity from integration sites in CLAD dogs treated successfully with gammaretroviral vector-mediated gene therapy. Gene Ther. 2008;15:1067-1071.

141. Bauer TR, Jr., Allen JM, Hai M, et al. Successful treatment of canine leukocyte adhesion deficiency by foamy virus vectors. Nat Med. 2008;14:93-97.

142. Bauer TR, Jr., Tuschong LM, Calvo KR, et al. Long-term follow-up of foamy viral vector-mediated gene therapy for canine leukocyte adhesion deficiency. Mol Ther. 2013;21:964-972.

143. Bauer TR, Jr., Olson EM, Huo Y, et al. Treatment of canine leukocyte adhesion deficiency by foamy virus vectors expressing CD18 from a PGK promoter. Gene Ther. 2011;18:553-559.

144. Chang AH, Stephan MT, Sadelain M. Stem cell-derived erythroid cells mediate long-term systemic protein delivery. Nat Biotechnol. 2006;24:1017-1021.

145. Hunter MJ, Tuschong LM, Fowler CJ, Bauer TR, Jr., Burkholder TH, Hickstein DD. Gene therapy of canine leukocyte adhesion deficiency using lentiviral vectors with human CD11b and CD18 promoters driving canine CD18 expression. Mol Ther. 2011;19:113-121.

146. Hunter MJ, Zhao H, Tuschong LM, et al. Gene therapy for canine leukocyte adhesion deficiency with lentiviral vectors using the murine stem cell virus and human phosphoglycerate kinase promoters. Hum Gene Ther. 2011;22:689-696.

147. Nelson EJ, Tuschong LM, Hunter MJ, Bauer TR, Jr., Burkholder TH, Hickstein DD. Lentiviral vectors incorporating a human elongation factor 1alpha promoter for the treatment of canine leukocyte

adhesion deficiency. Gene Ther. 2010;17:672-677.

148. Shen FW, Saga Y, Litman G, et al. Cloning of Ly-5 cDNA. Proc Natl Acad Sci U S A. 1985;82:7360-7363.

149. Almarza E, Segovia JC, Guenechea G, Gomez SG, Ramirez A, Bueren JA. Regulatory elements of the vav gene drive transgene expression in hematopoietic stem cells from adult mice. Exp Hematol. 2004;32:360-364.

150. Frenette PS, Mayadas TN, Rayburn H, Hynes RO, Wagner DD. Susceptibility to infection and altered hematopoiesis in mice deficient in both P- and E-selectins. Cell. 1996;84:563-574.

151. Hu Y, Smyth GK. ELDA: extreme limiting dilution analysis for comparing depleted and enriched populations in stem cell and other assays. J Immunol Methods. 2009;347:70-78.

152. Ramirez M, Segovia JC, Benet I, et al. Ex vivo expansion of umbilical cord blood (UCB) CD34(+) cells alters the expression and function of alpha 4 beta 1 and alpha 5 beta 1 integrins. Br J Haematol. 2001;115:213-221.

153. van Hennik PB, de Koning AE, Ploemacher RE. Seeding efficiency of primitive human hematopoietic cells in nonobese diabetic/severe combined immune deficiency mice: implications for stem cell frequency assessment. Blood. 1999;94:3055-3061.

154. Pear WS, Nolan GP, Scott ML, Baltimore D. Production of high-titer helper-free retroviruses by transient transfection. Proc Natl Acad Sci U S A. 1993;90:8392-8396.

155. Rasheed S, Nelson-Rees WA, Toth EM, Arnstein P, Gardner MB. Characterization of a newly derived human sarcoma cell line (HT-1080). Cancer. 1974;33:1027-1033.

156. Kishimoto TK, Hollander N, Roberts TM, Anderson DC, Springer TA. Heterogeneous mutations in the beta subunit common to the LFA-1, Mac-1, and p150,95 glycoproteins cause leukocyte adhesion deficiency. Cell. 1987;50:193-202.

157. Rothlein R, Springer TA. The requirement for lymphocyte function-associated antigen 1 in homotypic leukocyte adhesion stimulated by phorbol ester. J Exp Med. 1986;163:1132-1149.

158. Tang RH, Tng E, Law SK, Tan SM. Epitope mapping of monoclonal antibody to integrin alphaL beta2 hybrid domain suggests different requirements of affinity states for intercellular adhesion molecules (ICAM)-1 and ICAM-3 binding. J Biol Chem. 2005;280:29208-29216.

159. Burns S, Hardy SJ, Buddle J, Yong KL, Jones GE, Thrasher AJ. Maturation of DC is associated with changes in motile characteristics and adherence. Cell Motil Cytoskeleton. 2004;57:118-132.

160. Arnaout MA, Todd RF, 3rd, Dana N, Melamed J, Schlossman SF, Colten HR. Inhibition of phagocytosis of complement C3- or immunoglobulin G-coated particles and of C3bi binding by monoclonal antibodies to a monocyte-granulocyte membrane glycoprotein (Mol). J Clin Invest. 1983;72:171-179.

161. Hickstein DD, Locksley RM, Beatty PG, Smith A, Stone DM, Root RK. Monoclonal antibodies binding to the human neutrophil C3bi receptor have disparate functional effects. Blood. 1986;67:1054-1062.

162. Bauer TR, Schwartz BR, Liles WC, Ochs HD, Hickstein DD. Retroviral-mediated gene transfer of the leukocyte integrin CD18 into peripheral blood CD34+ cells derived from a patient with leukocyte adhesion deficiency type 1. Blood. 1998;91:1520-1526.

163. Tlili A, Erard M, Faure MC, et al. Stable accumulation of p67phox at the phagosomal membrane and ROS production within the phagosome. J Leukoc Biol. 2012;91:83-95.

164. Plachetka A, Chayka O, Wilczek C, Melnik S, Bonifer C, Klempnauer KH. C/EBPbeta induces chromatin opening at a cell-type-specific enhancer. Mol Cell Biol. 2008;28:2102-2112.

165. Williams S, Mustoe T, Mulcahy T, et al. CpG-island fragments from the HNRPA2B1/CBX3 genomic locus reduce silencing and enhance transgene expression from the hCMV promoter/enhancer in mammalian cells. BMC Biotechnol. 2005;5:17.

166. Antoniou M, Harland L, Mustoe T, et al. Transgenes encompassing dual-promoter CpG islands from the human TBP and HNRPA2B1 loci are resistant to heterochromatin-mediated silencing. Genomics. 2003;82:269-279.

167. Zhang F, Thornhill SI, Howe SJ, et al. Lentiviral vectors containing an enhancer-less ubiquitously acting chromatin opening element (UCOE) provide highly reproducible and stable transgene expression in hematopoietic cells. Blood. 2007;110:1448-1457.

168. Zhang F, Frost AR, Blundell MP, Bales O, Antoniou MN, Thrasher AJ. A ubiquitous chromatin opening element (UCOE) confers resistance to DNA methylation-mediated silencing of lentiviral vectors. Mol Ther. 2010;18:1640-1649.

169. Pfaff N, Lachmann N, Ackermann M, et al. A ubiquitous chromatin opening element prevents transgene silencing in pluripotent stem cells and their differentiated progeny. Stem Cells. 2013;31:488-499.

170. Ackermann M, Lachmann N, Hartung S, et al. Promoter and lineage independent anti-silencing activity of the A2 ubiquitous chromatin opening element for optimized human pluripotent stem cell-based gene therapy. Biomaterials. 2014;35:1531-1542.

171. Szulc J, Wiznerowicz M, Sauvain MO, Trono D, Aebischer P. A versatile tool for conditional gene expression and knockdown. Nat Methods. 2006;3:109-116.

172. Wiznerowicz M, Trono D. Conditional suppression of cellular genes: lentivirus vector-mediated drug-inducible RNA interference. J Virol. 2003;77:8957-8961.

173. Vigna E, Amendola M, Benedicenti F, Simmons AD, Follenzi A, Naldini L. Efficient Tet-dependent expression of human factor IX in vivo by a new self-regulating lentiviral vector. Mol Ther. 2005;11:763-775.

174. Ding ZM, Babensee JE, Simon SI, et al. Relative contribution of LFA-1 and Mac-1 to neutrophil adhesion and migration. J Immunol. 1999;163:5029-5038.

175. Papayannopoulou T, Priestley GV, Nakamoto B, Zafiropoulos V, Scott LM. Molecular pathways in bone marrow homing: dominant role of alpha(4)beta(1) over beta(2)-integrins and selectins. Blood. 2001;98:2403-2411.

176. Witkowska AM, Borawska MH. Soluble intercellular adhesion molecule-1 (sICAM-1): an overview. Eur Cytokine Netw. 2004;15:91-98.

177. Albella B, Segovia JC, Guenechea G, Pragnell IB, Bueren JA. Preserved long-term repopulation and differentiation properties of hematopoietic grafts subjected to ex vivo expansion with stem cell factor and interleukin 11. Transplantation. 1999;67:1348-1357.

178. Montini E, Cesana D, Schmidt M, et al. The genotoxic potential of retroviral vectors is strongly modulated by vector design and integration site selection in a mouse model of HSC gene therapy. J Clin Invest. 2009;119:964-975.

179. Forlow SB, Schurr JR, Kolls JK, Bagby GJ, Schwarzenberger PO, Ley K. Increased granulopoiesis through interleukin-17 and granulocyte colony-stimulating factor in leukocyte adhesion molecule-deficient mice. Blood. 2001;98:3309-3314.

180. Weinmann P, Scharffetter-Kochanek K, Forlow SB, Peters T, Walzog B. A role for apoptosis in the control of neutrophil homeostasis in the circulation: insights from CD18-deficient mice. Blood. 2003;101:739-746.

181. Szarka RJ, Wang N, Gordon L, Nation PN, Smith RH. A murine model of pulmonary damage induced by lipopolysaccharide via intranasal instillation. J Immunol Methods. 1997;202:49-57.

182. Ridger VC, Wagner BE, Wallace WA, Hellewell PG. Differential effects of CD18, CD29, and CD49 integrin subunit inhibition on neutrophil migration in pulmonary inflammation. J Immunol. 2001;166:3484-3490.

183. Winkler IG, Barbier V, Nowlan B, et al. Vascular niche E-selectin regulates hematopoietic stem cell

dormancy, self renewal and chemoresistance. Nat Med. 2012;18:1651-1657.

184. Szilvassy SJ, Humphries RK, Lansdorp PM, Eaves AC, Eaves CJ. Quantitative assay for totipotent reconstituting hematopoietic stem cells by a competitive repopulation strategy. Proc Natl Acad Sci U S A. 1990;87:8736-8740.

185. Adorno M, Sikandar S, Mitra SS, et al. Usp16 contributes to somatic stem-cell defects in Down's syndrome. Nature. 2013;501:380-384.

186. Mayadas TN, Cullere X. Neutrophil beta2 integrins: moderators of life or death decisions. Trends Immunol. 2005;26:388-395.

187. Whitlock BB, Gardai S, Fadok V, Bratton D, Henson PM. Differential roles for alpha(M)beta(2) integrin clustering or activation in the control of apoptosis via regulation of akt and ERK survival mechanisms. J Cell Biol. 2000;151:1305-1320.

188. Vermeulen M, Le Pesteur F, Gagnerault MC, Mary JY, Sainteny F, Lepault F. Role of adhesion molecules in the homing and mobilization of murine hematopoietic stem and progenitor cells. Blood. 1998;92:894-900.

189. Sahin AO, Buitenhuis M. Molecular mechanisms underlying adhesion and migration of hematopoietic stem cells. Cell Adh Migr. 2012;6:39-48.

190. Bonig H, Watts KL, Chang KH, Kiem HP, Papayannopoulou T. Concurrent blockade of alpha4-integrin and CXCR4 in hematopoietic stem/progenitor cell mobilization. Stem Cells. 2009;27:836-837.

191. Ramirez P, Rettig MP, Uy GL, et al. BIO5192, a small molecule inhibitor of VLA-4, mobilizes hematopoietic stem and progenitor cells. Blood. 2009;114:1340-1343.

192. Fuchs E, Tumbar T, Guasch G. Socializing with the neighbors: stem cells and their niche. Cell. 2004;116:769-778.

193. Boisset JC, Clapes T, Van Der Linden R, Dzierzak E, Robin C. Integrin alphaIIb (CD41) plays a role in the maintenance of hematopoietic stem cell activity in the mouse embryonic aorta. Biol Open. 2013;2:525-532.

194. Jacome A, Navarro S, Casado JA, et al. A simplified approach to improve the efficiency and safety of ex vivo hematopoietic gene therapy in fanconi anemia patients. Hum Gene Ther. 2006;17:245-250.

195. Tolar J, Adair JE, Antoniou M, et al. Stem cell gene therapy for fanconi anemia: report from the 1st international Fanconi anemia gene therapy working group meeting. Mol Ther. 2011;19:1193-1198.

196. Almarza E, Zhang F, Santilli G, et al. Correction of SCID-X1 using an enhancerless Vav promoter. Hum Gene Ther. 2011;22:263-270.

197. Zhang L, Thrasher AJ, Gaspar HB. Current progress on gene therapy for primary immunodeficiencies. Gene Ther. 2013;20:963-969.

198. Montini E, Cesana D, Schmidt M, et al. Hematopoietic stem cell gene transfer in a tumor-prone mouse model uncovers low genotoxicity of lentiviral vector integration. Nat Biotechnol. 2006;24:687-696.

199. Kaufmann KB, Brendel C, Suerth JD, et al. Alpharetroviral vector-mediated gene therapy for X-CGD: functional correction and lack of aberrant splicing. Mol Ther. 2013;21:648-661.

200. Rethwilm A. Foamy virus vectors: an awaited alternative to gammaretro- and lentiviral vectors. Curr Gene Ther. 2007;7:261-271.

201. Sjeklocha LM, Wong PY, Belcher JD, Vercellotti GM, Steer CJ. beta-Globin sleeping beauty transposon reduces red blood cell sickling in a patient-derived CD34(+)-based in vitro model. PLoS One. 2013;8:e80403.

202. Merten OW, Charrier S, Laroudie N, et al. Large-scale manufacture and characterization of a lentiviral vector produced for clinical ex vivo gene therapy application. Hum Gene Ther. 2011;22:343-356.

203. Mussolino C, Cathomen T. RNA guides genome engineering. Nat Biotechnol. 2013;31:208-209.

204. Perez-Pinera P, Ousterout DG, Gersbach CA. Advances in targeted genome editing. Current Opinion in Chemical Biology. 2012;16:268-277.

205. Tebas P, Stein D, Tang WW, et al. Gene editing of CCR5 in autologous CD4 T cells of persons infected with HIV. N Engl J Med. 2014;370:901-910.

206. Hofer U, Henley JE, Exline CM, Mulhern O, Lopez E, Cannon PM. Pre-clinical modeling of CCR5 knockout in human hematopoietic stem cells by zinc finger nucleases using humanized mice. J Infect Dis. 2013;208 Suppl 2:S160-164.

207. Garcia-Gomez M, Navarro S, Garcia-Bravo M, et al. Improved Clinically Applicable Lentiviral Vectors for the Gene Therapy of Pyruvate Kinase Deficiency. Human Gene Therapy. 2013;23:A113-A113.

208. Biffi A, Capotondo A, Fasano S, et al. Gene therapy of metachromatic leukodystrophy reverses neurological damage and deficits in mice. J Clin Invest. 2006;116:3070-3082.

209. Bosticardo M, Ghosh A, Du Y, Jenkins NA, Copeland NG, Candotti F. Self-inactivating retroviral vector-mediated gene transfer induces oncogene activation and immortalization of primary murine bone marrow cells. Mol Ther. 2009;17:1910-1918.

210. McBurney MW, Sutherland LC, Adra CN, Leclair B, Rudnicki MA, Jardine K. The mouse Pgk-1 gene promoter contains an upstream activator sequence. Nucleic Acids Res. 1991;19:5755-5761.

211. Scacheri PC, Crabtree JS, Novotny EA, et al. Bidirectional transcriptional activity of PGK-neomycin and unexpected embryonic lethality in heterozygote chimeric knockout mice. Genesis. 2001;30:259-263.

212. Taveau M, Stockholm D, Marchand S, Roudaut C, Le Bert M, Richard I. Bidirectional transcriptional activity of the Pgk1 promoter and transmission ratio distortion in Capn3-deficient mice. Genomics. 2004;84:592-595.

213. van Til NP, de Boer H, Mashamba N, et al. Correction of murine Rag2 severe combined immunodeficiency by lentiviral gene therapy using a codon-optimized RAG2 therapeutic transgene. Mol Ther. 2012;20:1968-1980.

214. Brendel C, Muller-Kuller U, Schultze-Strasser S, et al. Physiological regulation of transgene expression by a lentiviral vector containing the A2UCOE linked to a myeloid promoter. Gene Ther. 2012;19:1018-1029.

215. Knight S, Zhang F, Mueller-Kuller U, et al. Safer, silencing-resistant lentiviral vectors: optimization of the ubiquitous chromatin-opening element through elimination of aberrant splicing. J Virol. 2012;86:9088-9095.

216. Stein S, Scholz S, Schwable J, et al. From bench to bedside: preclinical evaluation of a self-inactivating gammaretroviral vector for the gene therapy of X-linked chronic granulomatous disease. Hum Gene Ther Clin Dev. 2013;24:86-98.

217. Mauro VP, Chappell SA. A critical analysis of codon optimization in human therapeutics. Trends Mol Med. 2014.

218. Jordan J, Beneke R, Hutler M, Veith A, Luft FC, Haller H. Regulation of MAC-1 (CD11b/CD18) expression on circulating granulocytes in endurance runners. Med Sci Sports Exerc. 1999;31:362-367.

219. Ryder MI, Fujitaki R, Lebus S, et al. Alterations of neutrophil L-selectin and CD18 expression by tobacco smoke: implications for periodontal diseases. J Periodontal Res. 1998;33:359-368.

220. Finn A, Moat N, Rebuck N, Klein N, Strobel S, Elliott M. Changes in neutrophil CD11b/CD18 and L-selectin expression and release of interleukin 8 and elastase in paediatric cardiopulmonary bypass. Agents Actions. 1993;38 Spec No:C44-46.

221. Palmer S, Hamblin AS. Increased CD11/CD18 expression on the peripheral blood leucocytes of patients with HIV disease: relationship to disease severity. Clin Exp Immunol. 1993;93:344-349.

222. Laurent T, Markert M, Von Fliedner V, et al. CD11b/CD18 expression, adherence, and chemotaxis of granulocyte in adult respiratory distress syndrome. Am J Respir Crit Care Med. 1994;149:1534-1538.

223. Jegga AG, Aronow BJ. Evolutionarily Conserved Noncoding DNA. eLS: John Wiley & Sons, Ltd; 2001.

224. Heckl D, Kowalczyk MS, Yudovich D, et al. Generation of mouse models of myeloid malignancy with combinatorial genetic lesions using CRISPR-Cas9 genome editing. Nat Biotechnol. 2014;32:941-946.

225. Mandal PankajÂ K, Ferreira LMR, Collins R, et al. Efficient Ablation of Genes in Human Hematopoietic Stem and Effector Cells using CRISPR/Cas9. Cell Stem Cell. 2014;15:643-652.

226. Jaako P, Debnath S, Olsson K, et al. Gene therapy cures the anemia and lethal bone marrow failure in mouse model for RPS19-deficient Diamond-Blackfan anemia. Haematologica. 2014.

227. Perumbeti A, Higashimoto T, Urbinati F, et al. A novel human gamma-globin gene vector for genetic correction of sickle cell anemia in a humanized sickle mouse model: critical determinants for successful correction. Blood. 2009;114:1174-1185.

228. Miller LJ, Bainton DF, Borregaard N, Springer TA. Stimulated mobilization of monocyte Mac-1 and p150,95 adhesion proteins from an intracellular vesicular compartment to the cell surface. J Clin Invest. 1987;80:535-544.

229. Ott MG, Schmidt M, Schwarzwaelder K, et al. Correction of X-linked chronic granulomatous disease by gene therapy, augmented by insertional activation of MDS1-EVI1, PRDM16 or SETBP1. Nat Med. 2006;12:401-409.

230. Stein S, Ott MG, Schultze-Strasser S, et al. Genomic instability and myelodysplasia with monosomy 7 consequent to EVI1 activation after gene therapy for chronic granulomatous disease. Nat Med. 2010;16:198-204.

231. Koldej RM, Carney G, Wielgosz MM, et al. Comparison of insulators and promoters for expression of the Wiskott-Aldrich syndrome protein using lentiviral vectors. Hum Gene Ther Clin Dev. 2013;24:77-85.

232. Flach J, Bakker ST, Mohrin M, et al. Replication stress is a potent driver of functional decline in ageing haematopoietic stem cells. Nature. 2014;512:198-202.

233. Norrman K, Fischer Y, Bonnamy B, Wolfhagen Sand F, Ravassard P, Semb H. Quantitative comparison of constitutive promoters in human ES cells. PLoS One. 2010;5:e12413.

234. Switonski M. Dog as a model in studies on human hereditary diseases and their gene therapy. Reprod Biol. 2014;14:44-50.

235. Trobridge GD, Horn PA, Beard BC, Kiem HP. Large animal models for foamy virus vector gene therapy. Viruses. 2012;4:3572-3588.

236. Lindemann D, Rethwilm A. Foamy virus biology and its application for vector development. Viruses. 2011;3:561-585.

237. Olszko ME, Trobridge GD. Foamy virus vectors for HIV gene therapy. Viruses. 2013;5:2585-2600.

238. Trobridge G, Josephson N, Vassilopoulos G, Mac J, Russell DW. Improved foamy virus vectors with minimal viral sequences. Mol Ther. 2002;6:321-328.

Appendix 1: Additional information

Table S1. List of monoclonal antibodies used for flow cytometry and cell sorting

Purpose	Reactivity	Antigen	Conjugation	Vendor	Catalog #	Clone
PB and BM murine β_2 integrin expression	Mouse	CD18	FITC	BD Pharmingen	553292	C71/16
	Mouse	CD11a	PE-Cy7	BD Pharmingen	558191	2D7
	Mouse	CD11b	PE	BD Pharmingen	553311	M1/70
	Mouse	CD11c	APC	BD Pharmingen	550261	HL3
	Mouse	CD3	PE	BD Pharmingen	553064	145-2C11
	Mouse	CD45R/B220	PE	BD Pharmingen	553090	RA3-6B2
	Mouse	GR1	FITC	BD Pharmingen	553128	RB6-8C5
Lin$^-$ sorting	Mouse	CD11b	FITC	BioLegend	101206	M1/70
	Mouse	CD45R/B220	FITC	Southern	1665-02	RA3-6B2
	Mouse	CD3	FITC	BD Pharmingen	553062	145-2C11
	Mouse	GR1	FITC	BD Pharmingen	553127	RB6-8C5
	Mouse	Ter119	FITC	eBioscience	11-5921	Ter119
LSK content and sorting	Mouse	CD11b	FITC	BioLegend	101206	M1/70
	Mouse	CD45R/B220	FITC	Southern	1665-02	RA3-6B2
	Mouse	CD3	FITC	BD Pharmingen	553062	145-2C11
	Mouse	GR1	FITC	BD Pharmingen	553127	RB6-8C5
	Mouse	Ter119	FITC	eBioscience	11-5921	Ter119
	Mouse	CD117/cKit	PE-Cy7	BD Pharmingen	558163	2B8
	Mouse	Sca1	PE	BD Pharmingen	553336	E13-161.7
LSK Cell Cycle status	Mouse	CD11b	FITC	BioLegend	101206	M1/70
	Mouse	CD45R/B220	FITC	Southern	1665-02	RA3-6B2
	Mouse	CD3	FITC	BD Pharmingen	553062	145-2C11
	Mouse	Gr1	FITC	BD Pharmingen	553127	RB6-8C5
	Mouse	Ter119	FITC	eBioscience	11-5921	Ter119
	Mouse	CD117/cKit	PE-Cy5	eBioscience	15-1171	2B8
	Mouse	Sca1	PE	BD Pharmingen	553336	E13-161.7
Hematopoietic progenitors Analysis	Mouse	CD3	Biotin	BD Pharmingen	553060	145-2C11
	Mouse	Gr1	Biotin	BD Pharmingen	553127	RB6-8C5
	Mouse	CD11b	Biotin	BD Pharmingen	553309	M1/70
	Mouse	CD45R/B220	Biotin	BD Pharmingen	553086	RA3-6B2
	Mouse	Ter119	Biotin	BD Pharmingen	553672	Ter119
	-	Biotin	A350	Molecular Probes	S11249	-
	Mouse	CD117/cKit	PE	BD Pharmingen	553355	2B8
	Mouse	Sca1	APC-Cy7	BioLegend	108125	D7
	Mouse	CD34	FITC	eBioscience	11-0341	RAM34
	Mouse	CD150	APC	BioLegend	115910	TC15-12F12.2
	Mouse	CD135	PE	BD Pharmingen	553842	ASF10.1
	Mouse	CD16/32	PerCP-eFluor 710	eBioscience	46-0161	93
LSK Integrin Analysis	Mouse	CD3	Biotin	BD Pharmingen	553060	145-2C11
	Mouse	Gr1	Biotin	BD Pharmingen	553127	RB6-8C5
	Mouse	Mac1	Biotin	BD Pharmingen	553309	M1/70
	Mouse	CD45R/B220	Biotin	BD Pharmingen	553086	RA3-6B2
	Mouse	Ter119	Biotin	BD Pharmingen	553672	Ter119
	-	Biotin	A350	Molecular Probes	S11249	-
	Mouse	CD117/cKit	PE	BD Pharmingen	553355	2B8
	Mouse	CD117/cKit	PE-Cy7	BD Pharmingen	558163	2B8
	Mouse	Sca1	APC-Cy7	BioLegend	108125	D7
	Mouse	CD18	FITC	BD Pharmingen	553292	C71/16
	Mouse	CD11a	APC	BD Pharmingen	550261	HL3
	Mouse	CD29	A488	ABD Serotec	MCA2298A488	HM BETA 1-1
	Mouse	CD49d	PE	BD Pharmingen	557420	9C10(MFR4.B)
PB aged neutrophils Analysis	Mouse	CD184/CXCR4	PE	eBioscience	12-9991-81	2B11
	Mouse	CD62L	FITC	BD Pharmingen	553150	MEL14
	Mouse	Gr1	Biotin	BD Pharmingen	553125	RB6-8C5
CRA	Human	CD4	PE	Miltenyi	130-098-134	MT-466
	Mouse	CD45.1/Ly5.1	PE	BioLegend	110708	A20
	Mouse	CD45.2/Ly5.2	FITC	BioLegend	109806	104

LDA	Mouse	CD45.2/Ly5.2	FITC	BioLegend	109806	104
	Mouse	CD3	PE-Cy5	BD Pharmingen	553065	145-2C11
	Mouse	CD45R/B220	PE	BD Pharmingen	553090	RA3-6B2
	Mouse	Gr1	PE	BD Pharmingen	553128	RB6-8C5
	Mouse	CD11b	Biotin	BD Pharmingen	553309	M1/70
	-	Biotin	PECy7	Molecular Probes	SA1012	-
hCD18/hCD11a expression in LCLs	Human	CD18	APC	BD Pharmingen	551060	6.7
	Human	CD11a	PE-Cy5	BD Pharmingen	551131	HI111
sICAM-1 binding Assay	Human	Fc IgG	PE	eBioscience	12-4998-82	Polyclonal
***Ex vivo* GT experiments: hCD18 and mCD11 subunits co-expression**	Human	CD18	APC	BD Pharmingen	551060	6.7
	Human	CD18	FITC	BioLegend	302106	TS1.18
	Mouse	CD11a	PE-Cy7	BD Pharmingen	558191	2D7
	Mouse	CD11b	PE	BD Pharmingen	553311	M1/70
	Mouse	CD11c	APC	BD Pharmingen	550261	HL3
***Ex vivo* GT experiments: hCD18 expression in different leukocyte subpopulations**	Human	CD18	APC	BD Pharmingen	551060	6.7
	Mouse	CD3	PE	BD Pharmingen	553064	145-2C11
	Mouse	CD3	FITC	BD Pharmingen	553062	145-2C11
	Mouse	CD45R/B220	PE	BD Pharmingen	553090	RA3-6B2
	Mouse	GR1	FITC	BD Pharmingen	553128	RB6-8C5
	Mouse	CD11b	FITC	BioLegend	101206	M1/70
***Ex vivo* GT experiments: hCD18 expression in BM LSK cells**	Human	CD18	APC	BD Pharmingen	551060	6.7
	Mouse	CD3	Biotin	BD Pharmingen	553060	145-2C11
	Mouse	Gr1	Biotin	BD Pharmingen	553127	RB6-8C5
	Mouse	Mac1	Biotin	BD Pharmingen	553309	M1/70
	Mouse	CD45R/B220	Biotin	BD Pharmingen	553086	RA3-6B2
	Mouse	Ter119	Biotin	BD Pharmingen	553672	Ter119
	Mouse	CD117/cKit				
	Mouse	Sca1				

Figure S1. Cloning strategy followed to generate the pCCL.PGK.CD18.Wpre* plasmid.

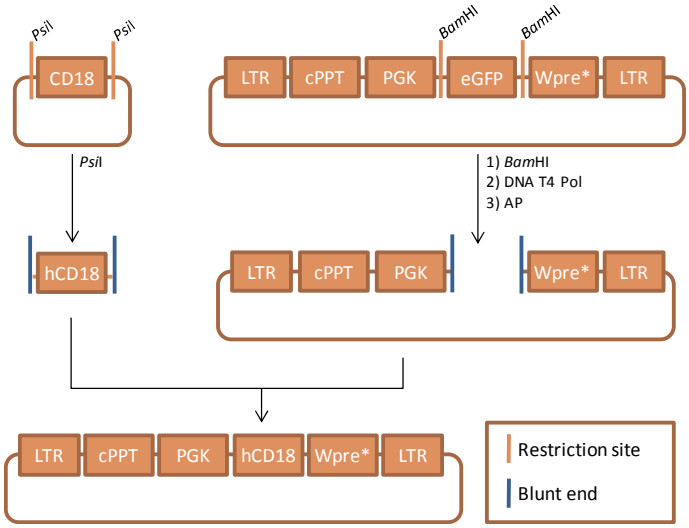

Figure S2. Cloning strategy followed to generate the pCCL.Chim.CD18.Wpre* plasmid.

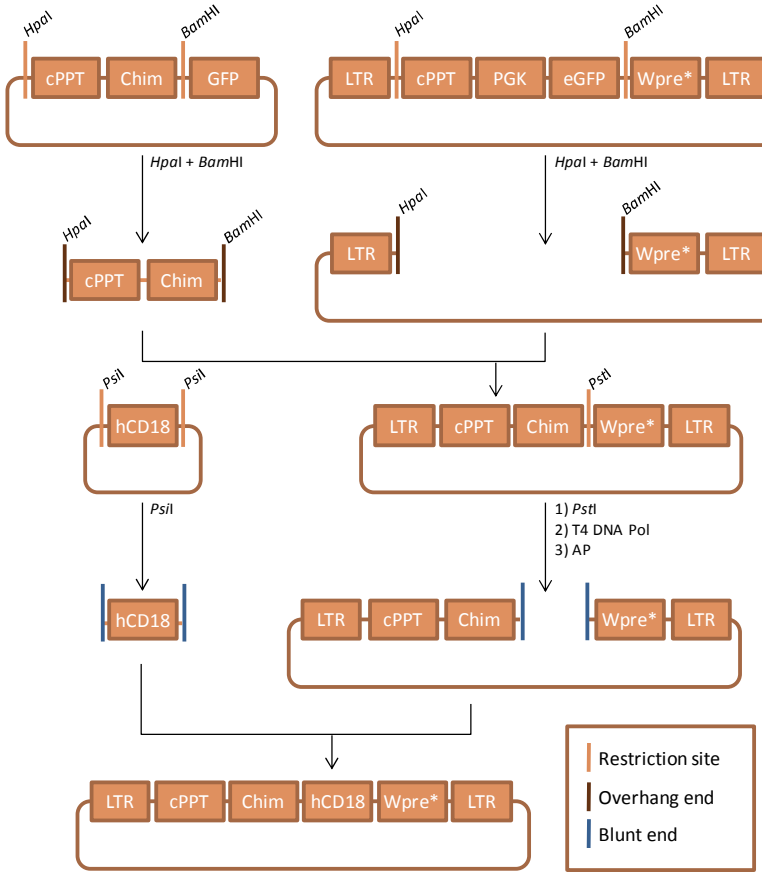

Figure S3. Cloning strategy followed to generate the pCCL.MIM.CD18.Wpre* plasmid.

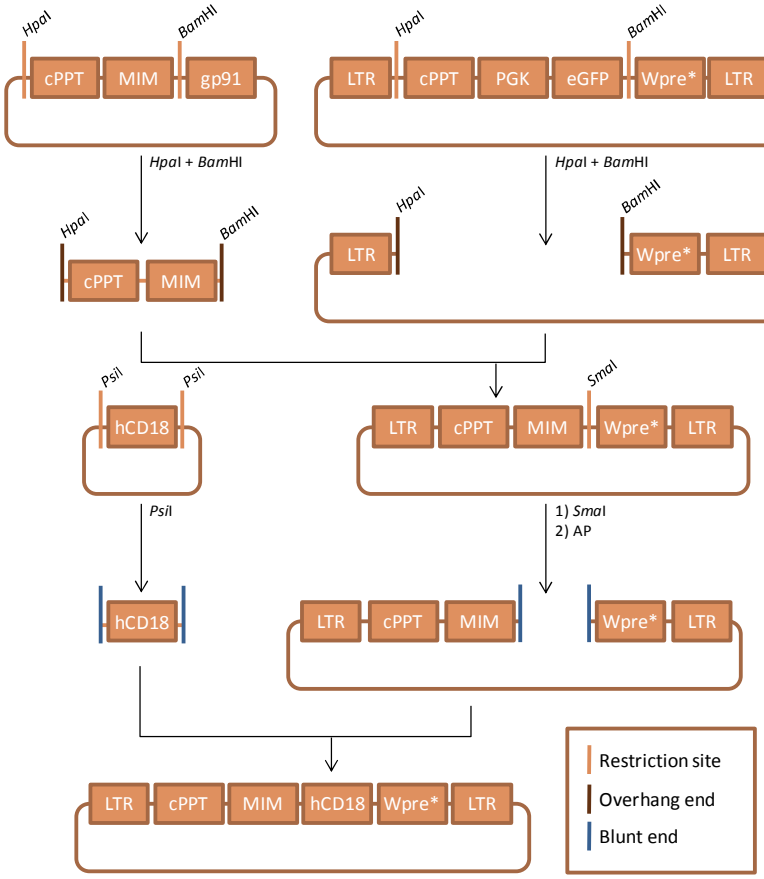

Figure S4. Cloning strategy followed to generate the pCCL.A2UCOE.CD18.Wpre* plasmid.

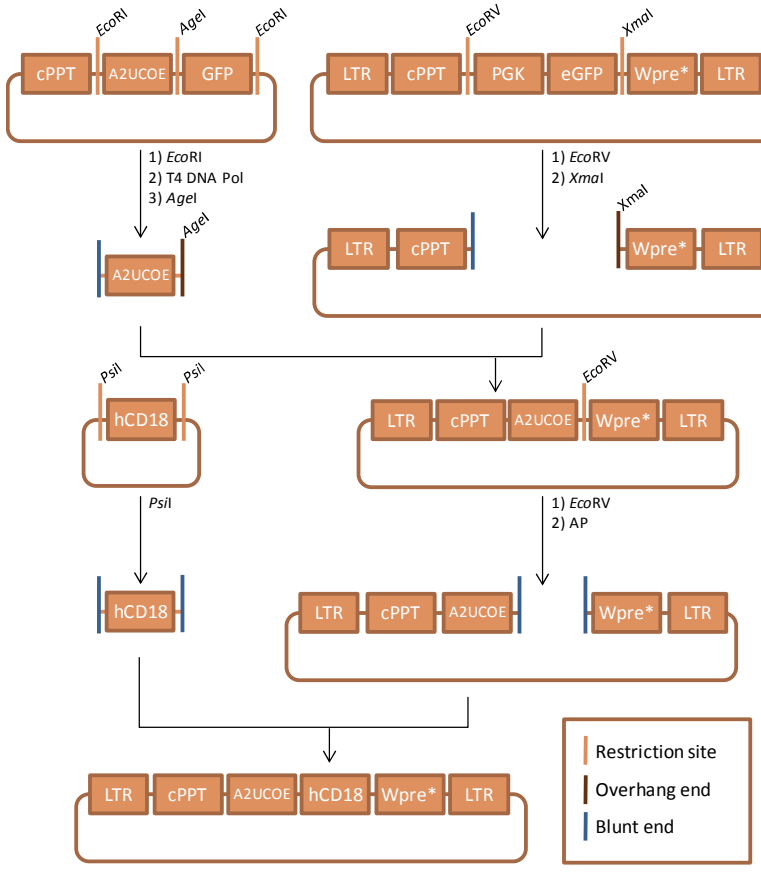

Figure S5. Cloning strategy followed to construct the lentiviral backbones containing the shRNA expression cassette.

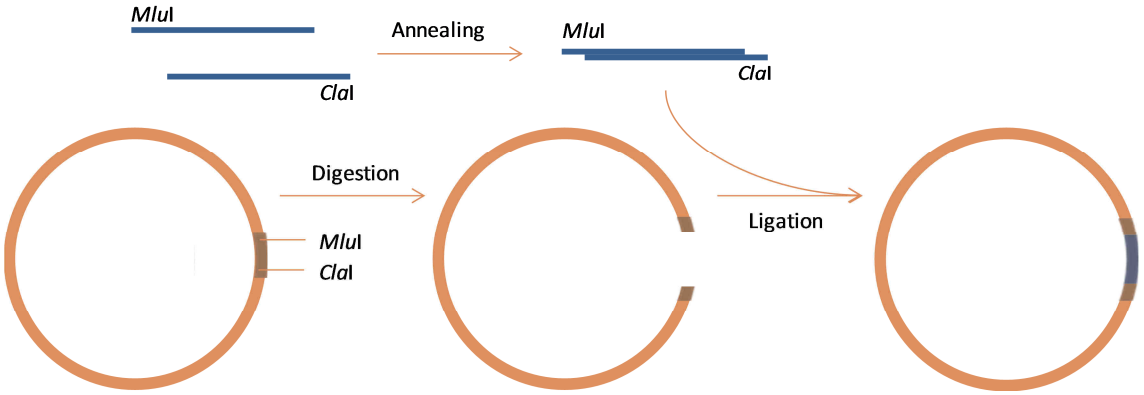

Appendix 2: Published articles related to the present doctoral thesis